



**TECHNISCHE
UNIVERSITÄT
WIEN**

DISSERTATION

A New Generation of Iron-based Hydrogenation Catalysts

ausgeführt zum Zwecke der Erlangung des akademischen Grades eines Doktors der
technischen Wissenschaften unter der Leitung von

Ao. Univ.Prof. Dr. Karl Kirchner

Institut für Angewandte Synthesechemie E163

eingereicht an der Technischen Universität Wien

Fakultät für Technische Chemie

von

Nikolaus Gorgas, MSc

Matr. Nr. 0509342

Esslinggasse 7, A-1010 Wien

Wien, April 2017

for ruth

Acknowledgements

First of all I would like to thank **Prof. Karl Kirchner** for giving me the opportunity to work in his research group and his supervision. Further, I want to thank him for many fruitful discussions and his enthusiasm for the subject of my thesis.

Special thanks to **Dr. Luca Gonsalvi**, **Dr. Federica Bertini** and **Dr. Irene Mellone** at the ICCOM-CNR in Florence for the successful collaboration and the invitation to work as a visiting researcher in their group. The COST-CARISMA action is gratefully acknowledged for the financial support of this short term scientific mission.

My particular acknowledgement goes also to **Prof. Luis Veiros** at the Instituto Superior Technico in Lisbon, who has been my virtual counterpart over the last years by supporting this work with a series of extensive DFT-calculations.

Moreover, I want to thank **Dr. Berthold Stöger** (TU-Wien) for performing single-crystal X-ray analysis and **Dr. Ernst Bitteneuer** (TU-Wien) for several ESI-MS measurements.

I would also like to thank all my former and current lab-colleagues, Özgür Öztopcu, Bernhard Bichler, Christian Schröder-Holzhacker, Sathiyamoorthy Murugesan, Sara R. M. M. de Aguiar, Mathias Glatz, Matthias Mastalir, Afroz Zirazadeh, Julian Brünig, Gerald Tomsu, Daniel Himmelbauer, Jan Pecak and Markus Rotter as well as the entire staff of the Institute of Applied Synthetic Chemistry at the Technical University of Vienna.

Finally, I want to thank my family and friends for their kind support and motivation during the whole time of my studies.

Preface – Aims and Structure of the Thesis

The catalytic reduction of polar multiple bonds such as carbonyl functionalities using molecular hydrogen plays a significant role in modern synthetic organic chemistry and is excellently performed by many transition metal complexes containing noble metals such as ruthenium, rhodium, or iridium. However, the limited availability of precious metals, their high price, and their toxicity diminish their attractiveness in the long run and more economical and environmentally friendly alternatives have to be found. Consequently, the development of well-defined base-metal catalysts of comparable activity would be desirable and is thus a major challenge for the development of more sustainable reduction reactions. As most abundant transition metal in the earth crust, iron constitutes a highly attractive alternative in order to surrogate traditional noble metals in catalysis.

Within this respect, the main objective of the current work was set on the development of novel type of iron-based hydrogenation catalysts of the general formula $[\text{Fe}(\text{PNP})(\text{H})(\text{CO})(\text{L})]$ that are supported by PNP-pincer ligands based on 2,6-diaminopyridine scaffolds. For this purpose, a series of iron hydride complexes has been synthesized, characterized and tested in the hydrogenative reduction of C-O double bonds. The work was complemented by detailed mechanistic studies in order to obtain better insight into the nature of catalyst action and activation.

This thesis is written as a cumulative work containing an introduction chapter and a compilation of four original papers that have already been published in established peer-review journals:

- (1) Gorgas, N.; Stöger, B.; Veiros, L. F.; Pittenauer, E.; Allmaier, G.; Kirchner, K. Efficient Hydrogenation of Ketones and Aldehydes Catalyzed by Well-Defined Iron(II) PNP Pincer Complexes: Evidence for an Insertion Mechanism. *Organometallics* **2014**, *33*, 6905–6914.
- (2) Gorgas, N.; Stöger, B.; Veiros, L. F.; Kirchner, K. Highly Efficient and Selective Hydrogenation of Aldehydes: A Well-Defined Fe(II) Catalyst Exhibits Noble-Metal Activity. *ACS Catal.* **2016**, *6*, 2664–2672.
- (3) Bertini, F.; Gorgas, N.; Stöger, B.; Peruzzini, M.; Veiros, L. F.; Kirchner, K.; Gonsalvi, L. Efficient and Mild Carbon Dioxide Hydrogenation to Formate Catalyzed by Fe(II) Hydrido Carbonyl Complexes Bearing 2,6-(Diaminopyridyl)diphosphine Pincer Ligands. *ACS Catal.* **2016**, *6*, 2889–2893.
- (4) Mellone, I.; Gorgas, N.; Bertini, F.; Peruzzini, M.; Kirchner, K.; Gonsalvi, L. Selective Formic Acid Dehydrogenation Catalyzed by Fe-PNP Pincer Complexes Based on the 2,6-Diaminopyridine Scaffold. *Organometallics* **2016**, *35*, 3344–3349.

The results reported in these publications are closely related to each other and comprise two major topics: (i) the hydrogenative reduction of aldehydes and ketones; (ii) the hydrogenation of carbon dioxide as well as the dehydrogenation of formic acid serving as hydrogen storage system.

Statement of Contribution:

The first two publications describe the synthesis and characterization of the novel iron complexes as well as their catalytic application in the hydrogenation of aldehydes and ketones. Nikolaus Gorgas (NG) is first author of these papers and his contribution includes the entire conceptual and experimental work as well as the preparation of the manuscripts.

The second part of this work was done in close collaboration with the group of Dr. Luca Gonsalvi at the ICCOM-CNR in Florence (Italy) and comprises two joint publications describing the application of these catalysts in the reversible (de)hydrogenation of carbon dioxide or formic acid as hydrogen storage materials. The contribution of NG to these publications was essential, including the preparation of catalysts, performing selected test reactions and all mechanistic experiments. Studies on the catalytic dehydrogenation of formic acid were done by NG at the ICCOM-CNR in Florence during a short term scientific mission (STSM) within the framework of the COST-CARISMA action.

Well-defined Iron Catalysts as Multi-talents for the Production, Activation, and Transfer of Dihydrogen

1.1 Introduction

Transformations using transition metal catalysts play a predominant role in modern synthetic chemistry. Since catalysis provides a sustainable and efficient approach for the production of bulk and fine chemicals, it became an indispensable part of countless industrial processes.¹ Traditionally, catalyst based on platinum-group metals like ruthenium, rhodium, iridium or platinum have been applied. However, the dependence on these scarce, expensive, and often toxic elements makes it highly attractive to develop for more sustainable alternatives by replacing them by abundant, cheap and environmentally friendly first-row transition metals.

Among them, iron constitutes one of the most promising candidates as surrogate for well-established noble metals in catalysis. Apart from the high natural abundance (iron is the most abundant transition metal in the Earth's crust) and low environmental impact, iron clearly shows its catalytic potential being an essential part of numerous enzymes that are involved in a wide variety of biological processes.² Despite these facts, iron has long been neglected for catalytic applications and only recently it became subject of intense investigations from many different academic and industrial research groups. The main reason might be the more complex coordination chemistry in comparison to many second- and third-row transition metals. For example, while those metals are known to undergo two electron reactions iron is often more prone to be engaged in one electron processes which often proceed *via* radical reactions and therefore increase the propensity for unselective and uncontrollable side reactions.³ Moreover, iron tends to adopt different spin state configurations which make the corresponding complexes coordinative labile but at the same time less reactive towards substrate binding.⁴ Therefore, new strategies and concepts have to be found in order to circumvent those unfavorable phenomena.

Although many examples of successful iron catalyzed transformations⁵ including cycloadditions, cross coupling reactions, oxidations, reductions, and olefin polymerizations have been reported in the last few years, the knowledge about distinctive requirements for active and selective catalytic systems is still poor. Most of these reactions just rely on *in-situ* assembled systems using simple and commercially available iron compounds, often in combination with achiral or chiral ligands. Thus, the identification of catalytically active species, key intermediates and pathways of the proceeding reactions gets usually impossible. This circumstance prevents improvements of the overall catalytic performance by specific structural and electronic modifications of the system. Consequently, the synthesis of isolated and structurally well-defined complexes combined with a fundamental understanding of reaction mechanisms appears to be a primary objective for the rational development of novel catalytic systems.

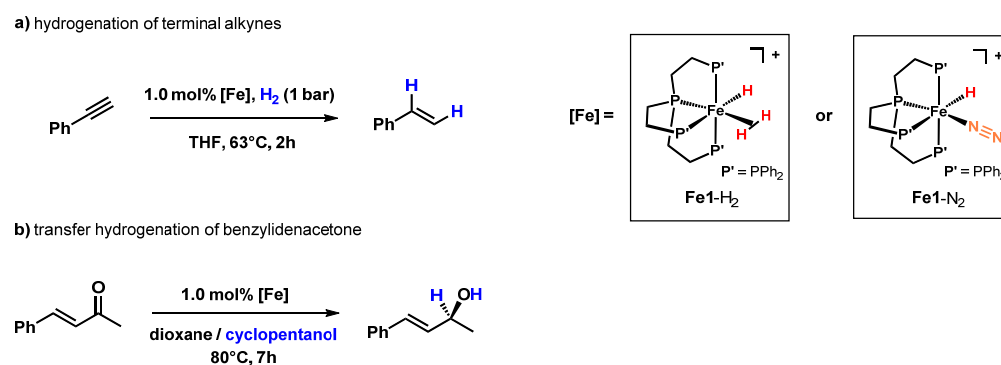
The success of organometallic catalysis mainly emerged from the huge structural diversity of

metal-ligand frameworks that facilitate optimization and therefore permit the development of “tailored-fit” catalysts for a large scope of specific substrates. Hence, novel iron based catalysts containing highly versatile ligand scaffolds that can be synthesized in a simple modular fashion and thus allow a systematic modifications in order to enhance the activity and selectivity of the of the system are highly desirable. Therefore, we will point out several common and characteristic features of selected well-defined iron based catalysts that even became competitive to their noble metal analogues by continuous improvements based on the sound knowledge of specific structure-activity relationships.

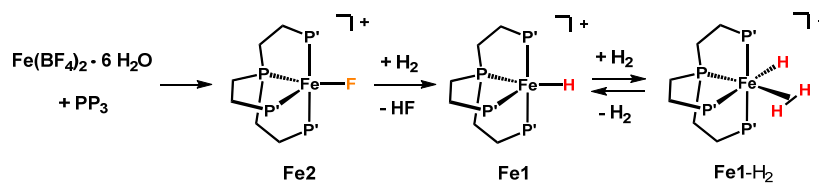
However, in terms of green and sustainable chemistry catalytic hydrogenation as one of the most important synthetic processes in industry represents a highly atom-efficient and clean methodology.⁶ Apart from synthetic applications, chemical hydrogen storage based on reversible hydrogenation/dehydrogenation of small molecules might be an attractive technology for future energy supply.⁷ For such processes iron based hydrogenation catalysts are highly desirable.⁸ In particular, reductions involving hydrogen transfer such as hydrogenations and transfer hydrogenations comprise a major group among the reactions catalyzed by iron compounds, which have been extensively investigated and well-understood over the last years.

1.2 Well-defined Iron-Tetraphosphine Catalysts

The first iron hydrogenation catalysts, based on a well-defined metal-ligand framework, have already been reported by *Bianchini et al.* in the late 1980s. Complexes of the type $[\text{Fe}(\text{PP}_3)(\text{H})(\text{H}_2)]^+$ (**Fe1-H₂**) and $[\text{Fe}(\text{PP}_3)(\text{H})(\text{N}_2)]^+$ (**Fe1-N₂**) were found to promote the selective hydrogenation of some terminal alkynes to alkenes^{9,10} as well as the transfer hydrogenation of benzylidenacetone¹¹ to the corresponding unsaturated alcohol (Scheme 1). Although these reactions were supposed to operate *via* two different mechanisms, the five coordinate monohydride complex $[\text{Fe}(\text{PP}_3)(\text{H})]^+$ has been proposed as common key intermediate in both cases.



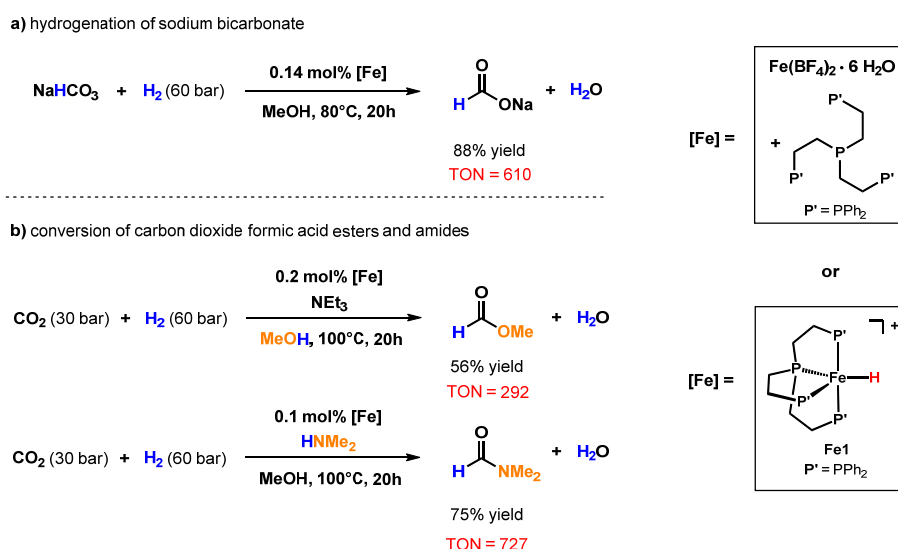
Scheme 1. Examples for the application of $[\text{Fe}(\text{PP}_3)(\text{H})(\text{H}_2)]^+$ and $[\text{Fe}(\text{PP}_3)(\text{H})(\text{N}_2)]^+$ in catalytic reductions reported by group of *Bianchini*.



Scheme 2. *In situ* formation of $[\text{Fe}(\text{PP}_3)(\text{H})]^+$ and $[\text{Fe}(\text{PP}_3)(\text{H})(\text{H}_2)]^+$ from $\text{Fe}(\text{BF}_4)_2$ and the respective ligand under an atmosphere of H_2 .

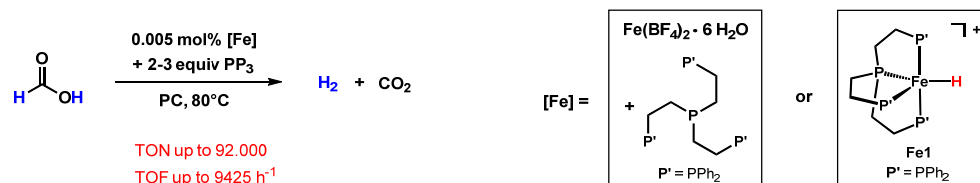
In 2010, the groups of *Beller* and *Laurenzy* re-discovered this system as they found that a combination of $\text{Fe}(\text{BF}_4)_2$ and the tetradentate ligand (PP_3), leading to the *in situ* formation of $[\text{Fe}(\text{PP}_3)(\text{H})]^+$ under the applied conditions (Scheme 2), promotes the hydrogenative reduction of sodium bicarbonate (Scheme 3).¹² At 80°C and 60 bar hydrogen pressure a TON of about 600 could be reached giving sodium formate in 88% yield. Moreover, this system is also capable for the hydrogenation carbon dioxide which was converted to formic acid esters (in presence of an alcohol) or amides (in presence of an amine).

In a subsequent publication, *Beller*, *Laurenzy*, *Ludwig* and co-workers reported on the production of hydrogen accomplished by the catalytic decomposition formic acid in presence of $[\text{Fe}(\text{PP}_3)(\text{H})]^+$ (Scheme 4).¹³ This system was found to be remarkably active. In presence of only 0.005 mol% of the iron precursor $\text{Fe}(\text{BF}_4)_2 \cdot 6\text{H}_2\text{O}$ together with a fourfold excess of the ligand a TOF of 9450 h^{-1} was observed at 80°C in propylene carbonate as the solvent. Moreover, the long term stability has been investigated under the same conditions by using a continuous setup. After a short induction period, a constant gas flow corresponding to a TOF of 5390 h^{-1} could be maintained over 16 hours resulting in an overall TON of more than 90.000. Notably, this system operates under acidic



Scheme 3. Iron catalyzed hydrogenation of bicarbonate/ CO_2 to formates

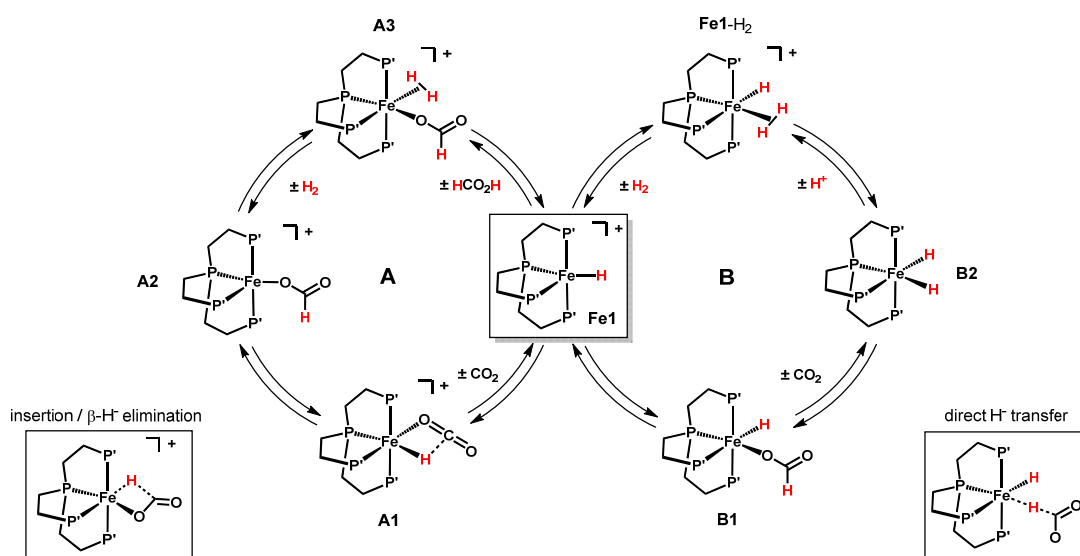
conditions, obviating the presence of a base. However, the addition of excess ligand was found to be essential for the catalytic performance, since significantly lower TOFs were reached when a 1:1 ratio of the iron-precursor and the ligand were employed in the reaction. This effect was even observed for the pre-synthesized complex $[\text{Fe}(\text{PP}_3)(\text{H})]^+$ which also showed increased activity in presence of an additional equivalent of PP_3 .



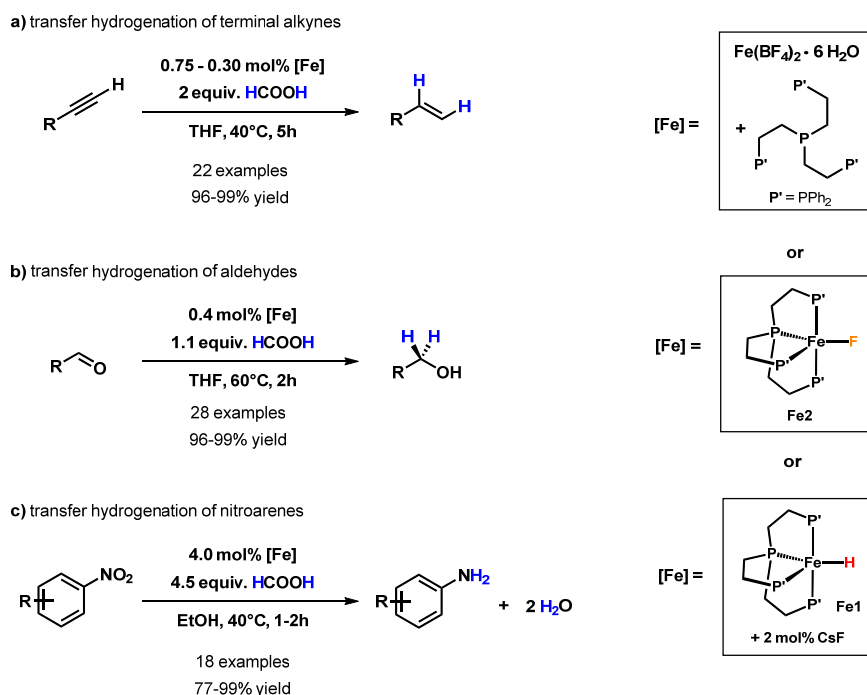
Scheme 4. Hydrogen production by the iron catalyzed decomposition of formic acid

Both the hydrogenation of carbon dioxide/bicarbonate and the reverse dehydrogenation of formic acid are considered to proceed *via* a similar reaction mechanism. Based on spectroscopic observations, two competing catalytic cycles have been proposed (Scheme 5),¹²⁻¹⁶ which have also been supported by the DFT-calculations of several other groups.¹⁷⁻²⁰ The key step in cycle A is supposed to be the reversible insertion/ β -hydride elimination of a CO_2 /formate-ligand between the cationic intermediates **A1** and **A2**, whereas the activation and release of CO_2 in cycle B takes place by a direct hydride transfer.

Beside the production of molecular hydrogen, formic acid could also be used as reductant in



Scheme 5. Mechanism of the iron catalyzed asymmetric transfer hydrogenation including catalyst activation and deactivation pathways.

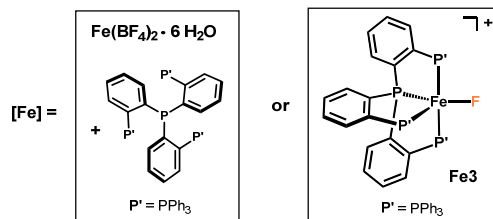
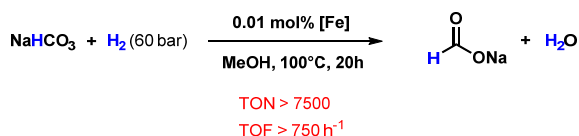


Scheme 6. Application of the iron-tetraphosphine system in transfer hydrogenations using formic acid as reductant.

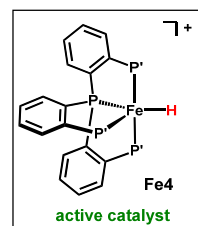
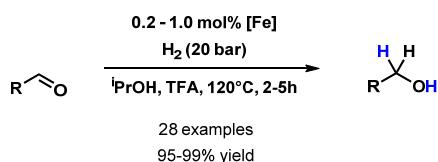
transfer hydrogenations catalyzed by the iron-tetraphos system (Scheme 6). In particular, *Beller* and co-workers developed general procedures for the reduction of nitroarenes to anilines,²¹ the conversion of terminal alkynes to alkenes²² and the selective hydrogenation of aldehydes.²³ All transformations take place under mild and essentially base-free condition. Notably, this system provides a high functional group tolerance and exhibits a remarkable degree of chemoselectivity, since other reducible functionalities including C-C double bonds, ketones or esters are not affected in course of the reaction. In contrast to the pure dehydrogenation of formic acid, the presence of fluoride anions appeared to be essential for the reaction to occur in the case of transfer hydrogenations. For example, comparable results were obtained for the *in situ* generated system and the pre-synthesized complex $[\text{Fe}(\text{PP}_3)(\text{F})]^+$, whereas $[\text{Fe}(\text{PP}_3)(\text{H})][\text{BPh}_4]$ was only active after addition of an external fluoride source.²¹ However, mechanistic proposals on the catalytic cycle remained mainly speculative.

In comparison to the successful applications of the iron-tetraphos system in hydrogen production and hydrogen transfer reductions by the use of formic acid, the performance of this catalyst in activating molecular hydrogen was only modest with the need for further improvements. This could be accomplished by the use of the structurally related complex **Fe4**, in which the phosphorous donors are connected via phenylene bridges (Scheme 7). For example, this catalyst achieved TONs of more than 7500 in the hydrogenation of sodium bicarbonate, being one order of magnitude more efficient compared to the corresponding complex **Fe1**.¹⁴ The improved hydrogenation performance of this system might be attributed to the higher thermal stability in comparison to complexes bearing ethylene

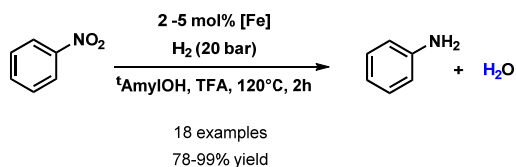
a) hydrogenation of carbon dioxide / bicarbonate



b) hydrogenation of aldehydes



c) hydrogenation of nitroarenes

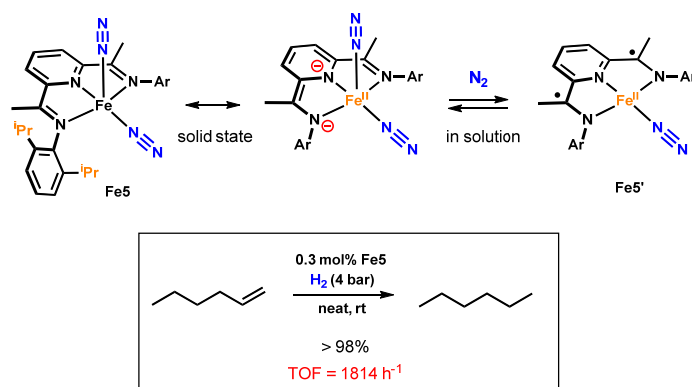


Scheme 7. Hydrogenations catalyzed by iron complexes supported by phenylene-bridged tetra-phosphine ligands

bridged phosphines. Moreover, **Fe4** has also been successfully employed as catalyst in the reduction of nitroarenes²⁴ and aldehydes²⁵ using molecular hydrogen. As in the case of corresponding transfer hydrogenations catalyzed by **Fe2**, high chemoselectivity over other reducible moieties has been observed for these reactions. Interestingly, the presence of trifluoroacetic acid is required to promote catalytic turnover, thus giving a rare example of a hydrogenation catalyst operating in acidic media.

1.3 Low Valent Iron-Dinitrogen Complexes

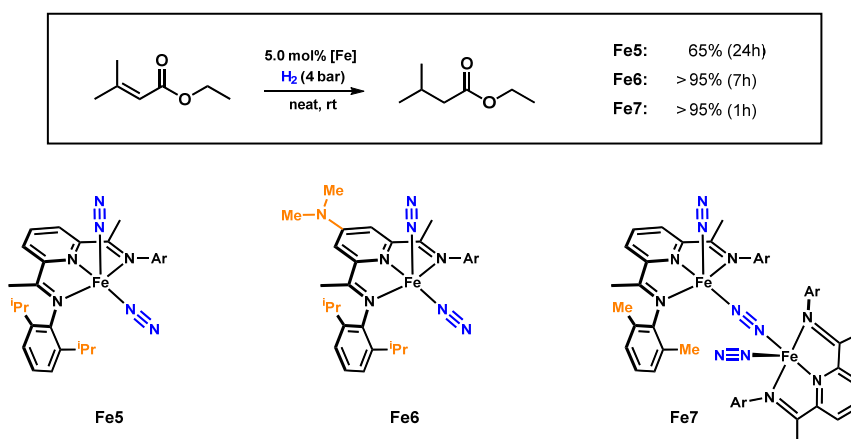
Another significant breakthrough in the field of iron catalyzed hydrogenations could be accomplished by the work of *Chirik* and co-workers on low valent iron(0) complexes bearing bis(imino)pyridine ligands. Initially, they had been inspired by the commonly known thermal and photochemical induced alkene hydrogenation methods using Fe(CO)₅, in which a Fe(CO)₃ intermediate is supposed to be the catalytically active species. As strong π-acidic tridentate ligands, aryl substituted bis(imino)pyridine scaffolds were considered to be suitable and modifiable surrogates for carbon monoxide in the putative iron tricarbonyl fragment, giving access to complexes, that in principle show an isolobal relationship to Fe(CO)₃. These considerations resulted in the preparation of the dinitrogen complex **Fe5** which was indeed found to be an effective pre-catalyst for the hydrogenation of alkenes and alkynes.²⁶



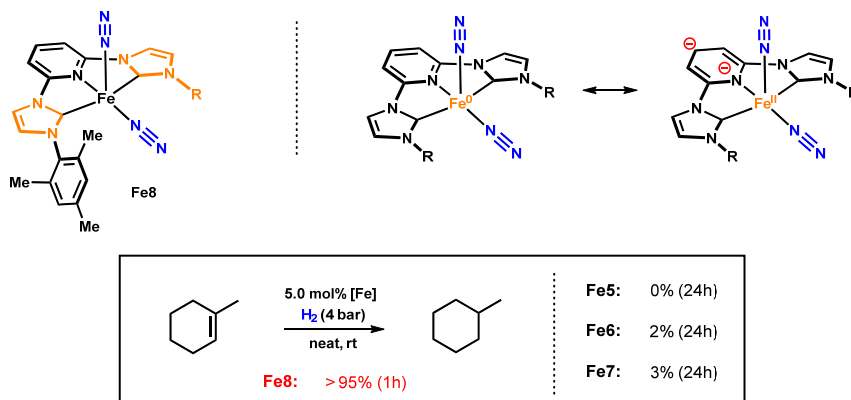
Scheme 8. Electronic structure of **Fe5** and its application in the hydrogenation of 1-hexene

Through spectroscopic and theoretical studies it could be shown, that this compound is best described as a resonance hybrid structure between an iron(0) and iron(II) form, with the ligand acting as a classical π -acceptor (Scheme 8).²⁷ In solution, one of the N_2 ligands dissociates under formation of the four coordinate complex **Fe5***, which possesses a different electronic structure to its five coordinate analogue. This compound is now more precisely described as an intermediate spin iron(II) complex, where two electrons have been transferred to the ligand, generating a triplet diradical dianion that is antiferromagnetically coupled to the metal center. In this state, the ligand is supposed to be potentially redox active. However, since details on the mechanism have not been reported, it remains an unresolved question if this kind of electron responsive metal-ligand cooperation is involved in the catalytic cycle of alkene hydrogenation.

Nevertheless, this catalyst exhibits high turnover frequencies under mild reaction conditions and low catalyst loadings.²⁶ Functional groups including fluorine substituents, ethers, substituted amines and α,β -unsaturated esters are tolerated by the catalyst.²⁸ Other substrates such as primary amines



Scheme 10. Improved catalytic performance in the hydrogenation of ethyl-3-methylbut-2-enoate by structural modifications of the catalysts



Scheme 11. Resonance structure of **Fe8** and its application in the hydrogenation of challenging trisubstituted unfunctionalized olefins

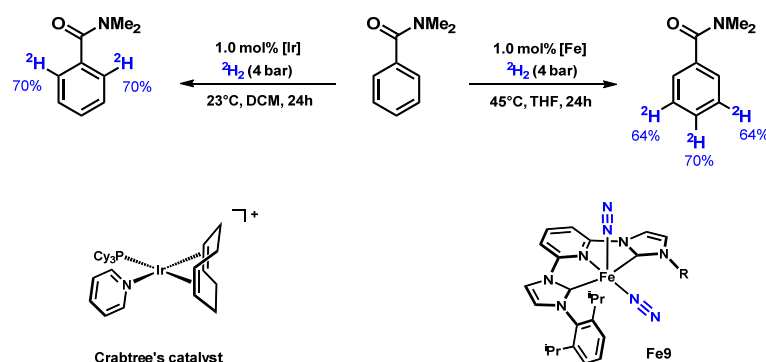
and most ketones were found to form inactive complexes with the catalyst or even cause decomposition as observed for α,β -unsaturated carbonyl compounds. Moreover, the reduction of unfunctionalized but sterically demanding tri- and tetrasubstituted alkenes appeared to be extremely difficult.

Subsequent ligand manipulations allowed for a detailed investigation of structure-activity relationships and finally lead to an improved overall catalyst performance.²⁹ For example, reducing the size of the aryl substituents (**Fe7**)³⁰ or introducing an electron donating dimethylamino group at the para-position of the pyridine backbone (**Fe6**)³¹ significantly increased the catalytic activity, especially with respect to highly challenging tri-substituted alkenes.

Further improvements could be accomplished through the catalytic evaluation of the more electron rich dinitrogen complex **Fe8**, originally reported by *Danopoulos* and co-workers,³² which features N-heterocyclic carbenes instead of imine groups. Although this complex is structurally related to its diimine analogues, again being considered as a hybrid resonance structure between an iron(0) and an iron(II) oxidation state, the formation of the corresponding four coordinate complexes, associated with the ligand's ability to participate in redox events, has not been observed, thus indicating that the hydrogenation of C-C double bonds apparently proceeds via a classical mechanism.³³

This new catalyst exhibits an improved catalytic activity in the hydrogenation of hindered, unfunctionalized alkenes.²⁹ At standard conditions (5 mol% cat., 4 bar H_2 , 23°C) even several trisubstituted olefins were quantitatively reduced. However, tetrasubstituted alkenes were found to be unaffected. Only 2,3-dimethyl-1H-indene could be reduced, which might be attributed to the fact that isomerization takes place prior to the hydrogenation of the C-C double bond.

Recently, complex **Fe9** has been successfully applied for deuterium and tritium labelling of pharmaceuticals by a direct hydrogen isotope exchange in aromatic and heteroaromatic rings of these substrates using $^2\text{H}_2$ or $^3\text{H}_2$ gas.³⁴ Common methods essentially rely on Iridium catalyst which are site selective due to *ortho*-directing groups.³⁵ Most beneficial, catalyst **Fe9** exhibits a complimentary



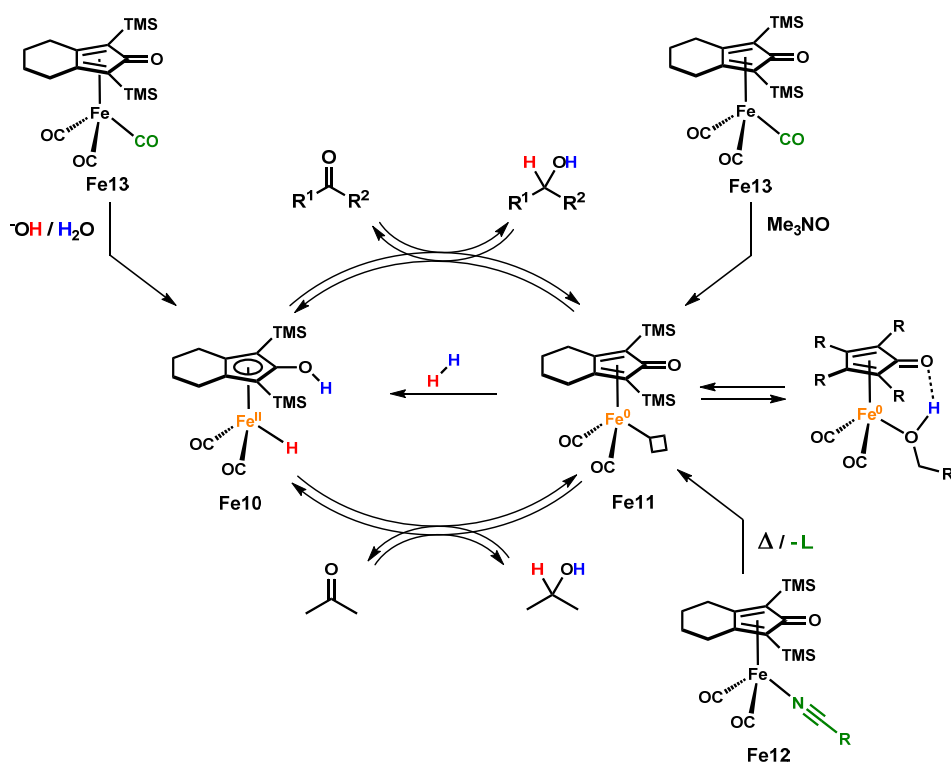
Scheme 12. Iron catalyzed radio-labelling in comparison to an state-of-the-art Ir-catalyst

selectivity since isotope exchange occurs at the most sterically accessible positions and does not require neighboring directing groups. Further advantages of this system include the high degree of incorporation, the use of polar aprotic solvents and the compatibility to various functional groups. Finally, the reactions were carried out at sub-atmospheric pressures being highly advantageous especially in the case of radio labelling.

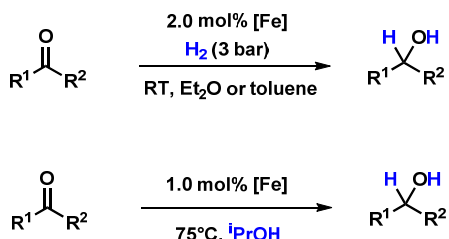
1.4 Knölker-Type Catalysts

Iron cyclopentadienone complexes comprise a major class of compounds capable of the catalytic activation and transfer of dihydrogen. In 2007, Casey and Guan discovered the catalytic potential of the (hydroxycyclopentadienyl)iron(II) dicarbonyl hydride **Fe10**. This complex, originally described by the group of Knölker,³⁶ was found to promote the hydrogenation of different carbonyl compounds including aldehydes, ketones and imines.³⁷ The reaction takes place under mild conditions (3 bar H₂, r.t.) and reaches a high level of chemoselectivity since a number of competitive substrates such as epoxides, esters as well as isolated alkenes and alkynes remain unaffected under the applied conditions. Only in the case of α,β -unsaturated substrates product mixtures have been obtained due to partial reduction of the conjugated C-C double bond.

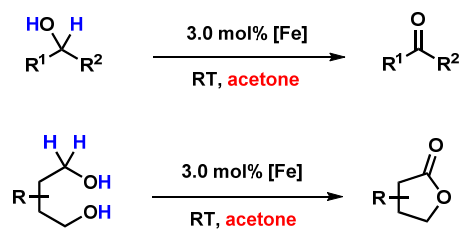
Detailed mechanistic studies provided strong evidence for a bifunctional reaction mechanism taking place in the outer coordination sphere of the metal.³⁸ **Fe10** contains two electronically coupled hydridic and acidic hydrogens that are transferred to the polarized double bond of the substrate in a concerted fashion (Scheme 13). Notably, this step is associated with a change in the oxidation state of the metal, resulting in the formation of an iron(0) species **Fe11** in which the cooperating ligand appears in the oxidized cyclopentadienone form. This coordinatively unsaturated intermediate is stabilized by the prior formed product alcohol which can easily dissociate from the complex, thus allowing for the coordination dihydrogen. In a second step, H₂ is cleaved heterolytically between the iron metal center and the ligand, which, accompanied by a further intramolecular redox-event, leads to the recovery of



hydrogenations and transfer hydrogenations



Oppenauer-type oxidations



Scheme 13. Mechanism and activation of *Knölker*-type complexes and their application in hydro-generative reductions as well as dehydrogenative oxidations of carbonyl/alcohol substrates.

the initial hydrido hydroxycyclopentadiene complex **Fe10**.

Since the hydrogen transfer between the catalyst and the substrate appeared to be reversible in the absence of H_2 , catalytic turnover can even be accomplished when an appropriate hydrogen source such as isopropanol is used. Moreover, the reverse transformation can be achieved in presence of a suitable hydrogen acceptor (e.g. acetone), so that this system can serve as a reduction or oxidation catalyst, respectively (Scheme 13). For example, in their initial paper *Casey* and *Guan* also described the transfer hydrogenation of acetophenone catalyzed by 1 mol% **Fe10** which was carried out in 2-propanol as the solvent.³⁷ In a subsequent publication, *Guan* et al. reported on an *Oppenauer*-type oxidation of primary and secondary alcohols in presence excess acetone to afford the corresponding

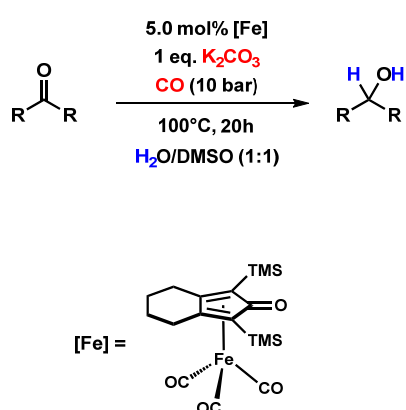
aldehydes and ketones, while the formation lactones was observed in the case of diol substrates.³⁹

This pioneering work on the basic reactivity of complex **Fe10** paved the way for further improvements of this system and the discovery of new applications.

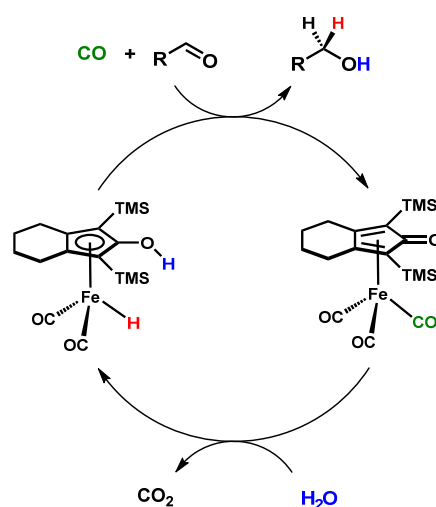
Apart from structural modifications of the cyclopentadienone ligand, significant progress has been achieved by the introduction of bench-stable catalyst precursors in order to avoid the use of the reactive but highly sensitive complex **Fe10** (Scheme 13). For example, nitrile ligated (cyclopentadienone)iron(0) dicarbonyl complexes **Fe12** have been used, which provide access to intermediate **Fe11** by the dissociation of the labile nitrile ligand at elevated temperatures.⁴⁰ Another approach was found by the selective mono-decarbonylation of the tricarbonyl precursor complex **Fe13**, which could be accomplished by the addition of trimethylamine *N*-oxide.⁴¹ Again, the unsaturated complex **Fe11** is generated *in situ* as one carbonyl ligand gets oxidized under the liberation of carbon dioxide. Alternatively, *Beller et al.* found that complex **Fe13** is effectively activated by treatment with potassium carbonate in the presence of water.⁴² Apparently, attack of a hydroxide anion on the carbonyl ligand induces a *Hieber*-type base reaction leading to the release of carbon dioxide and the generation of a hydride intermediate, which, after protonation of the cyclopentadienone ligand, is converted into the active catalyst **Fe10**.

Notably, the group of *Beller* could even demonstrated that this *Hieber*-type base reaction enables the system to promote the reduction of carbonyl compounds under water gas shift conditions in which carbon monoxide and water serve as the hydrogen source (Scheme 14).⁴³ For instance, under an atmosphere of CO (10 bar) and by using a H₂O/DMSO mixture as the solvent, a variety of different aromatic and aliphatic aldehydes could be converted into the corresponding primary alcohols in

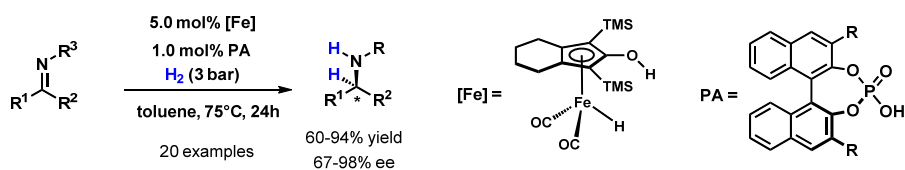
a) reduction of carbonyl substrates under water-gas shift conditions



b) proposed mechanistic cycle



Scheme 14. Reduction of aldehydes and ketones under water-gas shift conditions

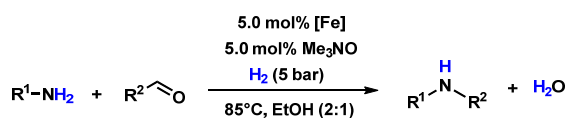


Scheme 15. Asymmetric hydrogenation of imines

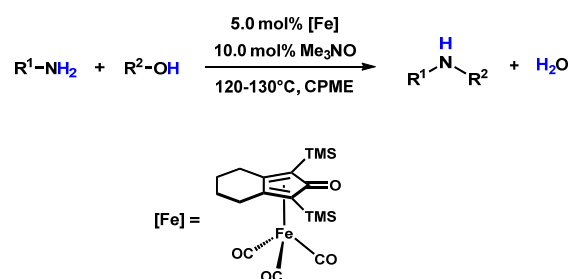
presence 0.5 -2.0 mol% of **Fe13** together with a stoichiometric amount of K_2CO_3 .

Beside the establishment of convenient catalyst precursors, several successful attempts to extend the scope of applications have been reported as well. For example, Knölker-type iron catalysts have been extensively used for the synthesis of amines. *Beller* and co-workers developed a general protocol for the stereoselective hydrogenation of imine substrates by using chiral Brønsted acid as co-catalyst in the reaction (Scheme 15).⁴⁴ In presence of 5 mol% of **Fe10** and 1 mol% of the enantiomerically pure phosphoric acid (PA) the resulting amines were obtained in good yields reaching up to 98% enantiomeric access. Moreover, *Renauld et al.* reported on the reductive amination of carbonyl substrates using molecular hydrogen (Scheme 16a).⁴⁵ A variety of aldehydes and ketones could be converted into the corresponding amines in high yields by using 5 mol% of complex **Fe13** activated by the addition of trimethylamine N-oxide. In some cases catalytic amounts of NH_4PF_6 were added to accelerate imine formation, thus avoiding the competitive hydrogenation of the C-O double bond. More recently, the groups of *Barta* and *Feringa* demonstrated that this system is

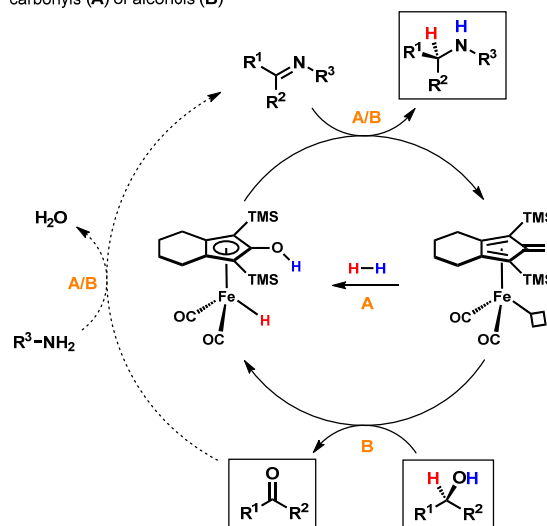
a) reductive amination of aldehydes and ketones (*Renauld 2012*)



b) alkylation of amines with alcohols (*Barta/Feringa 2014*)



c) mechanism of the catalytic formation of amines from carbonyls (A) or alcohols (B)



Scheme 16. Reductive amination of aldehydes and direct alkylation of amines with alcohols using an in situ generated *Knölker*-type catalyst

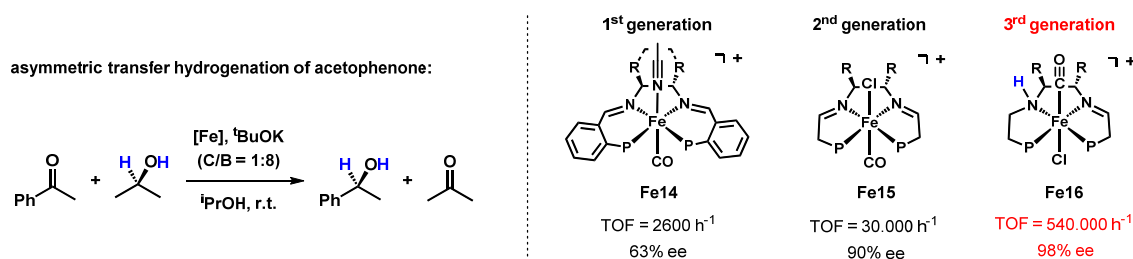
even capable to promote the direct amination of alcohols (Scheme 16b).⁴⁶ This reaction does not require the use of H₂, since it proceeds via a three-step mechanism involving catalytic autotransfer of dihydrogen (the so-called “hydrogen borrowing” concept). In particular, the alcohol substrate gets oxidized to the corresponding carbonyl compound by transferring two hydrogen atoms to the catalyst. The subsequent condensations reaction with an amine leads to the formation of an imine intermediate, which is finally hydrogenated to give the corresponding amine. Gratifyingly, the equivalent of dihydrogen consumed in this last step is provided by the initial dehydrogenation of the alcohol.

1.4 Chiral Tetradentate Iron-PNNP Catalysts

Morris and co-workers developed a series of well-defined iron based catalysts for the efficient asymmetric transfer hydrogenation of ketones. After their initial report in 2008, up to date the third generation of iron catalysts bearing chiral tetradentate PNNP ligands has been developed (Scheme 17).⁴⁷ The design of these complexes was driven by extensive mechanistic investigations, which gave insight in the mode of catalyst action and activation.

Upon activation with 8 equiv. of ^tBuOK in ⁱPrOH, catalysts of the first generation achieved TOFs up to 2600 h⁻¹ in the reduction of acetophenone affording the corresponding chiral alcohol in 63% ee (Scheme 17, **Fe14**).⁴⁸ However, iron nanoparticles were found to be the catalytically active species, apparently formed by the facile dissociation of the ligand under reducing conditions, since *o*-phenylene linkers in these complexes form rather flexible six membered chelate rings.⁴⁹ As a consequence, the next generation of Fe-PNNP contained ethylene linkers giving more stable 5,5,5 metallacycles instead of the former 6,5,6 system (Scheme 17, **Fe15**).⁵⁰ This change in the ligand structure prevented the formation of iron nanoparticles and gave rise to significantly more active and selective catalysts. For example, under very similar conditions 1-phenylethanol was obtained with up to 90% ee and a turnover frequency of more than 28.000 could be observed in the case of this substrate.

Mechanistic investigations revealed the formation of an enamido/amide complex **Fe17** as the catalytically active species.^{51,52} This intermediate receives a hydrogen equivalent from the ⁱPrOH solvent giving the hydrido enamido/amine complex **Fe18** which reduces the substrate ketone in the

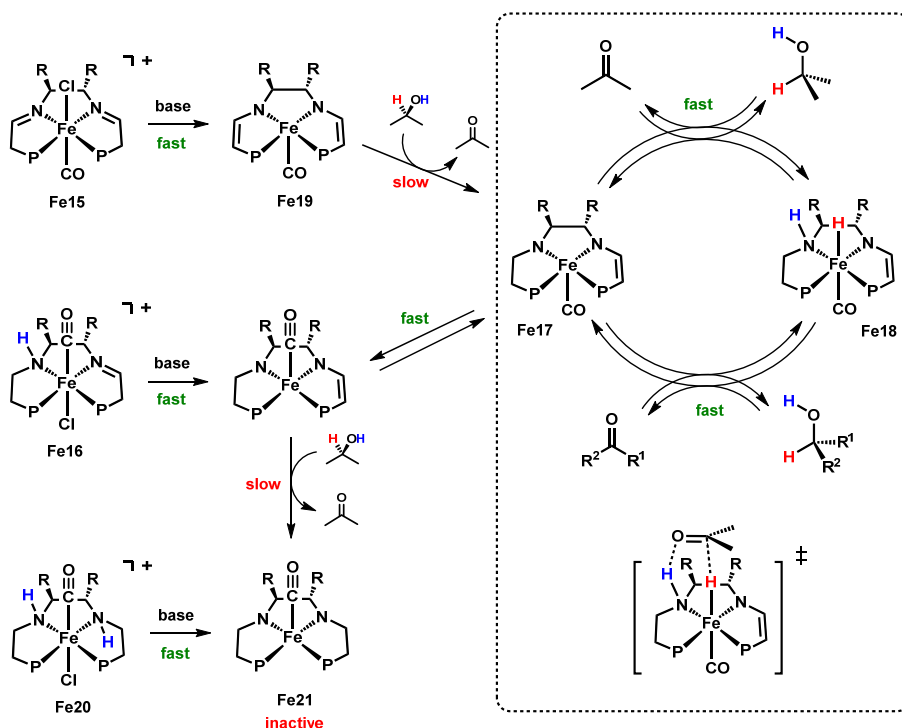


Scheme 17. Chiral iron-PNNP catalyst for the stereoselective transfer hydrogenation of ketones

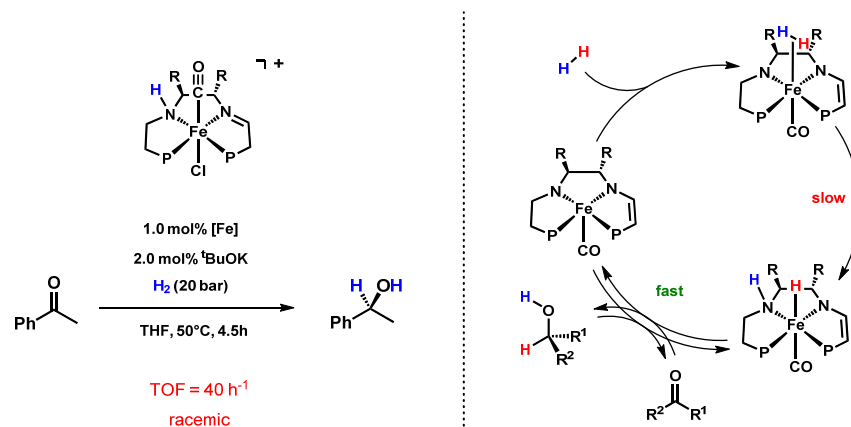
reverse reaction leading back to the initial enamido/amide complex. Activation of the catalyst precursor **Fe15** occurs *via* a two-step sequence. First, the acidic methylene groups of the imine linkers are rapidly deprotonated to give the bis-enamide complex **Fe19**. In a second step, taking place in the inner coordination sphere by the subsequent proton and hydride transfer from i PrOH, one of the enamide groups gets reduced to the amide present in active catalyst.

However, it was found that the catalytic performance of this system is mainly limited by the comparatively slow formation of the active species. The design of the next generation of pre-catalyst was therefore optimized towards a faster and more effective activation, which could finally be accomplished by the development of complexes based on a variety of amine-imine-diphosphine P-N-NH-P hybrid ligands (Scheme17, **Fe16**).⁵³ In contrast to the former bis-imine complexes, these pre-catalysts are activated in a single step obviating the slow reduction of one imine group. The fast activation takes the entire iron complex rapidly into the catalytic cycle, thus affording a much higher effective catalyst loading and a significantly enhanced catalytic performance of the system. Finally, a TOF of more than 540.000 h^{-1} could be observed in the reduction of acetophenone and the corresponding 1-phenylethanol was obtained with 98% ee.

Notably, the related bis-amine complex **Fe20** appeared to be catalytically inactive, demonstrating the significance of the amide/enamide structure in the active species.⁵⁴ Moreover, formation of the corresponding bis-amide intermediate was identified as a major catalyst deactivation pathway, caused



Scheme 18. Mechanism of the iron catalyzed asymmetric transfer hydrogenation including catalyst activation and deactivation pathways.



Scheme 19. Chiral iron-PNNP catalyst for the stereoselective hydrogenation of ketones

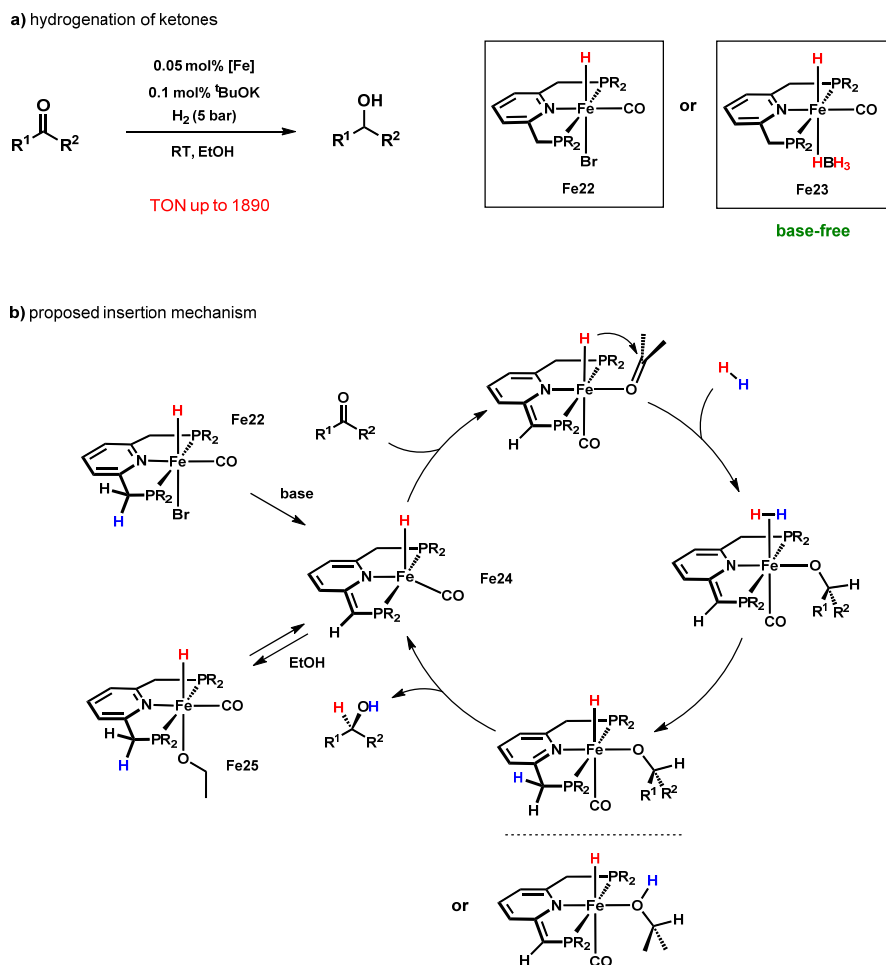
by the reduction of the enamide double bond of **Fe17**. At low base concentration, the active amido/enamido complex might be protonated by ⁱPrOH at the carbon in α -position to the phosphorus donor to give an amido/imine intermediate. Hydride transfer from the alkoxide to the imine, as previously shown for the activation step, irreversibly produces the bis-amide complex **Fe21**. Deactivation is suppressed in presence of excess ^tBuOK as the highest activities were observed in the range of 5 to 8 equivalents in respect to the catalyst.

In addition to their successful application in transfer hydrogenations complex **Fe17** has also been tested in the reduction of carbonyl compounds using hydrogen gas.⁵⁵ Although both the hydrogenation and transfer hydrogenation mostly proceed *via* the same intermediates, the use of dihydrogen instead of ⁱPrOH lead to a significantly lower activity and exhibited only poor enantioselectivity. Kinetic studies as well as a theoretical analysis of the mechanism by DFT-calculations identified the heterolytic cleavage of dihydrogen to be the rate determining step in the catalytic cycle, providing a reasonable explanation for the inferior performance of these catalysts in hydrogenation reactions in comparison to the outstanding activity and selectivity in transfer hydrogenations.

1.4 Hydrido Carbonyl Complexes Supported by PNP-Pincer Type Ligands

As demonstrated by a number of recent publications, iron hydride complexes bearing organophosphorus based PNP-pincer ligands proved to be highly effective and versatile systems for the hydrogenative reduction of carbonyl compounds.

In 2011 the group of *Milstein* reported on the iron(ii) hydrido carbonyl complex **Fe22** which is supported by a pyridine-based PNP pincer-type ligand (Scheme 20).⁵⁶ Upon activation with 2 equivalents of a strong base in ethanol, this complex was found to efficiently catalyze the



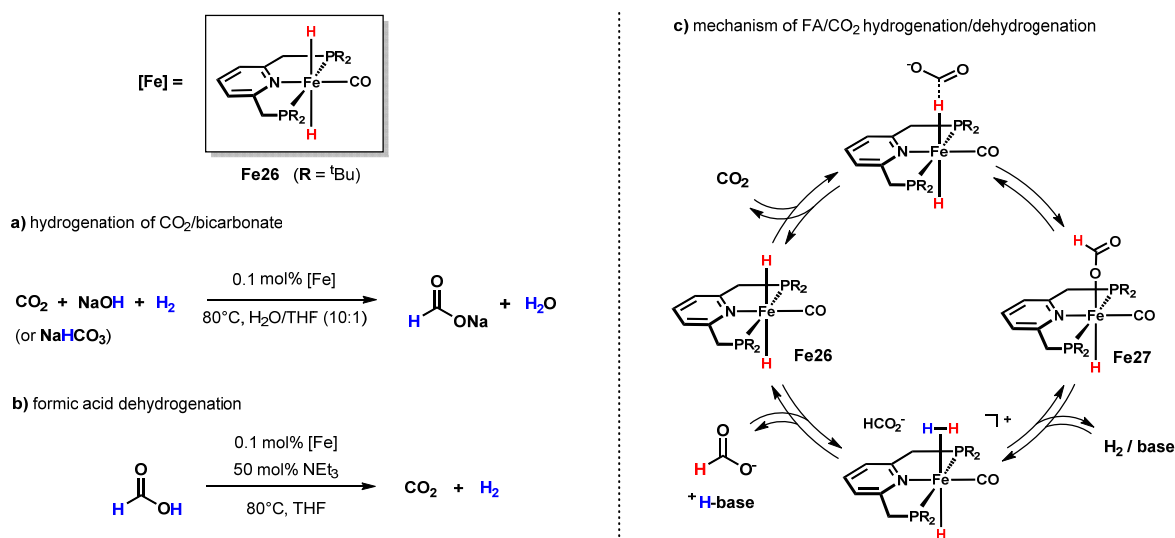
Scheme 20. Hydrogenation of ketones catalyzed by a PNP-supported iron hydrido carbonyl complex

hydrogenation of ketone substrates reaching turnover numbers of more than 1800 under mild conditions (4 bar H_2 , r.t.). Mechanistic studies based on stoichiometric experiments as well as DFT-calculations identified the deprotonated intermediate **Fe24** to be the catalytically active species in the reaction, which is thought to be stabilized by the reversible addition of the solvent alcohol to give the reprotonated hydrido alkoxide complex **Fe25**.⁵⁷ Since **Fe24** represents a formal 16 valence electron complex providing a free coordination site for an incoming substrate, the mechanism is considered to proceed *via* coordination of the ketone prior to its insertion into the metal hydride bond. In principle, two different pathways for the release of the product alcohol and the regeneration the initial intermediate **Fe24** were considered to be feasible. Either dihydrogen is activated by re-aromatization of the ligand followed by elimination of the product, which again leads to a de-aromatized system, or H_2 is directly cleaved between the iron metal center the product alkoxide without re-protonation of the methylene group in the linker. In accordance to the proposed inner-sphere mechanism, substrates containing a nitrile or amine functionality could not be hydrogenated, probably as a result of preferential coordination of these groups. Moreover, α,β -unsaturated ketones gave mixtures due to

partial hydrogenation of the C-C double bond. Noteworthy, the reaction takes place even without the addition of an external strong base by using the hydrido borohydride complex **Fe23**.⁵⁷ Apparently, the stoichiometric amount of a base necessary for catalyst activation might be generated by alcoholysis or by the reaction of the substrate with the free BH_4^- anion which can easily dissociate from the iron metal center.

Only poor catalytic activity was observed in the case of aldehydes, most obviously due to side reactions taking place under basic conditions. However, by employing NEt_3 as additive in the reaction, the efficiency of this system for the hydrogenation of aldehydes could be significantly increased and TONs of up to 4000 were obtained for several substrates, when the reaction was carried out at high pressures (30 bar) and in presence of excess $^t\text{BuOK}$ (cat./base-ratio = 1:25).⁵⁸ Interestingly, enhanced productivity was also observed in the presence of a large excess of acetophenone, which, however, was found to be unaffected during the reaction. Although no further investigations on the chemoselectivity of this catalyst have been provided, it is obvious that an alternative reaction mechanism is operating under these modified conditions. More recently, Hu *et al.* developed a general method for the chemoselective hydrogenation and transfer hydrogenation of aldehydes by using a similar iron(II) pincer complex supported by a 2,6-bis(phosphinito)pyridine ligand.⁵⁹ This reaction takes place under very mild conditions (4-8 bar H_2 , r.t.), albeit high catalyst loadings (5-10 mol%) were required to obtain the primary alcohols in reasonable yields. However, it was remarkable that this reaction did not proceed via a bifunctional mechanism, i.e. involving the pincer ligand.

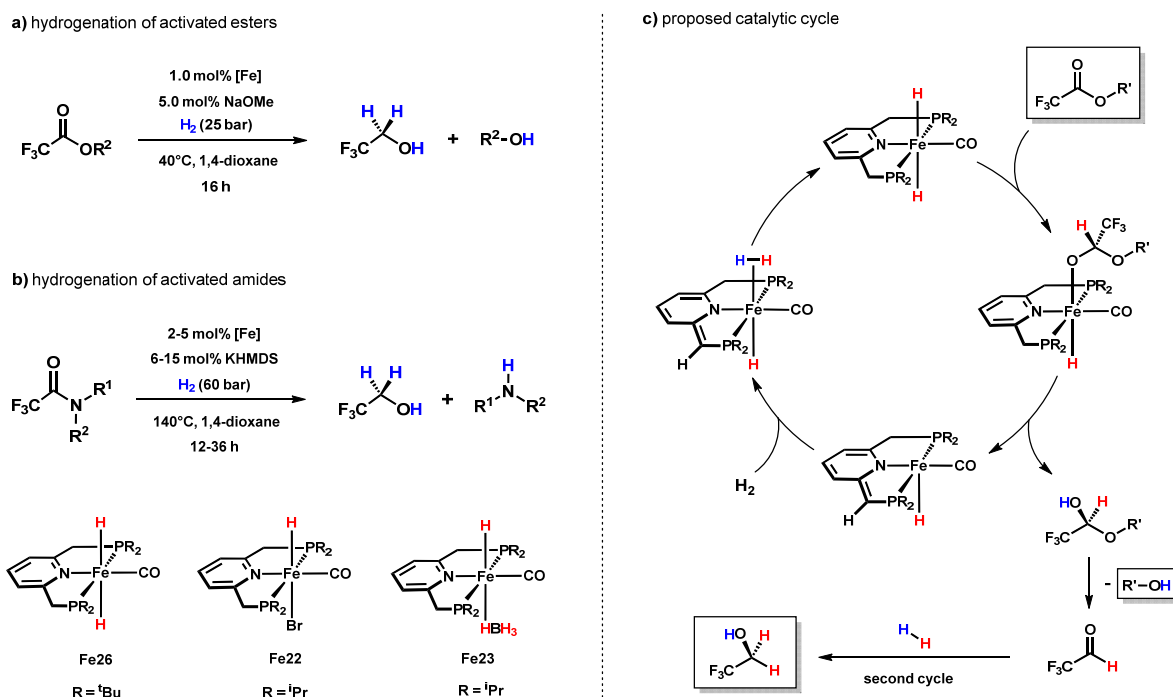
Milstein's group observed the formation of an iron(II) dihydride when complex **Fe26** was activated in presence of dihydrogen in aprotic solvents.⁵⁷ However, it appeared to be catalytically inactive for the reduction of ketones and the instability of this species did not allow for its isolation. In contrast to this, a stable dihydride compound could be obtained when the alkyl residues on the phosphorous were



Scheme 21. Hydrogenation of carbon dioxide and dehydrogenation of formic acid catalyzed by an iron(II) dihydride

replaced by more steric demanding *tert*-butyl groups.⁶⁰ Due to the strong mutual *trans*-influence on each other, it is well-known that transition metal hydrides become much more electrophilic when another H⁻ is located on the opposite position of the metal center. Thus, complex **Fe26** was found to promote the hydrogenation of more nucleophilic reaction partners, which, contrary to the case of ketones, proceeds via an *outer-sphere* attack of the hydride on the carbonyl carbon atom of the substrate.

For example, complex **Fe26** was successfully employed in the hydrogenative reduction of carbon dioxide and sodium bicarbonate to formate salts under low pressure in an aqueous solution of sodium hydroxide.⁶⁰ As revealed by stoichiometric experiments, the reaction of **Fe26** under one atmosphere of CO₂ leads to the immediate formation of the hydrido formate complex **Fe27** indicating an outer sphere attack of one hydride ligand. Replacement of the formate and H₂-coordination followed by a base assisted heterolytic cleavage of dihydrogen appears to be a plausible pathway for the regeneration of the initial dihydride complex. As formal reverse reaction, also the dehydrogenation of formic acid could be accomplished.⁶¹ By using 0.05 mol% of **Fe26** formic acid was quantitatively converted into carbon dioxide and dihydrogen within 3 hours and turnover numbers of up to 100000 could be reached after 10 days demonstrating the long-term stability of this catalyst. However, in contrast to the above mentioned iron(II) tetraphos systems, the presence of triethyl amine was found to be necessary for catalytic turnover. The reaction likely proceeds *via* protonation of **Fe26**, followed by the liberation of dihydrogen and the formation of the hydrido formate complex **Fe27**, which upon a non-classical beta-hydride elimination releases carbon dioxide and regenerates the initial iron(II) dihydride.



Scheme 22. Hydrogenation of activated esters and amides catalyzed by an iron(II) dihydride

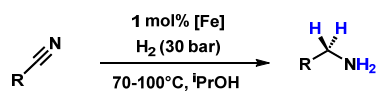
Moreover, the same iron catalyst was used for the reduction of trifluoroacetic esters to alcohols.⁶² Again, nucleophilic attack of the iron hydride to the carbonyl carbon atom probably seems to be the first step in the catalytic cycle. Loss of the resulting hemiacetal might be facilitated by the presence of the base generating a dearomatized species which leads to the recovery of the dihydride complex via addition of dihydrogen through a bifunctional metal-ligand cooperation. Obviously, the hemiacetal is in equilibrium with the corresponding aldehyde which might be reduced following a very similar mechanism. As reported more recently, even the corresponding trifluoro acetic amides could be hydrogenated by using **Fe26** albeit under much harsher reaction conditions had to be applied in these reactions. In this case, also complex **Fe22** and **Fe23** were found to be active, which under the applied condition might also form the corresponding iron(II) dihydride complex upon activation by a strong base or by the loss of BH₃ as dioxane adduct.⁶³

Inspired by the effectiveness of catalysts bearing pyridine-linked PNP-ligands several other research groups started investigations on iron hydrido carbonyl complexes which contain the structurally related aliphatic pincer ligands of the type HN(CH₂CH₂PR₂)₂. In general, replacing the pyridine fragment in the ligand's backbone by a secondary amine group afforded a novel family of catalysts that clearly exhibit enhanced reactivity. Consequently, this improvement not only lead to an extended scope of substrates but even resulted in a wider range of catalytic applications.

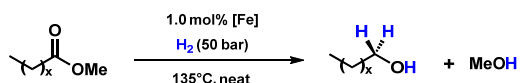
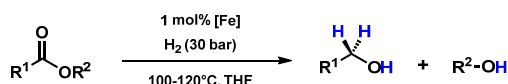
For example, such catalysts are capable for the hydrogenation of various carboxylic acid derivatives including essentially unactivated esters, amides and nitriles while pyridine based catalyst discovered by Milstein and co-workers have been restricted to the hydrogenative cleavage of much more reactive trifluoro acetyl moieties. Serving as catalyst precursors, hydrido borohydride complexes have been employed in these transformations, which generally do not require the presence of base or any other additives to promote catalyst activation or catalytic turnover. In particular, the group of Beller reported on the first iron catalyzed hydrogenation of aryl, alkyl, heterocyclic nitriles and dinitriles.⁶⁴ By using 1 mol% of complex **Fe28** the corresponding amines were obtained in high yields within 3h under optimized reaction conditions (ⁱPrOH, 60-130°C, 30 bar H₂). Shortly afterwards, complex **Fe28** was also found to promote hydrogenation of different esters and lactones to give the corresponding alcohols and diols.⁶⁵ Hydrogenation takes place under very similar conditions (1 mol% cat., THF, 100-120°C, 30 bar), although longer reaction times have been required (6-19h). At the same time, the groups of Guan and Fairweather independently reported on the hydrogenation of esters by using complex **Fe28**.⁶⁶ As demonstrated in their work, this system could even be applied for the transformation of some industrial important fatty acid esters taking place under neat conditions. More recently, several groups used complex **Fe28** for the hydrogenative reduction of various secondary and tertiary amides to afford the corresponding alcohols and amines.⁶⁷⁻⁶⁹

In any case, the iron(ii) *trans*-dihydride **Fe29** has been identified to be the active species, which is formed upon loss of BH₃ from the respective pre-catalysts **Fe28**. As already mentioned, the mutual *trans*-effect of the two hydride ligands leads to an elongation of the M-H bonds and thus significantly increases hydricity of this species. However, the improved activity in comparison to *Milstein's trans*-

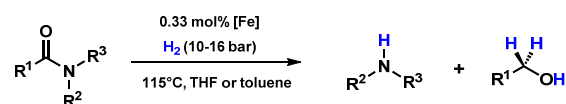
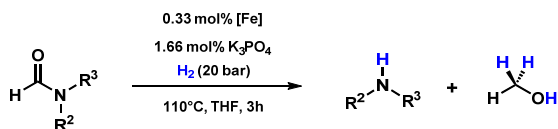
a) hydrogenation of nitriles to amines (Beller 2014)



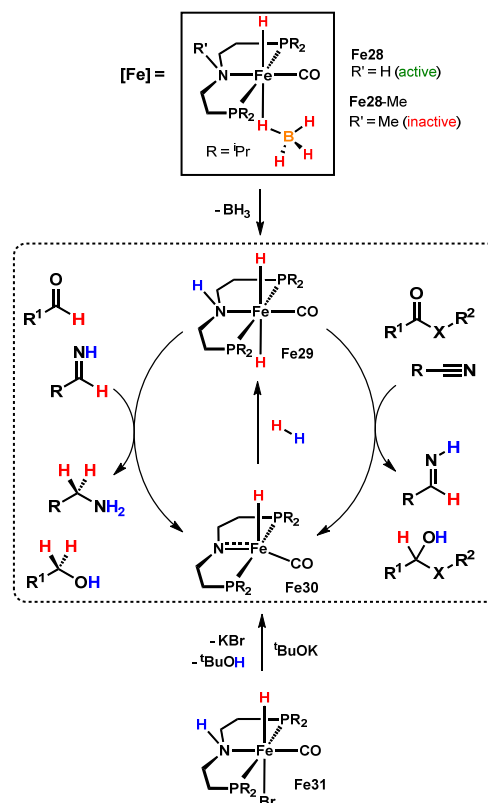
b) hydrogenation of esters to alcohols (Beller 2014 and Guan/Fairweather 2014)



c) hydrogenation of amides to alcohols and amines (Sanford 2016)



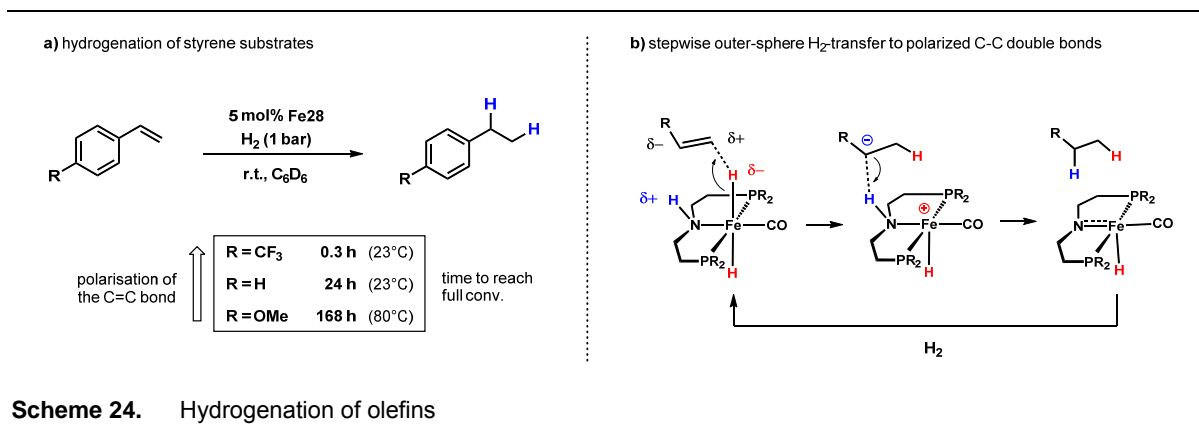
d) catalyst activation and proposed catalytic cycle



Scheme 23. Hydrogenation of carboxylic acid derivatives catalyzed by bifunctional aliphatic PNP hydrido carbonyl complexes

dihydride catalysts might be attributed to the fact that a secondary amine is directly bound to the iron metal center, thus arranging the NH proton and the hydride in a vicinal position. Hence, the two sites being adjacent and electronically coupled facilitate an outer sphere hydrogen (H^+ and H^-) transfer from the catalyst to the substrate.⁷⁰ Moreover, the remaining 16 valence electron complex is efficiently stabilized by the deprotonated nitrogen atom, which, as a strong π -donor bound to the metal, partially compensates its unsaturation. On the one hand, this assumption is supported by the fact that the related complex **Fe28-Me**, in which the amine proton was replaced by a methyl group, was found to be catalytically inactive.^{64,65} On the other hand, stoichiometric experiments indeed confirmed the formation of the five coordinated amido complex **Fe30** resulting from the reaction of the iron dihydride with the substrate. This complex, also accessible by the dehydrohalogenation of **Fe31** in presence of a strong base, could even be isolated, characterized and directly employed into reactions.^{71,72}

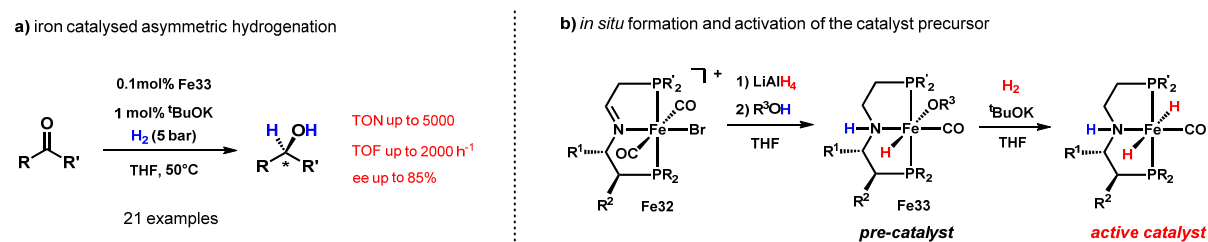
Notably, the *trans*-dihydride complex **Fe29** is even capable for the reduction of polarized C-C double bonds. This was already observed by *Beller*, *Guan* and *Fairweather* within their work on the hydrogenative reduction of esters, since methyl cinnamate was exclusively converted into the fully saturated alcohol whereas isolated C-C double bonds remained unaffected.^{65,66} More extensive



Scheme 24. Hydrogenation of olefins

studies have been reported by the group of *Williams*.⁷³ Test reactions carried out on an NMR scale using rather high catalyst loadings (5 mol% of **Fe28**) under 1 atm hydrogen pressure revealed that the tendency of this system for the hydrogenation of olefins strongly depends on the electronic properties of the C-C double bond, which was illustrated by employing different styrene derivatives in the reaction containing either electron withdrawing or donating functional groups in the 4-position of the substrate (Scheme 24a). For example, while 4-CF₃-styrene was quantitatively reduced to the corresponding ethylbenzene at room temperature within 20 minutes, the *para*-methoxy derivative required 7 days at 60°C to reach full conversion. Hydrogenation of nonpolar aliphatic alkenes has not been observed. Based on DFT-calculation, the reduction of polarized C-C double bonds presumably proceeds *via* a stepwise hydride/proton transfer from **Fe29** to the substrate involving metal-ligand cooperation (Scheme 24b).

Structural modifications of this catalyst could be accomplished as well. Apart from variations of the alkyl substituents on the phosphorous donors, even changes in ligand backbone have been reported. For example, *Morris et al.* developed catalysts for the asymmetric hydrogenation of polar double bonds by employing iron(II) catalysts bearing chiral PNP-ligands (Scheme 24).⁷⁴ Imine pincer complexes of the type [Fe(P-N-P')(CO)₂(Br)]BF₄ (**Fe32**) containing one chiral substituted ethylene linker and two different phosphorous donors could be prepared *via* an iron mediated template synthesis. The iron hydride pre-catalysts of the general formula [Fe(PNP)(H)(CO)(OR)] (**Fe33**) are formed *in-situ* as a mixture of isomers when the chiral dicarbonyl complexes **Fe32** are treated with

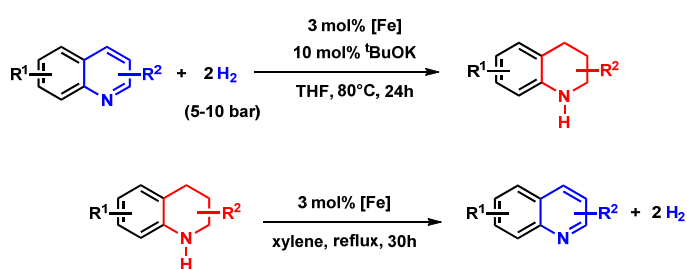


Scheme 24. Asymmetric hydrogenation of ketones

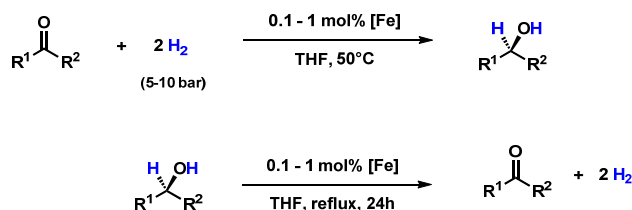
lithium aluminum hydride in THF followed by addition of an alcohol. With this system TOFs up to 2000 h⁻¹, TONs up to 5000, and enantioselectivities up to 85% could be obtained for a variety of pro-chiral ketone substrates. NMR-experiments revealed the formation of the corresponding dihydride complex when **Fe33** is treated with a strong base under an atmosphere of dihydrogen.⁷⁵ It should be mentioned that this system is only active in presence of excess ^tBuOK. As proposed by the authors, ^tBuOK might be essential for the generation of the respective amido complex from the otherwise more stable alkoxide complexes.

Another distinct characteristic has been discovered as the addition of dihydrogen to the five coordinated amido complex **Fe30** was found to be reversible. In particular, the dihydride complex **Fe29** can easily eliminate H₂ to form **Fe30** again. As a consequence, such catalysts are not only capable for hydrogenations but also allow for the reverse dehydrogenation of various substrates under liberation of molecular hydrogen. Since H₂ is the only side product of such reaction avoiding the production of any waste, this property constitutes a great advantage over other iron-based systems which require hydrogen acceptors.

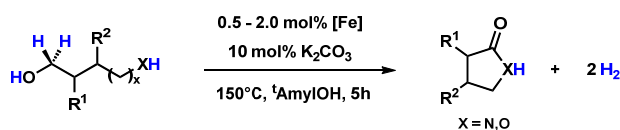
a) (de)hydrogenation of N-heterocyclic substrates (*Jones 2014*)



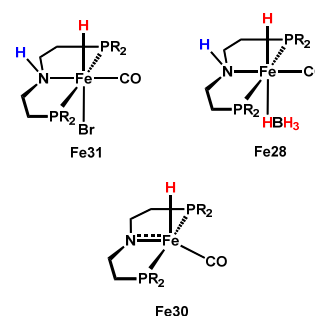
b) (de)hydrogenation of carbonyl/alcohol substrates (*Schneider/Jones 2014*)



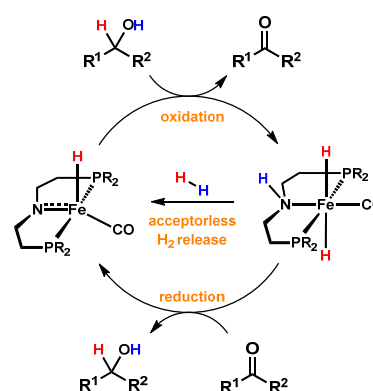
c) formation of lactones/lactams (*Beller 2015*)



d) complexes used for these transformations



e) reversible activation/liberation of H₂



Scheme 25. Application of bifunctional PNP hydrido carbonyl catalysts in hydrogenation- and dehydrogenation-reactions

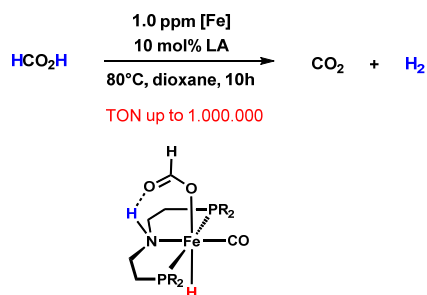
For example, *Jones et al.* reported on the reversible hydrogenation/dehydrogenation of N-heterocycles.⁷² On the one side, several secondary cyclic amines including tetrahydroquinoline, 2-methylindoline and 2,6-dimethylpiperidine could successfully be oxidized by using 3 mol% of **Fe28** in refluxing toluene. Running the reaction for 30 hours afforded the corresponding products in reasonable yields. Most feasible, the reaction proceeds via the initial dehydrogenation of the secondary amine fragment followed by isomerization of the resulting C-N to a C-C double bond. The partially oxidized amine is finally converted into the fully unsaturated product by undergoing a second dehydrogenation step. On the other hand, under a hydrogen pressure of only 5-10 bar and in presence of 3 mol% of **Fe31** together with 10 mol% ^tBuOK the unsaturated substrates could be converted back to the reduced tetra hydro analogues.

In a joined publication, the groups of *Schneider, Hazari* and *Jones* described the reversible hydrogenation and dehydrogenation of alcohols and the corresponding carbonyl compounds.⁷⁶ The hydrogenation of ketones could be accomplished with catalyst loading down to 0.05 mol% for some substrates which were quantitatively reduced to the corresponding secondary alcohols under mild conditions (50°C, 5 bar H₂). In contrast to *Morris'* system, the presence a base was not necessary for the reaction to take place. In reverse, alcohol dehydrogenation occurred under reflux conditions in presence of 0.1-1 mol% of **Fe28**. Secondary alcohols were efficiently converted into ketones while primary and diol substrates afforded the corresponding esters and lactones. Based on these studies, *Beller et al.* developed a general protocol for the production of lactones and lactams by using the catalytic dehydrogenation methodology.⁷⁷ A typical reaction was performed in a sealed reaction vessel at 150°C using 0.5 mol% of **Fe28** and 10 mol% of K₂CO₃ in ^tAmylOH. The presence of a base is not essential for the reaction to occur but resulted in an increased efficiency of the process, most obviously by facilitating the cyclisation step. This procedure allowed for the synthesis of a broad scoped of heterocyclic compounds from the corresponding 1,n-diols and 1,n-amino alcohols in good to excellent yields.

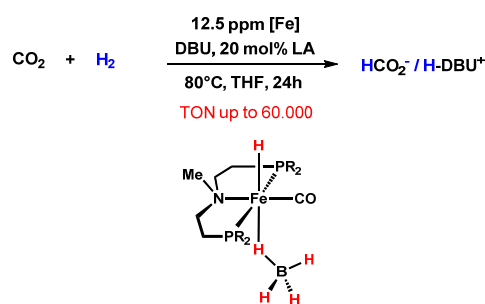
Apart from the synthetic applications, the dehydrogenation of small is of particular interest, since such substrates are considered as potential targets for chemical hydrogen storage.

Within this context, *Schneider, Hazari* and co-workers reported on the production of dihydrogen via the catalytic decomposition of formic acid.⁷¹ They predominantly used the isolated hydrido formate complex **Fe34**, which could be prepared by the reaction of formic acid with the amido complex **Fe30**. Initial test reactions carried out in presence of 0.1 mol% of **Fe34** and 50 mol% of triethyl amine at 80°C in dioxane gave comparable results to the iron based systems reported by the groups of *Milstein* and *Beller*. However, it was found that the catalytic activity significantly increases in presence of simple Lewis acid co-catalyst such as Li⁺, obviating the use of an additional base. In particular, a TON of nearly 1.000.000 and a TOF of approximately 200.000 could be reached by using only 1.0 ppm of the isolated hydrido formate in presence of 10 mol% of LiBF₄. Based on stoichiometric studies, **Fe29** and **Fe34** were identified as the key intermediates in this reaction, strongly resembling the mechanism previously proposed by *Milstein* for the related pyridine-based catalysts **Fe26**.⁶¹ In contrast to the

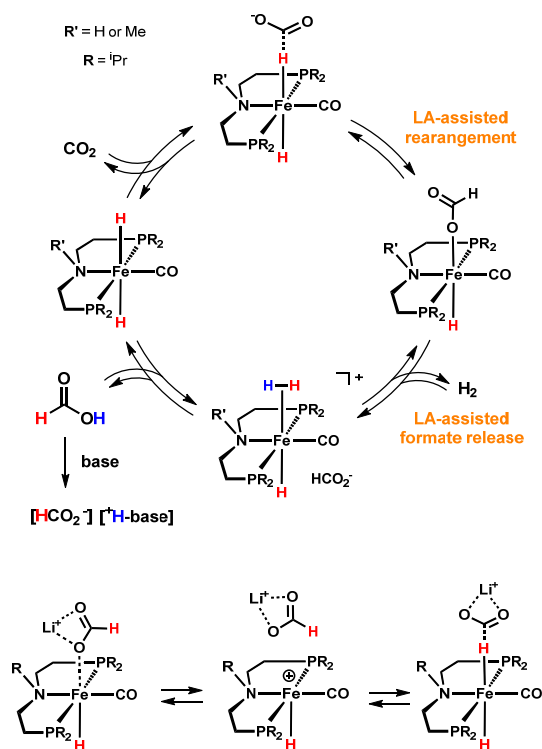
a) formic acid dehydrogenation (Schneider / Hazari 2014)



b) hydrogenation of carbon dioxide (Bernskoetter / Hazari 2015)



c) catalytic cycle for hydrogenation/dehydrogenation of CO₂/FA



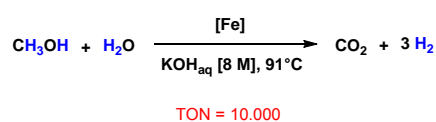
Scheme 26. Hydrogenation/dehydrogenation of CO₂/FA in presence of a Lewis-acid co-catalyst

dehydrogenation of alcohols and amines, this reaction does not involve metal-ligand cooperation. Decarboxylation of the iron formate intermediate is considered to be the rate determining step of the reaction. Since there is no vacant coordination site available on the metal, this formal β -hydride elimination presumably proceeds *via* an intermolecular rearrangement to an H-bound formate followed by the liberation of CO₂. However, the lithium cation was found to facilitate this process by stabilizing the negatively charged carboxylate group of the H-bound intermediate, thus being responsible for the greatly enhanced catalytic performance in presence of Lewis acid co-catalysts.

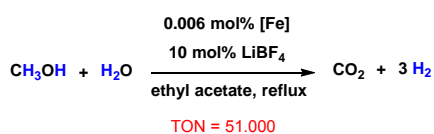
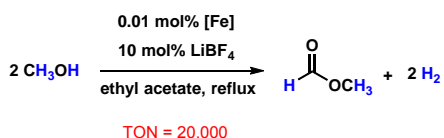
As subsequently reported by the groups of Bernskoetter and Hazari, the beneficial effect of Lewis acid co-catalysts on the catalytic activity of this system was also found to take place in the reverse process of CO₂ hydrogenation.⁷⁸ For example, without any additive a TON of 880 was obtained after 24 hours at catalyst loading of 0.02 mol%, which increased to more than 3000 in presence of LiOTf under otherwise identical conditions. Also complexes supported by the related amino methyl ligand were found to be active, further demonstrating that this reaction does not rely on a cooperative interaction between the NH group and the metal hydride. Surprisingly, these catalysts are significantly more effective for the hydrogenation of carbon dioxide, achieving turnover numbers of nearly 60.000 within 24 hours.

Already in 2013, *Beller et al.* found complexes **Fe28** and **Fe31** to be catalytically active for the production of dihydrogen through methanol dehydrogenation.⁷⁹ Carried out in an aqueous solution of sodium hydroxide at 91°C, TONs of up to 10.000 could be reached within 2 days. Both formate and carbonate/bicarbonate ions were observed by NMR spectroscopy, indicating that dehydrogenation of methanol proceeds beyond the stage of formaldehyde to formate and further to CO₂ which is trapped as carbonate under the basic conditions employed. In particular, the reaction likely proceeds *via* three sequential dehydrogenation steps. First, methanol gets oxidized to formaldehyde which, in presence of water, forms methanediol. In a second dehydrogenation step, this intermediate is converted to formic acid which finally decomposes to yield carbon dioxide and a third equivalent of H₂. More recently, *Bernskoetter, Holthausen* and *Hazari* re-examined the dehydrogenation of methanol by studying the effect of Lewis acid additives on the reaction.⁸⁰ As the last step of this dehydrogenation sequence involves the decarboxylation of a formate ion, an increase of catalytic activity could also be accomplished in this case. In contrast to the conditions applied by *Beller*, reactions were performed in absence of a base giving best results with ethyl acetate as the solvent. By using a 4:1 mixture of methanol and water in presence of 0.006 mol% of **Fe30** together with 10 mol% of LiBF₄ hydrogen production took place reaching turnover numbers of more than 50.000 after 4 days. In comparison, a reaction carried out at a catalyst loading of 0.5 mol% but without the addition of an additive yielded methyl formate as the major product, indicating that complete dehydrogenation to CO₂ is not occurring. Moreover, the hydrido formate **Fe34** was observed as the major iron containing species at the end of the reaction, apparently because decarboxylation is prevented in absence of the co-catalyst.

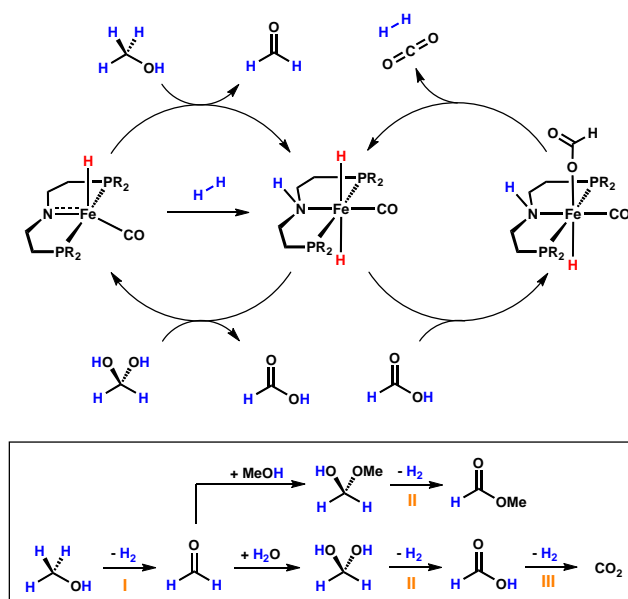
a) methanol dehydrogenation (*Beller 2013*)



a) LA assisted MeOH dehyd. (*Bernskoetter / Hazari 2015*)



c) two catalytic cycles involved in MeOH dehydrogenation



Scheme 27. Hydrogen production through the catalytic dehydrogenation of methanol

1.5 Conclusions and Perspectives

In conclusion, we described the development of some distinct families of well-defined iron-based catalysts that are active in a variety of hydrogenation and dehydrogenation reactions. These successful examples originated from the discovery of somehow privileged metal-ligand platforms that can efficiently support and stabilize the iron metal center or even participate in elementary steps of the reaction. The key aspects in the development of these catalysts have been the recognition of decisive structural features as well as the determination and optimization of proper reaction conditions that permit catalytic turnover. Moreover, mechanistic insights including catalyst activation and the identification of the reactive species revealed specific similarities and differences between the described systems. These catalysts already cover a broad scope of catalytic applications in some cases exhibiting activities and productivities that are competitive to well-established noble metal catalysts. However, the current knowledge about the nature and characteristics of active iron-based systems paved the way for conceptually and mechanistically well-founded research, which might lead to further developments and the discovery of novel catalyst extending the current scope and limitations of reactivity.

1.6 Reverences

- (1) Hartwig, J. F. *Organotransition Metal Chemistry: From Bonding to Catalysis*; University Science Books: Sausalito, Calif, 2010.
- (2) *Microbial Iron Metabolism: A Comprehensive Treatise*; Neilands, J. B., Ed.; Academic Press: New York, 1974.
- (3) *Catalysis without Precious Metals*; Bullock, R. M., Ed.; Wiley-VCH: Weinheim, 2010.
- (4) Benito-Garagorri, D.; Lagoja, I.; Veiros, L. F.; Kirchner, K. a. Reactivity of Coordinatively Unsaturated Iron Complexes towards Carbon Monoxide: To Bind or Not to Bind? *Dalton Trans.* **2011**, *40*, 4778–4792.
- (5) Bauer, I.; Knölker, H.-J. Iron Catalysis in Organic Synthesis. *Chem. Rev.* **2015**, *115*, 3170–3387.
- (6) *The Handbook of Homogeneous Hydrogenation*; de Vries, J. G., Elsevier, C. J., Eds.; Wiley-VCH Verlag GmbH: Weinheim, Germany, 2006.
- (7) Eberle, U.; Felderhoff, M.; Schüth, F. Chemical and Physical Solutions for Hydrogen Storage. *Angew. Chemie Int. Ed.* **2009**, *48*, 6608–6630.
- (8) Zell, T.; Langer, R. Iron-Catalyzed Hydrogenation and Dehydrogenation Reactions with Relevance to Reversible Hydrogen Storage Applications. *Recycl. Catal.* **2016**, *2*, 87–109.

- (9) Bianchini Claudio; Andrea Mell, Maurizio Peruzzini, F. V.; Zanobini, F. A Homogeneous Iron(II) System Capable of Selectively Catalyzing the Reduction of Terminal Alkynes to Alkenes and Buta-1,3-Dienes. *Organometallics* **1989**, *8*, 2080–2082.
- (10) Bianchini, C.; Meli, A.; Peruzzini, M.; Frediani, P.; Bohanna, C.; Esteruelas, M.; Oro, L. Selective Hydrogenation of 1-Alkynes To Alkenes Catalyzed By an Iron(II) Cis-Hydride η^2 -Dihydrogen Complex - a Case of Intramolecular Reaction Between η^2 -H₂ and σ -Vinyl Ligands. *Organometallics* **1992**, *11*, 138–145.
- (11) Bianchini, C.; Farnetti, E.; Graziani, M.; Peruzzini, M.; Polo, A. Chemoselective Hydrogen-Transfer Reduction of α,β -Unsaturated Ketones Catalyzed By Isostructural Iron(II), Ruthenium(II), and Osmium(II) Cis-Hydride η^2 -Dihydrogen Complexes. *Organometallics* **1993**, *12*, 3753–3761.
- (12) Federsel, C.; Boddien, A.; Jackstell, R.; Jennerjahn, R.; Dyson, P. J.; Scopelliti, R.; Laurency, G.; Beller, M. A Well-Defined Iron Catalyst for the Reduction of Bicarbonates and Carbon Dioxide to Formates, Alkyl Formates, and Formamides. *Angew. Chemie Int. Ed.* **2010**, *49*, 9777–9780.
- (13) Boddien, A.; Mellmann, D.; Gärtner, F.; Jackstell, R.; Junge, H.; Dyson, P. J.; Laurency, G.; Ludwig, R.; Beller, M. Efficient Dehydrogenation of Formic Acid Using an Iron Catalyst. *Science* **2011**, *333*, 1733–1736.
- (14) Ziebart, C.; Federsel, C.; Anbarasan, P.; Jackstell, R.; Baumann, W.; Spannenberg, A.; Beller, M. Well-Defined Iron Catalyst for Improved Hydrogenation of Carbon Dioxide and Bicarbonate. *J. Am. Chem. Soc.* **2012**, *134*, 20701–20704.
- (15) Mellmann, D.; Barsch, E.; Bauer, M.; Grabow, K.; Boddien, A.; Kammer, A.; Sponholz, P.; Bentrup, U.; Jackstell, R.; Junge, H.; Laurency, G.; Ludwig, R.; Beller, M. Base-Free Non-Noble-Metal-Catalyzed Hydrogen Generation from Formic Acid: Scope and Mechanistic Insights. *Chem. Eur. J.* **2014**, *20*, 13589–13602.
- (16) Mellmann, D.; Sponholz, P.; Junge, H.; Beller, M. Formic Acid as a Hydrogen Storage Material – Development of Homogeneous Catalysts for Selective Hydrogen Release. *Chem. Soc. Rev.* **2016**, *45*, 3954–3988.
- (17) Sánchez-De-Armas, R.; Xue, L.; Ahlquist, M. S. G. One Site Is Enough: A Theoretical Investigation of Iron-Catalyzed Dehydrogenation of Formic Acid. *Chem. Eur. J.* **2013**, *19*, 11869–11873.
- (18) Yang, L.; Wang, H.; Zhang, N.; Hong, S. The Reduction of Carbon Dioxide in Iron Biocatalyst Catalytic Hydrogenation Reaction: A Theoretical Study. *Dalt. Trans.* **2013**, *42*, 11186–11193.

- (19) Yang, X. Mechanistic Insights into Iron Catalyzed Dehydrogenation of Formic Acid: β -Hydride Elimination vs. Direct Hydride Transfer. *Dalton Trans.* **2013**, 2, 2–6.
- (20) Marcos, R.; Xue, L.; Sánchez-De-Armas, R.; Ahlquist, M. S. G. Bicarbonate Hydrogenation Catalyzed by Iron: How the Choice of Solvent Can Reverse the Reaction. *ACS Catal.* **2016**, 6, 2923–2929.
- (21) Wienhöfer, G.; Sorribes, I.; Boddien, A.; Westerhaus, F.; Junge, K.; Junge, H.; Llusar, R.; Beller, M. General and Selective Iron-Catalyzed Transfer Hydrogenation of Nitroarenes without Base. *J. Am. Chem. Soc.* **2011**, 133, 12875–12879.
- (22) Wienhöfer, G.; Westerhaus, F. a; Jagadeesh, R. V; Junge, K.; Junge, H.; Beller, M. Selective Iron-Catalyzed Transfer Hydrogenation of Terminal Alkynes. *Chem. Commun.* **2012**, 48, 4827–4829.
- (23) Wienhöfer, G.; Westerhaus, F. A.; Junge, K.; Beller, M. Fast and Selective Iron-Catalyzed Transfer Hydrogenations of Aldehydes. *J. Organomet. Chem.* **2013**, 744, 156–159.
- (24) Wienhöfer, G.; Baseda-Krüger, M.; Ziebart, C.; Westerhaus, F. a; Baumann, W.; Jackstell, R.; Junge, K.; Beller, M. Hydrogenation of Nitroarenes Using Defined Iron-Phosphine Catalysts. *Chem. Commun.* **2013**, 49, 9089–9091.
- (25) Wienhöfer, G.; Westerhaus, F. A.; Junge, K.; Ludwig, R.; Beller, M. A Molecularly Defined Iron-Catalyst for the Selective Hydrogenation of α,β -Unsaturated Aldehydes. *Chem. Eur. J.* **2013**, 19, 7701–7707.
- (26) Bart, S. C.; Lobkovsky, E.; Chirik, P. J. Preparation and Molecular and Electronic Structures of iron(0) Dinitrogen and Silane Complexes and Their Application to Catalytic Hydrogenation and Hydrosilation. *J. Am. Chem. Soc.* **2004**, 126, 13794–13807.
- (27) Stieber, S. C. E.; Milsman, C.; Hoyt, J. M.; Turner, Z. R.; Finkelstein, K. D.; Wieghardt, K.; Debeer, S.; Chirik, P. J. Bis(imino)pyridine Iron Dinitrogen Compounds Revisited: Differences in Electronic Structure between Four- and Five-Coordinate Derivatives. *Inorg. Chem.* **2012**, 51, 3770–3785.
- (28) Trovitch, R. J.; Lobkovsky, E.; Bill, E.; Chirik, P. J. Functional Group Tolerance and Substrate Scope in Bis(imino)pyridine Iron Catalyzed Alkene Hydrogenation. *Organometallics* **2008**, 27, 1470–1478.
- (29) Yu, R. P.; Darmon, J. M.; Hoyt, J. M.; Margulieux, G. W.; Turner, Z. R.; Chirik, P. J. High-Activity Iron Catalysts for the Hydrogenation of Hindered, Unfunctionalized Alkenes. *ACS Catal.* **2012**, 2, 1760–1764.
- (30) Russell, S. K.; Darmon, J. M.; Lobkovsky, E.; Chirik, P. J. Synthesis of Aryl-Substituted

Bis(imino) Pyridine Iron Dinitrogen Complexes. *Inorg. Chem.* **2010**, *49*, 2782–2792.

- (31) Darmon, J. M.; Turner, Z. R.; Lobkovsky, E.; Chirik, P. J. Electronic Effects in 4-Substituted Bis(imino)pyridines and the Corresponding Reduced Iron Compounds. *Organometallics* **2012**, *31*, 2275–2285.
- (32) Danopoulos, A.; Wright, J.; Motherwell, W. B. Molecular N₂ Complexes of Iron Stabilised by N-Heterocyclic “Pincer” Dicarbene Ligands. *Chem. Commun.* **2005**, *6*, 784–786.
- (33) Darmon, J. M.; Yu, R. P.; Semproni, S. P.; Turner, Z. R.; Stieber, S. C. E.; Debeer, S.; Chirik, P. J. Electronic Structure Determination of Pyridine N-Heterocyclic Carbene Iron Dinitrogen Complexes and Neutral Ligand Derivatives. *Organometallics* **2014**, *33*, 5423–5433.
- (34) Yu, R. P.; Hesk, D.; Rivera, N.; Pelczer, I.; Chirik, P. J. Iron-Catalyzed Tritiation of Pharmaceuticals. *Nature* **2016**, *529*, 195–199.
- (35) Nilsson, G. N.; Kerr, W. J. The Development and Use of Novel Iridium Complexes as Catalysts for Ortho-Directed Hydrogen Isotope Exchange Reactions. *J. Label. Compd. Radiopharm.* **2010**, *53*, 662–667.
- (36) Knölker, H.-J.; Baum, E.; Goesmann, H.; Klauss, R. Demetalation of Tricarbonyl(cyclopentadienone)iron Complexes Initiated by a Ligand Exchange Reaction with NaOH – X-Ray Analysis of a Complex with Nearly Square-Planar Coordinated Sodium. *Angew. Chemie Int. Ed.* **1999**, *38*, 2064–2066.
- (37) Casey, C. P.; Hairong, G. An Efficient and Chemoselective Iron Catalyst for the Hydrogenation of Ketones. *J. Am. Chem. Soc.* **2007**, *129*, 5816–5817.
- (38) Casey, C. P.; Guan, H. Cyclopentadienone Iron Alcohol Complexes: Synthesis, Reactivity, and Implications for the Mechanism of Iron-Catalyzed Hydrogenation of Aldehydes. *J. Am. Chem. Soc.* **2009**, *131*, 2499–2507.
- (39) Coleman, M. G.; Brown, A. N.; Bolton, B. A.; Guan, H. Iron-Catalyzed Oppenauer-Type Oxidation of Alcohols. *Adv. Synth. Catal.* **2010**, *352*, 967–970.
- (40) Plank, T. N.; Drake, J. L.; Kim, D. K.; Funk, T. W. Air-Stable, Nitrile-Ligated (Cyclopentadienone)iron Dicarbonyl Compounds as Transfer Reduction and Oxidation Catalysts. *Adv. Synth. Catal.* **2012**, *354*, 597–601.
- (41) Moyer, S. A.; Funk, T. W. Air-Stable Iron Catalyst for the Oppenauer-Type Oxidation of Alcohols. *Tetrahedron Lett.* **2010**, *51*, 5430–5433.
- (42) Fleischer, S.; Zhou, S.; Junge, K.; Beller, M. General and Highly Efficient Iron-Catalyzed Hydrogenation of Aldehydes, Ketones, and α,β -Unsaturated Aldehydes. *Angew. Chemie Int.*

Ed. **2013**, *52*, 5120–5124.

- (43) Tlili, A.; Schranck, J.; Neumann, H.; Beller, M. Discrete Iron Complexes for the Selective Catalytic Reduction of Aromatic, Aliphatic, and α,β -Unsaturated Aldehydes under Water-Gas Shift Conditions. *Chem. Eur. J.* **2012**, 1–6.
- (44) Zhou, S.; Fleischer, S.; Junge, K.; Beller, M. Cooperative Transition-Metal and Chiral Brønsted Acid Catalysis: Enantioselective Hydrogenation of Imines to Form Amines. *Angew. Chemie Int. Ed.* **2011**, *50*, 5120–5124.
- (45) Pagnoux-Ozherelyeva, A.; Pannetier, N.; Mbaye, M. D.; Gaillard, S.; Renaud, J. L. Knölker's Iron Complex: An Efficient in Situ Generated Catalyst for Reductive Amination of Alkyl Aldehydes and Amines. *Angew. Chemie Int. Ed.* **2012**, *51*, 4976–4980.
- (46) Yan, T.; Feringa, B. L.; Barta, K. Iron Catalyzed Direct Alkylation of Amines with Alcohols. *Nat. Commun.* **2014**, *5*, 5602.
- (47) Sues, P. E.; Demmans, K. Z.; Morris, R. H. Rational Development of Iron Catalysts for Asymmetric Transfer Hydrogenation. *Dalt. Trans* **2014**, *43*, 7650–7667.
- (48) Sui-Seng, C.; Freutel, F.; Lough, A. J.; Morris, R. H. Highly Efficient Catalyst Systems Using Iron Complexes with a Tetradentate PNNP Ligand for the Asymmetric Hydrogenation of Polar Bonds. *Angew. Chemie - Int. Ed.* **2008**, *47*, 940–943.
- (49) Sonnenberg, J. F.; Coombs, N.; Dube, P. A.; Morris, R. H. Iron Nanoparticles Catalyzing the Asymmetric Transfer Hydrogenation of Ketones. *J. Am. Chem. Soc.* **2012**, *134*, 5893–5899.
- (50) Mikhailine, A.; Lough, A. J.; Morris, R. H. Efficient Asymmetric Transfer Hydrogenation of Ketones Catalyzed by an Iron Complex Containing a P - N - N - P Tetradentate Ligand Formed by Template Synthesis. **2009**, *260*, 1394–1395.
- (51) Mikhailine, A. A.; Maishan, M. I.; Lough, A. J.; Morris, R. H. The Mechanism of Efficient Asymmetric Transfer Hydrogenation of Acetophenone Using an Iron(II) Complex Containing an (S,S)-Ph₂PCH₂CH=NCHPhCHPhN=CHCH₂PPh₂ Ligand: Partial Ligand Reduction Is the Key. *J. Am. Chem. Soc.*, 2012, *134*, 12266–12280.
- (52) Prokopchuk, D. E.; Morris, R. H. Inner-Sphere Activation, Outer-Sphere Catalysis: Theoretical Study on the Mechanism of Transfer Hydrogenation of Ketones Using iron(II) PNNP Eneamido Complexes. *Organometallics* **2012**, *31*, 7375–7385.
- (53) Zuo, W.; Lough, A. J.; Li, Y. F.; Morris, R. H. Amine(imine)diphosphine Iron Catalysts for Asymmetric Transfer Hydrogenation of Ketones and Imines. *Science* **2013**, *342*, 1080–1083.
- (54) Zuo, W.; Prokopchuk, D. E.; Lough, A. J.; Morris, R. H. Details of the Mechanism of the

- Asymmetric Transfer Hydrogenation of Acetophenone Using the Amine(imine)diphosphine Iron Precatalyst: The Base Effect and the Enantiodetermining Step. *ACS Catal.* **2016**, *6*, 301–314.
- (55) Zuo, W.; Tauer, S.; Prokopchuk, D.; Morris, R. Catalysts Containing Amine (Imine) Diphosphine P-NH-NP Ligands Catalyze Both the Asymmetric Hydrogenation and Asymmetric Transfer Hydrogenation of Ketones. *Organometallics* **2014**, *33*, 5791–5801.
- (56) Langer, R.; Leitus, G.; Ben-David, Y.; Milstein, D. Efficient Hydrogenation of Ketones Catalyzed by an Iron Pincer Complex. *Angew. Chemie Int. Ed.* **2011**, *50*, 2120–2124.
- (57) Langer, R.; Iron, M. A.; Konstantinovski, L.; Diskin-Posner, Y.; Leitus, G.; Ben-David, Y.; Milstein, D. Iron Borohydride Pincer Complexes for the Efficient Hydrogenation of Ketones under Mild, Base-Free Conditions: Synthesis and Mechanistic Insight. *Chem. Eur. J.* **2012**, *18*, 7196–7209.
- (58) Zell, T.; Ben-David, Y.; Milstein, D. Highly Efficient, General Hydrogenation of Aldehydes Catalyzed by PNP Iron Pincer Complexes. *Catal. Sci. Technol.* **2015**, *5*, 822–826.
- (59) Mazza, S.; Scopelliti, R.; Hu, X. Chemoselective Hydrogenation and Transfer Hydrogenation of Aldehydes Catalyzed by Iron(II) PONOP Pincer Complexes. *Organometallics* **2015**, *34*, 1538–1545.
- (60) Langer, R.; Diskin-Posner, Y.; Leitus, G.; Shimon, L. J. W.; Ben-David, Y.; Milstein, D. Low-Pressure Hydrogenation of Carbon Dioxide Catalyzed by an Iron Pincer Complex Exhibiting Noble Metal Activity. *Angew. Chemie Int. Ed.* **2011**, *50*, 9948–9952.
- (61) Zell, T.; Butschke, B.; Ben-David, Y.; Milstein, D. Efficient Hydrogen Liberation from Formic Acid Catalyzed by a Well-Defined Iron Pincer Complex under Mild Conditions. *Chem. Eur. J.* **2013**, *19*, 8068–8072.
- (62) Zell, T.; Ben-David, Y.; Milstein, D. Unprecedented Iron-Catalyzed Ester Hydrogenation. Mild, Selective, and Efficient Hydrogenation of Trifluoroacetic Esters to Alcohols Catalyzed by an Iron Pincer Complex. *Angew. Chemie Int. Ed.* **2014**, *53*, 4685–4689.
- (63) Garg, J. A.; Chakraborty, S.; Ben-David, Y.; Milstein, D. Unprecedented Iron-Catalyzed Selective Hydrogenation of Activated Amides to Amines and Alcohols. *Chem. Commun.* **2016**, *52*, 5285–5288.
- (64) Bornschein, C.; Werkmeister, S.; Wendt, B.; Jiao, H.; Alberico, E.; Baumann, W.; Junge, H.; Junge, K.; Beller, M. Mild and Selective Hydrogenation of Aromatic and Aliphatic (Di)nitriles with a Well-Defined Iron Pincer Complex. *Nat. Commun.* **2014**, *5* (May), 4111.
- (65) Werkmeister, S.; Junge, K.; Wendt, B.; Alberico, E.; Jiao, H.; Baumann, W.; Junge, H.; Gallou, F.; Beller, M. Hydrogenation of Esters to Alcohols with a Well-Defined Iron Complex. *Angew.*

Chemie Int. Ed. **2014**, *53*, 8722–8726.

- (66) Chakraborty, S.; Dai, H.; Bhattacharya, P.; Neil, T.; Gibson, M. S.; Krause, J. A.; Guan, H.; Fairweather, N. T. Iron-Based Catalysts for the Hydrogenation of Esters to Alcohols. *J. Am. Chem. Soc.* **2014**, *136*, 7869.
- (67) Jayarathne, U.; Zhang, Y.; Hazari, N.; Bernskoetter, W. H. Selective Iron-Catalyzed Deaminative Hydrogenation of Amides. *Organometallics*, **2017**, *36*, 409–416
- (68) Schneck, F.; Assmann, M.; Balmer, M.; Harms, K.; Langer, R. Selective Hydrogenation of Amides to Amines and Alcohols Catalyzed by Improved Iron Pincer Complexes. *Organometallics* **2016**, *35*, 1931–1943.
- (69) Rezayee, N. M.; Samblanet, D. C.; Sanford, M. S. Iron-Catalyzed Hydrogenation of Amides to Alcohols and Amines. *ACS Catal.* **2016**, *6*, 6377–6383.
- (70) Eisenstein, O.; Crabtree, R. H. Outer Sphere Hydrogenation Catalysis. *New J. Chem.* **2013**, *37*, 21–27.
- (71) Bielinski, E. a; Lagaditis, P. O.; Zhang, Y.; Mercado, B. Q.; Würtele, C.; Bernskoetter, W. H.; Hazari, N.; Schneider, S. Lewis Acid Assisted Formic Acid Dehydrogenation Using a Pincer Supported Iron Catalyst. *J. Am. Chem. Soc.* **2014**, 1–4.
- (72) Chakraborty, S.; Brennessel, W. W.; Jones, W. D. A Molecular Iron Catalyst for the Acceptorless Dehydrogenation and Hydrogenation of N-Heterocycles. *J. Am. Chem. Soc.* **2014**, *136*, 8564–8567.
- (73) Xu, R.; Chakraborty, S.; Bellows, S. M.; Yuan, H.; Cundari, T. R.; Jones, W. D. Iron-Catalyzed Homogeneous Hydrogenation of Alkenes under Mild Conditions by a Stepwise, Bifunctional Mechanism. *ACS Catal.* **2016**, *6*, 2127–2135.
- (74) Lagaditis, P. O.; Sues, P. E.; Sonnenberg, J. F.; Wan, K. Y.; Lough, A. J.; Morris, R. H. Iron(II) Complexes Containing Unsymmetrical P–N–P' Pincer Ligands for the Catalytic Asymmetric Hydrogenation of Ketones and Imines. *J. Am. Chem. Soc.* **2014**, *136*, 1367–1380.
- (75) Sonnenberg, J. F.; Wan, K. Y.; Sues, P. E.; Morris, R. H. Ketone Asymmetric Hydrogenation Catalyzed by P–NH–P' Pincer Iron Catalysts: An Experimental and Computational Study. *ACS Catal.* **2016**, 316–326.
- (76) Chakraborty, S.; Lagaditis, P. O.; Förster, M.; Bielinski, E. A.; Hazari, N.; Holthausen, M. C.; Jones, W. D.; Schneider, S. Well-Defined Iron Catalysts for the Acceptorless Reversible Dehydrogenation-Hydrogenation of Alcohols and Ketones. *ACS Catal.* **2014**, *4*, 3994–4003.
- (77) Peña-López, M.; Neumann, H.; Beller, M. Iron(II) Pincer-Catalyzed Synthesis of Lactones and

Lactams through a Versatile Dehydrogenative Domino Sequence. *ChemCatChem* **2015**, *7*, 865–871.

- (78) Zhang, Y.; MacIntosh, A. D.; Wong, J. L.; Bielinski, E. A.; Williard, P. G.; Mercado, B. Q.; Hazari, N.; Bernskoetter, W. H. Iron Catalyzed CO₂ Hydrogenation to Formate Enhanced by Lewis Acid Co-Catalysts. *Chem. Sci.* **2015**, *6*, 4291–4299.
- (79) Alberico, E.; Sponholz, P.; Cordes, C.; Nielsen, M.; Drexler, H. J.; Baumann, W.; Junge, H.; Beller, M. Selective Hydrogen Production from Methanol with a Defined Iron Pincer Catalyst under Mild Conditions. *Angew. Chemie Int. Ed.* **2013**, *52*, 14162–14166.
- (80) Bielinski, E. A.; Förster, M.; Zhang, Y.; Bernskoetter, W. H.; Hazari, N.; Holthausen, M. C. Base-Free Methanol Dehydrogenation Using a Pincer-Supported Iron Compound and Lewis Acid Co-Catalyst. *ACS Catal.* **2015**, *5*, 2404–2415.

Results and Discussion – Part I

Efficient Hydrogenation of Ketones and Aldehydes Catalyzed by Well-Defined Iron(II) PNP Pincer Complexes: Evidence for an Insertion Mechanism.

Reprinted with permission from *Organometallics* **2014**, 33, 6905–6914. Copyright 2014 American Chemical Society.

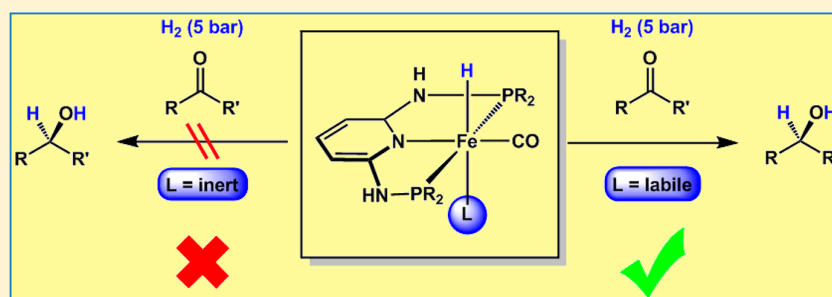
Efficient Hydrogenation of Ketones and Aldehydes Catalyzed by Well-Defined Iron(II) PNP Pincer Complexes: Evidence for an Insertion Mechanism

Nikolaus Gorgas,[†] Berthold Stöger,[‡] Luis F. Veiros,[§] Ernst Pittenauer,[‡] Günter Allmaier,[‡] and Karl Kirchner^{*,†}

[†]Institute of Applied Synthetic Chemistry and [‡]Institute of Chemical Technologies and Analytics, Vienna University of Technology, Getreidemarkt 9, A-1060 Vienna, Austria

[§]Centro de Química Estrutural, Instituto Superior Técnico, Universidade de Lisboa, Avenida Rovisco Pais No. 1, 1049-001 Lisboa, Portugal

Supporting Information



ABSTRACT: We have prepared and structurally characterized a new class of Fe(II) PNP pincer hydride complexes $[\text{Fe}(\text{PNP-}i\text{Pr})(\text{H})(\text{CO})(\text{L})]^n$ ($\text{L} = \text{Br}^-$, CH_3CN , pyridine, PMe_3 , SCN^- , CO , BH_4^- ; $n = 0, +1$) based on the 2,6-diaminopyridine scaffold where the PiPr_2 moieties of the PNP ligand are connected to the pyridine ring via NH and/or NMe spacers. Complexes $[\text{Fe}(\text{PNP-}i\text{Pr})(\text{H})(\text{CO})(\text{L})]^n$ with labile ligands ($\text{L} = \text{Br}^-$, CH_3CN , BH_4^-) and NH spacers are efficient catalysts for the hydrogenation of both ketones and aldehydes to alcohols under mild conditions, while those containing inert ligands ($\text{L} = \text{pyridine}$, PMe_3 , SCN^- , CO) are catalytically inactive. Interestingly, complex $[\text{Fe}(\text{PNP}^{\text{Me}}-i\text{Pr})(\text{H})(\text{CO})(\text{Br})]$, featuring NMe spacers, is an efficient catalyst for the chemoselective hydrogenation of aldehydes. The first type of complexes involves deprotonation of the PNP ligand as well as heterolytic dihydrogen cleavage via metal-alkoxide cooperation, but no reversible aromatization/deprotonation of the PNP ligand. In the case of the N-methylated complex the mechanism remains unclear, but obviously does not allow bifunctional activation of dihydrogen. The experimental results complemented by DFT calculations strongly support an insertion of the $\text{C}=\text{O}$ bond of the carbonyl compound into the $\text{Fe}-\text{H}$ bond.

INTRODUCTION

The catalytic reduction of polar multiple bonds via molecular hydrogen plays a significant role in modern synthetic organic chemistry. This reaction is excellently performed by many transition metal complexes containing noble metals such as ruthenium, rhodium, or iridium.¹ However, the limited availability of precious metals, their high price, and their toxicity diminish their attractiveness in the long run, and more economical and environmentally friendly alternatives have to be found. In this respect, the preparation of well-defined iron-based catalysts of comparable activity would be desirable.² Iron is the most abundant transition metal in the earth's crust and is ubiquitously available. Accordingly, it is not surprising that the field of iron-catalyzed hydrogenations of polar multiple bonds is rapidly evolving, as shown by several recent examples.^{3–7}

It is interesting to note that many of these hydrogenations involve ligand–metal bifunctional catalysis (metal–ligand

cooperation);⁸ that is, the complexes contain electronically coupled hydride and acidic hydrogen atoms as a result of heterolytic dihydrogen cleavage that may be transferred to polar unsaturated substrates in an outer-sphere fashion or may be transferred via hydride migration (inner-sphere mechanism). An effective way of bond activation by metal–ligand cooperation involves aromatization/dearomatization of the ligand in pincer-type complexes. In particular, pincer ligands in which a central pyridine-based backbone is connected with $-\text{CH}_2\text{PR}_2$ and/or $-\text{CH}_2\text{NR}_2$ substituents were shown to exhibit this behavior.⁹ This has resulted in the development of novel and unprecedented iron catalysis where this type of cooperation plays a key role in the heterolytic cleavage of H_2 .⁴ In the case of ketones and aldehydes, most efficient are

Received: September 26, 2014

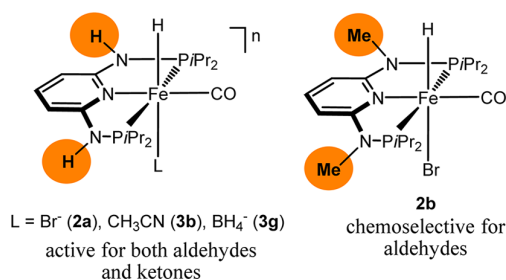
Published: November 17, 2014

complexes of the types $[\text{Fe}(\text{PNP}^{\text{CH}_2\text{-iPr}})(\text{CO})(\text{H})(\text{Br})]$ and $[\text{Fe}(\text{PNP}^{\text{CH}_2\text{-iPr}})(\text{CO})(\text{H})(\kappa^1\text{-BH}_4)]$, where the bromide and BH_4^- ligands are labile, facilitating the coordination of the substrates. It has thus been suggested by Milstein that this reaction proceeds via an inner-sphere mechanism involving insertion of the carbonyl compounds into the Fe–H bond.^{4a,c}

We are currently focusing on the synthesis and reactivity of iron complexes containing PNP pincer ligands based on the 2,6-diaminopyridine scaffold. In these ligands the aromatic pyridine ring and the phosphine moieties are connected via NH, *N*-alkyl, or *N*-aryl linkers. The advantage of these ligands is that both substituents of the phosphine and amine sites can be systematically varied in a modular fashion, which has a decisive effect on the outcome of reactions.¹⁰ Recently we prepared the cationic Fe(II) hydride complex $\text{cis-}[\text{Fe}(\text{PNP-}i\text{Pr})(\text{CO})_2\text{H}]^+$, which involved reversible NH activation as well as heterolytic dihydrogen cleavage via metal–PNP ligand cooperation.¹¹ This complex turned out to be catalytically inactive for the hydrogenation of ketones and aldehydes, which was attributed to the fact that this complex is substitutionally inert and/or that the basicity of the hydride is too low.

Herein we report the synthesis, characterization, and catalytic activity of a series of neutral iron hydride complexes of the type $[\text{Fe}(\text{PNP-}i\text{Pr})(\text{CO})(\text{H})(\text{Br})]$ (**2a–c**) where the PiPr_2 moieties of the PNP ligand are connected to the pyridine ring via NH and/or NMe spacers (Scheme 1). In addition, the synthesis of a

Scheme 1. Two Types of Highly Reactive Iron PNP Pincer Hydrogenation Catalysts



series of neutral and cationic hydride complexes of the type $[\text{Fe}(\text{PNP-}i\text{Pr})(\text{CO})(\text{H})(\text{L})]^n$ (**3a–g**) ($n = +1, 0$) where L = CH₃CN, pyridine, PMe₃, $\kappa^1\text{-N}$ -coordinated SCN[−], and $\kappa^1\text{-coordinated BH}_4^-$ is described. All complexes featuring labile ligands L (Br[−], CH₃CN, BH₄[−]) are efficient catalysts for the hydrogenation of ketones and aldehydes to alcohols under mild conditions. Moreover, the *N*-methylated complex **2b** is a chemoselective catalyst for the reduction of aldehydes. The first example of catalytic hydrogenation of aldehyde that is chemoselective against ketone was recently reported by Beller.¹² However, this reaction required elevated temperatures

(120 °C) and a high H₂ pressure (20 bar). The experimental results are complemented by DFT calculations.

RESULTS AND DISCUSSION

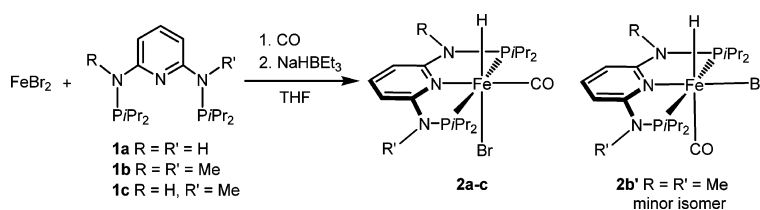
The synthesis of complexes $[\text{Fe}(\text{PNP-}i\text{Pr})(\text{CO})(\text{H})(\text{Br})]$ (**2a–c**) was accomplished in 63–67% isolated yields by treatment of anhydrous FeBr₂ with 1 equiv of the corresponding PNP-*i*Pr ligands **1a–c** in THF in the presence of CO and subsequent addition of 1.1 equiv of Na[HBET₃] (Scheme 2). This reaction proceeds via the intermediacy of the dibromo complexes $[\text{Fe}(\text{PNP-}i\text{Pr})(\text{CO})(\text{Br})_2]$, which, in principle, can be isolated in pure form as shown previously,¹³ but are labile, slowly losing CO, and were thus directly used without prior isolation. In the case of the symmetrical *N*-methylated PNP-*i*Pr ligand **1b**, two isomers were obtained in a ca. 2.7:1 ratio with the hydride ligand being *trans* to the bromide and to the CO ligand, respectively, which could not be separated. All hydride complexes are air sensitive both in the solid state and in solution.

Characterization was accomplished by elemental analysis and by ¹H, ¹³C{¹H}, and ³¹P{¹H} NMR and IR spectroscopy. The ¹H NMR spectrum confirmed the presence of one hydride ligand, which appeared at −21.4, −21.6, and −21.8 ppm, respectively, as a well-resolved triplet with a ²J_{HP} coupling constant of about 57 Hz. Isomer **2b'** exhibits the hydride resonance at −1.1 ppm. In the ¹³C{¹H} NMR spectrum the most noticeable resonance is the low-field resonance of the carbonyl carbon atom *trans* to the pyridine nitrogen observed as a triplet in the range 217.1–222.7 ppm (*J*_{CP} about 13–23 Hz). The ³¹P{¹H} NMR spectra of complexes **2a** and **2b** give rise to a singlet at 147.1 and 164.0 ppm, respectively, while in the case of **2c** two doublets centered at 165.0 and 147.2 ppm are observed. In the IR spectrum the strong bands for CO stretching frequencies are found in the range 1901 to 1903 cm^{−1}.

The solid-state structure of **2a** was determined by single-crystal X-ray diffraction. A structural view is depicted in Figure 1 with selected bond distances given in the caption. Complex **2a** adopts a distorted octahedral geometry around the metal center with the hydride ligand being in *cis* position to a CO ligand. The PNP ligand is coordinated to the iron center in a typical tridentate meridional mode, with a P1–Fe1–P2 angle of 164.58(4)°. The hydride and the N–H atoms could be unambiguously located in the difference Fourier maps. The Fe–H distance was refined to 1.46(2) Å.

Complexes **2a–c** are substitutionally labile. This has been exemplarily studied in more detail with **2a** (Scheme 3). Dissolution of **2a** in MeOH-*d*₄ resulted in an immediate replacement of the Br[−] ligand to give the cationic complex $[\text{Fe}(\text{PNP-}i\text{Pr})(\text{H})(\text{CO})(\text{MeOH-}d_4)]^+$ (**3a**), as evident by a new hydride resonance at −26.6 ppm and a ³¹P{¹H} signal at 140.6 ppm. Interestingly, in ethanol dissociation of the bromide

Scheme 2. Synthesis of Hydride Complexes 2a–c



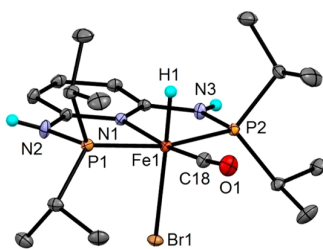


Figure 1. Structural view of $[\text{Fe}(\text{PNP-}i\text{Pr})(\text{H})(\text{CO})(\text{Br})]\cdot\text{CH}_2\text{Cl}_2$ (**2a**· CH_2Cl_2) showing 50% thermal ellipsoids (CH_2Cl_2 and most hydrogen atoms omitted for clarity). Selected bond lengths (Å) and angles (deg): Fe1–P1 2.1927(6), Fe1–P2 2.1927(6), Fe1–N1 2.022(1), Fe1–Br1 2.5269(6), Fe1–C18 1.731(1), Fe1–H1 1.46(2), P1–Fe1–P2 164.58(1), N1–Fe1–C18 171.95(4).

ligand is much less pronounced and Br^- is only partially replaced by EtOH. This might also contribute to the fact that higher catalytic activities are achieved in this solvent perhaps due to diminished competition between substrate and solvent for a free coordination site (*vide infra*). The addition of $\text{L} = \text{CH}_3\text{CN}$, pyridine, PMe_3 , SCN^- , CO, and BH_4^- leads to the formation of the corresponding cationic or neutral complexes $[\text{Fe}(\text{PNP-}i\text{Pr})(\text{H})(\text{CO})(\text{L})]^n$ (**3b–g**) as shown in Scheme 3. Complexes **3b–g** could also be isolated in pure form by reacting **2a** with the respective ligands CH_3CN (neat), pyridine, PMe_3 , SCN^- (Na^+ salt), BH_4^- (Na^+ salt), and CO in both the absence and presence of silver salts in 83–97% isolated yields. These complexes exhibit the characteristic hydride resonances at -18.6 , -20.1 , -11.1 , -19.8 , -7.5 , and -18.2 , ppm, respectively. In the case of **3g** the BH_4^- ligand gives rise to a broad signal at -3.61 ppm (4H). The observation of a broad four-proton resonance in this region of the ^1H NMR spectrum is typical for κ^1 -coordinated BH_4^- ligands of iron complexes and indicates dynamic behavior of this ligand.^{4c}

Structural views of **3b**, **3c**, **3d**, **3e**, and **3g** are depicted in Figures 2–6 with selected bond distances given in the captions.

The lability of complexes **2a** and **3b–g** was also studied by ESI-MS. Solutions of these complexes in CH_3CN were subjected to ESI-MS analysis in the positive ion mode (the neutral complexes were investigated in the presence of NaCl to obtain cationic sodiated species). In the case of $[\text{Fe}(\text{PNP-}i\text{Pr})(\text{H})(\text{CO})(\text{Br})]$ (**2a**), $[\text{Fe}(\text{PNP-}i\text{Pr})(\text{H})(\text{CO})(\text{CH}_3\text{CN})]^+$ (**3b**), and $[\text{Fe}(\text{PNP-}i\text{Pr})(\text{H})(\text{CO})(\kappa^1\text{-BH}_4)]$ (**3g**) the cationic fragment $[\text{Fe}(\text{PNP-}i\text{Pr})(\text{H})(\text{CO})]^+$ (m/z 426.1) was found as the predominant species, while for all other complexes $[\text{Fe}(\text{PNP-}i\text{Pr})(\text{H})(\text{CO})(\text{py})]^+$ (**3c**), $[\text{Fe}(\text{PNP-}i\text{Pr})(\text{H})(\text{CO})(\text{PMe}_3)]^+$ (**3d**), $[\text{Fe}(\text{PNP-}i\text{Pr})(\text{H})(\text{CO})(\kappa^1\text{-N-SCN})]$ (**3e**), and $[\text{Fe}(\text{PNP-}i\text{Pr})(\text{H})(\text{CO})_2]^+$ (**3f**) the intact complexes $[\text{M}]^+$ ($m/$

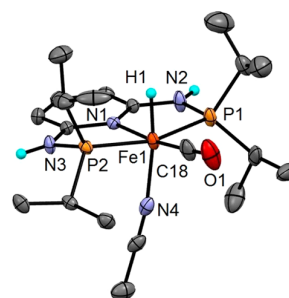


Figure 2. Structural view of $[\text{Fe}(\text{PNP-}i\text{Pr})(\text{H})(\text{CO})(\text{CH}_3\text{CN})]\text{Br}$ (**3b**) showing 50% thermal ellipsoids (bromide counterion and most hydrogen atoms omitted for clarity). Only one of the two crystallographically independent complexes is shown. Selected bond lengths (Å) and angles (deg): Fe1–P1 2.1986(10), Fe1–P2 2.2028(10), Fe1–N1 1.998(2), Fe1–N4 1.984(2), Fe1–C18 1.738(3), Fe1–H1 1.460(6), P1–Fe1–P2 162.87(3), N1–Fe1–C18 173.7(1).

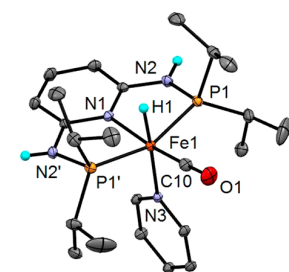
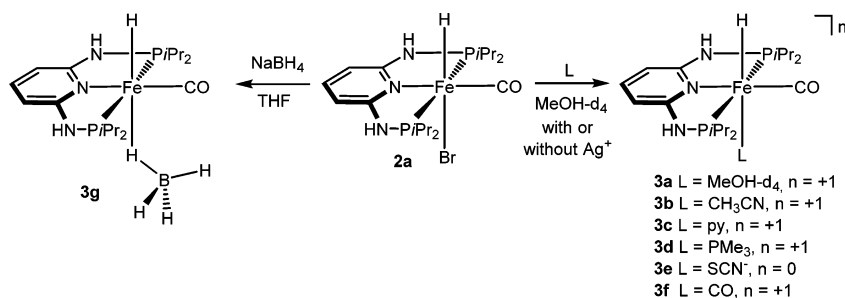


Figure 3. Structural view of $[\text{Fe}(\text{PNP-}i\text{Pr})(\text{H})(\text{CO})(\text{py})]\text{BF}_4$ (**3c**) showing 50% thermal ellipsoids (most hydrogen atoms and BF_4^- anion omitted for clarity). Selected bond lengths (Å) and angles (deg): Fe1–P1 2.1915(3), Fe1–N1 2.017(1), Fe1–N3 2.068(1), Fe1–C10 1.738(2), Fe1–H1 1.46(2), P1–Fe1–P2 158.56(1), N1–Fe1–C10 171.31 (6).

z 505.1, 502.2, 507.1 (as $[\text{M} + \text{Na}]^+$, and 456.1) were observed as major fragments. We also investigated an EtOH solution of **2a** in the presence of KO t Bu in the hopes of detecting the alkoxide complex $[\text{Fe}(\text{PNP-}i\text{Pr})(\text{H})(\text{CO})(\text{OEt})]$. However, only the fragment at m/z 426.1 was detected as the major species. These observations are in accord with the fact that the ligands Br^- , OEt^- , BH_4^- , and CH_3CN *trans* to the hydride ligand are substitutionally labile, while pyridine, PMe_3 , SCN^- , and CO are substitutionally inert.

The catalytic activity of all hydride complexes was investigated in the hydrogenation of ketones and aldehydes. In preliminary experiments various solvents were tested for the

Scheme 3. Substitution of the Bromide Ligand in **2a** by $\text{MeOH-}d_4$, CH_3CN , Pyridine, PMe_3 , SCN^- , CO, and BH_4^-



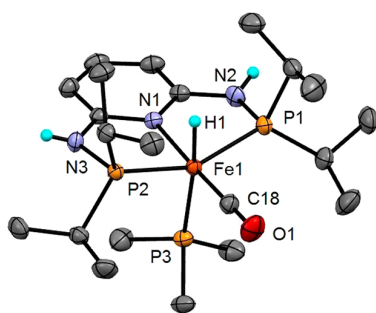


Figure 4. Structural view of $[\text{Fe}(\text{PNP-}i\text{Pr})(\text{H})(\text{CO})(\text{PMe}_3)]\text{BF}_4$ (**3d**) showing 50% thermal ellipsoids (most hydrogen atoms and BF_4^- anion omitted for clarity). Selected bond lengths (Å) and angles (deg): Fe1–P1 2.1952(4), Fe1–P2 2.1886(4), Fe1–N1 2.007(1), Fe1–C18 1.730(2), Fe1–P3 2.2753(5), Fe1–H1 1.46(2), P1–Fe1–P2 154.89(2), N1–Fe1–C18 176.68(7).

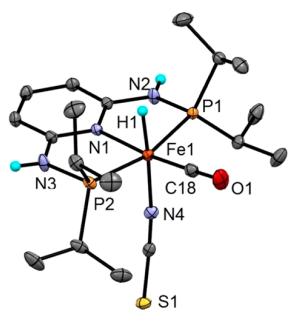


Figure 5. Structural view of $[\text{Fe}(\text{PNP-}i\text{Pr})(\text{H})(\text{CO})(\kappa^1\text{-N-SCN})]$ (**3e**) showing 50% thermal ellipsoids (most hydrogen atoms omitted for clarity). Selected bond lengths (Å) and angles (deg): Fe1–P1 2.1884(7), Fe1–P2 2.1871(7), Fe1–N1 2.018(1), Fe1–N4 1.989(1), Fe1–C18 1.738(2), Fe1–H1 1.49(2), P1–Fe1–P2 164.78(1), N1–Fe1–C18 172.84(5).

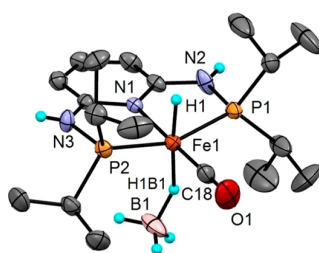


Figure 6. Structural view of $[\text{Fe}(\text{PNP-}i\text{Pr})(\text{H})(\text{CO})(\kappa^1\text{-BH}_4)]$ (**3g**) showing 50% thermal ellipsoids (most hydrogen atoms omitted for clarity). Selected bond lengths (Å) and angles (deg): Fe1–P1 2.1885(7), Fe1–P2 2.1873(7), Fe1–N1 1.998(2), Fe1–C18 1.733(2), Fe1–B1 2.72(1), Fe1–H1 1.46(2), Fe1–H1B1 1.67(2), P1–Fe1–P2 159.99(3), N1–Fe1–C18 178.13(9).

hydrogenation of acetophenone using 1.0 mol % **2a**, 2.0 mol % KOtBu, and 5 bar hydrogen at ambient temperature (25 °C, Table 1). The hydrogenation reaction takes place only in alcoholic solutions, with ethanol being by far the best solvent, giving *rac*-1-phenylethanol in essentially quantitative yield. Moreover, in the absence of base and/or H_2 no reaction takes place, indicating that **2a** is not an active catalyst for transfer hydrogenation. The amount of the catalyst precursor could be reduced to 0.1 mol %. In this case 77% isolated yield was reached within 1 h, which corresponds to a TOF of 770 h^{-1} .

Table 1. Iron-Catalyzed Hydrogenation of Acetophenone^a

$$\text{Ph-C(=O)-Me} \xrightarrow[\text{solvent, 2h, RT}]{\begin{matrix} \text{H}_2 \text{ (5 bar)} \\ 1.0 \text{ mol \% } \mathbf{2a} \\ 2.0 \text{ mol \% KOtBu} \end{matrix}} \text{Ph-CH(OH)-Me}$$

entry	solvent	yield [%] ^b	TOF [h^{-1}]
1	THF		
2	MeOH	36	18
3	<i>i</i> PrOH	58	29
4	<i>t</i> AmylOH	89	45
5	EtOH	99	50

^aReaction conditions: **2a** (0.025 mmol, 1.0 mol %), KOtBu (0.05 mmol), substrate (2.5 mmol), solvent (5 mL), H_2 (5 bar), 2 h. ^bYields were determined by ^1H NMR.

However, in terms of a better reproducibility 0.5 mol % catalyst was used for all subsequent reactions.

In contrast to **2a**, under the same reaction conditions, as well as with even 5 mol %, complex **2b**, bearing NMe linkers, was completely inactive for the reduction of ketones, while **2c**, containing one NH and one NMe linker, was catalytically active but with a significantly lower activity than **2a** (28% yield). On the other hand, the catalytic activity of both $[\text{Fe}(\text{PNP-}i\text{Pr})(\text{H})(\text{CO})(\text{CH}_3\text{CN})]^+$ (**3b**) and $\text{Fe}(\text{PNP-}i\text{Pr})(\text{H})(\text{CO})(\kappa^1\text{-BH}_4)]$ (**3g**) was similar to that of **2a** (94% yield). The reaction with **3g** could be performed even without addition of an external base, although slightly higher temperatures were required to achieve comparable activities (50 °C) since base has to be generated by alcoholysis of free BH_4^- .¹⁴ Similar observations were recently made by Milstein.^{4c} In sharp contrast to the substitutionally labile complexes **2a**, **3b**, and **3g**, the inert compounds **3c–f** were catalytically inactive.

On the basis of these results, we investigated the scope and limitations of catalyst **2a** using various substrates (Table 2). Halogen substituents had no notable influence on the catalytic activity, while the reaction with 4-methoxyacetophenone and 4-nitroacetophenone resulted in significantly lower yields (entries 5 and 6). Likewise, for simple ketones such as cyclohexanone and benzophenone lower activity was observed. In the presence of a nitrile or primary amine substituents on the aromatic system no reaction was observed, presumably due to preferential coordination of these groups to the iron center, thus blocking a vacant coordination site to accommodate an incoming substrate (entries 7 and 8). The same result was found for 4-acetylpyridine. This is in line with the observation that **3c**, containing a strongly bound pyridine ligand, is catalytically inactive. The reduction of 2-acetylpyridine was extremely efficient, giving full conversion even after 1 h (TOF = 200 h^{-1} , entry 11). In this case, coordination of pyridine is obviously hampered due to the bulky acetyl substituent in the *ortho* position of the pyridine unit. The reduction of *trans*-4-phenylbutenone resulted in mixtures, where reduction of the double bond also took place (entry 13). Finally, the hydrogenation of aldehydes was tested with complexes **2a** and **2b** as catalysts utilizing benzaldehyde, 4-isopropylbenzaldehyde, cyclohexane carboxaldehyde, picolinealdehyde, and isonicotinaldehyde (Table 3). Under the standard reaction conditions, low conversions were observed (entry 1). However, an increase of the catalyst loading to 5.0 mol % and reduction of the reaction time to 10 min afforded the respective alcohols in nearly quantitative yield. In the case of isonicotinaldehyde

Table 2. Iron-Catalyzed Hydrogenation of Ketones^a

$\text{R}-\text{C}(=\text{O})-\text{R}' \xrightarrow[\text{solvent, 2h, RT}]{\text{H}_2 (5 \text{ bar}), 0.5 \text{ mol \% } \mathbf{2a}, 1.0 \text{ mol \% KOtBu}} \text{R}-\text{C}(\text{OH})-\text{R}'$				
Entry	Substrate	Product	Yield ^d [%]	TOF [h ⁻¹]
1			99	100
2 ^b	R = H		77	770
3	R = Cl		99	100
4	R = Br		99	100
5	R = OMe		34	34
6	R = NO ₂		47	47
7	R = NH ₂			
8	R = CN			
9			30	30
10			64	64
11 ^c			99	200
12			-	-
13			10	100
			45	
			45	

^aReaction conditions: **2a** (0.0125 mmol), KOtBu (0.025 mmol), substrate (2.5 mmol), EtOH (5 mL), H₂ (5 bar), 2 h. ^bReaction conditions: **2a** (0.0025 mmol), KOtBu (0.005), substrate (2.5 mmol), EtOH (3 mL), 1 h. ^cReaction time: 1 h. ^dYields were determined by ¹H NMR.

(entry 6) no reaction took place, again due to strong coordination of the pyridine moiety.

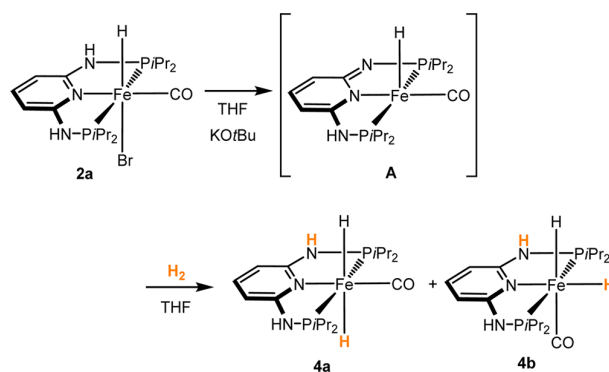
In order to gain a mechanistic understanding of the catalytic hydrogenation of aldehydes and ketones, some stoichiometric reactions of **2a** were investigated. Treatment of **2a** in THF with KOtBu resulted in an immediate color change from orange to deep red. In the ¹H NMR spectrum hydride signals were no longer present, but in the IR spectrum two strong absorptions at 1872 and 1822 cm⁻¹ were observed ($\nu_{\text{Fe-H}}$ and ν_{CO}). This may be tentatively assigned to the formation of [Fe(PNP-^H-iPr)(H)(CO)] (**A**) as a result of dehydrohalogenation. In this context it is important to note that a series of related iron PNP pincer complexes were prepared and even structurally characterized recently by Schneider¹⁵ and Jones.¹⁶ The formation of the Fe(0) dicarbonyl complex [Fe(PNP-iPr)(CO)₂] can be ruled out by comparison with an authentic sample.¹¹ Moreover, purging the solution with H₂ afforded a mixture of the *trans* and *cis* dihydride complexes [Fe(PNP-iPr)(CO)(H)₂] (**4a,b**) (Scheme 4). Such a reaction does not take place with [Fe(PNP-iPr)(CO)₂]. The ¹H NMR spectrum of the mixture at room temperature exhibited a triplet at -9.02 ppm for the

Table 3. Iron-Catalyzed Hydrogenation of Aldehydes^a

$\text{R}-\text{CHO} \xrightarrow[\text{EtOH, 10 min, RT}]{\text{H}_2 (5 \text{ bar}), 5 \text{ mol \% } \mathbf{2a} \text{ or } \mathbf{2b}, 10 \text{ mol \% KOtBu}} \text{R}-\text{CH}_2\text{OH}$				
Entry	Substrate	Product	Yield ^d [%]	TOF [h ⁻¹]
1 ^b			23	23
2			99	120
3			99	120
4 ^c			99	60
5			99	120
6				

^aReaction conditions: **2a** or **2b** (0.125 mmol), KOtBu (0.25 mmol), substrate (2.5 mmol), EtOH (5 mL), H₂ (5 bar), 10 min. ^bReaction conditions: **2a** (0.0125 mmol), KOtBu (0.025 mmol), substrate (2.5 mmol), EtOH (5 mL), H₂ (5 bar), 2 h. ^cReaction time: 20 min. ^dYields were determined by ¹H NMR.

Scheme 4. Dehydrohalogenation of **2a** with KOtBu in THF to Give **A** and Subsequent Addition of H₂ to Afford a Mixture of the *trans* and *cis* Dihydride Complexes **4a** and **4b**



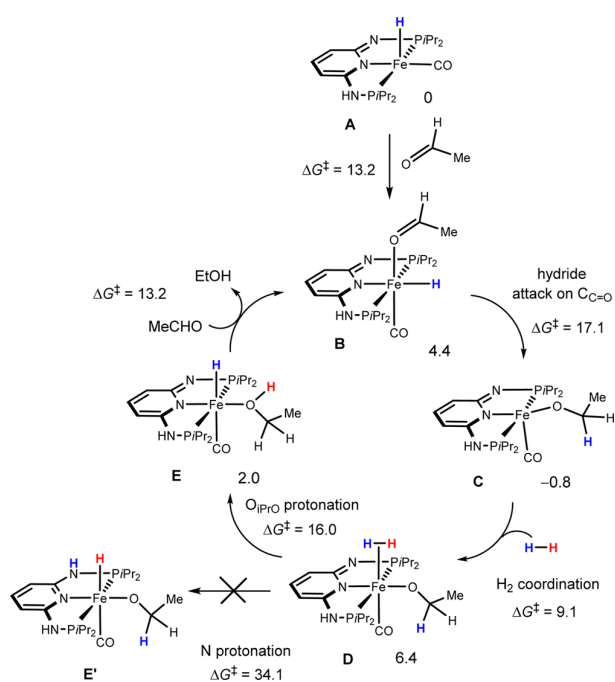
trans-dihydride **4a** and only one broad signal at -13.4 ppm for the *cis*-dihydride **4b** due to fast exchange between the two hydrides. Complexes **4a** and **4b** did not show any significant reactivity toward acetophenone even after 1 day, suggesting that these are not active species in the catalytic reduction of ketones. Our findings are fully consistent with Milstein's discoveries based on the related iron pincer complex [Fe(PNP-CH₂-iPr)(H)(CO)(κ¹-BH₄)],^{4c} but strongly contrast the recently reported computational study by Yang on the iron-catalyzed reduction of acetophenone.¹⁷ In his calculated mechanism, the reaction proceeds via *trans*-[Fe(PNP-iPr)(CO)(H)₂] (**4a**) and involves an outer-sphere hydrogen transfer from this complex to the carbonyl carbon atom of acetophenone in EtOH as solvent. Accordingly, we believe that this mechanism is not operative in our system with respect to ketone reduction, although *trans*-dihydride iron PNP complexes were shown to be important species in other reactions.^{4b,d,e,13,15,16,18} The reduction of aldehydes, in

particular with **2b**, remains mechanistically unclear at this stage, and the involvement of dihydride complexes cannot be ruled out.

In sharp contrast to the above observations in THF, when KOtBu was added to an EtOH solution of **2a** in the presence of dihydrogen, no changes in the IR, ^1H NMR, and $^{31}\text{P}\{^1\text{H}\}$ NMR spectra were observed. This again emphasizes the particular role of EtOH as solvent apparently preventing the formation of **4a** and **4b**.

Preliminary DFT calculations¹⁹ were carried out to establish a reasonable mechanism using the hydrogenation of acetaldehyde with **2a** as model. A summary of these results with the most relevant points along the catalytic cycle is presented in Scheme 5. Loss of a labile bromide ligand and

Scheme 5. Catalytic Cycle Calculated for an Inner-Sphere Mechanism^a



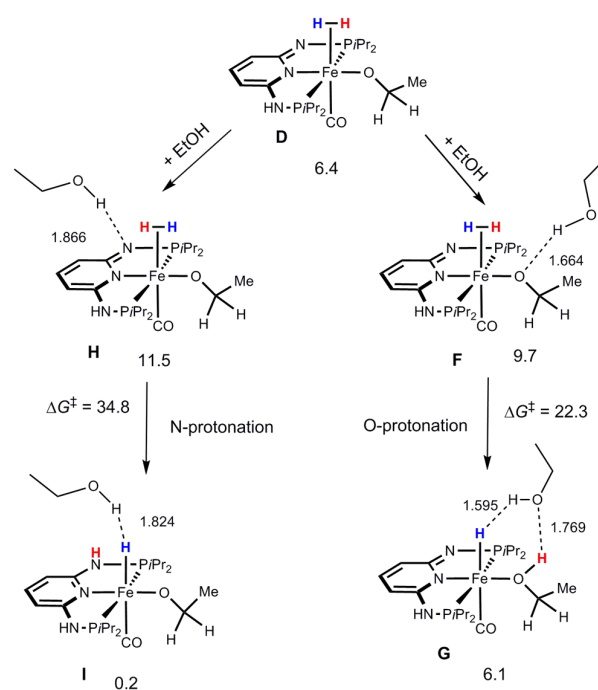
^aFree energy values (in kcal/mol) referred to $[\text{Fe}(\text{PNP}^{\text{H}}\text{-iPr})(\text{H})(\text{CO})]$ (**A**).

deprotonation of an NH group in the catalytic precursor **2a** will produce a five-coordinated complex, $[\text{Fe}(\text{PNP}^{\text{H}}\text{-iPr})(\text{H})(\text{CO})]$ (**A**), that is the starting point in the mechanistic investigations and also the reference for all free energy values. The catalytic cycle depicted in Scheme 5 starts with the occupation of the free coordination site in **A** by the substrate (in **B**). Then there is nucleophilic attack of the hydride on the carbonyl C atom with formation of the alkoxide complex, **C**. The reaction proceeds with coordination of dihydrogen (**D**) and subsequent protonation of the O atom with formation of the alcohol and regeneration of the hydride (**E**). The cycle is closed by ligand exchange with liberation of one molecule of the product and coordination of another substrate from **E** back to **B**. The highest energy barrier along the cycle corresponds to the hydride migration step, and its value (17.1 kcal/mol) indicates a facile reaction. It has to be emphasized that the PNP ligand is not involved in dihydrogen activation but remains deprotonated throughout the catalytic cycle, acting as a strongly

electron-donating anionic ligand. In fact, the activation barrier for dihydrogen splitting involving protonation of the PNP N atom, corresponding to reversible aromatization/dearomatization of that ligand to afford **E'**, is considerably higher (34.1 kcal/mol) than the one associated with protonation of the O atom of the alkoxide producing the final alcohol product as shown in Scheme 5 (16.0 kcal/mol).

The dihydrogen splitting step was also studied with the inclusion of one explicit solvent molecule (ethanol) in the calculations (Scheme 6). In fact, the ethanol molecule acting as

Scheme 6. Dihydrogen Splitting via O- and N-Protonation Calculated with One Explicit EtOH Molecule^a



^aFree energy values (in kcal/mol) are referred to $[\text{Fe}(\text{PNP}^{\text{H}}\text{-iPr})(\text{H})(\text{CO})]$ (**A**) and H-bond distances in Å.

a proton shuttle could alter the most favorable path and change the conclusions above. The results obtained are shown in Scheme 6 and indicate that O-protonation of the alkoxide ligand remains the preferred pathway for the reaction, with a barrier 12.5 kcal/mol lower than the value calculated for protonation of the PNP N atom. The O-protonation step calculated with an explicit solvent molecule (EtOH), represented in Scheme 6, has a free energy barrier 6.3 kcal/mol higher than the same process calculated without the ethanol molecule (cf. Scheme 5) due to the rise in the entropy term originated by the presence of that extra molecule. If one compares energy values, the barrier becomes 5 kcal/mol lower in the case with the extra ethanol molecule. This result confirms that the PNP ligand remains deprotonated and, thus, dearomatized along the entire cycle and means that N–H acidity has no active part in the reaction mechanism that should not be classified as bifunctional catalysis in this case.

It is also interesting to note that deprotonation of the PNP ligand is accompanied by a substantial increase of the ligand charge. In fact, in the N-protonated counterpart of **A**, $[\text{Fe}(\text{PNP}^{\text{H}}\text{-iPr})(\text{H})(\text{CO})]^+$, the PNP ligand is more positive ($C_{\text{PNP}} = 1.03$)

than the same ligand in **A** ($C_{\text{PNP}} = 0.14$). Accordingly, the hydride in the cationic complex is also electron poorer than the equivalent ligand in **A**, $C_{\text{H}} = -0.14$ and -0.16 , respectively, indicating that **A** should be a better active species in a reaction where the key step is hydride nucleophilic attack on the substrate carbonyl C atom.

CONCLUSION

In conclusion, we have prepared a new class of Fe(II) PNP pincer hydride complexes $[\text{Fe}(\text{PNP-}i\text{Pr})(\text{CO})(\text{H})(\text{L})]^n$ (**2a–c**, **3a–g**) ($n = +1, 0$) based on the 2,6-diaminopyridine scaffold where the PiPr_2 moieties of the PNP ligand connect to the pyridine ring via NH and/or NMe spacers and where the complexes feature both labile (Br^- , CH_3CN , BH_4^-) and inert (pyridine, PMe_3 , SCN^- , CO) coligands. Complexes with labile ligands are efficient catalysts for the hydrogenation of ketones and aldehydes to alcohols under mild conditions. These reactions take place at room temperature with turnover frequencies up to 770 h^{-1} using 5 bar hydrogen pressure and seem to involve heterolytic dihydrogen cleavage via metal-alkoxide cooperation, with the PNP ligand not being involved in dihydrogen activation. The PNP ligand remains deprotonated throughout the catalytic cycle, acting as a strongly electron donating anionic ligand. The catalytic reactions do not proceed in aprotic solvents, but require alcoholic solutions, with EtOH being the best solvent. EtOH prevents the formation of dihydride species, which are catalytically inactive, and seems to stabilize the dearomatized $16e$ intermediate **A** due to reversible EtOH coordination. The experimental results complemented by DFT calculations strongly support an inner-sphere mechanism, i.e., insertion of the C=O bond of the carbonyl compound into the Fe–H bond. Finally, the chemoselectivity of **2b** toward aldehydes vs ketones is remarkable and may be synthetically useful. This reaction apparently also does not proceed via a bifunctional mechanism. Detailed mechanistic studies, in particular the reaction of catalyst **2b** where the mechanism remains unclear, as well as catalyst optimizations are currently under way.

EXPERIMENTAL SECTION

General Procedures. All manipulations were performed under an inert atmosphere of argon by using Schlenk techniques or in an MBraun inert-gas glovebox. The solvents were purified according to standard procedures.²⁰ The deuterated solvents were purchased from Aldrich and dried over 4 Å molecular sieves. The ligands N,N' -bis(diisopropylphosphino)-2,6-diaminopyridine (PNP-*i*Pr) (**1a**),²¹ N,N' -bis(diisopropylphosphino)- N,N' -dimethyl-2,6-diaminopyridine (PNP^{Me}-*i*Pr) (**1b**), and N,N' -bis(diisopropylphosphino)- N -methyl-2,6-diaminopyridine (PNP^{HMe}-*i*Pr) (**1c**)²² and complex $[\text{Fe}(\text{PNP-}i\text{Pr})(\text{H})(\text{CO})_2]\text{SbF}_6$ (**3f**) were prepared according to the literature.¹¹ ^1H , $^{13}\text{C}\{^1\text{H}\}$, and $^{31}\text{P}\{^1\text{H}\}$ NMR spectra were recorded on Bruker AVANCE-250 and AVANCE-400 spectrometers. ^1H and $^{13}\text{C}\{^1\text{H}\}$ NMR spectra were referenced internally to residual protio-solvent and solvent resonances, respectively, and are reported relative to tetramethylsilane ($\delta = 0$ ppm). $^{31}\text{P}\{^1\text{H}\}$ NMR spectra were referenced externally to H_3PO_4 (85%) ($\delta = 0$ ppm). All mass spectrometric measurements were performed on an Esquire 3000^{plus} 3D-quadrupole ion trap mass spectrometer (Bruker Daltonics, Bremen, Germany) in positive-ion mode electrospray ionization (ESI-MS). All mass calculations are based on the lowest mass (i.e. most abundant) iron isotope (^{56}Fe -isotope).

General Procedure for the Hydrogenation Reactions. All hydrogenation reactions were performed at ambient temperature (25°C) under a hydrogen atmosphere of 5 bar using a 90 mL Fisher-Porter tube, which was flushed several times with hydrogen gas prior

to the addition of the reaction solution. For the preparation of the reaction solutions a vial was charged with the specified amount of catalyst, substrate, and EtOH. Subsequently, KO^tBu was added and the solution was taken up into a syringe and transferred to the Fisher-Porter tube. After stirring the solution for the stated time, pressure was carefully released, diethyl ether (20 mL) was added, and the reaction was quenched by addition of an aqueous solution of H_3PO_4 (0.5 M, 0.5 mL). The organic phase was separated, washed with brine, and dried over MgSO_4 . The solvent was removed under reduced pressure, and the isolated product was characterized by NMR spectroscopy.

Syntheses. $[\text{Fe}(\text{PNP-}i\text{Pr})(\text{H})(\text{CO})\text{Br}]$ (2a**).** Anhydrous FeBr_2 (190 mg, 0.88 mmol) and **1a** (300 mg, 0.88 mmol) were dissolved in 12 mL of THF. The immediately formed yellow suspension was stirred for 1 h at room temperature before CO was bubbled through the reaction mixture for 10 min. During this time the color of the suspension changed from yellow to blue. The reaction mixture was cooled to 0°C , and a solution of $\text{Na}[\text{HBEt}_3]$ in toluene (0.97 mL, 1 M, 0.97 mmol) was slowly added. The reaction mixture was stirred for 30 min at 0°C , in which time the color changed from blue to dark red. After an additional 60 min at room temperature the solution was filtered and the solvent was removed under reduced pressure. The dark residue was taken up in THF (3 mL), and the product was precipitated by addition of *n*-hexane (15 mL). The precipitate was separated from the supernatant solution, washed with *n*-pentane (3×10 mL), and dried under vacuum to afford a bright yellow powder. Yield: 298 mg (67%). Anal. Calcd for $\text{C}_{18}\text{H}_{34}\text{BrFeN}_3\text{O}_2$: C, 42.71; H, 6.77; N, 8.30. Found: C, 42.57; H, 6.83; N, 8.33. ^1H NMR (δ , CD_2Cl_2 , 20°C): 7.17 (t, $J = 8.0$ Hz, 1H, py^4), 6.11 (d, $J = 8.0$ Hz, 2H, $\text{py}^{3,5}$), 5.54 (bs, 2H, NH), 3.24 (m, 2H, $\text{CH}(\text{CH}_3)_2$), 2.51 (m, 2H, $\text{CH}(\text{CH}_3)_2$), 1.56 (dd, $J = 7.9$ Hz, $J = 17.6$, 6H, $\text{CH}(\text{CH}_3)_2$), 1.44 (dd, $J = 6.4$ Hz, $J = 11.9$, 6H, $\text{CH}(\text{CH}_3)_2$), 1.21 (dd, $J = 7.0$ Hz, $J = 17.1$, 6H, $\text{CH}(\text{CH}_3)_2$), 1.00 (dd, $J = 6.8$ Hz, $J = 14.2$, 6H, $\text{CH}(\text{CH}_3)_2$), -21.36 (t, $^2J_{\text{HP}} = 56.6$, 1H, FeH). $^{13}\text{C}\{^1\text{H}\}$ NMR (δ , CD_2Cl_2 , 20°C): 222.7 (br, CO), 160.8 (t, $^2J_{\text{CP}} = 9.9$ Hz, $\text{py}^{2,6}$), 138.7 (s, py^4), 97.4 (s, $\text{py}^{3,5}$), 30.3 (t, $^1J_{\text{CP}} = 10.7$ Hz, $\text{CH}(\text{CH}_3)_2$), 27.4 (t, $^1J_{\text{CP}} = 12.9$ Hz, $\text{CH}(\text{CH}_3)_2$), 19.6 (s, $\text{CH}(\text{CH}_3)_2$), 18.8 (s, $\text{CH}(\text{CH}_3)_2$), 18.5 (s, $\text{CH}(\text{CH}_3)_2$), 17.2 (s, $\text{CH}(\text{CH}_3)_2$). $^{31}\text{P}\{^1\text{H}\}$ NMR (δ , CD_2Cl_2 , 20°C): 147.1. IR (ATR, cm^{-1}): 1902 (ν_{CO}). ESI-MS (m/z , EtOH); pos. ion: 426.1 $[\text{M} - \text{Br}]^+$, 398.2 $[\text{M} - \text{Br} - \text{CO}]^+$.

$[\text{Fe}(\text{PNP}^{\text{Me}}-i\text{Pr})(\text{H})(\text{CO})\text{Br}]$ (2b**).** This complex was prepared analogously to **2a** using **1b** (300 mg, 0.81 mmol), FeBr_2 (175 mg, 0.81 mg), and $\text{Na}[\text{HBEt}_3]$ (0.89 mL, 1 M in toluene, 0.89 mmol) as starting materials. The product was obtained as a mixture of two isomers in a 2.7:1 ratio (**2b**, **2b'**). Yield: 276 mg (64%) of a red-orange powder. Anal. Calcd for $\text{C}_{20}\text{H}_{38}\text{BrFeN}_3\text{O}_2$: C, 44.96; H, 7.17; N, 7.87. Found: C, 44.86; H, 7.22; N, 7.07. **2b**: ^1H NMR (δ , CD_2Cl_2 , 20°C): 7.44 (t, $J = 8.3$ Hz, 1H, py^4), 6.02 (d, $J = 8.3$ Hz, 2H, $\text{py}^{3,5}$), 3.10 (s, 3H, NCH_3), 2.80 (m, 2H, $\text{CH}(\text{CH}_3)_2$), 2.55 (m, 2H, $\text{CH}(\text{CH}_3)_2$), 1.72 (dd, $J = 7.3$ Hz, $J = 16.6$, 6H, $\text{CH}(\text{CH}_3)_2$), 1.60 (dd, $J = 7.3$ Hz, $J = 14.5$, 6H, $\text{CH}(\text{CH}_3)_2$), 1.22 (dd, $J = 7.3$ Hz, $J = 16.8$, 6H, $\text{CH}(\text{CH}_3)_2$), 0.83 (dd, $J = 7.0$ Hz, $J = 14.1$, 6H, $\text{CH}(\text{CH}_3)_2$), -21.84 (t, $^2J_{\text{HP}} = 57.5$, 1H, FeH). $^{13}\text{C}\{^1\text{H}\}$ NMR (δ , CD_2Cl_2 , 20°C): 222.7 (t, $^2J_{\text{CP}} = 22.4$ Hz, CO), 162.6 (t, $^2J_{\text{CP}} = 11.4$ Hz, $\text{py}^{2,6}$), 138.9 (s, py^4), 96.6 (s, $\text{py}^{3,5}$), 34.0 (s, NCH_3), 33.6 (t, $^1J_{\text{CP}} = 9.3$ Hz, $\text{CH}(\text{CH}_3)_2$), 31.2 (t, $^1J_{\text{CP}} = 14.8$ Hz, $\text{CH}(\text{CH}_3)_2$), 21.7 (s, $\text{CH}(\text{CH}_3)_2$), 20.3 (t, $^2J_{\text{CP}} = 3.6$ Hz, $\text{CH}(\text{CH}_3)_2$), 18.3 (s, $\text{CH}(\text{CH}_3)_2$), 17.8 (t, $^2J_{\text{CP}} = 5.0$ Hz, $\text{CH}(\text{CH}_3)_2$). $^{31}\text{P}\{^1\text{H}\}$ NMR (δ , CD_2Cl_2 , 20°C): 164.0 (s). IR (ATR, cm^{-1}): 1903 (ν_{CO}). **2b'**: ^1H NMR (δ , CD_2Cl_2 , 20°C): 7.13 (t, $J = 8.2$ Hz, 1H, py^4), 5.65 (d, $J = 8.2$ Hz, 2H, $\text{py}^{3,5}$), 3.04 (m, 2H, $\text{CH}(\text{CH}_3)_2$), 2.97 (s, 3H, NCH_3), 2.83 (m, 2H, $\text{CH}(\text{CH}_3)_2$), 1.61 (dd, $J = 7.4$ Hz, $J = 16.1$, 6H, $\text{CH}(\text{CH}_3)_2$), 1.54 (dd, $J = 7.0$ Hz, $J = 14.3$, 6H, $\text{CH}(\text{CH}_3)_2$), 1.50 (dd, $J = 7.4$ Hz, $J = 16.3$, 6H, $\text{CH}(\text{CH}_3)_2$), 1.29 (dd, $J = 7.0$ Hz, $J = 14.3$, 6H, $\text{CH}(\text{CH}_3)_2$), -1.08 (t, $^2J_{\text{HP}} = 57.1$, 1H, FeH). $^{13}\text{C}\{^1\text{H}\}$ NMR (δ , CD_2Cl_2 , 20°C): 217.1 (t, $^2J_{\text{CP}} = 13.0$ Hz, CO), 163.5 (t, $^2J_{\text{CP}} = 9.8$ Hz, $\text{py}^{2,6}$), 137.0 (s, py^4), 95.4 (s, $\text{py}^{3,5}$), 33.3 (s, NCH_3), 31.6 (t, $^1J_{\text{CP}} = 12.9$ Hz, $\text{CH}(\text{CH}_3)_2$), 31.3 (t, $^1J_{\text{CP}} = 8.6$ Hz, $\text{CH}(\text{CH}_3)_2$), 19.2 (t, $^2J_{\text{CP}} = 3.7$ Hz, $\text{CH}(\text{CH}_3)_2$), 18.8 (s, $\text{CH}(\text{CH}_3)_2$), 18.7 (t, $^2J_{\text{CP}} = 2.3$ Hz, $\text{CH}(\text{CH}_3)_2$), 18.3 (s, $\text{CH}(\text{CH}_3)_2$). $^{31}\text{P}\{^1\text{H}\}$ NMR (δ , CD_2Cl_2 , 20°C): 161.6. IR (ATR, cm^{-1}): 1903 (ν_{CO}).

[Fe(PNP^H-Me-*i*Pr)(H)(CO)Br] (2c). This complex was prepared analogously to **2a** using **1c** (300 mg, 0.84 mmol), FeBr₂ (181 mg, 0.84 mg), and Na[HB(Et₃)₃] (0.92 mL, 1 M in toluene, 0.92 mmol) as starting materials. Yield: 275 mg (63%) of an orange powder. Anal. Calcd for C₁₉H₃₆BrFeN₃OP₂: C, 43.87; H, 6.98; N, 8.08. Found: C, 43.59; H, 7.19; N, 7.96. ¹H NMR (δ, CD₂Cl₂, 20 °C): 7.31 (t, *J* = 7.8 Hz, 1H, py⁴), 6.22 (d, *J* = 7.8 Hz, 1H, py^{3,5}), 5.91 (d, *J* = 7.8 Hz, 1H, py^{3,5}), 5.61 (bs, 1H, NH), 2.80 (m, 1H, CH(CH₃)₂), 3.07 (d, *J* = 3.1 Hz, 3H, NCH₃), 2.75 (m, 1H, CH(CH₃)₂), 2.53 (m, 2H, CH(CH₃)₂), 1.72 (dd, *J* = 6.9 Hz, *J* = 17.4 Hz, 3H, CH(CH₃)₂), 1.55 (dd, *J* = 7.3 Hz, *J* = 13.6 Hz, 3H, CH(CH₃)₂), 1.52 (dd, *J* = 7.8 Hz, *J* = 9.5 Hz, 3H, CH(CH₃)₂), 1.44 (dd, *J* = 7.1 Hz, *J* = 10.7 Hz, 3H, CH(CH₃)₂), 1.26 (dd, *J* = 6.8 Hz, *J* = 17.0 Hz, 3H, CH(CH₃)₂), 1.18 (dd, *J* = 6.9 Hz, *J* = 17.4 Hz, 3H, CH(CH₃)₂), 0.94 (dd, *J* = 6.7 Hz, *J* = 14.4 Hz, 3H, CH(CH₃)₂), 0.88 (dd, *J* = 6.7 Hz, *J* = 14.4 Hz, 3H, CH(CH₃)₂), -21.64 (t, ²*J*_{HP} = 57.2 Hz, FeH). ¹³C{¹H} NMR (δ, CD₂Cl₂, 20 °C): 222.5 (br, CO), 162.4 (br, py^{2,6}), 161.0 (br, py^{2,6}), 138.9 (s, py⁴), 98.2 (d, ³*J*_{CP} = 6.8 Hz, py^{3,5}), 95.7 (d, ³*J*_{CP} = 6.8 Hz, py^{3,5}), 33.5 (d, ¹*J*_{CP} = 21.7 Hz, CH(CH₃)₂), 33.4 (d, ²*J*_{CP} = 12.1 Hz, NCH₃), 31.7 (d, ¹*J*_{CP} = 28.6 Hz, CH(CH₃)₂), 29.0 (d, ¹*J*_{CP} = 22.8 Hz, CH(CH₃)₂), 27.1 (d, ¹*J*_{CP} = 24.1 Hz, CH(CH₃)₂), 21.1 (s, CH(CH₃)₂), 20.4 (d, ²*J*_{CP} = 8.8 Hz, CH(CH₃)₂), 19.5 (d, ²*J*_{CP} = 8.8 Hz, CH(CH₃)₂), 18.7 (d, ²*J*_{CP} = 10.1 Hz, CH(CH₃)₂), 18.5 (s, CH(CH₃)₂), 18.3 (s, CH(CH₃)₂), 18.0 (d, ²*J*_{CP} = 9.4 Hz, CH(CH₃)₂), 17.1 (d, ²*J*_{CP} = 7.9 Hz, CH(CH₃)₂). ³¹P{¹H} NMR (δ, CD₂Cl₂, 20 °C): 165.0 (d, *J*_{PP} = 145.1 Hz), 147.2 (d, *J*_{PP} = 145.1 Hz). IR (ATR, cm⁻¹): 1901 (ν_{CO}).

[Fe(PNP-*i*Pr)(H)(CO)(CH₃CN)BF₄] (3b). To a solution of **2a** (150 mg, 0.30 mmol) in CH₃CN (10 mL) was added AgBF₄ (58 mg, 0.30 mmol). After stirring for 5 min at room temperature, the precipitate was filtered off and the solvent was removed under reduced pressure. The product was washed twice with diethyl ether and dried under vacuum to afford a pale green powder. Yield: 148 mg (93%). Anal. Calcd for C₂₀H₃₇BF₄FeN₄OP₂: C, 43.35; H, 6.73; N, 10.11. Found: C, 43.28; H, 6.78; N, 10.02. ¹H NMR (δ, acetone-*d*₆, 20 °C): 7.64 (s, 2H, NH), 7.63 (t, *J* = 7.9 Hz, 1H, py⁴), 6.33 (d, *J* = 7.9 Hz, 2H, py^{3,5}), 2.67 (m, 4H, CH(CH₃)₂), 2.40 (s, 3H, CH₃CN), 1.53 (m, 12H, CH(CH₃)₂), 1.22 (dd, *J* = 7.1 Hz, *J* = 17.4 Hz, 6H, CH(CH₃)₂), 1.06 (dd, *J* = 6.9 Hz, *J* = 14.8 Hz, 6H, CH(CH₃)₂), -18.55 (t, ²*J*_{HP} = 53.3 Hz, 1H, FeH). ¹³C{¹H} NMR (δ, CD₂Cl₂, 20 °C): 218.7 (t, ²*J*_{CP} = 21.7 Hz, CO), 161.1 (t, ²*J*_{CP} = 9.0 Hz, py^{2,6}), 140.3 (s, py⁴), 127.2 (s, CH₃CN), 98.9 (s, py^{3,5}), 31.0 (t, ¹*J*_{CP} = 10.2 Hz, CH(CH₃)₂), 29.8 (t, ¹*J*_{CP} = 15.4 Hz, CH(CH₃)₂), 19.4 (s, CH(CH₃)₂), 18.2 (s, CH(CH₃)₂), 4.5 (s, CH₃CN). ³¹P{¹H} NMR (δ, CD₂Cl₂, 20 °C): 145.6. IR (ATR, cm⁻¹): 1929 (ν_{CO}). ESI-MS (*m/z*, EtOH); pos. ion: 426.1 [M - CH₃CN]⁺, 398.1 [M - CH₃CN - CO]⁺. Crystals suitable for X-ray crystallography were grown with Br⁻ as counterion (analogously prepared without the addition of a silver salt as halide scavenger) by slow evaporation of a CH₃CN/THF (1:1) solution.

[Fe(PNP-*i*Pr)(H)(CO)(py)BF₄] (3c). To a solution of **2a** (150 mg, 0.30 mmol) in CH₃OH (8 mL) was added pyridine (36 μL, 0.45 mmol). After stirring for 5 min at room temperature, AgBF₄ (58 mg, 0.30 mmol) was added and the reaction mixture was stirred for an additional 5 min. The dark precipitate was filtered off, and the solvent was removed under reduced pressure. The residue was washed twice with diethyl ether and dried under vacuum to afford a yellow powder. Yield: 150 mg (83%). Anal. Calcd for C₂₃H₃₉BF₄FeN₄OP₂: C, 46.65; H, 6.64; N, 9.46. Found: C, 47.07; H, 6.95; N, 9.29. ¹H NMR (δ, MeOH-*d*₄, 20 °C): 10.00–6.55 (broad and unresolved signals, 4H, pyridine-H^{2,3,5,6}), 7.77 (t, *J* = 7.6 Hz, 1H, pyridine-H⁴), 7.46 (t, *J* = 8.0 Hz, 1H, py⁴), 6.34 (d, *J* = 8.0 Hz, 2H, py^{3,5}), 2.50 (m, 2H, CH(CH₃)₂), 1.89 (m, 2H, CH(CH₃)₂), 1.28–1.19 (m, 12H, CH(CH₃)₂), 1.07 (dd, *J* = 6.8 Hz, *J* = 14.3 Hz, 6H, CH(CH₃)₂), 0.93 (dd, *J* = 7.5 Hz, *J* = 15.6 Hz, 6H, CH(CH₃)₂), -20.08 (t, ²*J*_{HP} = 52.9 Hz, 1H, FeH). ¹³C{¹H} NMR (δ, MeOH-*d*₄, 20 °C): 220.3 (t, ²*J*_{CP} = 22.8 Hz, CO), 163.0 (t, ²*J*_{CP} = 9.0 Hz, py^{2,6}), 141.0 (d, ³*J*_{CP} = 13.6 Hz, pyridine-C^{2,6}), 138.8 (s, pyridine-C⁴), 138.5 (s, py⁴), 126.9 (s, pyridine-C^{3,5}), 99.3–98.6 (unresolved signal), 30.3 (t, ¹*J*_{CP} = 16.3 Hz, CH(CH₃)₂), 18.9 (s, CH(CH₃)₂), 18.7 (s, CH(CH₃)₂), 18.3 (s, CH(CH₃)₂), 17.5 (s, CH(CH₃)₂). ³¹P{¹H} NMR (δ, MeOH-*d*₄, 20 °C): 142.3. IR (ATR,

cm⁻¹): 1906 (ν_{CO}). ESI-MS (*m/z*, EtOH); pos. ion: 505.1 [M]⁺, 426.1 [M - C₅H₅N]⁺.

[Fe(PNP-*i*Pr)(H)(CO)(PMe₃)BF₄] (3d). To a solution of **2a** (150 mg, 0.30 mmol) in CH₃OH (8 mL) was added PMe₃ (47 mL, 0.45 mmol). After stirring for 5 min at room temperature, AgBF₄ (58 mg, 0.30 mmol) was added and the reaction mixture was stirred for an additional 5 min. The dark precipitate was filtered off, and the solvent of the filtrate was removed *in vacuo*. The residue was washed twice with *n*-pentane and dried under high vacuum to give an off-white powder. Yield: 172 mg (97%). Anal. Calcd for C₂₁H₄₃BF₄FeN₃OP₃: C, 42.81; H, 7.36; N, 7.13. Found: C, 42.94; H, 7.58; N, 7.58. ¹H NMR (δ, MeOH-*d*₄, 20 °C): 7.31 (t, *J* = 7.8 Hz, 1H, py⁴), 6.22 (d, *J* = 7.8 Hz, 2H, py^{3,5}), 2.73 (m, 2H, CH(CH₃)₂), 2.62 (m, 2H, CH(CH₃)₂), 1.58–1.45 (m, 12H, CH(CH₃)₂), 1.25 (m, 6H, CH(CH₃)₂), 1.23 (d, *J* = 7.2 Hz, 3H, P(CH₃)₃), 0.99 (dd, *J* = 6.8 Hz, *J* = 14.7 Hz, 6H, CH(CH₃)₂), -11.09 (dt, ²*J*_{HP} = 35.7 Hz, ²*J*_{HP} = 60.7 Hz, 1H, FeH). ¹³C{¹H} NMR (δ, MeOH-*d*₄, 20 °C): 220.5 (dt, *J*_{CP} = 15.2 Hz, *J*_{CP} = 23.2 Hz, CO), 162.0 (t, *J*_{CP} = 8.4 Hz, py^{2,6}), 140.7 (s, py⁴), 98.9 (s, py^{3,5}), 34.7 (t, *J*_{CP} = 11.7 Hz, CH(CH₃)₂), 28.7 (dt, *J*_{CP} = 8.0 Hz, *J*_{CP} = 14.8 Hz, CH(CH₃)₂), 19.8 (t, *J*_{CP} = 4.6 Hz, CH(CH₃)₂), 19.0 (t, *J*_{CP} = 4.6 Hz, CH(CH₃)₂), 18.8 (d, *J*_{CP} = 23.2 Hz, P(CH₃)₃), 17.9 (s, CH(CH₃)₂), 17.4 (bs, CH(CH₃)₂). ³¹P{¹H} NMR (δ, MeOH-*d*₄, 20 °C): 147.3 (d, *J* = 25.6 Hz, 2P, PIP₂), 2.9 (t, *J* = 25.6 Hz, PMe₃). IR (ATR, cm⁻¹): 1910 (ν_{CO}). ESI-MS (*m/z*, EtOH); pos. ion: 502.2 [M]⁺, 426.1 [M - PMe₃]⁺.

[Fe(PNP-*i*Pr)(H)(CO)(κ⁻¹-N-SCN)] (3e). To a solution of **2a** (150 mg, 0.30 mmol) in THF (10 mL) was added NaSCN (27 mg, 0.33 mmol). After stirring for 1 h at room temperature, the solution was filtered and the solvent was removed under reduced pressure. The product was washed twice with diethyl ether and dried under vacuum to afford an off-white powder. Yield: 136 mg (93%). Anal. Calcd for C₁₉H₃₄FeN₄OP₂S: C, 47.12; H, 7.08; N, 11.57. Found: C, 47.18; H, 7.13; N, 11.42. ¹H NMR (δ, DMSO-*d*₆, 20 °C): 8.26 (s, 2H, NH), 7.26 (t, *J* = 7.9 Hz, 1H, py⁴), 6.13 (d, *J* = 7.9 Hz, 2H, py^{3,5}), 2.48 (m, 2H, CH(CH₃)₂), 2.41 (m, 2H, CH(CH₃)₂), 1.44 (m, 6H, CH(CH₃)₂), 1.38 (m, 6H, CH(CH₃)₂), 1.12 (m, 6H, CH(CH₃)₂), 0.95 (m, 6H, CH(CH₃)₂), -19.84 (t, ²*J*_{HP} = 52.1 Hz, 1H, FeH). ¹³C{¹H} NMR (δ, DMSO-*d*₆, 20 °C): 220.7 (t, ²*J*_{CP} = 24.1 Hz, CO), 161.0 (t, ²*J*_{CP} = 9.6 Hz, py^{2,6}), 138.7 (s, py⁴), 137.4 (d, ³*J*_{CP} = 5.4 Hz, SCN), 96.6 (s, py^{3,5}), 29.5 (t, ¹*J*_{CP} = 10.6 Hz, CH(CH₃)₂), 27.8 (t, ¹*J*_{CP} = 14.9 Hz, CH(CH₃)₂), 18.8 (s, CH(CH₃)₂), 17.9 (s, CH(CH₃)₂), 17.8 (s, CH(CH₃)₂), 17.4 (s, CH(CH₃)₂). ³¹P{¹H} NMR (δ, CD₂Cl₂, 20 °C): 146.6. IR (ATR, cm⁻¹): 2074 (ν_{NCS}), 1921 (ν_{CO}). ESI-MS (*m/z*, EtOH, NaCl); pos. ion: 507.1 [M + Na]⁺, 426.1 [M - SCN]⁺, 398.2 [M - SCN - CO]⁺.

[Fe(PNP-*i*Pr)(H)(CO)(κ⁻¹-BH₄)] (3g). *Method A.* To a solution of **2a** (200 mg, 0.40 mmol) in THF (24 mL) was added sodium borohydride (76 mg, 2.00 mmol). After stirring for 6 h at room temperature, the solution was filtered and the solvent was removed under reduced pressure. The residue was dissolved in THF (1.0 mL), and the product was precipitated by addition of *n*-pentane. The bright yellow powder was washed twice with *n*-pentane and dried under vacuum. Yield: 132 mg (75%).

Method B. To a suspension of [Fe(PNP-*i*Pr)(CO)(Br)₂] (200 mg, 0.40 mmol) in EtOH (10 mL) was added sodium borohydride (65 mg, 1.71 mmol). An immediate gas evolution took place, and the initially blue suspension turned into a dark orange solution within 5 min. After stirring the reaction mixture for 30 min, all volatiles were removed under reduced pressure. The residue was dissolved in dichloromethane (10 mL), the resulting solution was filtered, and the solvent was removed under vacuum. Yield: 136 mg (91%). Anal. Calcd for C₁₈H₃₈BF₄FeN₃OP₂: C, 49.01; H, 8.68; N, 9.53. Found: C, 48.95; H, 8.61; N, 9.77. ¹H NMR (δ, CD₂Cl₂, 20 °C): 7.17 (t, *J* = 7.9 Hz, 1H, py⁴), 6.13 (d, *J* = 7.9 Hz, 2H, py^{3,5}), 5.43 (bs, 2H, NH), 3.01 (m, 2H, CH(CH₃)₂), 2.50 (m, 2H, CH(CH₃)₂), 1.50 (dd, *J* = 7.6 Hz, *J* = 17.7 Hz, 6H, CH(CH₃)₂), 1.42 (dd, *J* = 7.0 Hz, *J* = 12.5 Hz, 6H, CH(CH₃)₂), 1.22 (dd, *J* = 7.0 Hz, *J* = 17.4 Hz, 6H, CH(CH₃)₂), 1.05 (dd, *J* = 6.7 Hz, *J* = 14.4 Hz, 6H, CH(CH₃)₂), -3.61 (br, 4H, BH₄), -18.12 (t, ²*J*_{HP} = 52.1 Hz, 1H, FeH). ¹³C{¹H} NMR (δ, CD₂Cl₂, 20 °C): 160.8 (t, ²*J*_{CP} = 9.1 Hz, py^{2,6}), 138.5 (s, py⁴), 97.3 (s, py^{3,5}), 31.4

($t, {}^1J_{\text{CP}} = 10.6$ Hz, $\text{CH}(\text{CH}_3)_2$), 27.8 ($t, {}^1J_{\text{CP}} = 13.2$ Hz, $\text{CH}(\text{CH}_3)_2$), 19.5 ($t, {}^2J_{\text{CP}} = 3.8$ Hz, $\text{CH}(\text{CH}_3)_2$), 18.6 ($t, {}^2J_{\text{CP}} = 4.6$ Hz, $\text{CH}(\text{CH}_3)_2$), 18.4 ($s, \text{CH}(\text{CH}_3)_2$), 17.4 ($s, \text{CH}(\text{CH}_3)_2$), the CO resonance could not be observed. ${}^{31}\text{P}\{^1\text{H}\}$ NMR (δ , CD_2Cl_2 , 20 °C): 151.2. IR (ATR, cm^{-1}): 1911 (ν_{CO}). ESI-MS (m/z , EtOH); pos. ion: 426.1 [$\text{M} - \text{BH}_4$] $^+$, 398.1 [$\text{M} - \text{BH}_4 - \text{CO}$] $^+$.

X-ray Structure Determination. X-ray diffraction data of **2a**, **CD₂Cl₂**, **3b**, **3c**, **3e**, and **3f** were collected at $T = 100$ K (**3f**: $T = 200$ K due to a phase transition at lower temperatures) in a dry stream of nitrogen on Bruker Kappa APEX II diffractometer systems using graphite-monochromatized Mo $K\alpha$ radiation ($\lambda = 0.710$ 73 Å) and fine sliced φ - and ω -scans. Data of **3d** were collected at $T = 185$ K on a Bruker SMART APEX diffractometer using ω -scans. Data were reduced to intensity values with SAINT, and an absorption correction was applied with the multiscan approach implemented in SADABS.²³ The structures were solved by charge flipping using SUPERFLIP²⁴ and refined against F with JANA2006.²⁵ Non-hydrogen atoms were refined anisotropically. The H atoms connected to C atoms were placed in calculated positions and thereafter refined as riding on the parent atoms. H atoms connected to N, B, and Fe atoms were located in difference Fourier maps. The Fe–H distances were restrained. The N–H distances were restrained in **2a**· CD_2Cl_2 and **3d**, whereas the N–H atoms in the remaining models were freely refined. In **3f**, the B–H distances were restrained to 1.000(1) Å. Molecular graphics were generated with the program MERCURY.²⁶ Crystal data and experimental details are given in Tables S1 and S2.

Computational Details. All calculations were performed using the Gaussian 09 software package²⁷ on the Phoenix Linux Cluster of the Vienna University of Technology. The optimized geometries were obtained with the B3LYP functional.²⁸ That functional includes a mixture of Hartree–Fock²⁹ exchange with DFT¹⁹ exchange–correlation, given by Becke’s three-parameter functional with the Lee, Yang, and Parr correlation functional, which includes both local and nonlocal terms. The basis set used for the geometry optimizations (basis b1) consisted of the Stuttgart/Dresden ECP (SDD) basis set³⁰ to describe the electrons of iron and a standard 6-31G(d,p) basis set³¹ for all other atoms. Transition-state optimizations were performed with the Synchronous Transit-Guided Quasi-Newton Method (STQN) developed by Schlegel et al.,³² following extensive searches of the potential energy surface. Frequency calculations were performed to confirm the nature of the stationary points, yielding one imaginary frequency for the transition states and none for the minima. Each transition state was further confirmed by following its vibrational mode downhill on both sides and obtaining the minima presented on the energy profiles. Atomic charges were obtained by means of a natural population analysis (NPA).³³ The electronic energies (E_{b1}) obtained at the B3LYP/b1 level of theory were converted to free energy at 298.15 K and 1 atm (G_{b1}) by using zero-point energy and thermal energy corrections based on structural and vibration frequency data calculated at the same level.

Single-point energy calculations were performed using the M06 functional and a standard 6-311++G(d,p) basis set,³⁴ on the geometries optimized at the B3LYP/b1 level. The M06 functional is a hybrid meta-GGA functional developed by Truhlar and Zhao,³⁵ and it was shown to perform very well for the kinetics of transition metal molecules, providing a good description of weak and long-range interactions.³⁶ Solvent effects (ethanol) were considered in the M06/6-311++G(d,p)//B3LYP/b1 energy calculations using the polarizable continuum model (PCM) initially devised by Tomasi and co-workers³⁷ with radii and nonelectrostatic terms of the SMD solvation model, developed by Truhler et al.³⁸ The free energy values presented ($G_{\text{b2}}^{\text{soln}}$) were derived from the electronic energy values obtained at the M06/6-311++G(d,p)//B3LYP/b1 level, including solvent effects ($E_{\text{b2}}^{\text{soln}}$), according to the following expression: $G_{\text{b2}}^{\text{soln}} = E_{\text{b2}}^{\text{soln}} + G_{\text{b1}} - E_{\text{b1}}$.

■ ASSOCIATED CONTENT

■ Supporting Information

Coordinates of the optimized structures, ${}^1\text{H}$, ${}^{13}\text{C}\{^1\text{H}\}$, and ${}^{31}\text{P}\{^1\text{H}\}$ NMR spectra of all complexes, crystallographic data and technical details in CIF format for **2a**, **3b**, **3e** (CCDC 1010393–1010395) and **3c**, **3d**, **3g** (CCDC 1023528–1023530). This material is available free of charge via the Internet at <http://pubs.acs.org>.

■ AUTHOR INFORMATION

Corresponding Author

*E-mail: kkirch@mail.tuwien.ac.at.

Notes

The authors declare no competing financial interest.

■ ACKNOWLEDGMENTS

Financial support by the Austrian Science Fund (FWF) is gratefully acknowledged (Project No. P24583-N28), and L.F.V. and L.P.F. acknowledge Fundação para a Ciência e Tecnologia, Projecto Estratégico - PEst-OE/QUI/UI0100/2013 and PEst-OE/FIS/UI0261/2014, respectively. The X-ray center of the Vienna University of Technology is acknowledged for financial support and for providing access to the single-crystal diffractometer.

■ REFERENCES

- (1) (a) Noyori, R.; Ohkuma, T. *Angew. Chem., Int. Ed.* **2001**, *40*, 40–73. (b) Noyori, R. *Angew. Chem., Int. Ed.* **2013**, *52*, 79–92. (c) de Vries, J. G.; Elsevier, C. J., Eds. *Handbook of Homogeneous Hydrogenation*; Wiley-VCH: Weinheim, 2007. (d) Johnson, N. B.; Lennon, I. C.; Moran, P. H.; Ramsden, J. A. *Acc. Chem. Res.* **2007**, *40*, 1291–1299. (e) Dub, P. A.; Ikariya, T. *ACS Catal.* **2012**, *2*, 1718–1741.
- (2) For recent reviews on iron-catalyzed reaction see: (a) Morris, R. H. *Chem. Soc. Rev.* **2009**, *38*, 2282–2291. (b) Enthaler, S.; Junge, K.; Beller, M. *Angew. Chem., Int. Ed.* **2008**, *47*, 3317–3321. (c) Gaillard, S.; Renaud, J.-L. *ChemSusChem* **2008**, *1*, 505–509. (d) Bauer, G.; Kirchner, K. A. *Angew. Chem., Int. Ed.* **2011**, *50*, 5798–5800. (e) Bullock, R. M. *Science* **2013**, *342*, 1054–1055. (f) Sues, P. E.; Demmans, Z.; Morris, R. H. *Dalton Trans.* **2014**, *43*, 7650–7667.
- (3) (a) Casey, C. P.; Guan, H. *J. Am. Chem. Soc.* **2007**, *129*, 5816–5817. (b) Casey, C. P.; Guan, H. *J. Am. Chem. Soc.* **2009**, *131*, 2499–2507.
- (4) (a) Langer, R.; Leitius, G.; Ben-David, Y.; Milstein, D. *Angew. Chem., Int. Ed.* **2011**, *50*, 2120–2124. (b) Langer, R.; Diskin-Posner, Y.; Leitius, G.; Shimon, L. J.; Ben-David, Y.; Milstein, D. *Angew. Chem., Int. Ed.* **2011**, *50*, 9948–9952. (c) Langer, R.; Iron, M. A.; Konstantinovski, L.; Diskin-Posner, Y.; Leitius, G.; Ben-David, Y.; Milstein, D. *Chem.—Eur. J.* **2012**, *18*, 7196–7209. (d) Zell, T.; Butschke, B.; Ben-David, Y.; Milstein, D. *Chem.—Eur. J.* **2013**, *19*, 8068–8072. (e) Zell, T.; Ben-David, Y.; Milstein, D. *Angew. Chem., Int. Ed.* **2014**, *53*, 4685–4689.
- (5) Berkessel, A.; Reichau, S.; von der Höh, A.; Leconte, N.; Neudörfl, J.-M. *Organometallics* **2011**, *30*, 3880–3887.
- (6) (a) Sui-Seng, C.; Freutel, F.; Lough, A. J.; Morris, R. H. *Angew. Chem., Int. Ed.* **2008**, *47*, 940–943. (b) Sui-Seng, C.; Haque, F. N.; Hadzovic, A.; Pütz, A.-M.; Reuss, V.; Meyer, N.; Lough, A. J.; Zimmer-De Iulius, M.; Morris, R. H. *Inorg. Chem.* **2009**, *48*, 735–743. (c) Lagaditis, P. O.; Sues, P. E.; Sonnenberg, J. F.; Wan, K. Y.; Lough, A. J.; Morris, R. H. *J. Am. Chem. Soc.* **2014**, *136*, 1367–1380. (d) Zuo, W.; Tauer, S.; Prokopchuk, D. E.; Morris, R. H. *Organometallics* **2014**, *33*, 5791–5801. (e) Sonnenberg, J. F.; Lough, A. J.; Morris, R. H. *Organometallics* **2014**, in press.
- (7) (a) Tlili, A.; Schranck, J.; Neumann, H.; Beller, M. *Chem.—Eur. J.* **2012**, *18*, 15935–15939. (b) Fleischer, S.; Zhou, S.; Junge, K.; Beller, M. *Angew. Chem., Int. Ed.* **2013**, *52*, 5120–5124.

- (8) (a) Crabtree, R. H. *New J. Chem.* **2011**, *35*, 18–23. (b) Grützmacher, H. *Angew. Chem., Int. Ed.* **2008**, *47*, 1814–1818. (c) van der Vlugt, J. I.; Reek, J. N. H. *Angew. Chem., Int. Ed.* **2009**, *48*, 8832–8846.
- (9) (a) Gunanathan, C.; Milstein, D. *Acc. Chem. Res.* **2011**, *44*, 588–602. (b) Gunanathan, C.; Milstein, D. *Top. Organomet. Chem.* **2011**, *37*, 55–84. (c) Poverenov, E.; Milstein, D. *Top. Organomet. Chem.* **2013**, *40*, 21–47. (d) Chang, Y.-H.; Nakajima, Y.; Tanaka, H.; Yoshizawa, K.; Ozawa, F. *J. Am. Chem. Soc.* **2013**, *135*, 11791–11794.
- (10) (a) Bichler, B.; Glatz, M.; Stöger, B.; Mereiter, K.; Veiros, L. F.; Kirchner, K. *Dalton Trans.* **2014**, *43*, 14517–15419. (b) de Aguiar, S. R. M. M.; Öztöpcü, Ö.; Stöger, B.; Mereiter, K.; Veiros, L. F.; Pittenauer, E.; Allmaier, G.; Kirchner, K. *Dalton Trans.* **2014**, *43*, 14669–14679.
- (11) Bichler, B.; Holzhaecker, C.; Stöger, B.; Puchberger, M.; Veiros, L. F.; Kirchner, K. *Organometallics* **2013**, *32*, 4114–4121.
- (12) Wienhöfer, G.; Westerhaus, F. A.; Junge, K.; Ludwig, R.; Beller, M. *Chem.—Eur. J.* **2013**, *19*, 7701–7707.
- (13) Benito-Garagorri, D.; Alves, L. G.; Puchberger, M.; Mereiter, K.; Veiros, L. F.; Calhorda, M. J.; Carvalho, M. D.; Ferreira, L. P.; Godinho, M.; Kirchner, K. *Organometallics* **2009**, *28*, 6902–6914.
- (14) Sandoval, C. A.; Ohkuma, T.; Muniz, K.; Noyori, R. *J. Am. Chem. Soc.* **2003**, *125*, 13490–13503.
- (15) Bielinski, E. A.; Lagaditis, P. O.; Zhang, Y.; Mercado, B. Q.; Würtele, C.; Bernskoetter, W. H.; Hazari, N.; Schneider, S. *J. Am. Chem. Soc.* **2014**, *136*, 10234–10237.
- (16) Chakraborty, S.; Brennessel, W. W.; Jones, W. D. *J. Am. Chem. Soc.* **2014**, *136*, 8564–8567.
- (17) Yang, Y. *Inorg. Chem.* **2011**, *50*, 12836–12843.
- (18) Chakraborty, S.; Dai, H.; Bhattacharya, P.; Fairweather, N. T.; Gibson, M. S.; Krause, J. A.; Guan, H. *J. Am. Chem. Soc.* **2014**, *136*, 7869–7872.
- (19) Parr, R. G.; Yang, W. *Density Functional Theory of Atoms and Molecules*; Oxford University Press: New York, 1989.
- (20) Perrin, D. D.; Armarego, W. L. F. *Purification of Laboratory Chemicals*, 3rd ed.; Pergamon: New York, 1988.
- (21) Benito-Garagorri, D.; Becker, E.; Wiedermann, J.; Lackner, W.; Pollak, M.; Mereiter, K.; Kisala, J.; Kirchner, K. *Organometallics* **2006**, *25*, 1900–1913.
- (22) Öztöpcü, Ö.; Holzhaecker, C.; Puchberger, M.; Weil, M.; Mereiter, K.; Veiros, L. F.; Kirchner, K. *Organometallics* **2013**, *32*, 3042–3052.
- (23) Bruker computer programs: APEX2, SAINT, and SADABS; Bruker AXS Inc.: Madison, WI, 2012.
- (24) Palatinus, L.; Chapuis, G. *J. Appl. Crystallogr.* **2007**, *40*, 786–790.
- (25) Petříček, V.; Dušek, M.; Palatinus, L. *JANA2006, the crystallographic computing system*; Institute of Physics: Praha, Czech Republic, 2006.
- (26) Macrae, C. F.; Edgington, P. R.; McCabe, P.; Pidcock, E.; Shields, G. P.; Taylor, R.; Towler, M.; van de Streek, J. *J. Appl. Crystallogr.* **2006**, *39*, 453.
- (27) Frisch, M. J.; Trucks, G. W.; Schlegel, H. B.; Scuseria, G. E.; Robb, M. A.; Cheeseman, J. R.; Scalmani, G.; Barone, V.; Mennucci, B.; Petersson, G. A.; Nakatsuji, H.; Caricato, M.; Li, X.; Hratchian, H. P.; Izmaylov, A. F.; Bloino, J.; Zheng, G.; Sonnenberg, J. L.; Hada, M.; Ehara, M.; Toyota, K.; Fukuda, R.; Hasegawa, J.; Ishida, M.; Nakajima, T.; Honda, Y.; Kitao, O.; Nakai, H.; Vreven, T.; Montgomery, J. A., Jr.; Peralta, J. E.; Ogliaro, F.; Bearpark, M.; Heyd, J. J.; Brothers, E.; Kudin, K. N.; Staroverov, V. N.; Kobayashi, R.; Normand, J.; Raghavachari, K.; Rendell, A.; Burant, J. C.; Iyengar, S. S.; Tomasi, J.; Cossi, M.; Rega, N.; Millam, J. M.; Klene, M.; Knox, J. E.; Cross, J. B.; Bakken, V.; Adamo, C.; Jaramillo, J.; Gomperts, R.; Stratmann, R. E.; Yazyev, O.; Austin, A. J.; Cammi, R.; Pomelli, C.; Ochterski, J. W.; Martin, R. L.; Morokuma, K.; Zakrzewski, V. G.; Voth, G. A.; Salvador, P.; Dannenberg, J. J.; Dapprich, S.; Daniels, A. D.; Farkas, Ö.; Foresman, J. B.; Ortiz, J. V.; Cioslowski, J.; Fox, D. J. *Gaussian 09, Revision A.02*; Gaussian, Inc.: Wallingford, CT, 2009.
- (28) (a) Becke, A. D. *J. Chem. Phys.* **1993**, *98*, 5648–5652. (b) Miehlich, B.; Savin, A.; Stoll, H.; Preuss, H. *Chem. Phys. Lett.* **1989**, *157*, 200–206. (c) Lee, C.; Yang, W.; Parr, G. *Phys. Rev. B* **1988**, *37*, 785–789.
- (29) Hehre, W. J.; Radom, L.; Schleyer, P. v. R.; Pople, J. A. *Ab Initio Molecular Orbital Theory*; John Wiley & Sons: New York, 1986.
- (30) (a) Haeusermann, U.; Dolg, M.; Stoll, H.; Preuss, H. *Mol. Phys.* **1993**, *78*, 1211–1224. (b) Kuechle, W.; Dolg, M.; Stoll, H.; Preuss, H. *J. Chem. Phys.* **1994**, *100*, 7535–7542. (c) Leininger, T.; Nicklass, A.; Stoll, H.; Dolg, M.; Schwerdtfeger, P. *J. Chem. Phys.* **1996**, *105*, 1052–1059.
- (31) (a) McLean, A. D.; Chandler, G. S. *J. Chem. Phys.* **1980**, *72*, 5639–5648. (b) Krishnan, R.; Binkley, J. S.; Seeger, R.; Pople, J. A. *J. Chem. Phys.* **1980**, *72*, 650–654. (c) Wachters, A. J. H. *J. Chem. Phys.* **1970**, *52*, 1033–1036. (d) Hay, P. J. *J. Chem. Phys.* **1977**, *66*, 4377–4384. (e) Raghavachari, K.; Trucks, G. W. *J. Chem. Phys.* **1989**, *91*, 1062–1065. (f) Binning, R. C., Jr.; Curtiss, L. A. *J. Comput. Chem.* **1990**, *11*, 1206. (g) McGrath, M. P.; Radom, L. *J. Chem. Phys.* **1991**, *94*, 511–516.
- (32) (a) Peng, C.; Ayala, P. Y.; Schlegel, H. B.; Frisch, M. J. *J. Comput. Chem.* **1996**, *17*, 49–56. (b) Peng, C.; Schlegel, H. B. *Isr. J. Chem.* **1993**, *33*, 449–454.
- (33) (a) Carpenter, J. E.; Weinhold, F. *J. Mol. Struct. (Theochem)* **1988**, *169*, 41–62. (b) Carpenter, J. E. Ph.D. Thesis. University of Wisconsin, Madison, WI, 1987. (c) Foster, J. P.; Weinhold, F. *J. Am. Chem. Soc.* **1980**, *102*, 7211–7218. (d) Reed, A. E.; Weinhold, F. *J. Chem. Phys.* **1983**, *78*, 4066–4073. (e) Reed, A. E.; Weinhold, F. *J. Chem. Phys.* **1985**, *83*, 1736–1740. (f) Reed, A. E.; Weinstock, R. B.; Weinhold, F. *J. Chem. Phys.* **1985**, *83*, 735–746. (g) Reed, A. E.; Curtiss, L. A.; Weinhold, F. *Chem. Rev.* **1988**, *88*, 899–926. (h) Weinhold, F.; Carpenter, J. E. *The Structure of Small Molecules and Ions*; Plenum: New York, 1988; p 227.
- (34) (a) McClean, A. D.; Chandler, G. S. *J. Chem. Phys.* **1980**, *72*, 5639–5648. (b) Krishnan, R.; Binkley, J. S.; Seeger, R.; Pople, J. A. *J. Chem. Phys.* **1980**, *72*, 650–654. (c) Wachters, A. J. H. *J. Chem. Phys.* **1970**, *52*, 1033–1036. (d) Hay, P. J. *J. Chem. Phys.* **1977**, *66*, 4377–4384. (e) Raghavachari, K.; Trucks, G. W. *J. Chem. Phys.* **1989**, *91*, 1062–1065. (f) Binning, R. C., Jr.; Curtiss, L. A. *J. Comput. Chem.* **1990**, *11*, 1206–1216. (g) McGrath, M. P.; Radom, L. *J. Chem. Phys.* **1991**, *94*, 511–516. (h) Clark, T.; Chandrasekhar, J.; Spitznagel, G. W.; Schleyer, P. v. R. *J. Comput. Chem.* **1983**, *4*, 294–301. (i) Frisch, M. J.; Pople, J. A.; Binkley, J. S. *J. Chem. Phys.* **1984**, *80*, 3265–3269.
- (35) Zhao, Y.; Truhlar, D. G. *Theor. Chem. Acc.* **2008**, *120*, 215–241.
- (36) (a) Zhao, Y.; Truhlar, D. G. *Acc. Chem. Res.* **2008**, *41*, 157–167. (b) Zhao, Y.; Truhlar, D. G. *Chem. Phys. Lett.* **2011**, *502*, 1–13.
- (37) (a) Cancès, M. T.; Mennucci, B.; Tomasi, J. *J. Chem. Phys.* **1997**, *107*, 3032–3041. (b) Cossi, M.; Barone, V.; Mennucci, B.; Tomasi, J. *J. Chem. Phys. Lett.* **1998**, *286*, 253–260. (c) Mennucci, B.; Tomasi, J. *J. Chem. Phys.* **1997**, *106*, 5151–5158. (d) Tomasi, J.; Mennucci, B.; Cammi, R. *Chem. Rev.* **2005**, *105*, 2999–3094.
- (38) Marenich, A. V.; Cramer, C. J.; Truhlar, D. G. *J. Phys. Chem. B* **2009**, *113*, 6378–6396.

Supporting Information

Efficient Hydrogenation of Ketones and Aldehydes Catalyzed by Well-defined Iron(II) PNP Pincer Complexes – Evidence for an Insertion Mechanism

Nikolaus Gorgas, Berthold Stöger, Luis F. Veiros, Ernst Pittenauer, Günter Allmaier, and Karl
Kirchner*

Details for the crystal structure determinations	S2-S3
Coordinates of the optimized structures	S4-S12
NMR spectra of all complexes	S13-S36

Table S1. Details for the crystal structure determinations of **2a**·CD₂Cl₂, **3b**, and **3c**.

	2a ·CD ₂ Cl ₂	3b	3c
formula	C ₁₉ H ₃₄ BrCl ₂ D ₂ FeN ₃ OP ₂	C ₂₀ H ₃₇ BrFeN ₄ OP ₂	C ₂₃ H ₃₉ BF ₄ FeN ₄ OP ₂
fw	593.1	547.2	592.2
cryst.size, mm	0.67 x 0.35 x 0.08	0.44 x 0.34 x 0.03	0.65 x 0.32 x 0.32
color, shape	yellow rhombic prism	dark red triangular plate	yellow irregular rod
crystal system	orthorhombic	orthorhombic	orthorhombic
space group	<i>Pna</i> 2 ₁ (no. 33)	<i>Pbca</i> (no. 61)	<i>Pnma</i> (no. 62)
<i>a</i> , Å	18.885(3)	16.083(3)	14.2000(4)
<i>b</i> , Å	13.024(2)	19.993(3)	11.2801(6)
<i>c</i> , Å	10.5229(19)	31.806(5)	17.5587(7)
<i>V</i> , Å ³	2588.3(8)	10227(3)	2812.5(2)
<i>T</i> , K	100	100	100
<i>Z</i>	4	16	4
ρ_{calc} , g cm ⁻³	1.5216	1.4217	1.3981
μ , mm ⁻¹ (MoK α)	2.472	2.296	0.700
<i>F</i> (000)	1216	4544	1240
absorption corrections, <i>T</i> _{min}	multi-scan, 0.37–0.82	multi-scan, 0.41–0.94	multi-scan, 0.76–0.86
θ range, deg	1.90–39.36	1.28–27.55	1.84–32.69
no. of rflns measd	184112	364570	47499
<i>R</i> _{int}	0.0583	0.0558	0.0282
no. of rflns unique	15162	11779	5364
no. of rflns <i>I</i> > 3 σ (<i>I</i>)	14174	9118	4567
no. of params / restraints	275 / 3	529 / 2	191 / 1
<i>R</i> (<i>I</i> > 3 σ (<i>I</i>)) ^a	0.0264	0.0393	0.0266
<i>R</i> (all data)	0.0298	0.0575	0.0339
<i>wR</i> (<i>I</i> > 3 σ (<i>I</i>))	0.0323	0.0496	0.0367
<i>wR</i> (all data)	0.0326	0.0505	0.0374
Goof	1.77	2.77	2.16
Diff.Four.peaks min/max, eÅ ⁻³	-0.72 / 0.95	-2.10 / 1.25	-0.28 / 0.50

^a $R = \sum ||F_o| - |F_c|| / \sum |F_o|$, $wR = \sum w(|F_o| - |F_c|) / \sum w|F_o|$, $\text{Goof} = \{\sum [w(F_o^2 - F_c^2)^2] / (n-p)\}^{1/2}$

Table S2. Details for the crystal structure determinations of **3d**, **3e**, and **3f**.

	3d	3e	3g
formula	C ₂₁ H ₄₃ BF ₄ FeN ₃ OP ₃	C ₁₉ H ₃₄ FeN ₄ OP ₂ S	C ₁₈ H ₃₈ BFeN ₃ OP ₂
fw	589.2	484.4	441.1
cryst.size, mm	0.84 x 0.72 x 0.12	0.56 x 0.30 x 0.18	0.46 x 0.39 x 0.10
color, shape	colourless plate	yellow rhombic prism	dark yellow rhombic prism
crystal system	monoclinic	orthorhombic	monoclinic
space group	<i>P2₁/c</i> (no. 14)	<i>Pbca</i> (no. 61)	<i>P2₁/c</i> (no. 14)
a, Å	8.5095(2)	11.641(3)	11.5662(10)
b, Å	20.2457(5)	15.517(3)	13.0257(12)
c, Å	17.1097(5)	26.757(6)	15.2625(14)
β, °	97.9075(14)	90	90.122(3)
V, Å ³	2919.64(13)	4833.3(18)	2299.4(4)
T, K	185	100	200
Z	4	8	4
ρ _{calc} , g cm ⁻³	1.3399	1.3308	1.2738
μ, mm ⁻¹ (MoKα)	0.725	0.859	0.807
F(000)	1240	2048	944
absorption corrections, T _{min} -	Multi-scan, 0.55–0.92	multi-scan, 0.74–0.86	multi-scan, 0.79–0.90
θ range, deg	2.01–30.10	2.32–30.15	2.06–30.12
no. of rflns measd	32570	146427	83935
R _{int}	0.0396	0.0422	0.0541
no. of rflns unique	8547	7120	6775
no. of rflns >3σ(I)	6955	6030	4600
no. of params / restraints	359 / 3	265 / 0	283 / 4
R (I > 3σ(I)) ^a	0.0348	0.0231	0.0495
R (all data)	0.0441	0.0316	0.0884
wR (I > 3σ(I))	0.0480	0.0324	0.0493
wR (all data)	0.0491	0.0331	0.0512
GooF	1.92	1.99	2.19
Diff.Four.peaks min/max, eÅ ⁻³	-0.20 / 0.61	-0.22 / 0.33	-0.50 / 0.78

^a $R = \sum ||F_o| - |F_c|| / \sum |F_o|$, $wR = \sum w(|F_o| - |F_c|) / \sum w|F_o|$, $GooF = \{\sum [w(F_o^2 - F_c^2)^2] / (n-p)\}^{1/2}$

Atomic Coordinates for all the optimized molecules (B3LYP/b1)

H₂				H	2.421871	-2.645702	-1.754347
H	-0.678813	-0.385346	-1.963920	H	4.027324	-2.610825	-1.009749
H	-0.260100	-0.948947	-1.721497	H	4.229726	-0.577429	1.209487
MeCHO				H	3.438859	-0.086776	3.518913
O	-1.508785	-0.866646	2.778154	H	1.791109	0.161921	2.918071
C	-2.379402	-1.528287	2.258381	H	3.083206	1.266753	2.419963
H	-3.128246	-1.051073	1.585301	H	3.503730	-2.465920	2.653776
C	-2.553790	-3.013522	2.446278	H	3.096404	-2.845910	-0.977319
H	-1.785528	-3.406290	3.114404	H	1.835904	-2.296766	2.085211
H	-2.501392	-3.519207	1.474275	H	-0.000451	-0.687436	1.281223
H	-3.550240	-3.221267	2.855048	B			
EtOH				Fe	-0.014546	0.191874	0.488396
O	-1.031893	-1.236576	1.818657	P	-2.276649	-0.072253	0.300877
H	-0.366069	-1.610226	2.410959	P	2.262645	-0.088199	0.250002
C	-2.309896	-1.547836	2.362110	N	0.012861	-1.205487	-1.024357
H	-2.443435	-1.087000	3.354292	N	-2.303316	-1.353844	-0.845535
H	-3.034408	-1.075067	1.691092	N	2.386598	-1.080676	-1.094077
C	-2.570062	-3.049177	2.442633	C	-1.127687	-1.752596	-1.496043
H	-1.861952	-3.535882	3.124534	C	-1.166458	-2.659440	-2.550277
H	-2.462223	-3.509950	1.456303	C	0.062610	-3.011133	-3.135820
H	-3.580202	-3.253549	2.814256	C	1.244089	-2.481770	-2.671196
A				C	1.239333	-1.564079	-1.573910
Fe	-0.001323	-0.430433	-0.169896	C	-3.200479	-0.829682	1.754653
P	-2.222105	-0.158446	-0.096030	C	-4.572816	-1.430008	1.416197
P	2.233549	-0.111236	-0.071816	C	-3.280979	0.110900	2.969064
N	0.026411	1.564428	-0.197418	C	-3.493673	1.182412	-0.426700
N	-2.306349	1.551295	-0.243126	C	-3.436735	2.528689	0.316150
N	2.406722	1.564377	-0.083682	C	-3.286123	1.374019	-1.937980
C	-1.126188	2.297700	-0.221421	C	3.158533	-1.053594	1.602753
C	-1.153990	3.681489	-0.236979	C	4.471474	-1.681279	1.110888
C	0.084099	4.358222	-0.221418	C	3.355393	-0.270773	2.909828
C	1.266156	3.665621	-0.181952	C	3.471059	1.331746	-0.089746
C	1.265852	2.232245	-0.152029	C	3.554104	1.678981	-1.583026
C	-3.326012	-0.710586	-1.518551	C	3.207796	2.575772	0.773463
C	-4.694917	-0.014943	-1.571219	C	0.012470	-0.779116	1.922490
C	-3.473712	-2.239021	-1.605222	O	0.024476	-1.346479	2.938631
C	-3.162437	-0.568919	1.482251	H	-3.161797	-1.745453	-1.208429
C	-2.897001	-2.020126	1.921346	H	-2.107463	-3.072414	-2.896396
C	-2.786114	0.409440	2.606580	H	0.074800	-3.715007	-3.964644
C	3.281896	-0.627117	-1.552026	H	2.203256	-2.747127	-3.098585
C	4.662662	0.047877	-1.552801	H	-2.531441	-1.656541	2.020866
C	3.392996	-2.143631	-1.770023	H	-4.964977	-1.968065	2.286535
C	3.165567	-0.690522	1.454060	H	-4.518777	-2.149708	0.593296
C	2.850888	0.224427	2.647252	H	-5.308602	-0.661470	1.155574
C	2.884075	-2.161025	1.802115	H	-3.576139	-0.458342	3.857197
C	0.039771	-2.171227	-0.323905	H	-4.032536	0.894099	2.824955
O	0.063779	-3.334001	-0.386348	H	-2.321254	0.589256	3.181083
H	-3.167416	2.075817	-0.174185	H	-4.495337	0.757654	-0.279875
H	-2.096420	4.216498	-0.265788	H	-4.193122	3.211133	-0.088729
H	0.094000	5.445239	-0.236928	H	-2.459885	3.006533	0.200145
H	2.228336	4.161717	-0.159718	H	-3.620070	2.428608	1.387808
H	-2.744249	-0.377168	-2.388809	H	-4.022444	2.089112	-2.323203
H	-5.234498	-0.325013	-2.473165	H	-3.403979	0.438926	-2.490268
H	-4.603321	1.074457	-1.610668	H	-2.289173	1.759337	-2.165949
H	-5.322529	-0.280105	-0.713550	H	2.457830	-1.873789	1.801886
H	-3.927850	-2.511628	-2.564277	H	4.842263	-2.399068	1.852601
H	-4.129246	-2.624704	-0.817973	H	5.256718	-0.929130	0.971860
H	-2.513407	-2.756724	-1.532790	H	4.323929	-2.198945	0.160641
H	-4.232199	-0.455044	1.260850	H	3.712171	-0.943294	3.698741
H	-3.481962	-2.245740	2.820062	H	2.428776	0.191051	3.262480
H	-1.839143	-2.158986	2.160854	H	4.108687	0.516391	2.794555
H	-3.166750	-2.754569	1.158870	H	4.449180	0.927640	0.199444
H	-3.338001	0.152221	3.517560	H	4.358668	2.405388	-1.753728
H	-3.018927	1.446287	2.351284	H	2.623725	2.122217	-1.952626
H	-1.716391	0.351938	2.830569	H	3.748199	0.785175	-2.178607
H	2.703021	-0.204563	-2.385769	H	4.034950	3.289027	0.670272
H	5.153874	-0.105830	-2.521118	H	3.098352	2.339220	1.834259
H	5.317424	-0.382023	-0.786264	H	2.293341	3.091163	0.464965
H	4.574120	1.120144	-1.367478	H	-0.002999	1.334700	1.511937
H	3.857335	-2.345746	-2.742428	O	0.028618	1.632232	-1.001339
				C	0.042328	2.849565	-0.858406
				H	0.012656	3.267111	0.160744

C	0.099321	3.800575	-2.010760	N	0.068068	1.825298	-0.062466
H	-0.757549	4.484183	-1.968017	N	-2.260032	1.859633	-0.239015
H	0.999584	4.421433	-1.922699	N	2.438608	1.730474	0.092784
H	0.109598	3.265967	-2.961871	C	-1.056661	2.573545	-0.170994
C				C	-1.046257	3.962127	-0.211920
Fe	-0.078992	-0.025022	0.314977	C	0.205105	4.599903	-0.137890
P	-2.330659	-0.203630	-0.129821	C	1.364620	3.869631	-0.029937
P	2.220208	-0.201518	0.125430	C	1.315077	2.441174	0.003373
N	0.030766	-1.584328	-0.996807	C	-3.260287	-0.452058	-1.473362
N	-2.304857	-1.615109	-1.101340	C	-4.688071	0.106815	-1.569167
N	2.401454	-1.575897	-0.819447	C	-3.236511	-1.983206	-1.625142
C	-1.086390	-2.177784	-1.495516	C	-3.367742	-0.086021	1.511530
C	-1.055936	-3.274644	-2.345006	C	-3.465435	-1.573909	1.898587
C	0.205225	-3.804468	-2.676358	C	-2.873026	0.758873	2.696953
C	1.354920	-3.247329	-2.174271	C	3.324918	-0.399932	-1.454091
C	1.287848	-2.110540	-1.306869	C	4.711756	0.262735	-1.417985
C	-3.522689	-0.659557	1.242597	C	3.424286	-1.898141	-1.771175
C	-4.964836	-0.911331	0.777664	C	3.273827	-0.557136	1.540139
C	-3.460799	0.314188	2.432834	C	3.022354	0.324789	2.772309
C	-3.184153	1.057217	-1.225555	C	3.006510	-2.038474	1.853181
C	-3.492271	2.372482	-0.490777	C	0.043257	-0.468787	-1.702546
C	-2.320510	1.312566	-2.472558	O	0.082332	-0.637964	-2.845979
C	3.299467	-0.596977	1.610049	H	-3.101981	2.418439	-0.275593
C	4.758927	-0.872699	1.216860	H	-1.971200	4.521090	-0.298122
C	3.183902	0.376561	2.792166	H	0.250943	5.685618	-0.166959
C	3.137105	1.075461	-0.920767	H	2.339894	4.337065	0.024478
C	2.317386	1.371111	-2.187071	H	-2.675329	-0.025847	-2.298319
C	3.579696	2.374195	-0.235331	H	-5.134358	-0.185513	-2.526118
C	-0.090712	-1.008254	1.738893	H	-4.714760	1.200839	-1.524188
O	-0.108381	-1.608828	2.731645	H	-5.333663	-0.286523	-0.777212
H	-3.131293	-2.000728	-1.538031	H	-3.547410	-2.253776	-2.640024
H	-1.976347	-3.706084	-2.722117	H	-3.930231	-2.467502	-0.932272
H	0.263638	-4.666523	-3.336078	H	-2.242483	-2.397692	-1.445459
H	2.338114	-3.636433	-2.407493	H	-4.364630	0.281473	1.232061
H	-3.098355	-1.616251	1.574993	H	-3.973668	-1.668398	2.864820
H	-5.561666	-1.303285	1.608743	H	-2.472293	-2.026849	1.973847
H	-5.019583	-1.646695	-0.032398	H	-4.038917	-2.152107	1.170499
H	-5.447394	0.009492	0.434569	H	-3.605589	0.707435	3.509794
H	-4.004786	-0.112506	3.282701	H	-2.733474	1.811129	2.433921
H	-3.920470	1.277848	2.198718	H	-1.926889	0.377896	3.095559
H	-2.432125	0.504177	2.748087	H	2.750945	0.078916	-2.258063
H	-4.128024	0.593295	-1.546113	H	5.189582	0.172193	-2.400619
H	-3.881661	3.107915	-1.204032	H	5.372337	-0.225210	-0.692549
H	-2.584901	2.777042	-0.034961	H	4.635070	1.321278	-1.161060
H	-4.246219	2.245755	0.290534	H	3.912734	-2.034490	-2.743029
H	-2.860467	1.965026	-3.167858	H	2.447201	-2.384320	-1.819536
H	-2.074578	0.387410	-3.001475	H	4.030673	-2.428894	-1.030004
H	-1.385935	1.813335	-2.201401	H	4.326630	-0.432782	1.257845
H	2.856176	-1.551621	1.923375	H	3.701060	0.028248	3.580388
H	5.301015	-1.298282	2.069608	H	2.001703	0.206681	3.156493
H	5.280668	0.045429	0.925477	H	3.181650	1.381045	2.545682
H	4.811878	-1.581386	0.386814	H	3.568517	-2.336337	2.746285
H	3.726725	-0.028221	3.654325	H	3.311338	-2.699719	1.038318
H	2.145289	0.530844	3.096640	H	1.943134	-2.218180	2.041201
H	3.617093	1.355698	2.567645	O	-0.317835	-2.080119	0.533244
H	4.030852	0.514888	-1.223151	C	0.175775	-3.187656	-0.148020
H	2.907438	1.979625	-2.882618	H	-0.131555	-3.202187	-1.216343
H	1.407059	1.931632	-1.946127	C	-0.325829	-4.478617	0.505442
H	2.035475	0.450300	-2.704928	H	-1.420496	-4.516931	0.489704
H	4.164309	2.975869	-0.941975	H	0.059448	-5.363369	-0.016020
H	4.212194	2.196358	0.638155	H	-0.004420	-4.524799	1.551486
H	2.727063	2.981517	0.079035	H	1.281551	-3.215362	-0.159689
H	-0.010589	2.474119	2.661729	H	0.430868	-0.130650	1.719330
O	-0.365049	1.742025	0.772188	H	-0.328255	0.055004	1.740810
C	0.348007	2.596813	1.623209	E			
H	1.423555	2.363894	1.642960	Fe	-0.070778	-0.216731	-0.123927
C	0.157823	4.056036	1.207710	P	-2.289673	0.117994	0.187751
H	0.699655	4.729226	1.882390	P	2.191362	0.095321	0.037720
H	0.525438	4.217962	0.188512	N	-0.019915	1.813364	-0.159951
H	-0.902355	4.328953	1.230458	N	-2.333712	1.824214	0.047421
D				N	2.351315	1.746140	-0.165677
Fe	-0.016970	-0.215396	0.034711	C	-1.149253	2.551338	-0.088034
P	-2.277474	0.160033	0.001901	C	-1.162334	3.942060	-0.133385
P	2.292744	0.065051	0.054981	C	0.077678	4.592691	-0.245817
				C	1.247931	3.870777	-0.279110

C	1.216370	2.444350	-0.201070	C	3.365409	-0.462329	-1.327577
C	-3.622592	-0.451329	-1.033676	C	4.805313	0.059647	-1.222132
C	-3.403555	-1.915192	-1.454871	C	3.319108	-1.981548	-1.582636
C	-3.686217	0.445184	-2.280494	C	3.117969	-0.324763	1.656591
C	-3.154754	-0.173145	1.836588	C	2.575257	0.521461	2.817783
C	-3.330745	-1.669388	2.144217	C	3.050941	-1.821719	2.002659
C	-2.429228	0.545139	2.982253	C	0.015071	-0.224728	-2.015763
C	3.404944	-0.578521	-1.246342	O	0.007917	-0.267600	-3.173464
C	4.687766	0.264585	-1.329149	H	-3.197110	2.225647	-0.123207
C	3.746924	-2.068012	-1.094964	H	-2.195939	4.431369	-0.161087
C	3.056732	-0.313063	1.673499	H	-0.051619	5.709471	-0.064675
C	2.821852	0.799649	2.702709	H	2.119249	4.476926	0.006111
C	2.628139	-1.674773	2.241843	H	-2.887467	-0.066670	-2.218351
C	-0.055213	-0.362127	-1.918365	H	-5.325816	-0.495160	-2.180184
O	-0.012535	-0.449834	-3.075315	H	-4.949952	0.856161	-1.113444
H	-3.178794	2.364669	0.172755	H	-5.301131	-0.743461	-0.434831
H	-2.097561	4.488275	-0.079388	H	-3.564073	-2.376662	-2.591084
H	0.108410	5.678473	-0.293562	H	-3.620759	-2.719273	-0.861722
H	2.219438	4.345129	-0.340888	H	-2.064372	-2.379334	-1.634412
H	-4.582724	-0.381558	2.703210	H	-4.167240	0.308730	1.637222
H	-4.252318	-2.266055	-2.052737	H	-4.076190	-1.651602	2.919458
H	-3.292087	-2.593666	-0.604881	H	-2.533449	-2.157429	2.214632
H	-2.506095	-1.999014	-2.075369	H	-4.007361	-2.188228	1.239219
H	-4.452153	0.066483	-2.967270	H	-3.159545	0.532496	3.654126
H	-2.732362	0.447546	-2.816971	H	-2.390625	1.653855	2.520149
H	-3.932568	1.481345	-2.038978	H	-1.553242	0.168766	2.985892
H	-4.152947	0.277025	1.722801	H	2.885043	0.031723	-2.182346
H	-3.771715	-1.796442	3.139355	H	5.352588	-0.173039	-2.142943
H	-2.366055	-2.186303	2.135788	H	5.350035	-0.410464	-0.396567
H	-3.991779	-2.168739	1.430238	H	4.852712	1.146486	-1.088146
H	-3.001645	0.432668	3.910396	H	3.702089	-2.197445	-2.586582
H	-2.310257	1.613490	2.782640	H	2.300993	-2.372698	-1.490658
H	-1.431405	0.125570	3.135335	H	3.955375	-2.520382	-0.872311
H	2.854163	-0.446922	-2.186890	H	4.167350	-0.046729	1.487150
H	5.282382	-0.042241	-2.198485	H	3.130438	0.288154	3.733594
H	5.315778	0.127269	-0.441023	H	1.517636	0.302091	2.990434
H	4.450274	1.326002	-1.412060	H	2.671200	1.594525	2.629409
H	4.336696	-2.408970	-1.953854	H	3.595545	-2.007303	2.935735
H	2.858539	-2.704845	-1.038875	H	3.491100	-2.454222	1.229033
H	4.349430	-2.252120	-0.198720	H	2.014329	-2.138116	2.142540
H	4.129979	-0.352570	1.446935	O	0.242118	-2.178030	-0.348850
H	3.360817	0.576658	3.631970	C	-0.254888	-3.042961	0.609734
H	1.756136	0.886717	2.941780	H	-0.036027	-2.704041	1.645044
H	3.159618	1.764473	2.319864	C	0.325992	-4.450537	0.424413
H	3.221528	-1.929690	3.128198	H	1.416725	-4.432201	0.526518
H	2.754424	-2.495045	1.525970	H	-0.080019	-5.152755	1.164059
H	1.579765	-1.633972	2.565028	H	0.091494	-4.827498	-0.577198
O	-0.192404	-2.305552	0.309886	H	-1.363038	-3.134928	0.565199
C	-0.006391	-3.391118	-0.620040	H	0.019392	-0.266782	1.338791
H	-0.816510	-3.287911	-1.343174	H	3.170454	2.298247	0.074546
C	-0.067738	-4.739066	0.081478				
H	-1.021159	-4.865960	0.602678	F			
H	0.037685	-5.547630	-0.649089	Fe	0.658618	0.323937	0.242970
H	0.742192	-4.845690	0.812384	P	2.846866	-0.194447	0.706141
H	0.939643	-3.262434	-1.156591	P	-1.647953	0.225617	-0.099055
H	0.463144	-2.367174	1.019185	O	1.618188	1.415817	-3.072865
H	0.018774	-0.094737	1.416007	N	0.340015	-1.629771	0.729677
				N	2.622979	-1.830691	1.174330
E'				N	-1.968362	-1.382956	0.219831
Fe	0.016392	-0.204375	-0.210302	C	1.362282	-2.433505	1.113047
P	-2.198497	0.002341	0.018163	C	1.197832	-3.777241	1.424116
P	2.201442	0.046286	0.057355	C	2.022059	2.431362	-3.971211
N	-0.009337	1.847693	-0.114455	C	-0.100384	-4.308557	1.324766
N	-2.315149	1.735837	-0.197139	C	-1.156193	-3.522485	0.929183
N	2.303373	1.788229	-0.027108	C	-0.948836	-2.143554	0.613883
C	-1.182174	2.519547	-0.146928	H	1.264547	3.230986	-4.033253
C	-1.239440	3.921698	-0.130801	C	3.647593	0.558152	2.232675
C	-0.039834	4.623431	-0.077954	C	5.022595	-0.036494	2.573192
C	1.174372	3.946901	-0.037637	C	3.678519	2.096201	2.229535
C	1.150216	2.543504	-0.058618	H	2.960529	2.908259	-3.639838
C	-3.320048	-0.603744	-1.364093	C	4.189718	-0.309300	-0.600742
C	-4.802335	-0.220457	-1.257206	C	4.688745	-1.070475	-1.062027
C	-3.124718	-2.109467	-1.623310	C	2.223617	1.820896	-5.351273
C	-3.201983	-0.170565	1.604994	C	3.715794	-1.139793	-1.805583
C	-3.467710	-1.629058	2.007920	C	-2.818591	1.107974	1.088269
C	-2.533460	0.595494	2.756461	C	-4.254181	0.567895	0.978446

C	-2.790852	2.641777	1.053977	C	-2.817152	1.131677	1.006001
H	1.294897	1.362132	-5.704625	C	-4.253753	0.627157	0.798649
C	-2.350701	0.537847	-1.819757	C	-2.765637	2.664241	1.063116
C	-1.997302	-0.613065	-2.773829	H	3.145902	2.723216	-4.717747
C	-1.935450	1.891332	-2.418741	C	-2.241583	0.626350	-1.878233
H	2.993636	1.043488	-5.317294	C	-1.826173	-0.490019	-2.845661
C	0.365496	0.915131	1.879485	C	-1.857587	2.011269	-2.419751
O	0.167354	1.282542	2.957080	H	1.579651	3.533491	-4.520402
H	3.392404	-2.438162	1.422193	C	0.382302	0.918753	2.026292
H	2.532119	2.583107	-6.074826	O	0.177948	1.246243	3.119846
H	2.044651	-4.382537	1.727091	H	3.297396	-2.417056	1.650175
H	-0.265494	-5.356392	1.562275	H	1.927785	2.629689	-6.006248
H	-2.164151	-3.908019	0.840829	H	1.922936	-4.339601	1.913970
H	2.939600	0.242431	3.009951	H	-0.372190	-5.311503	1.564735
H	5.348720	0.321641	3.555971	H	-2.200776	-3.849053	0.696365
H	5.005462	-1.130572	2.619750	H	3.099011	0.398818	2.973398
H	5.785590	0.262803	1.847695	H	5.526721	0.371257	3.414700
H	3.952402	2.454559	3.228117	H	5.060373	-1.135352	2.630231
H	4.416575	2.490567	1.526451	H	5.886691	0.131380	1.704595
H	2.709957	2.527333	1.969993	H	4.284955	2.551022	2.914257
H	5.015479	-0.844803	-0.110998	H	4.604707	2.392278	1.186563
H	5.432789	0.939022	-1.855664	H	2.942359	2.572246	1.760183
H	3.863604	1.662247	-1.465383	H	4.959519	-1.122730	-0.015686
H	5.164754	1.636973	-0.258209	H	5.467439	0.307058	-1.996728
H	4.578444	-1.383909	-2.435964	H	3.918938	1.140490	-1.817495
H	3.248578	-2.082583	-1.504810	H	5.177325	1.306601	-0.574121
H	3.014814	-0.565197	-2.419546	H	4.403227	-1.939264	-2.279897
H	-2.419254	0.783311	2.057609	H	3.218902	-2.555636	-1.114583
H	-4.844762	0.918125	1.833214	H	2.788659	-1.215468	-2.179168
H	-4.752924	0.929937	0.072550	H	-2.472869	0.752209	1.977297
H	-4.264999	-0.524030	0.969689	H	-4.882774	0.928825	1.645076
H	-3.386970	3.037307	1.884597	H	-4.705908	1.053203	-0.104603
H	-1.780547	3.045945	1.148690	H	-4.274894	-0.461876	0.718184
H	-3.228124	3.032415	0.129652	H	-3.413672	3.029210	1.869038
H	-3.437888	0.525597	-1.672441	H	-1.758229	3.039763	1.260724
H	-2.543639	-0.486864	-3.715815	H	-3.125095	3.120005	0.134283
H	-0.930349	-0.614736	-3.024708	H	-3.332476	0.581498	-1.773485
H	-2.258439	-1.582426	-2.343899	H	-2.272766	-0.317791	-3.832914
H	-2.455265	2.043261	-3.372347	H	-0.738335	-0.528592	-2.966656
H	-2.183914	2.737298	-1.772904	H	-2.151147	-1.464513	-2.475407
H	-0.860500	1.915208	-2.619612	H	-2.288732	2.160865	-3.417364
O	1.227825	2.053621	-0.532762	H	-2.219644	2.825820	-1.786225
C	0.742756	3.308951	-0.146014	H	-0.771810	2.110448	-2.509629
H	0.692033	3.399492	0.955555	O	1.256951	2.293003	-0.373940
C	1.639790	4.432975	-0.670423	C	0.751005	3.590463	-0.030976
H	2.660873	4.322748	-0.290169	H	0.646025	3.593549	1.057017
H	1.258687	5.412718	-0.358239	C	1.698407	4.692352	-0.487275
H	1.683893	4.420376	-1.764369	H	2.686171	4.573168	-0.032886
H	-0.285701	3.485228	-0.510766	H	1.301014	5.672398	-0.202512
H	1.186183	-0.320875	-1.269852	H	1.818372	4.682300	-1.575985
H	0.433933	-0.134378	-1.398479	H	-0.246334	3.734310	-0.464138
H	1.483130	1.790826	-2.155976	H	1.352272	0.644097	-2.425038
				H	0.823667	-0.139653	-1.140361
				H	1.381057	2.232498	-1.345313
G							
Fe	0.671487	0.372713	0.340984	H			
P	2.840455	-0.239131	0.732379	Fe	0.480024	0.273632	0.501791
P	-1.574568	0.285859	-0.147944	P	2.668764	-0.128340	1.052136
O	1.730008	1.431471	-2.883934	P	-1.802623	0.069981	0.106476
N	0.307654	-1.575862	0.804482	O	-3.794700	-3.450135	-0.796514
N	2.541191	-1.786082	1.419097	N	0.238298	-1.685717	1.023008
N	-1.947587	-1.325431	0.108108	N	2.499734	-1.743137	1.610945
C	1.288951	-2.387249	1.257289	N	-2.047821	-1.567023	0.390602
C	1.101078	-3.733975	1.548585	C	1.283521	-2.423184	1.474676
C	1.501273	1.382691	-4.294648	C	1.182595	-3.774024	1.780348
C	-0.185345	-4.262959	1.346095	C	-5.167663	-3.429524	-0.456301
C	-1.201186	-3.469737	0.869070	C	-0.064261	-4.389375	1.579219
C	-0.965063	-2.088550	0.579410	C	-1.140479	-3.671976	1.110696
H	1.988637	0.493078	-4.717298	C	-0.999254	-2.280098	0.832484
C	3.785567	0.588887	2.138665	H	-5.539927	-4.456435	-0.567226
C	5.137885	-0.053032	2.481880	C	3.400138	0.741126	2.546955
C	3.907963	2.113432	1.982835	C	4.769010	0.200969	2.988759
H	0.426481	1.305640	-4.506471	C	3.409948	2.274721	2.426194
C	4.142459	-0.638002	-0.568101	H	-5.315517	-3.155408	0.601275
C	4.703503	0.609693	-1.270687	C	4.037077	-0.221741	-0.229311
C	2.073925	2.642899	-4.921594	C	4.344620	1.164100	-0.827262
C	3.601275	-1.648963	-1.591266				

C	-5.987752	-2.498015	-1.350121	C	3.063152	-1.128969	0.076930
C	3.698436	-1.236570	-1.332977	C	3.781696	0.005040	-0.679585
C	-3.015825	0.896293	1.290000	C	-1.177171	-5.026403	-2.197141
C	-4.430993	0.307239	1.188742	C	2.377413	-2.083211	-0.909071
C	-3.044181	2.430061	1.236544	C	-3.318465	2.163575	0.995658
H	-5.857764	-2.772109	-2.401813	C	-4.820019	2.062490	0.684124
C	-2.476175	0.395854	-1.623853	C	-2.831818	3.614445	0.857094
C	-2.128392	-0.751875	-2.585597	H	-2.241797	-5.053673	-1.944769
C	-2.011704	1.750724	-2.185187	C	-2.762445	0.923761	-1.676187
H	-5.668609	-1.457028	-1.229772	C	-2.440653	-0.388745	-2.403384
C	0.138167	0.928427	2.096236	C	-2.066456	2.105017	-2.380598
O	-0.084998	1.358464	3.145987	H	-0.637247	-5.620939	-1.453653
H	3.284919	-2.303655	1.913954	C	-0.234116	1.495244	2.242577
H	-7.055558	-2.554709	-1.106430	O	-0.361421	2.084475	3.235778
H	2.043690	-4.325252	2.141291	H	1.864066	-2.530154	2.560902
H	-0.174816	-5.449872	1.789801	H	-1.040475	-5.490070	-3.179703
H	-2.100035	-4.129763	0.907222	H	0.069395	-3.966498	3.290596
H	2.666391	0.471669	3.317332	H	-2.391489	-4.384532	3.202985
H	5.045062	0.643446	3.952179	H	-3.871482	-2.784760	1.983161
H	4.769902	-0.828613	3.123125	H	2.162481	0.413307	3.478961
H	5.558169	0.459673	2.275536	H	4.533901	-0.025207	4.024558
H	3.593042	2.714963	3.412484	H	3.795455	-1.502110	3.411410
H	4.203153	2.624652	1.760229	H	4.866546	-0.545071	2.372789
H	2.462810	2.664369	2.048859	H	3.702916	2.283966	3.250628
H	4.923706	-0.590787	0.304458	H	4.120148	1.838968	1.594889
H	5.034861	1.054429	-1.671144	H	2.490386	2.405671	1.964568
H	3.429376	1.649844	-1.178541	H	3.797290	-1.702354	0.660114
H	4.819525	1.828562	-0.101483	H	4.358757	-0.417670	-1.510078
H	4.579489	-1.393063	-1.964712	H	3.052835	0.716943	-1.079229
H	3.395094	-2.207243	-0.930548	H	4.480889	0.552186	-0.041853
H	2.899239	-0.869250	-1.985177	H	3.140046	-2.607440	-1.496947
H	-2.604906	0.597815	2.262887	H	1.751316	-2.827426	-0.410333
H	-5.043325	0.677214	2.019387	H	1.742324	-1.519747	-1.597553
H	-4.930900	0.608306	0.261724	H	-3.166351	1.865767	2.041807
H	-4.412080	-0.783317	1.235943	H	-5.385110	2.703472	1.370401
H	-3.651969	2.814477	2.063664	H	-5.046369	2.400121	-0.332398
H	-2.048952	2.872449	1.321634	H	-5.214354	1.047308	0.800172
H	-3.498248	2.790815	0.308094	H	-3.389467	4.254151	1.550869
H	-3.567933	0.411785	-1.511937	H	-1.769856	3.716772	1.086557
H	-2.547967	-0.529955	-3.573805	H	-2.999050	4.005874	-0.150925
H	-1.044948	-0.859783	-2.718990	H	-3.849724	1.074902	-1.693629
H	-2.530735	-1.708555	-2.247712	H	-2.883573	-0.364430	-3.405861
H	-2.408421	1.883808	-3.198380	H	-1.358786	-0.502569	-2.511819
H	-2.358386	2.595066	-1.584321	H	-2.818842	-1.268913	-1.877130
H	-0.919595	1.808815	-2.232520	H	-2.299324	2.083021	-3.451350
O	0.998771	1.950208	-0.348656	H	-2.389573	3.075571	-1.995389
C	0.526419	3.217637	-0.022781	H	-0.981242	2.030580	-2.254616
H	0.646500	3.452912	1.056594	O	0.841945	1.794618	-0.387986
C	1.274887	4.285148	-0.825964	C	0.782791	3.165224	-0.204041
H	2.347010	4.253650	-0.603697	H	0.928968	3.469696	0.857620
H	0.902180	5.290068	-0.593034	C	1.851085	3.873752	-1.045794
H	1.149171	4.108735	-1.899552	H	2.853214	3.544419	-0.749881
H	-0.554687	3.332947	-0.229455	H	1.795231	4.963673	-0.929184
H	1.080227	-0.383215	-1.010203	H	1.719818	3.630702	-2.105977
H	0.327167	-0.238792	-1.161380	H	-0.202864	3.594314	-0.489071
H	-3.327589	-2.697910	-0.362421	H	-0.556933	-2.123750	-0.881076
				H	-0.069801	-0.403643	-0.519383
				H	-3.950200	-0.762625	0.668463
I				J			
Fe	-0.117048	0.491949	0.760011	Fe	0.800253	-0.037471	-0.230906
P	1.839816	-0.424788	1.311590	P	-0.140223	-2.066011	0.059112
P	-2.231408	0.882284	0.120971	P	1.322900	2.152405	-0.346582
O	-0.869591	-3.047110	-0.906742	N	-1.054249	0.643042	0.194526
N	-0.908431	-1.193594	1.617518	N	-1.736771	-1.558477	0.497426
N	1.254481	-1.829204	2.161779	N	-0.253359	2.810858	-0.063508
N	-2.964436	-0.561245	0.763836	C	-2.063388	-0.221093	0.507500
C	-0.098252	-2.105642	2.204004	C	-3.352641	0.219531	0.823587
C	-0.602486	-3.264977	2.808997	C	-3.596764	1.588079	0.829759
C	-0.668367	-3.592506	-2.201878	C	-2.580307	2.489824	0.534985
C	-1.972427	-3.493582	2.744477	C	-1.314114	1.982055	0.227971
C	-2.806812	-2.603902	2.078712	C	-0.470222	-3.111954	-1.468626
C	-2.227177	-1.467030	1.498169	C	-1.259641	-4.400847	-1.187527
H	-1.207204	-3.010480	-2.966301	C	0.794905	-3.386400	-2.301710
C	2.892706	0.364499	2.660589	C	0.337095	-3.210378	1.458098
C	4.083870	-0.481617	3.135427	C	1.705769	-3.869748	1.214631
C	3.321450	1.806552	2.340707				
H	0.398120	-3.578528	-2.477183				

H	-3.915211	1.880192	-2.764189
H	-2.930841	0.408857	-2.792795
H	-2.202326	1.925398	-2.283734
H	2.447410	-1.756561	1.749280
H	4.822799	-2.177484	2.093988
H	5.279915	-0.703875	1.241499
H	4.505524	-2.034343	0.351896
H	3.313060	-0.770914	3.770836
H	2.181923	0.410386	3.104012
H	3.926455	0.650160	2.933969
H	4.525943	0.519217	-0.504335
H	4.274366	2.130216	-2.297440
H	2.549196	2.332568	-1.982396
H	3.158023	0.772358	-2.551311
H	4.751067	2.953172	0.036884
H	4.292599	2.010331	1.455530
H	3.092615	2.998059	0.628895
H	-0.039399	1.475977	1.294922
O	-0.033379	1.731967	-1.288524
C	0.294319	2.689790	-0.573582
H	1.274223	2.700986	-0.084442
C	-0.481500	3.970995	-0.479340
H	-0.653284	4.226382	0.571177
H	0.134694	4.774486	-0.903914
H	-1.427573	3.916015	-1.017371

TS_{C-D}

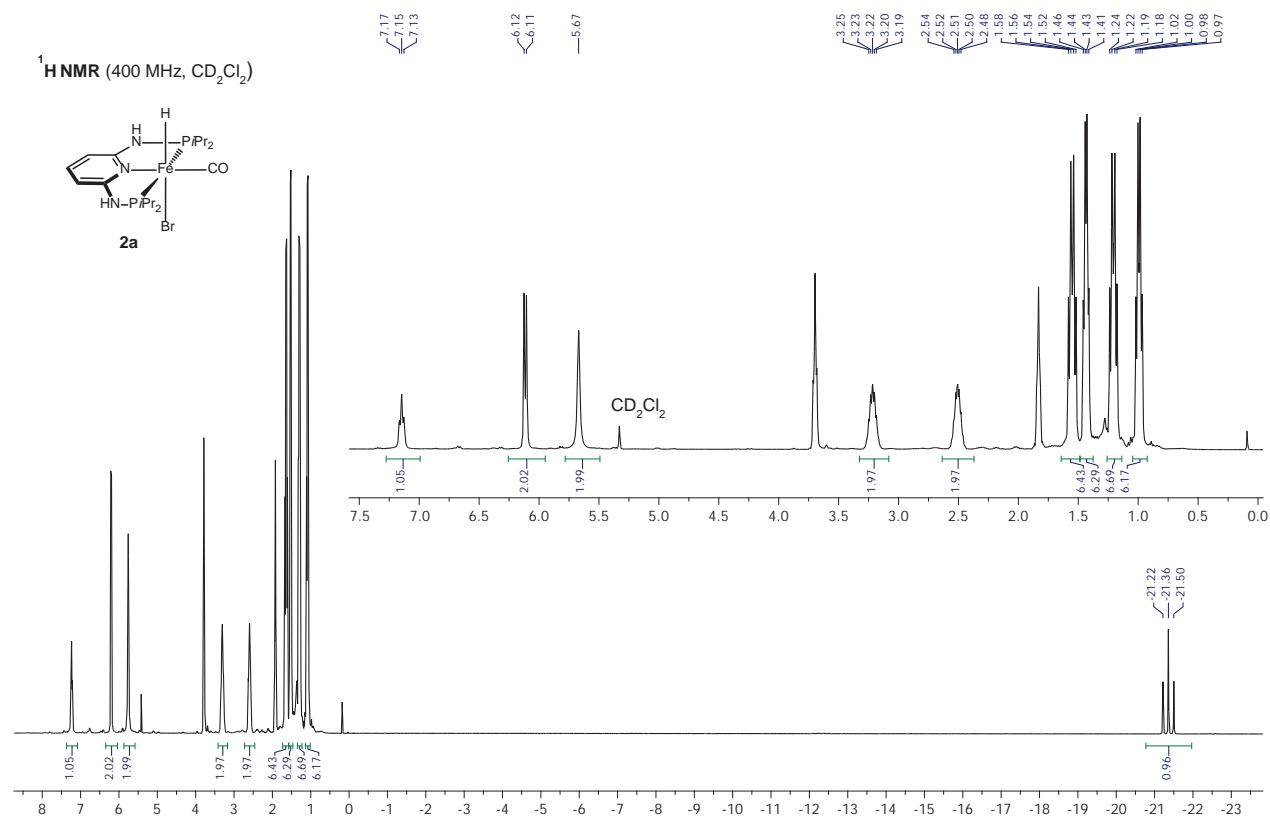
Fe	-0.057185	-0.411525	-0.418654
P	-2.342194	-0.001145	-0.355570
P	2.267371	-0.143190	-0.358689
N	0.041120	1.621127	-0.308685
N	-2.294623	1.709881	-0.444178
N	2.419146	1.522444	-0.312542
C	-1.078315	2.393205	-0.342390
C	-1.053797	3.779977	-0.287556
C	0.204501	4.405534	-0.220179
C	1.358171	3.661322	-0.216095
C	1.296799	2.233294	-0.278340
C	-3.299526	-0.476628	-1.899408
C	-4.718236	0.103175	-1.993276
C	-3.282789	-1.993481	-2.161972
C	-3.492174	-0.346737	1.094284
C	-3.572869	-1.850624	1.412955
C	-3.089961	0.456672	2.341486
C	3.296485	-0.617181	-1.865029
C	4.644213	0.120358	-1.901969
C	3.470726	-2.129611	-2.059764
C	3.312097	-0.757213	1.106602
C	3.321366	0.258239	2.259340
C	2.932946	-2.159319	1.604179
C	-0.000848	-0.530997	-2.139923
O	0.030179	-0.658738	-3.292801
H	-3.124718	2.287030	-0.430616
H	-1.976405	4.349144	-0.307722
H	0.258573	5.490367	-0.176292
H	2.340662	4.114895	-0.178225
H	-2.688289	0.001620	-2.675039
H	-5.136595	-0.101764	-2.985041
H	-4.735076	1.189804	-1.856751
H	-5.393527	-0.346673	-1.258136
H	-3.567532	-2.189706	-3.201280
H	-3.997702	-2.521075	-1.523950
H	-2.295182	-2.427790	-1.987912
H	-4.483109	0.003689	0.774310
H	-4.192478	-2.002542	2.304083
H	-2.578186	-2.262886	1.600460
H	-4.022296	-2.425347	0.599740
H	-3.863779	0.343957	3.108943
H	-2.975772	1.523516	2.131671
H	-2.150797	0.092410	2.764515
H	2.687079	-0.234959	-2.693345
H	5.112563	-0.014980	-2.884131
H	5.342760	-0.273676	-1.155185
H	4.511350	1.188243	-1.717834
H	3.990179	-2.325508	-3.004788
H	2.513971	-2.657675	-2.091045

H	4.076616	-2.571351	-1.260924
H	4.331397	-0.800891	0.702641
H	4.047699	-0.059945	3.016812
H	2.345120	0.321332	2.749537
H	3.588815	1.256124	1.908101
H	3.569745	-2.433267	2.453902
H	3.064856	-2.925237	0.835963
H	1.891752	-2.199616	1.936874
O	-0.380607	-2.163391	0.156877
C	0.194632	-3.364092	-0.268168
H	-0.169326	-3.633632	-1.278784
C	-0.162367	-4.498673	0.693307
H	-1.249001	-4.617218	0.759333
H	0.268995	-5.449128	0.357565
H	0.215437	-4.283886	1.698599
H	1.291335	-3.296928	-0.348557
H	0.046170	-0.584244	2.151238
H	0.120037	0.139013	2.313732

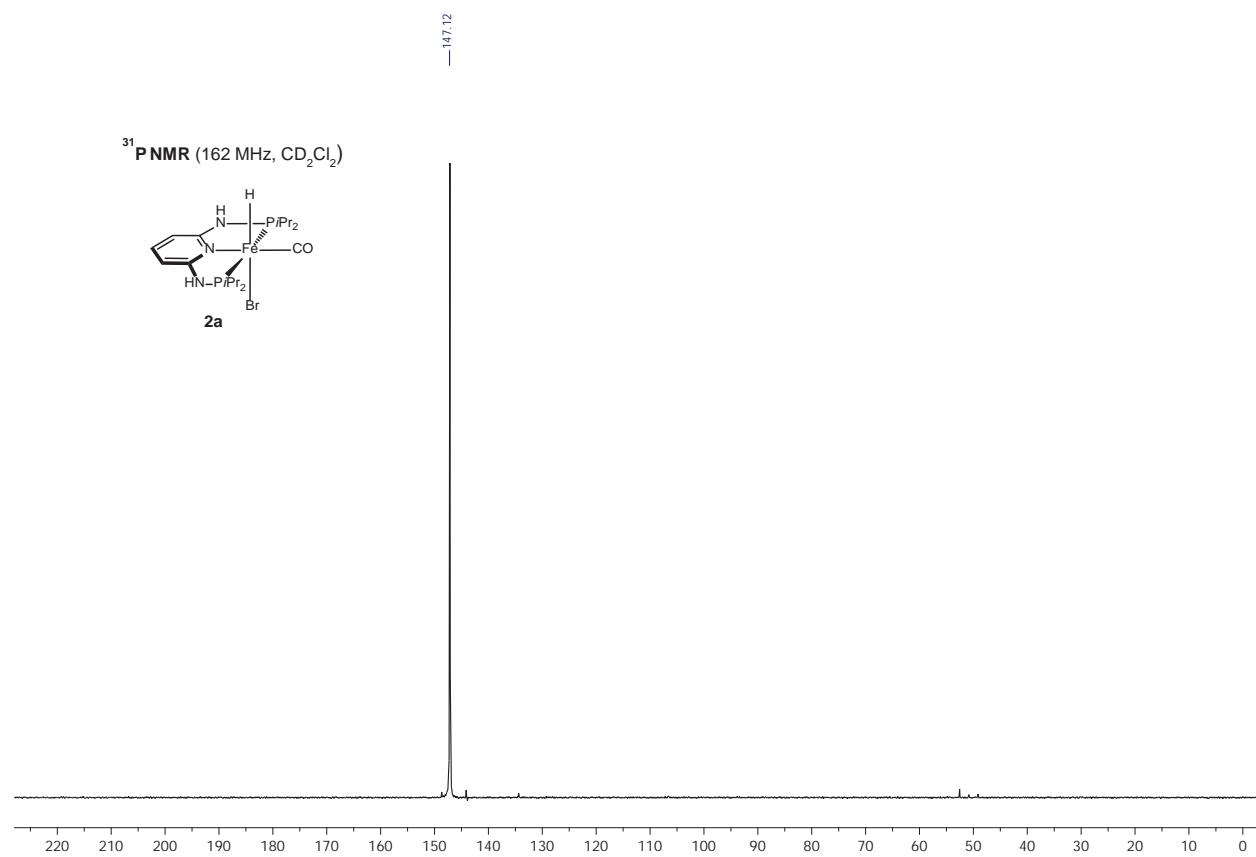
TS_{D-E}

Fe	-0.040116	-0.189355	-0.121297
P	-2.288063	0.200853	-0.031282
P	2.265178	0.071814	-0.009853
N	0.062691	1.842770	-0.090692
N	-2.268686	1.906404	-0.195954
N	2.435444	1.736250	-0.048986
C	-1.057669	2.604785	-0.146469
C	-1.038442	3.993767	-0.159755
C	0.218634	4.623197	-0.130775
C	1.374330	3.881720	-0.090374
C	1.315153	2.452568	-0.075461
C	-3.348561	-0.344574	-1.480895
C	-4.803991	0.143115	-1.435026
C	-3.258742	-1.856320	-1.756736
C	-3.317186	-0.063660	1.517025
C	-3.560033	-1.554018	1.811873
C	-2.674249	0.645290	2.720054
C	3.351309	-0.464357	-1.453967
C	4.789232	0.063662	-1.336987
C	3.316074	-1.958243	-1.802801
C	3.209486	-0.404049	1.556932
C	2.743397	0.451786	2.743930
C	3.176102	-1.896016	1.912544
C	0.012931	-0.268203	-1.894877
O	0.061105	-0.339970	-3.048210
H	-3.106419	2.471430	-0.158499
H	-1.963178	4.558238	-0.200860
H	0.271361	5.708957	-0.142493
H	2.355921	4.338599	-0.073042
H	-2.842177	0.173366	-2.305862
H	-5.302364	-0.083209	-2.384283
H	-4.878677	1.225488	-1.285579
H	-5.374186	-0.352596	-0.642766
H	-3.680185	-2.072853	-2.744675
H	-3.824972	-2.438313	-1.024299
H	-2.226555	-2.213024	-1.734611
H	-4.283361	0.419976	1.315306
H	-4.065197	-1.659963	2.778523
H	-2.618203	-2.108071	1.849862
H	-4.195231	-2.026104	1.058062
H	-3.342883	0.575602	3.585347
H	-2.486024	1.704210	2.522504
H	-1.722706	0.180104	2.992299
H	2.865867	0.080358	-2.274532
H	5.304967	-0.043550	-2.298649
H	5.367301	-0.500910	-0.596696
H	4.796220	1.119458	-1.055919
H	3.848564	-2.130149	-2.745541
H	2.295680	-2.329313	-1.926951
H	3.809130	-2.568994	-1.039592
H	4.244183	-0.117631	1.331169
H	3.381090	0.255380	3.614137
H	1.712626	0.213448	3.028493
H	2.797311	1.516146	2.506135
H	3.795776	-2.079844	2.798317
H	3.556638	-2.534112	1.110582

C	-0.125877	-4.267518	1.195257	C	0.451907	-2.142921	2.065280
C	-1.158367	-3.480187	0.746700	C	0.080990	-3.338488	2.691129
C	-0.942899	-2.092612	0.474874	C	-1.201376	-3.209614	-1.808384
H	0.698938	1.140998	-4.181755	C	-1.255608	-3.728524	2.611018
C	3.734681	0.641373	2.094987	C	-2.175636	-2.962804	1.905012
C	5.064527	-0.000712	2.517048	C	-1.747868	-1.772999	1.288260
C	3.862458	2.164653	1.922299	H	-0.322531	-3.306076	-2.461272
H	0.934929	2.813575	-3.672552	C	3.444881	0.553715	1.913703
C	4.234405	-0.567949	-0.611039	C	4.567589	-0.269822	2.562957
C	4.891449	0.686646	-1.209424	C	3.995883	1.724899	1.080472
C	2.590923	1.987191	-4.781159	H	-0.943638	-3.672666	-0.843212
C	3.705879	-1.491770	-1.720796	C	3.222136	-1.255876	-0.441536
C	-2.802798	1.091920	1.084092	C	3.217154	-0.373319	-1.704228
C	-4.247819	0.592566	0.926537	C	-2.389340	-3.934406	-2.432394
C	-2.745987	2.620793	1.203395	C	2.709361	-2.667889	-0.761201
H	3.097496	1.027498	-4.924746	C	-3.115548	1.245523	1.904570
C	-2.392532	0.647303	-1.852001	C	-4.603182	0.860391	1.899427
C	-1.947129	-0.397974	-2.884510	C	-2.898273	2.723484	2.274186
C	-2.160309	2.075740	-2.363241	H	-2.641747	-3.489457	-3.399404
H	3.329968	2.705943	-4.419583	C	-3.064909	-1.248046	-1.151875
C	0.403826	0.896022	1.883187	C	-2.186204	1.112962	-2.410837
O	0.218625	1.213658	2.979173	C	-3.559692	2.700350	-1.029587
H	3.333698	-2.395720	1.516329	H	-3.268692	-3.863363	-1.784194
H	2.219273	2.30163	-5.753835	C	0.214569	1.272871	2.091949
H	1.986284	-4.325573	1.746679	O	0.306338	1.821634	3.109049
H	-0.297658	-5.320328	1.404587	H	2.453294	-2.333507	2.425530
H	-2.158233	-3.866203	0.592624	H	-2.161058	-4.995388	-2.585096
H	3.004375	0.458987	2.893468	H	0.820009	-3.940361	3.208704
H	5.411166	0.447519	3.454984	H	-1.573924	-4.647911	3.094780
H	4.969494	-1.077596	2.691989	H	-3.213979	-3.253403	1.806609
H	5.849888	0.157108	1.771042	H	2.825721	0.970986	2.716139
H	4.140522	2.619630	2.879575	H	5.205655	0.388636	3.163011
H	4.636442	2.429968	1.196660	H	4.180660	-1.041320	3.236992
H	2.925242	2.611820	1.584895	H	5.211704	-0.750687	1.818944
H	4.989731	-1.120954	-0.033312	H	4.507833	2.436703	1.737003
H	5.666939	0.379666	-1.920938	H	4.727429	1.378400	0.342774
H	4.154661	1.283883	-1.753227	H	3.196082	2.248320	0.549227
H	5.373985	1.310245	-0.452428	H	4.251632	-1.337974	-0.069027
H	4.546139	-1.838776	-2.333193	H	3.833762	-0.843604	-2.479079
H	3.195859	-2.373464	-1.321863	H	2.201822	-0.251215	-2.088936
H	3.016552	-0.949981	-2.371819	H	3.609828	0.628058	-1.518971
H	-2.411814	0.670061	2.019400	H	3.308919	-3.100351	-1.569897
H	-4.833295	0.863918	1.813081	H	2.770965	-3.342992	0.097109
H	-4.741633	1.051353	0.062462	H	1.668938	-2.643450	-1.097599
H	-4.276290	-0.493065	0.809873	H	-2.625811	0.643190	2.683641
H	-3.327157	2.944204	2.075001	H	-5.038577	1.044088	2.888855
H	-1.727258	2.993612	1.331206	H	-5.175135	1.453548	1.178672
H	-3.180772	3.114297	0.328505	H	-4.733819	-0.195544	1.652721
H	-3.466853	0.502600	-1.683705	H	-3.219877	2.890611	3.308631
H	-2.499898	-0.250655	-3.820068	H	-1.851596	3.026300	2.202071
H	-0.880635	-0.309813	-3.113785	H	-3.483282	3.393464	1.640502
H	-2.136257	-1.410848	-2.522598	H	-3.937296	0.587143	-1.242748
H	-2.650456	2.208685	-3.335004	H	-2.709347	1.566943	-3.261049
H	-2.562386	2.836517	-1.689232	H	-1.228549	1.624696	-2.273483
H	-1.095160	2.277991	-2.503341	H	-1.982349	0.071366	-2.655818
O	1.250590	2.240267	-0.419594	H	-4.031627	2.991815	-1.974410
C	0.639418	3.494140	-0.180126	H	-4.300028	2.837986	-0.239989
H	0.519471	3.622883	0.904827	H	-2.732269	3.395367	-0.853917
C	1.489177	4.634988	-0.734963	O	0.800893	1.864759	-0.517377
H	2.485778	4.634333	-0.282823	C	0.510738	3.192464	-0.232283
H	1.015352	5.601062	-0.528287	H	0.970125	3.534334	0.722143
H	1.609429	4.542823	-1.819766	C	1.019325	4.104300	-1.353047
H	-0.367804	3.535802	-0.619764	H	2.101500	3.987817	-1.478676
H	1.192837	0.386387	-1.822497	H	0.807450	5.158756	-1.136004
H	0.749337	-0.222206	-1.375041	H	0.544605	3.841071	-2.304202
H	1.583863	2.017432	-1.519377	H	-0.578825	3.372417	-0.108614
				H	-0.507116	-1.059783	-1.226591
				H	0.136599	-0.445463	-0.929625
				H	-2.195958	-1.537008	-0.690176
TS_{H-I}							
Fe	0.127816	0.396606	0.567169				
P	2.206663	-0.436156	0.918202				
P	-2.172433	0.630476	0.389124				
O	-1.487329	-1.826073	-1.646227				
N	-0.448366	-1.363211	1.426233				
N	1.770318	-1.697235	2.035850				
N	-2.585396	-1.057931	0.445014				



S13



S14

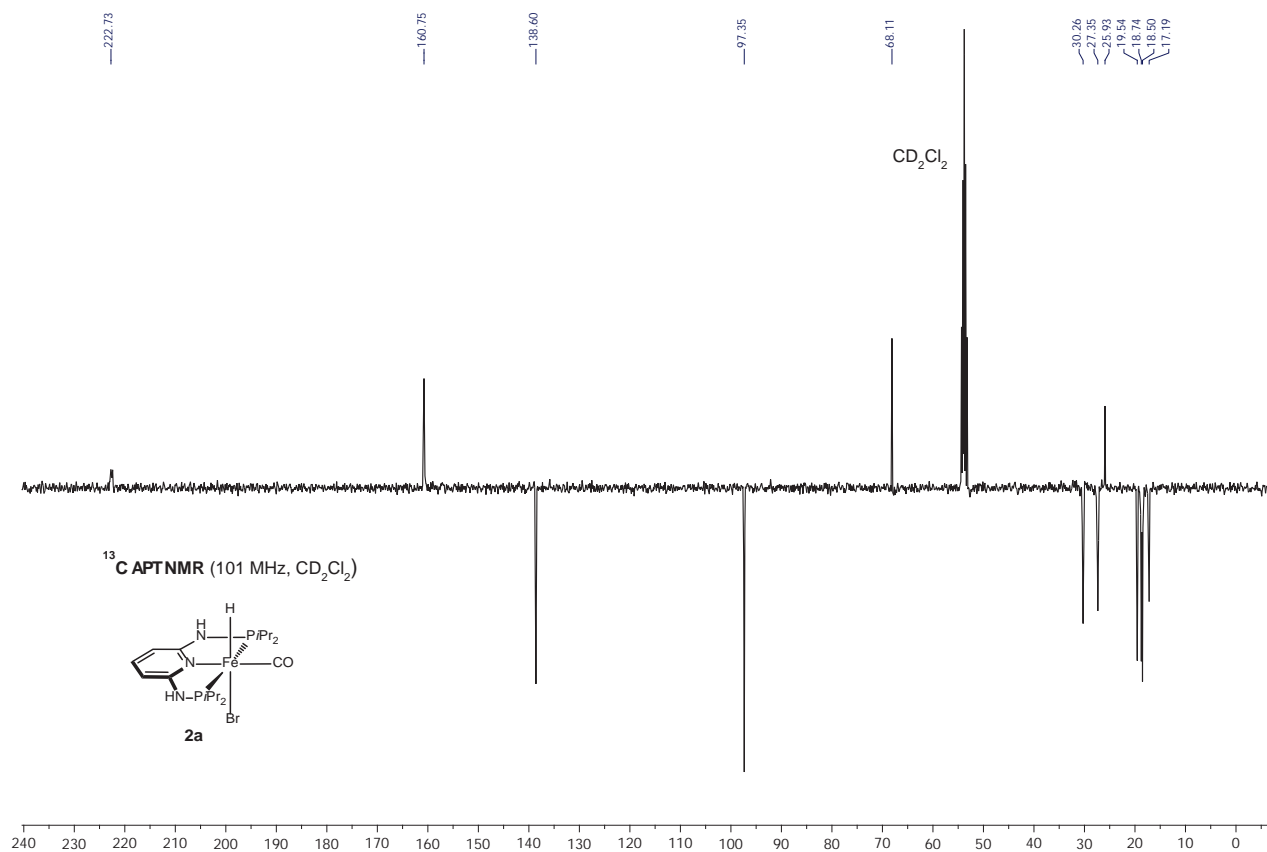


Figure S3. ¹³C{¹H} APT NMR spectrum of complex **2a**.

S15

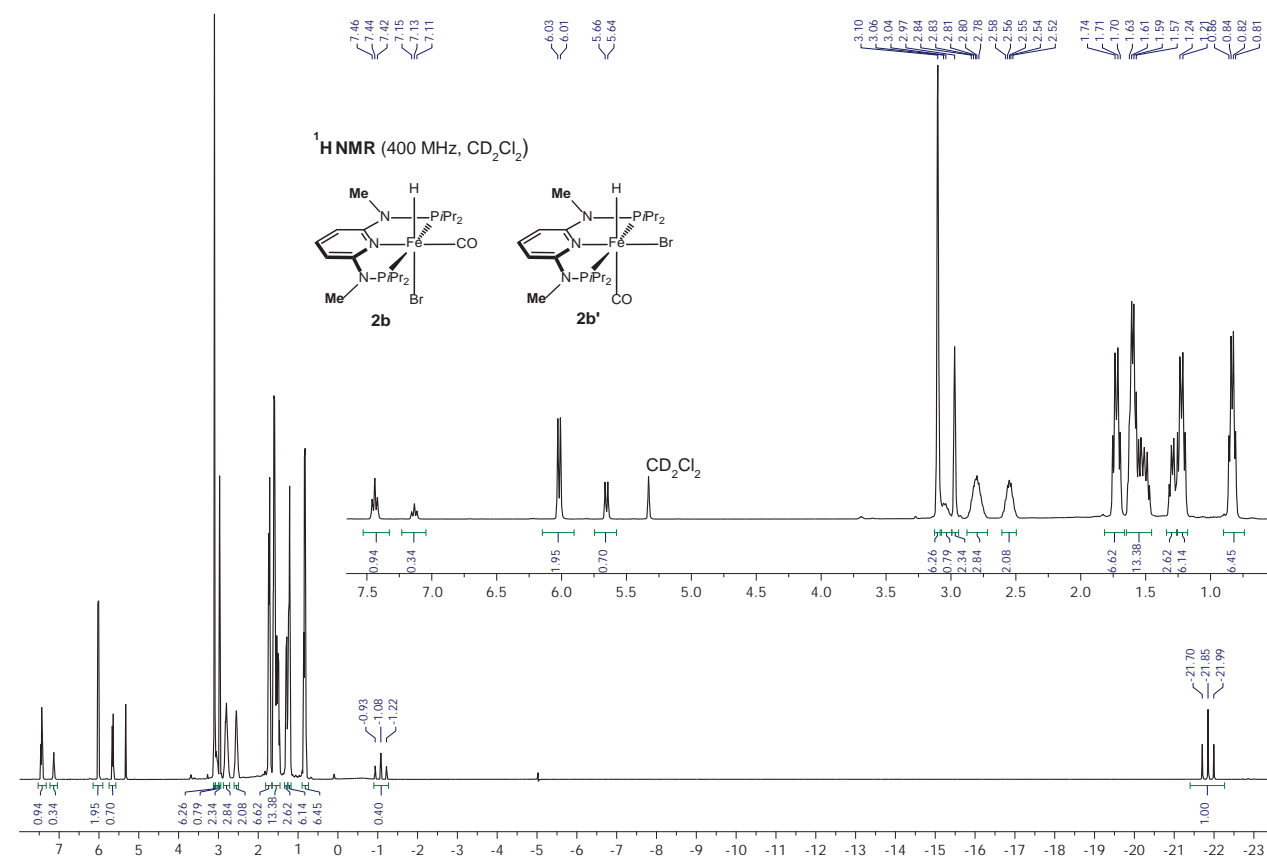


Figure S4. ¹H NMR spectrum of complex **2b**.

S16

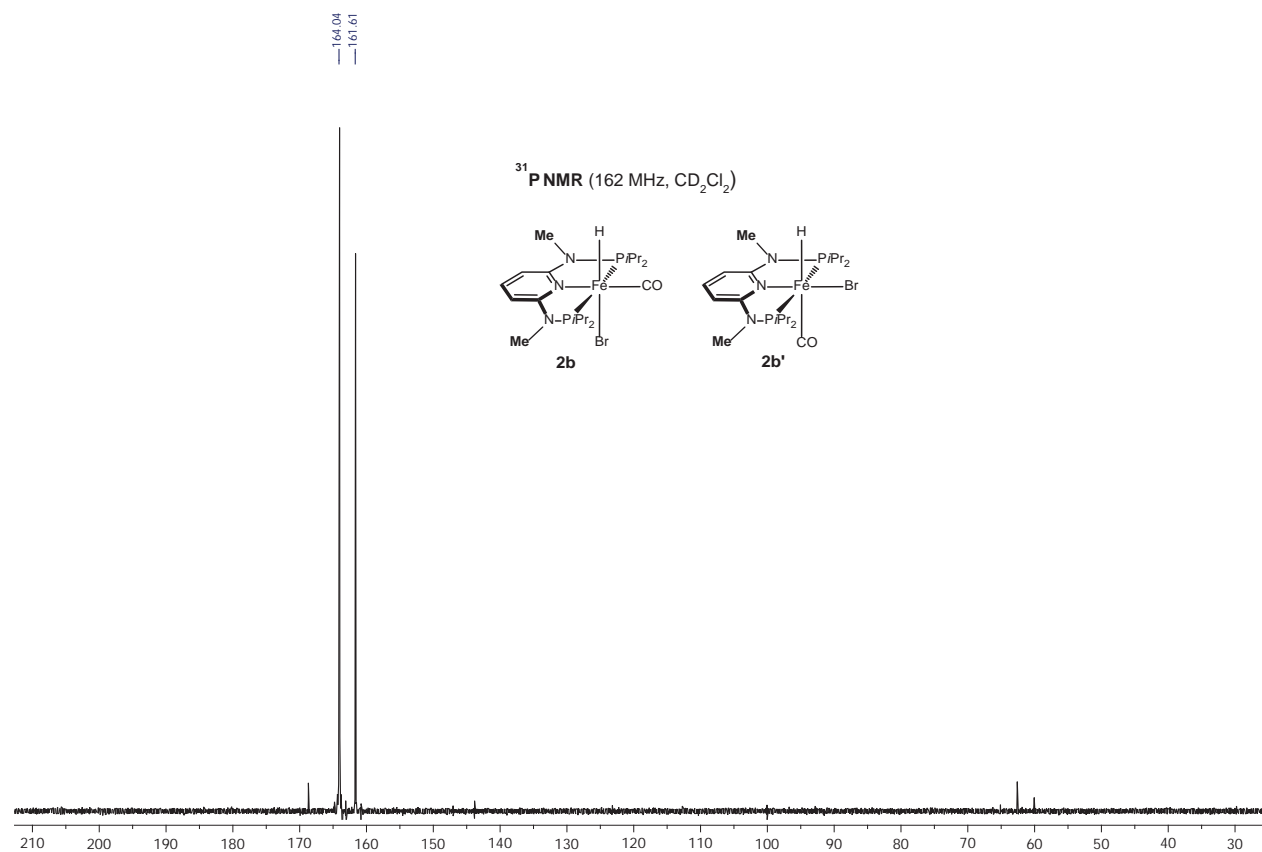


Figure S5. ³¹P{¹H} NMR spectrum of complex **2b**.

S17

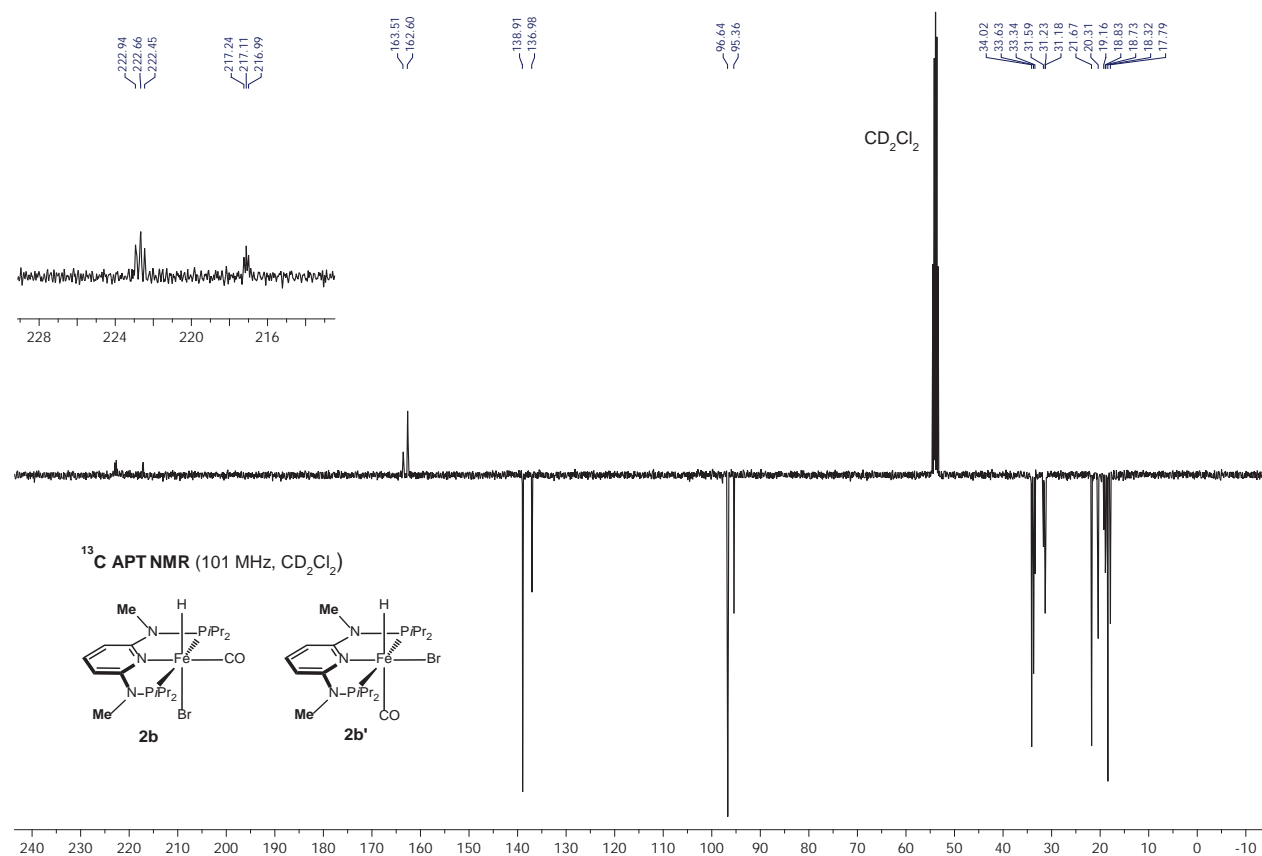


Figure S6. ¹³C{¹H} APT NMR spectrum of complex **2b**.

S18

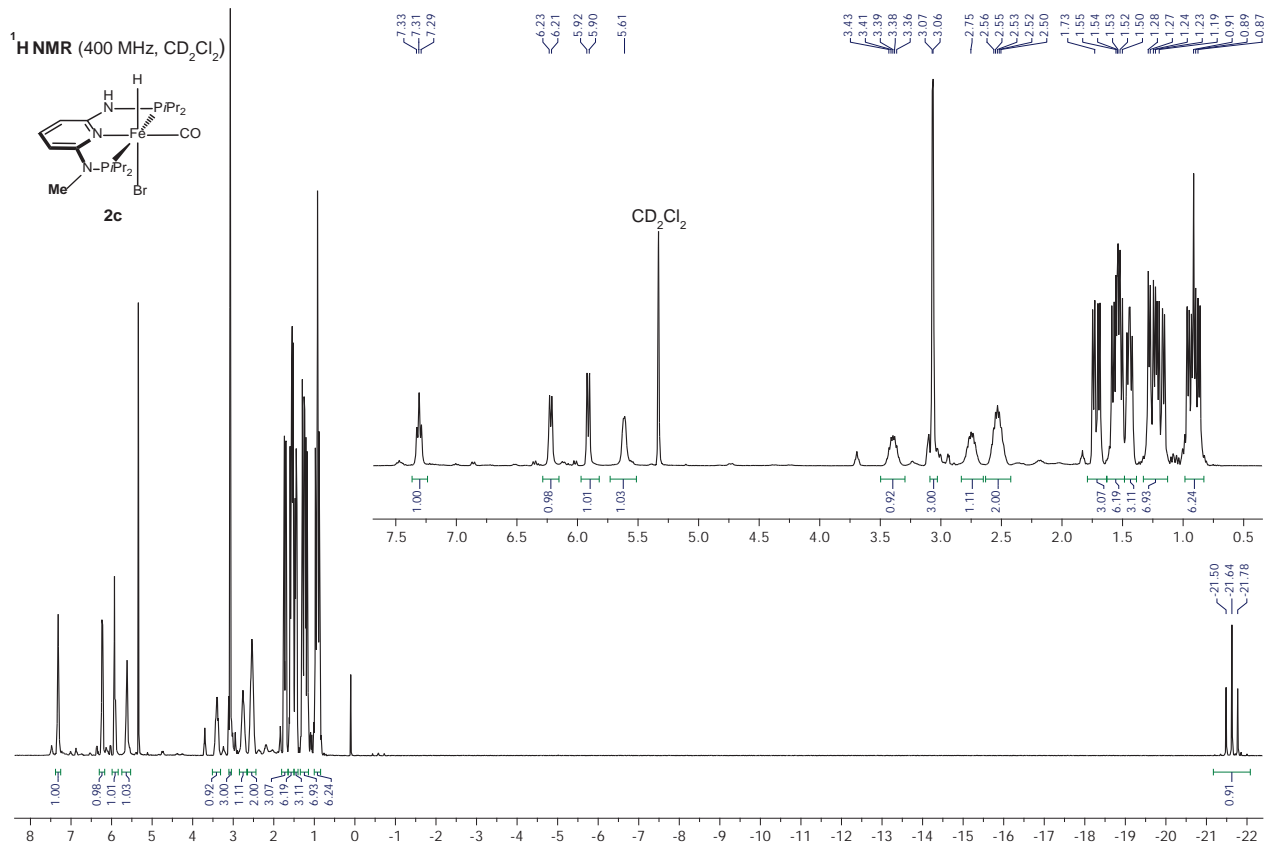


Figure S7. ¹H NMR spectrum of complex **2c**.

S19

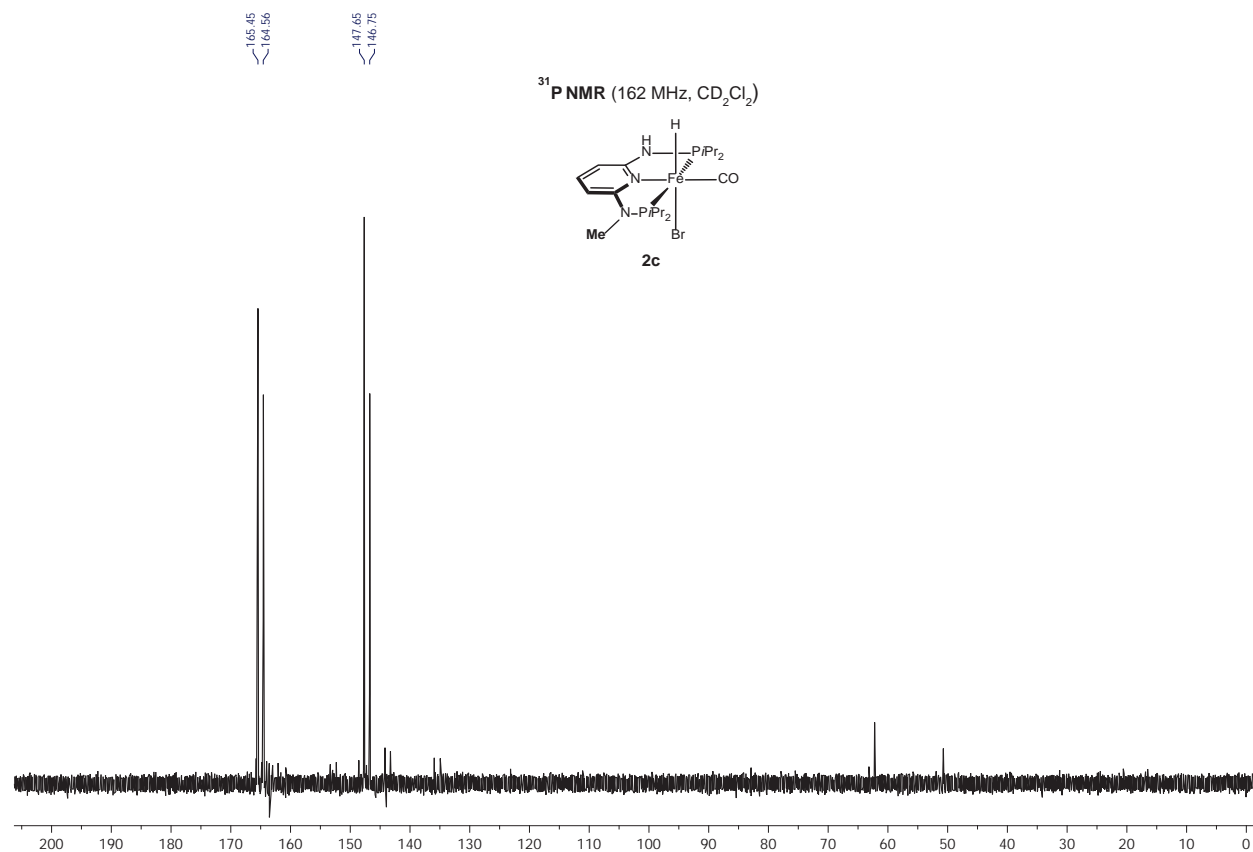


Figure S8. ³¹P{¹H} NMR spectrum of complex **2c**.

S20

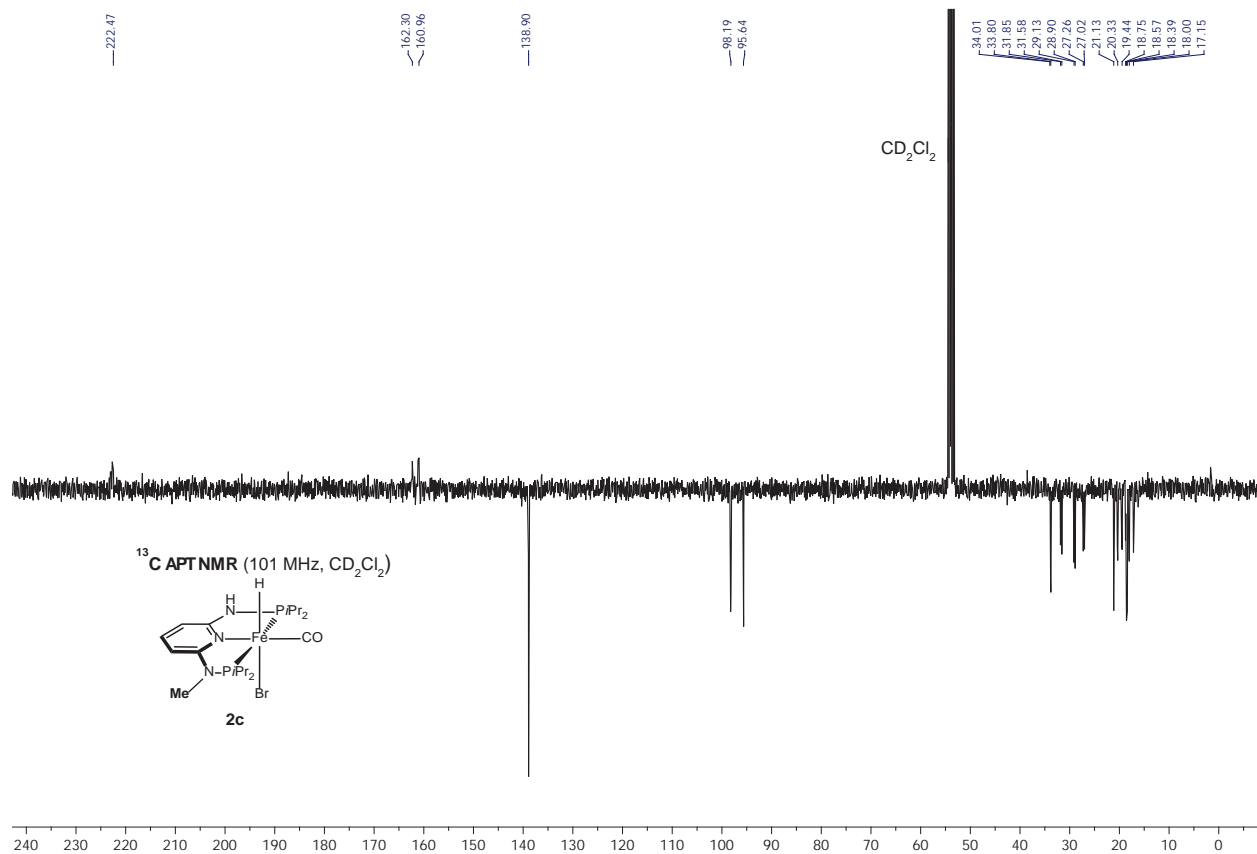


Figure S9. ¹³C{¹H} APT NMR spectrum of complex **2c**.

S21

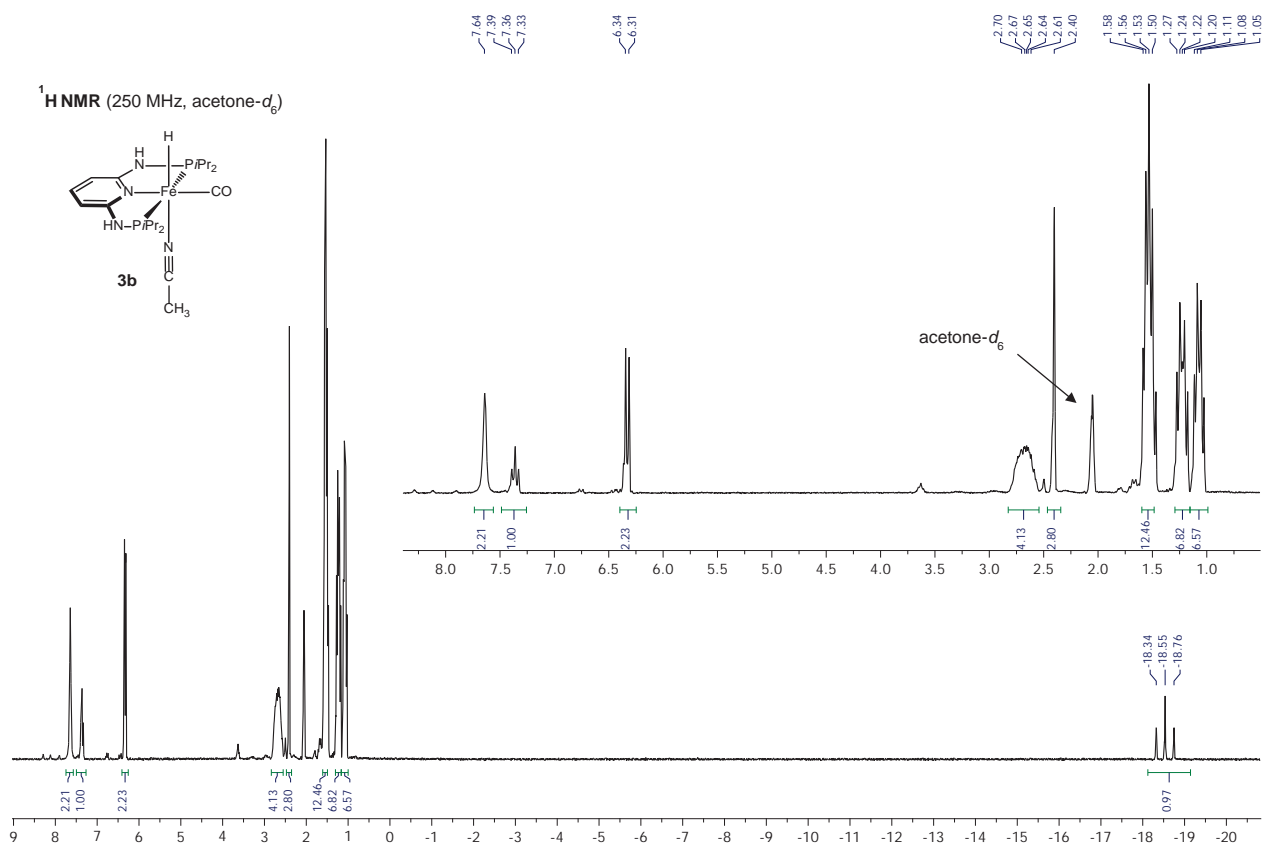


Figure S10. ¹H NMR spectrum of complex **3b**.

S22

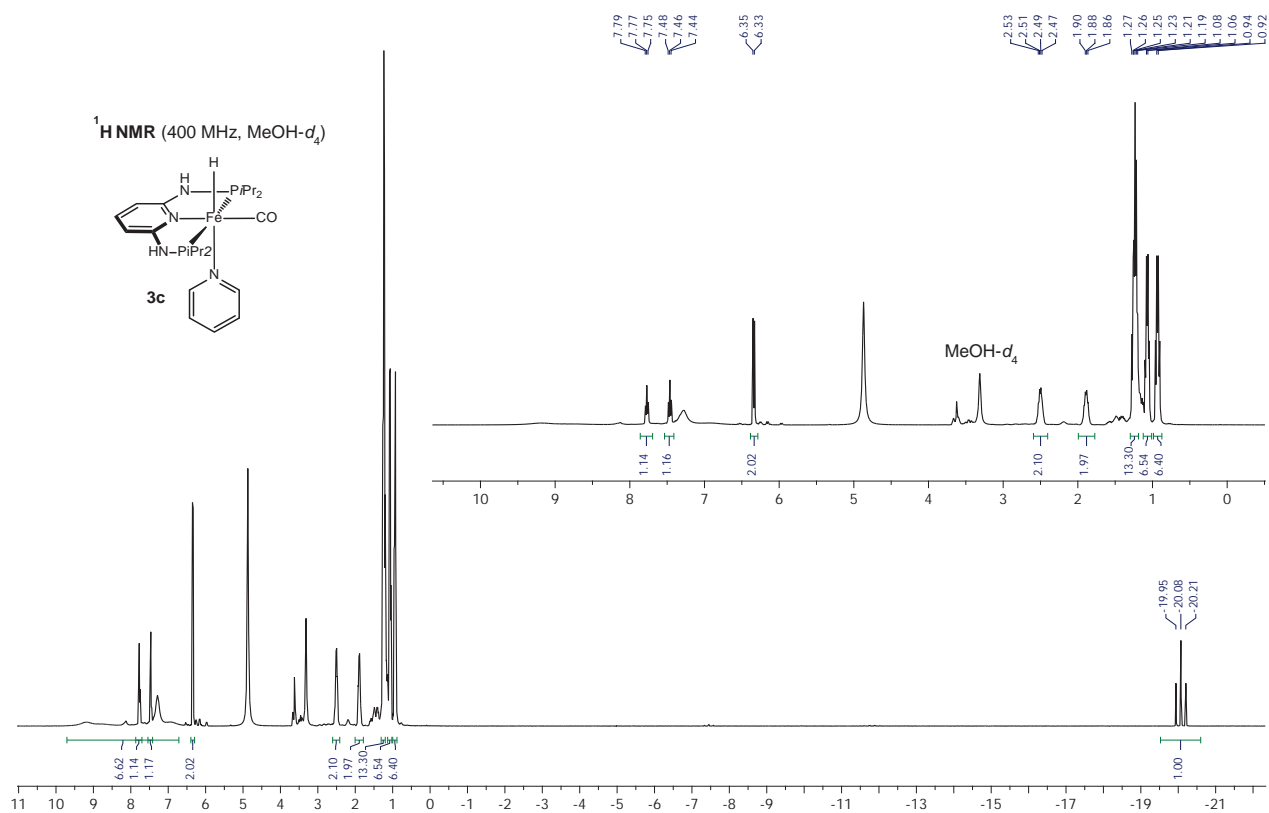


Figure S13. ¹H NMR spectrum of complex **3c**.

S25

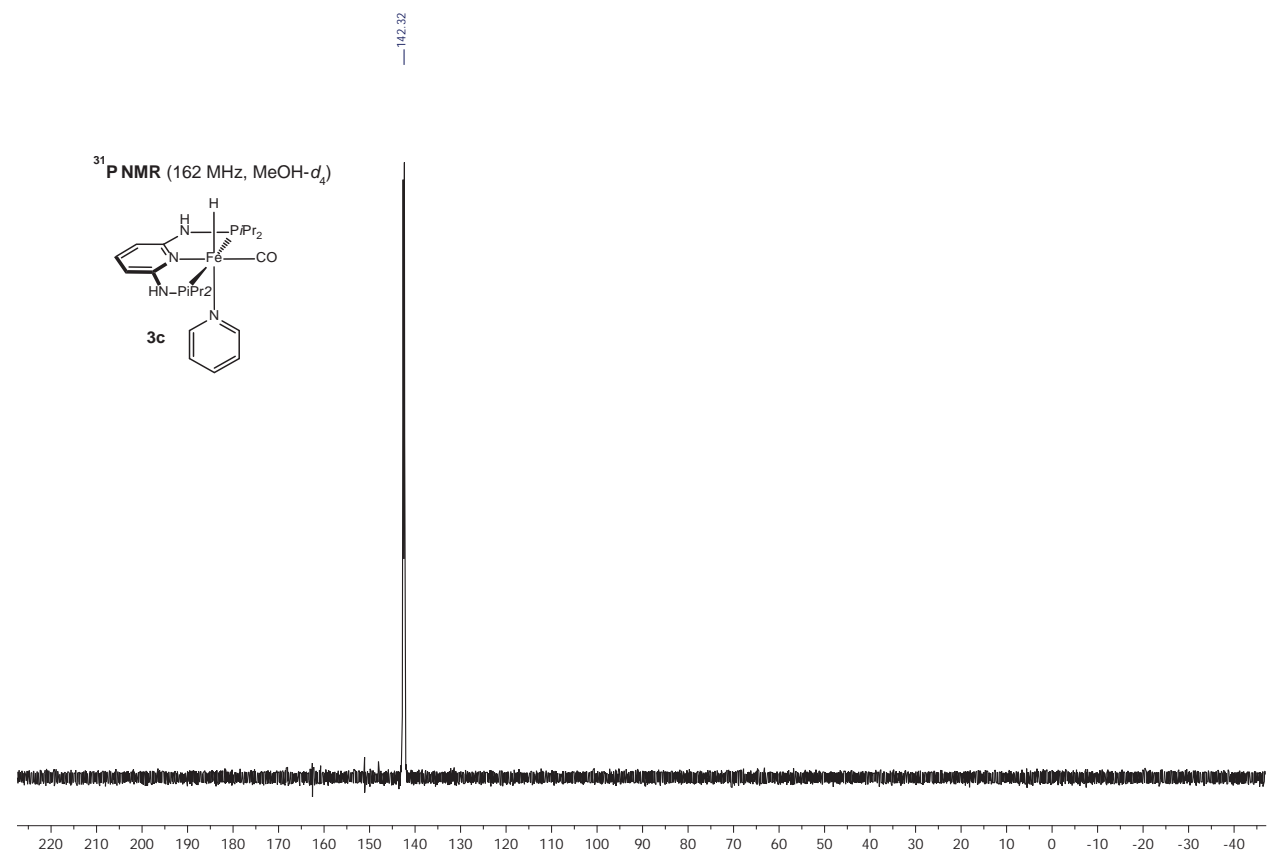


Figure S14. ³¹P{¹H} NMR spectrum of complex **3c**.

S26

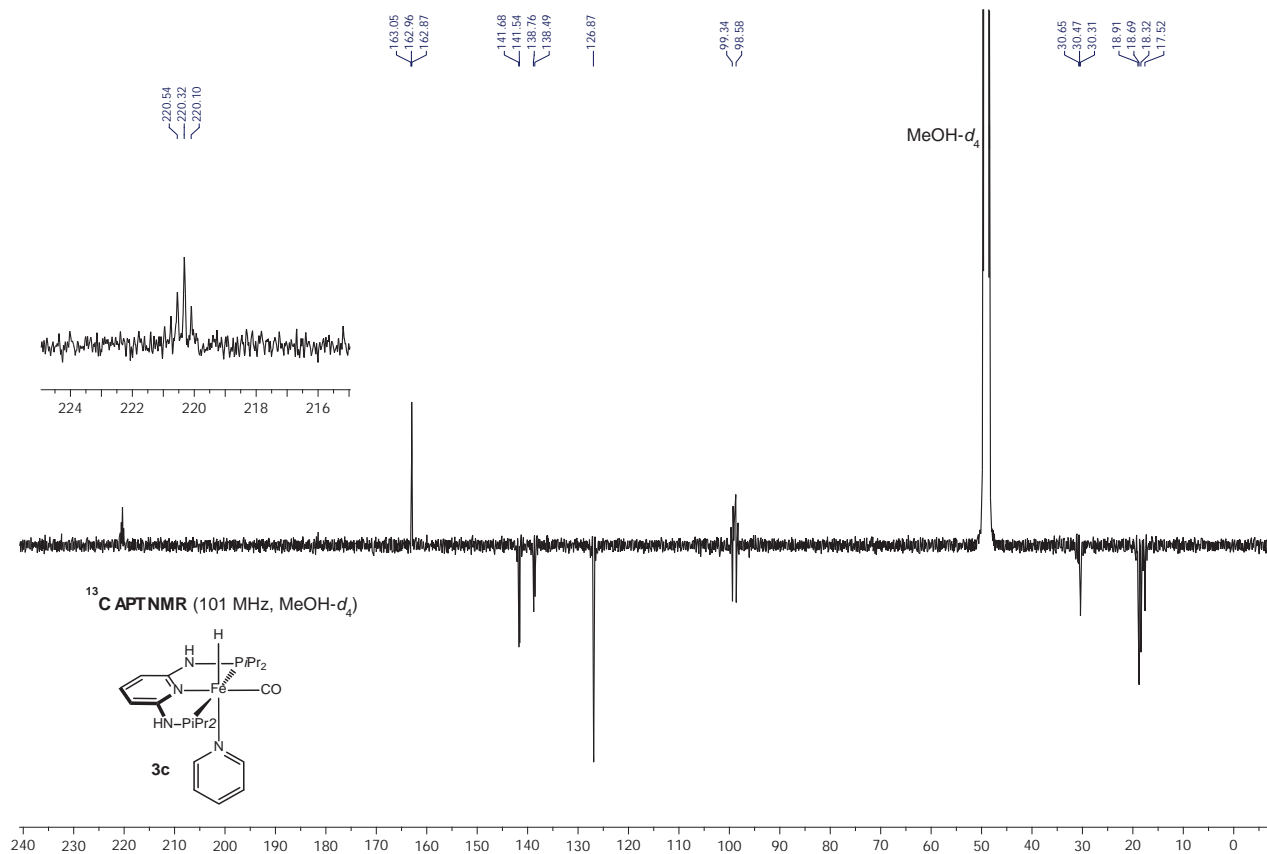


Figure S15. ¹³C{¹H} APT NMR spectrum of complex **3c**.

S27

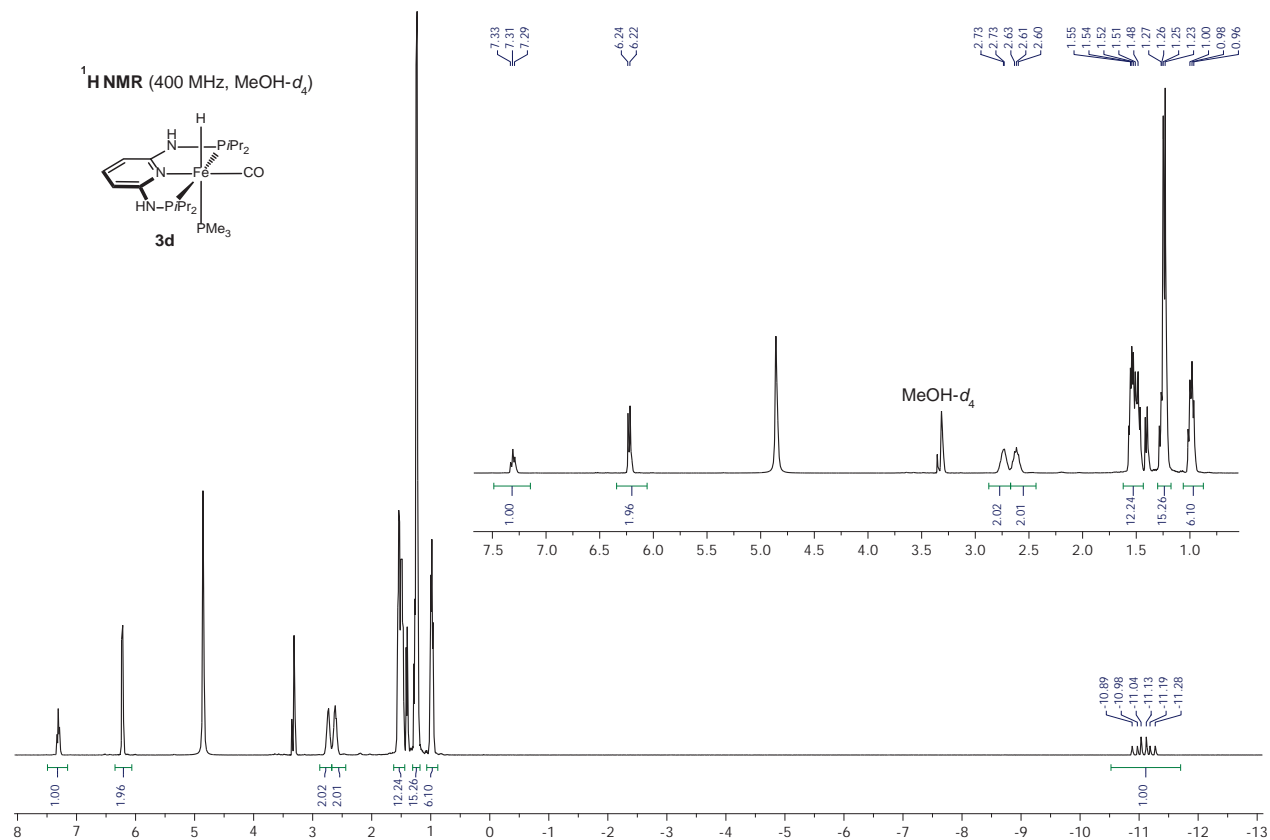


Figure S16. ¹H NMR spectrum of complex **3d**.

S28

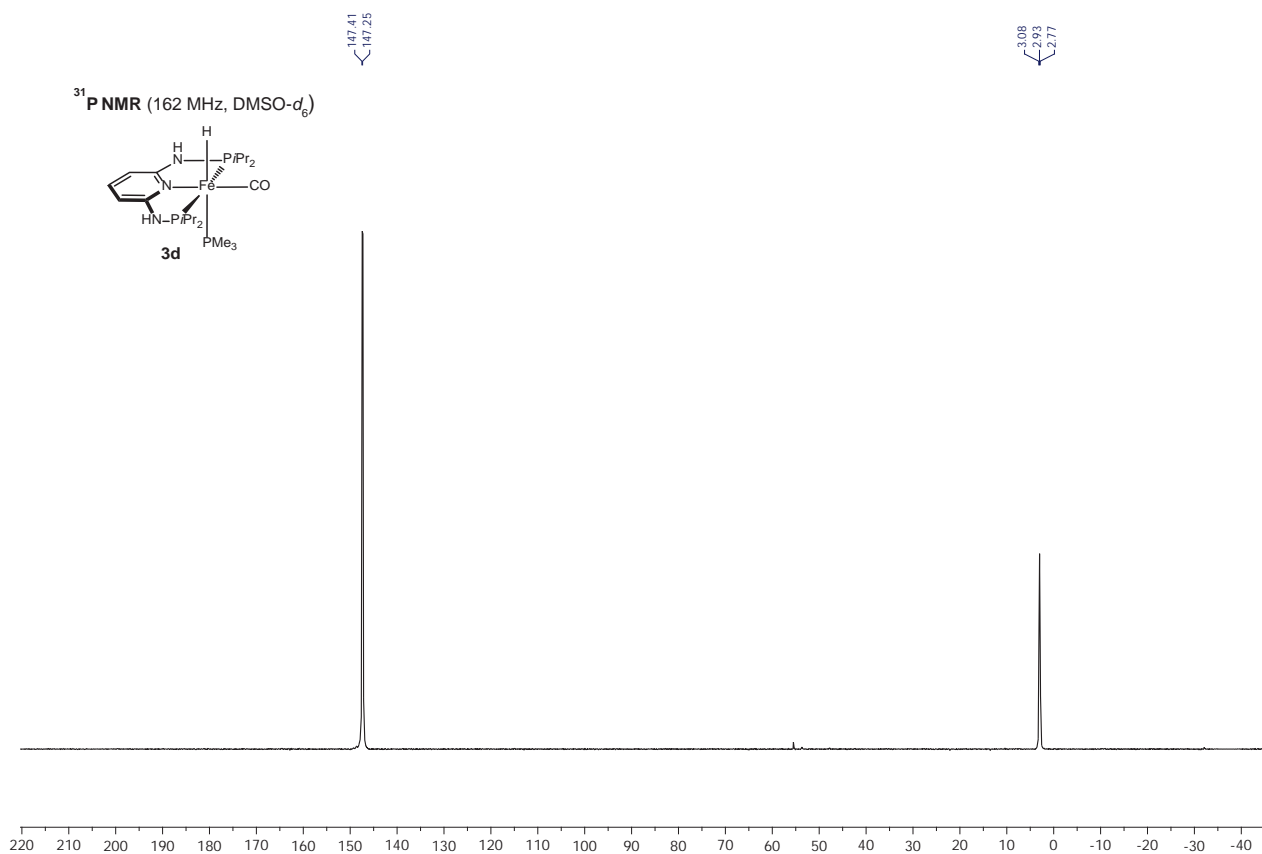


Figure S17. ³¹P{¹H} NMR spectrum of complex **3d**.

S29

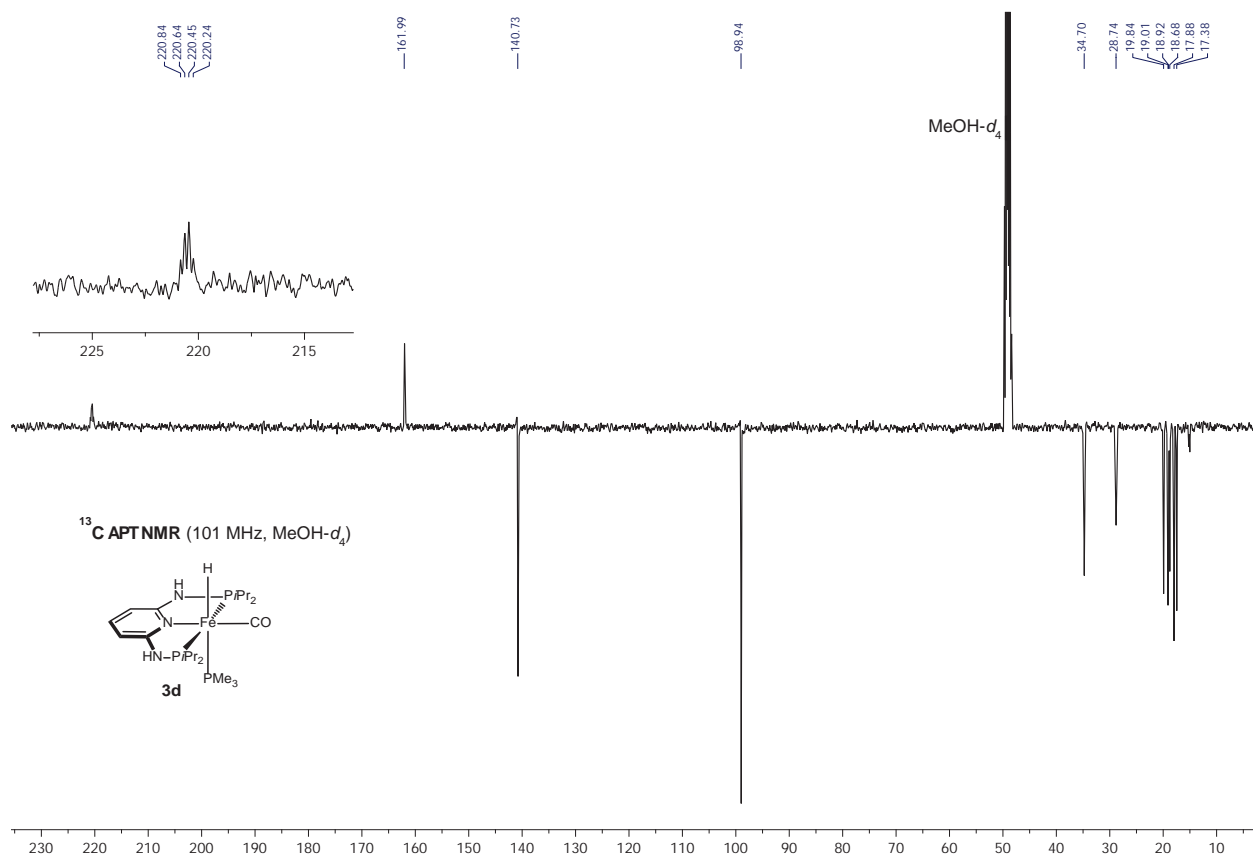


Figure S18. ¹³C{¹H} APT NMR spectrum of complex **3d**.

S30

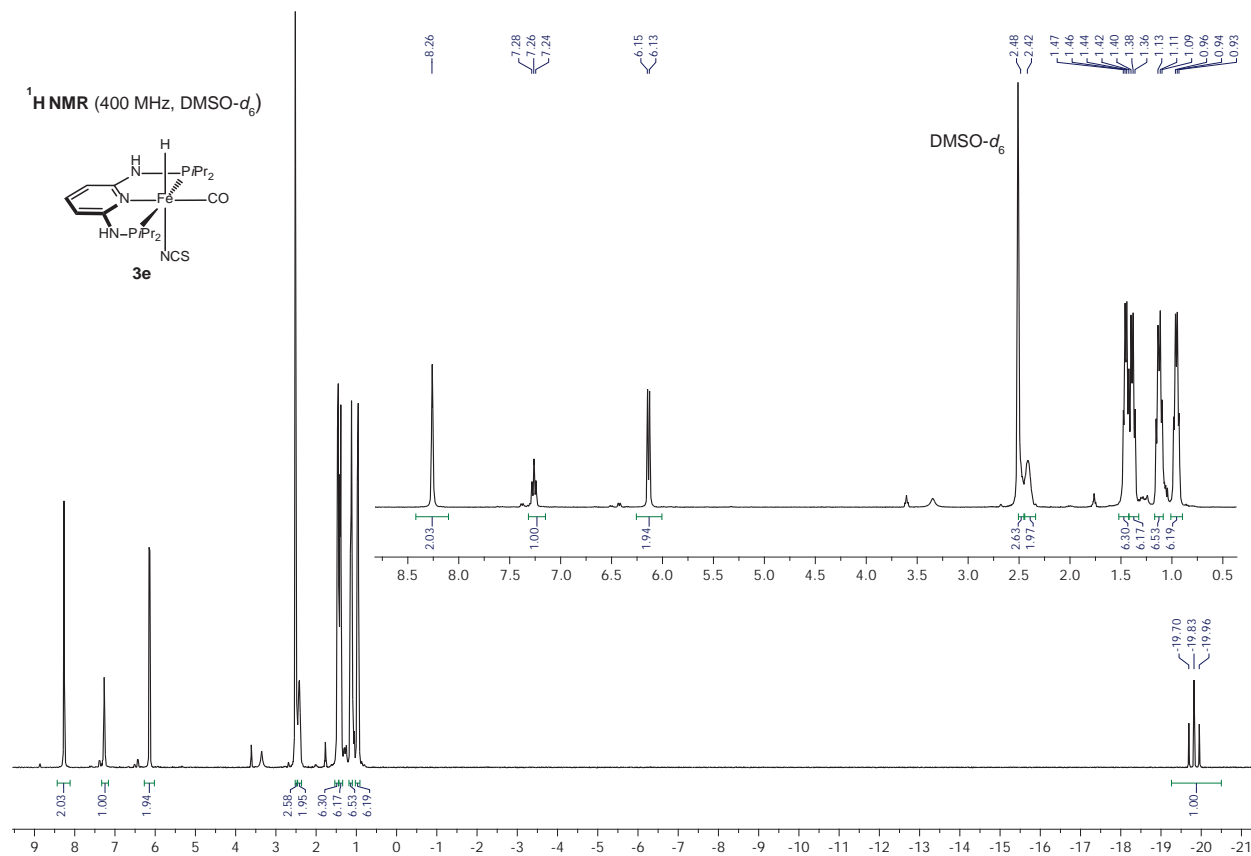


Figure S19. ¹H NMR spectrum of complex **3e**.

S31

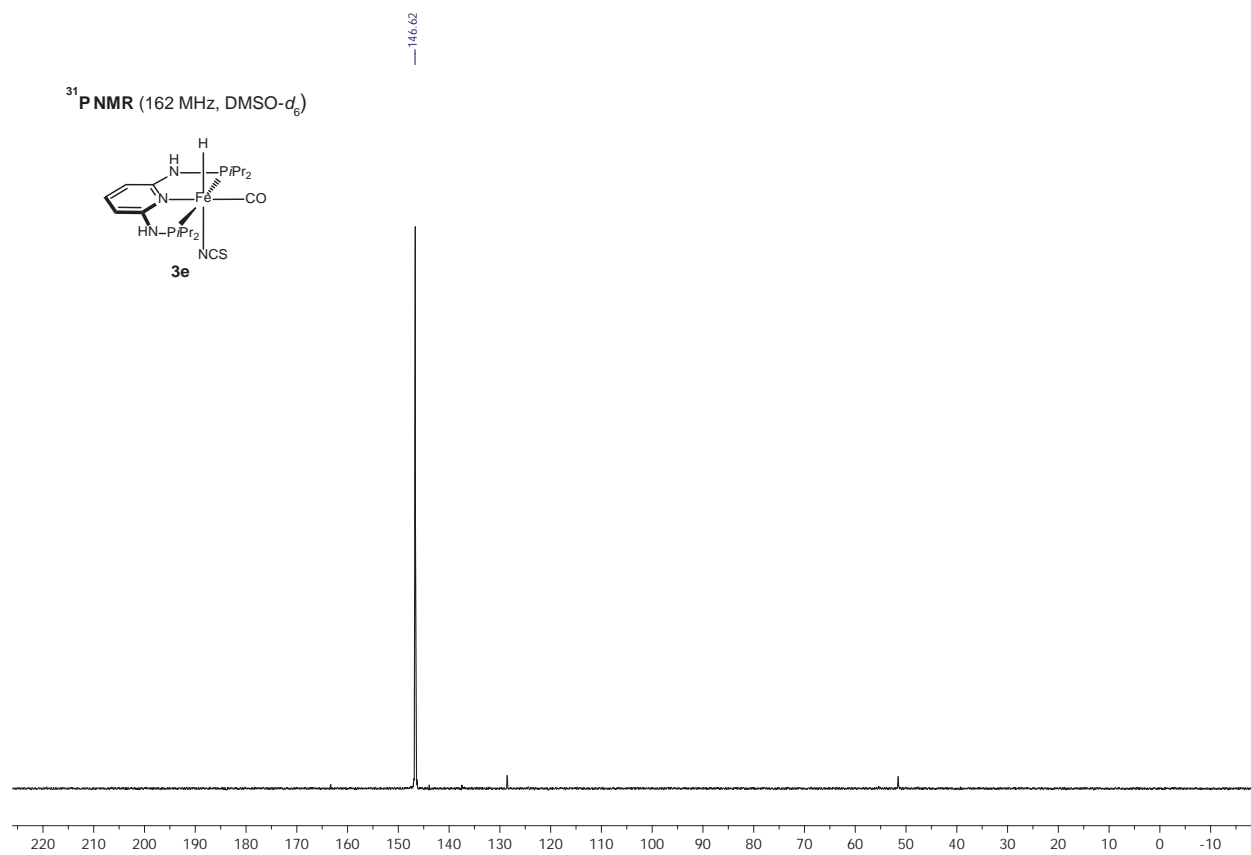


Figure S20. ³¹P{¹H} NMR spectrum of complex **3e**.

S32

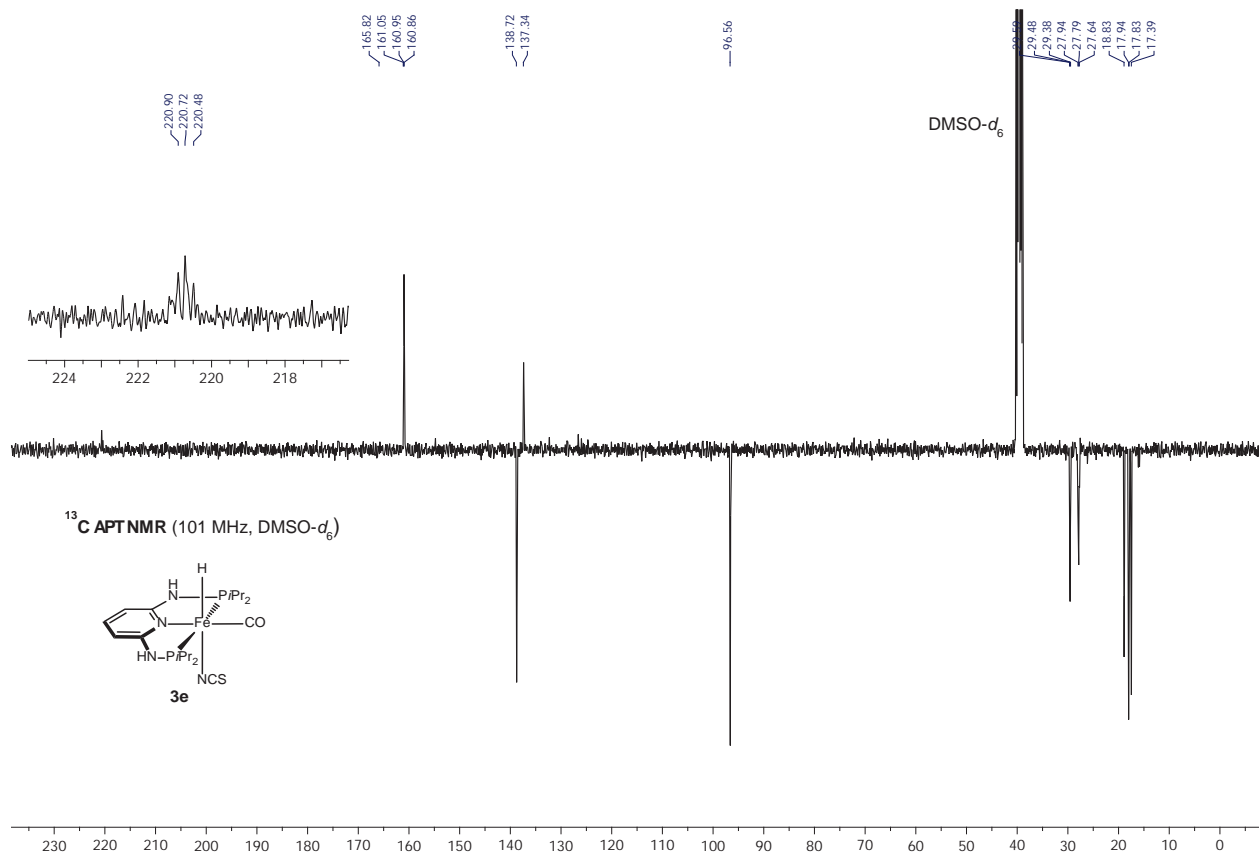


Figure S21. ¹³C{¹H} APT NMR spectrum of complex **3e**.

S33

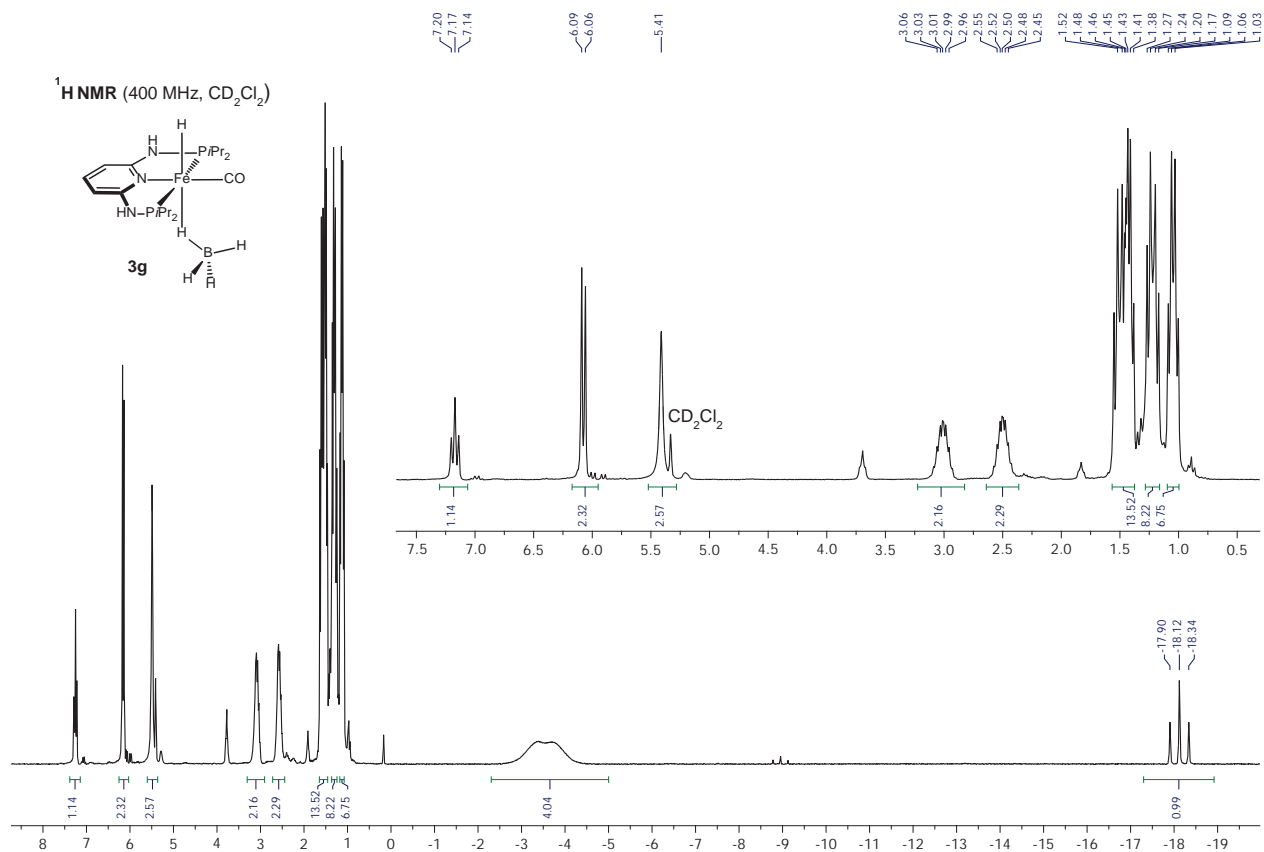
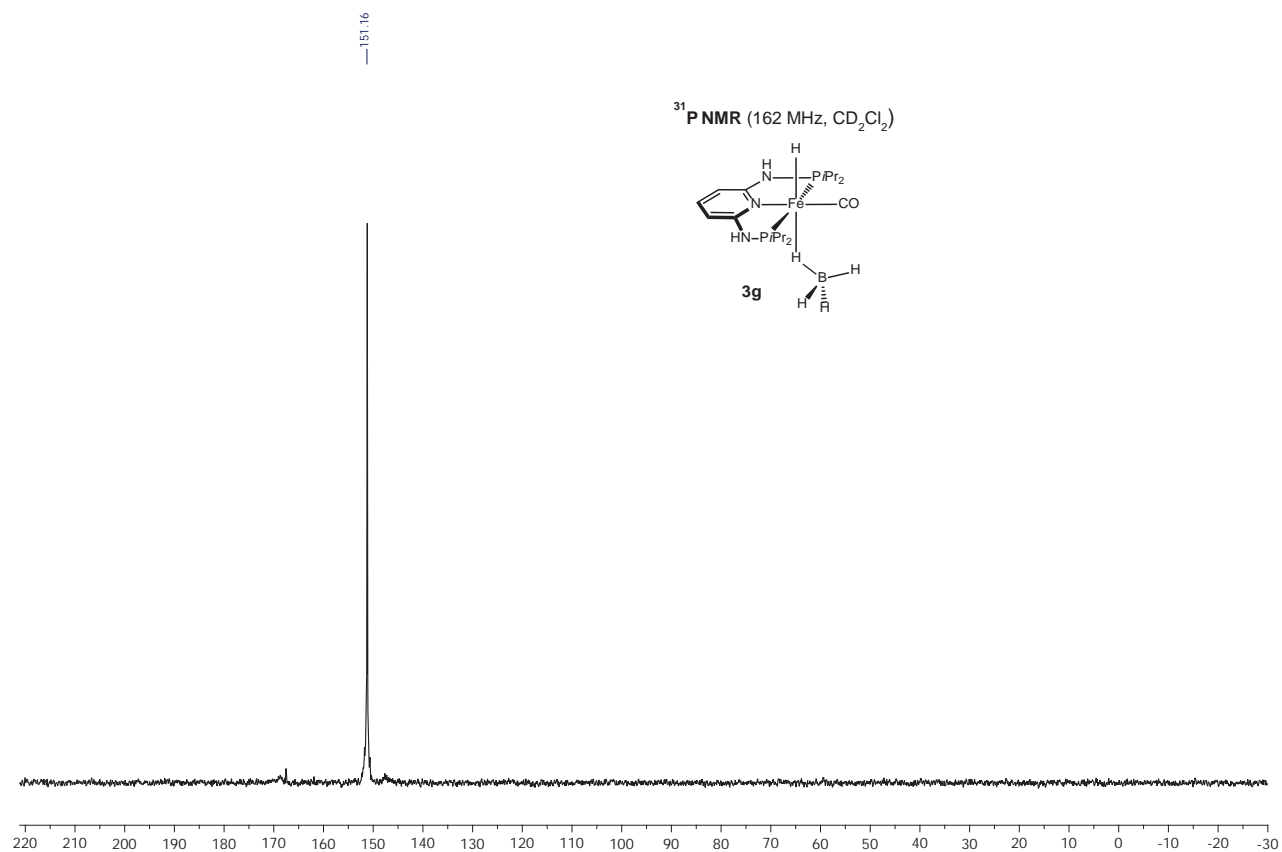
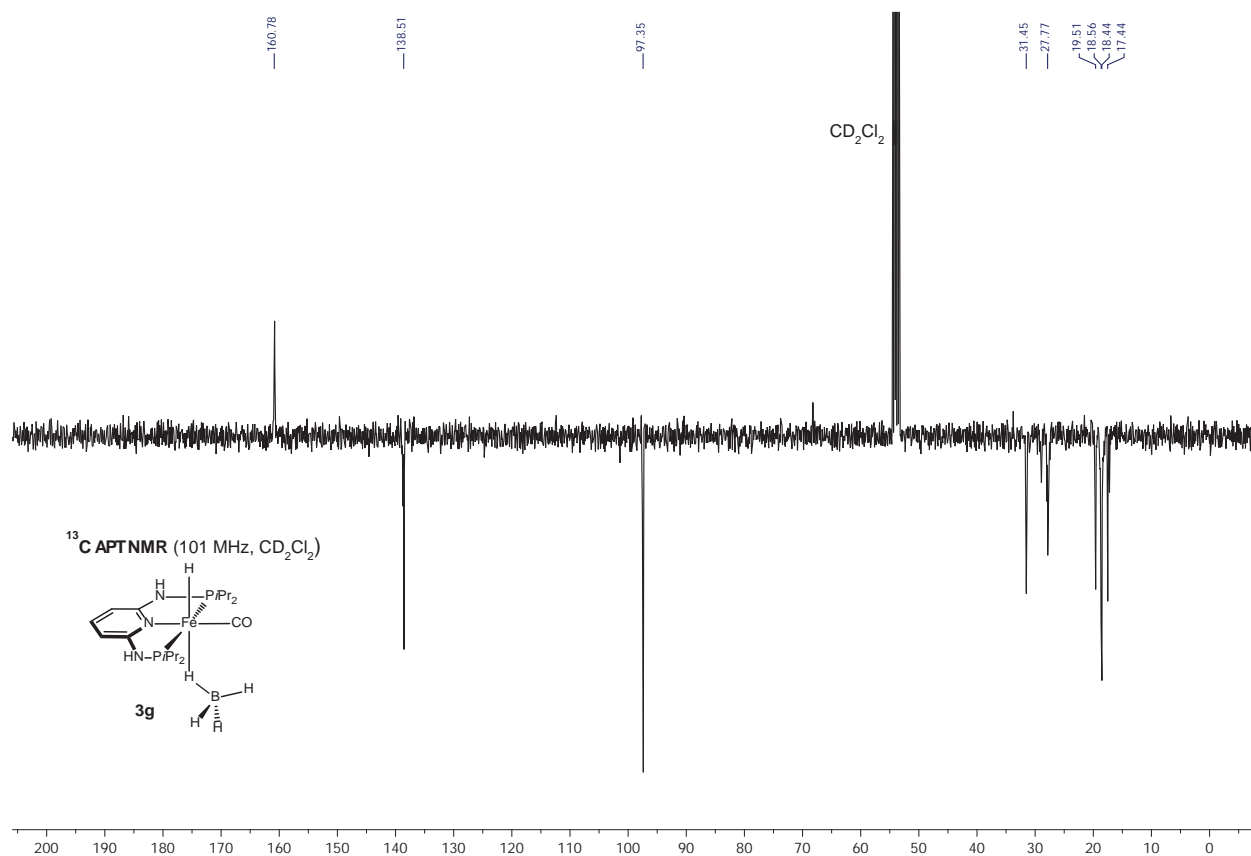


Figure S22. ¹H NMR spectrum of complex **3g**.

S34



S35



S36

Results and Discussion – Part II

Highly Efficient and Selective Hydrogenation of Aldehydes: A Well-Defined Fe(II) Catalyst Exhibits Noble-Metal Activity.

Reprinted with permission from *ACS Catal.* **2016**, *6*, 2664–2672. Copyright 2016 American Chemical Society.



Highly Efficient and Selective Hydrogenation of Aldehydes: A Well-Defined Fe(II) Catalyst Exhibits Noble-Metal Activity

Nikolaus Gorgas,[†] Berthold Stöger,[‡] Luis F. Veiros,[§] and Karl Kirchner^{*,†}

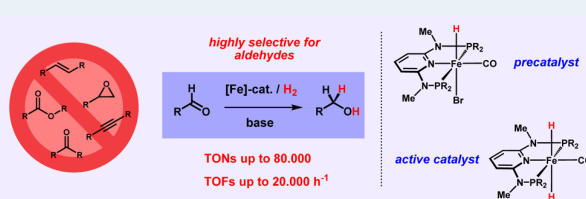
[†]Institute of Applied Synthetic Chemistry and [‡]Institute of Chemical Technologies and Analytics, Vienna University of Technology, Getreidemarkt 9, A-1060 Vienna, Austria

[§]Centro de Química Estrutural, Instituto Superior Técnico, Universidade de Lisboa, Av. Rovisco Pais No. 1, 1049-001 Lisboa, Portugal

Supporting Information

ABSTRACT: The synthesis and application of $[\text{Fe}(\text{PNP}^{\text{Me}}\text{-iPr})(\text{CO})(\text{H})(\text{Br})]$ and $[\text{Fe}(\text{PNP}^{\text{Me}}\text{-iPr})(\text{H})_2(\text{CO})]$ as catalysts for the homogeneous hydrogenation of aldehydes is described. These systems were found to be among the most efficient catalysts for this process reported to date and constitute rare examples of a catalytic process which allows selective reduction of aldehydes in the presence of ketones and other reducible functionalities. In some cases, TONs and TOFs of up to 80000 and 20000 h^{-1} , respectively, were reached. On the basis of stoichiometric experiments and computational studies, a mechanism which proceeds via a *trans*-dihydride intermediate is proposed. The structure of the hydride complexes was also confirmed by X-ray crystallography.

KEYWORDS: aldehyde hydrogenation, iron pincer complexes, homogeneous catalysis, mechanistic studies, DFT calculations



INTRODUCTION

Efficiency and selectivity constitute decisive factors in the development of sustainable chemical processes, especially regarding industrial large-scale applications. Within this context, the catalytic reduction of carbonyl compounds using molecular hydrogen represents a green and economical method to access valuable alcohols for the production of a large number of fine and bulk chemicals.¹ Over the last few decades, a wide variety of highly productive homogeneous catalysts based on noble metals have been developed for this purpose. However, the selective hydrogenation of carbonyl compounds over other reducible functional groups is still a challenging task. Although significant progress has been made concerning the selective reduction of carbonyl groups in the presence of C=C double bonds,² only few examples of catalysts are known which exhibit full selectivity for aldehydes over ketones. In particular, such reactions are important for the production of flavors,³ fragrances,³ and pharmaceuticals.⁴ Very recently, Dupau and co-workers reported a general and highly efficient method for the chemoselective base-free ruthenium-catalyzed hydrogenation of aldehydes in the presence of ketones. By using the ruthenium complex $[\text{Ru}(\text{en})(\text{dppe})(\text{OCO}t\text{Bu})_2]$ (Chart 1), a variety of different ketoaldehydes could be hydrogenated, reaching turnover numbers of up to 40000.⁵ Surprisingly, apart from some quite less effective examples,⁶ this system remains the only example of a noble-metal-based homogeneous hydrogenation catalyst which allows selective reduction of aldehydes in the presence of ketones.

However, it is a major attractive goal to replace scarce, toxic, and expensive noble metals by environmentally friendly and

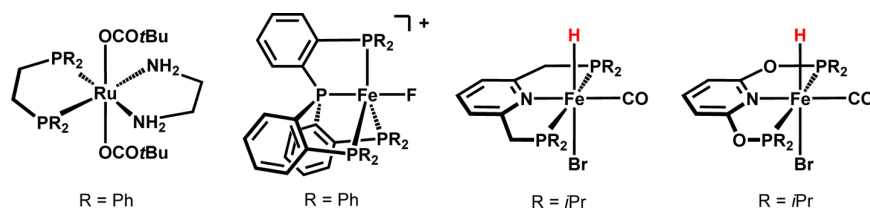
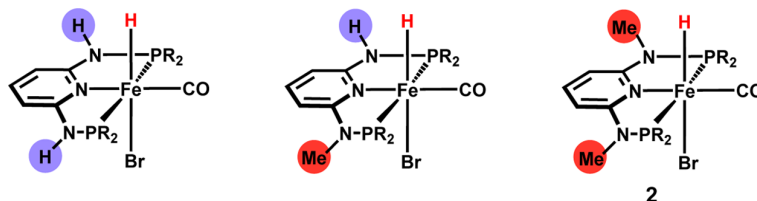
abundant first-row transition metals.^{7,8} Among them, iron appears to be one of the most attractive alternatives.⁹ In recent years, significant progress has been achieved in the development of iron-based hydrogenation catalysts.¹⁰ Interestingly, some of these systems proved to be selective for the reduction of aldehydes in the presence of other carbonyl moieties.^{11–13} In 2013, Beller and co-workers reported on an Fe(II) tetraphos system (Chart 1) which represents the first example of a homogeneous hydrogenation catalyst exhibiting full chemoselectivity for the reduction of aldehydes.¹¹ Various substrates including aromatic, aliphatic, and α,β -unsaturated aldehydes could be efficiently converted into the corresponding primary alcohols, while other carbonyl moieties such as ketones and esters were not reduced. Turnover numbers up to 2000 could be achieved at 140 °C and a hydrogen pressure of 40 bar. Even higher TONs were obtained by the group of Milstein using an Fe(II) hydrido carbonyl pincer complex (Chart 1).¹² This complex was found to be highly active also for the hydrogenation of ketones, while its performance in the reduction of aldehydes was only modest.^{10g} However, by employing NEt_3 as an additive in the reaction, the efficiency of this system could be significantly increased and TONs of up to 4000 were obtained for several substrates under 30 bar of H_2 and a reaction temperature of 40 °C. Interestingly, enhanced productivity was also observed in the presence of a large excess of acetophenone, which, however, was found to be unaffected

Received: February 12, 2016

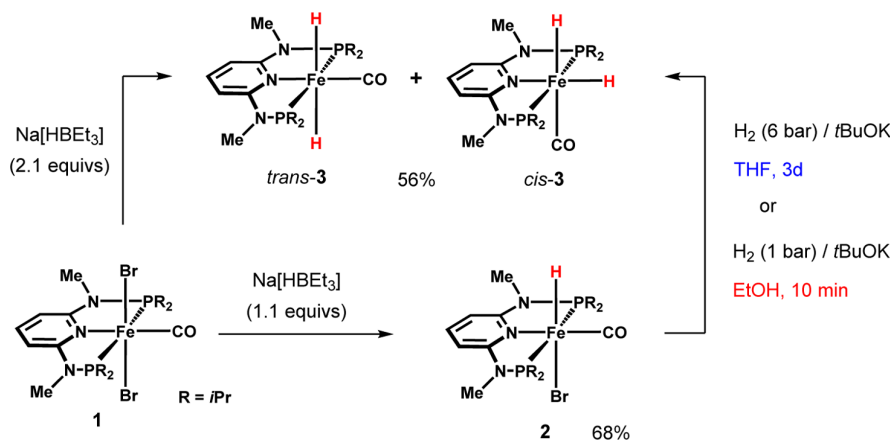
Revised: March 10, 2016

Published: March 11, 2016



Chart 1. Well-Defined Catalysts for the Chemoselective Reduction of Aldehydes^{5,11–13}Chart 2. Iron Hydride Complexes Based on the 2,6-Diaminopyridine Scaffold (R = *i*Pr)

Scheme 1. Synthesis of Complexes 2 and 3 (Mixture of Cis and Trans Isomers)



under these conditions. Although briefly mentioned, no further investigations on the chemoselectivity of this catalyst have been provided. More recently, Hu et al. developed a general method for the chemoselective hydrogenation and transfer hydrogenation of aldehydes by using a similar iron(II) pincer complex supported by a 2,6-bis(phosphinito)pyridine ligand (Chart 1).¹³ This reaction takes place under very mild conditions (4–8 bar of H₂, room temperature), although high catalyst loadings (5–10 mol %) were required to obtain the primary alcohols in reasonable yields. However, it was remarkable that this reaction did not proceed via a bifunctional mechanism: i.e., involving the pincer ligand.^{9d}

Within this context, our group recently reported on the synthesis and reactivity of iron hydride complexes containing PNP pincer ligands based on a 2,6-diaminopyridine scaffold (Chart 2).¹⁴ In these ligands the aromatic pyridine ring and the phosphine moieties are connected via *N*-H or *N*-methyl linkers. The advantage of these ligands is that both substituents on the phosphine and amine sites can be systematically varied in a modular fashion, which has a decisive effect on the outcome of the reactions. Complexes featuring at least one *N*-H spacer in the ligand backbone efficiently catalyze the hydrogenation of ketones under mild conditions.

On the basis of detailed experimental and computational studies it could be shown that this reaction proceeds via an

inner-sphere mechanism in which the catalytically active species is formed by deprotonation of the *N*-H group. In accordance with the proposed mechanism, no reaction took place when the complex [Fe(PNP^{Me}-*i*Pr)(CO)(H)(Br)] (2), which is not capable of this kind of metal–ligand cooperation, was tested. Surprisingly, aldehydes could still be reduced with this complex under the same reaction conditions, thus pointing to an alternative reaction mechanism which allows complete chemoselectivity of aldehydes over ketones. However, these results were just preliminary and the way in which complex 2 is able to promote this reaction remained unclear. In this paper, we provide a detailed catalytic and mechanistic study for the chemoselective reduction of aldehydes using complex 2, which was found to be the most efficient iron-based hydrogenation catalyst reported to date, displaying unprecedented high turnover numbers surpassing even those of noble-metal catalysts.

RESULTS AND DISCUSSION

The monohydride complex [Fe(PNP^{Me}-*i*Pr)(CO)(H)(Br)] (2) was prepared as described previously by the reaction of [Fe(PNP^{Me}-*i*Pr)(CO)(Br)₂] (1) with Na[HBET₃] (1.1 equiv) in THF (Scheme 1). With this procedure typically two isomers were formed.¹⁴ The major isomer of 2, with the hydride ligand

being trans to the bromide ligand, could be isolated in pure form in 68% isolated yield.

Interestingly, by using 2 equiv of Na[HBET₃] the corresponding iron(II) dihydride complexes **3** are obtained, which exist of a mixture of *cis* (major) and *trans* isomers (minor) in an approximate ratio of 1.0:0.7 (Scheme 1). These new complexes could be isolated in 56% yield and were fully characterized by a combination of elemental analysis and ¹H, ¹³C{¹H}, and ³¹P{¹H} NMR and IR spectroscopy. The ³¹P{¹H} NMR spectrum displays two signals at 191.1 and 189.2 ppm for the *cis* and *trans* isomers, respectively. In the ¹³C{¹H} NMR spectrum two triplets centered at 224.7 and 219.5 ppm were observed for the carbonyl ligands, while only one mutual strong band at 1880 cm⁻¹ was found for the CO vibration in the IR spectrum. In the ¹H NMR spectrum, *trans*-**3** exhibits a sharp triplet at -8.76 ppm (*J*_{PH} = 42.9 Hz) while a broad signal centered at -13.02 ppm is observed for *cis*-**3** due to fast interchange of the two hydride ligands. This could be proved by recording NMR spectra at variable temperatures in THF-*d*₆ (Figure 1).

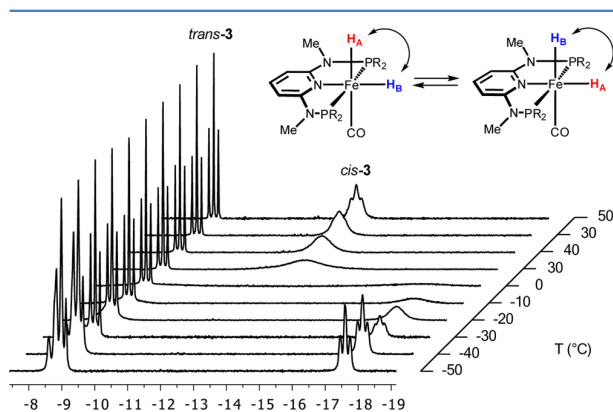


Figure 1. Variable-temperature ¹H NMR spectra of complexes **3** (300 MHz, THF-*d*₆, hydride region). Complex *cis*-**3** gives rise to signals at -8.82 (H_A) and -17.64 ppm (H_B) at -50 °C. At this temperature the signal of H_A is superimposed with that of the hydrides of *trans*-**3** (-8.76 ppm).

Upon cooling, the broad signal originating from the *cis* isomer starts to split into two separate triplets centered at -8.82 and -17.64 ppm, respectively, while the evolution of a single triplet resonance was observed at higher temperatures. In addition, all iron hydride complexes described above could be crystallized and their solid-state structures were determined by X-ray diffraction. Structural views of **2** and **3** are depicted in Figures 2 and 3 with selected bond distances given in the captions.

Alternatively, the iron dihydride could also be prepared in situ by the reaction of complex **2** with *t*BuOK (1.1 equiv) under an atmosphere of H₂. Since **2** is not capable of activating dihydrogen in a bifunctional manner, the formation of **3** likely involves intermolecular cleavage of H₂ with support of the iron center and the external base. The rate of hydrogen cleavage strongly depends on the solvent. Immediate formation of **3** was observed in EtOH (1 bar of H₂), while the same reaction carried out in THF required, even under a hydrogen pressure of 5 bar, up to 3 days in order to achieve complete conversion.

Stoichiometric experiments revealed that **3** readily reacts with aldehydes. Again, significant differences were observed, depend-

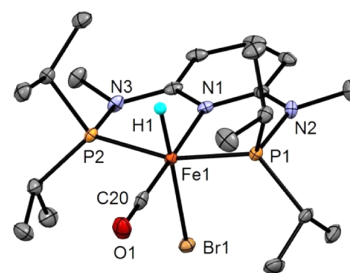


Figure 2. Structural view of [Fe(PNP^{Me}-*i*Pr)(CO)(H)(Br)] (**2**) showing 50% thermal ellipsoids (most H atoms and second independent molecule omitted for clarity). Selected bond lengths (Å) and angles (deg): Fe1-Br1 2.5159(4), Fe1-P1 2.1679(6), Fe1-P2 2.1764(6), Fe1-N1 2.0097(16), Fe1-C20 1.749(2), Fe1-H1 1.46(3); P1-Fe1-P2 161.99(2), N1-Fe1-C20 177.64(9).

ing on the choice of the solvent. The addition of 1 equiv of benzaldehyde to a solution of the iron dihydride in an aprotic solvent (Scheme 2) resulted in the formation of a new iron hydride species, which was, however, present only in small concentrations. This new compound, exhibiting a characteristic triplet resonance at -23.55 ppm (*J*_{PH} = 55.5 Hz) in the hydride region of the ¹H spectrum together with a singlet at 164.9 ppm in the ³¹P{¹H} NMR spectrum, was identified as the alkoxide complex **4** generated by the insertion of the aldehyde into one of the metal-hydride bonds of **3** (Figure 4). The intensity of this signal did not change over time but grew with an increase in the amount of added substrate. Thus, addition of up to 20 equiv of aldehyde was necessary to observe complete conversion of the iron dihydride. Moreover, no reaction took place when the solution of the in situ generated hydrido alkoxide complex was exposed to dihydrogen (24 h, 6 bar).

In contrast to this, the iron dihydride immediately disappeared after the addition of 1 equiv of benzaldehyde when the reaction was carried out in ethanol (Scheme 3). In this case, two new complexes were observed in the ¹H and ³¹P{¹H} NMR spectra. The first complex was again found to be the hydrido alkoxide **4** resulting from substrate insertion, displaying just slightly deviating chemical shifts due to the different solvent. The second complex exhibits a triplet resonance at -26.38 ppm (*J*_{PH} = 58.9 Hz) in the ¹H spectrum which correlates to a signal at 159.4 ppm in the ³¹P{¹H} NMR spectrum and was identified as a cationic species, in which the alkoxide trans to the hydride is replaced by a solvent molecule (**4'**). This complex could be independently synthesized by treatment of **2** with silver salts in ethanol. Purging this mixture with dihydrogen led immediately to the re-formation of the iron dihydride **3**. These findings strongly indicate that the use of a protic solvent is essential for the hydrogenation reaction by stabilizing and solvating the alkoxo ligand trans to the hydride. In particular, this effect appears to be responsible for the irreversibility of the insertion step by preventing β-hydride elimination of the coordinated alkoxide. In the same way, the coordination of dihydrogen to the iron metal center might be facilitated, thus accelerating the rate of H₂ activation. It is worth noting that complex **3** did not react with acetophenone, presumably due to the lower electrophilicity of ketones.

Since the reactivity of a transition-metal hydride is mainly affected by its coligand in the *trans* position, we therefore expected that only the *trans* isomer is reactive toward aldehydes and that both isomers are in equilibrium with one another (Scheme 4).¹⁵

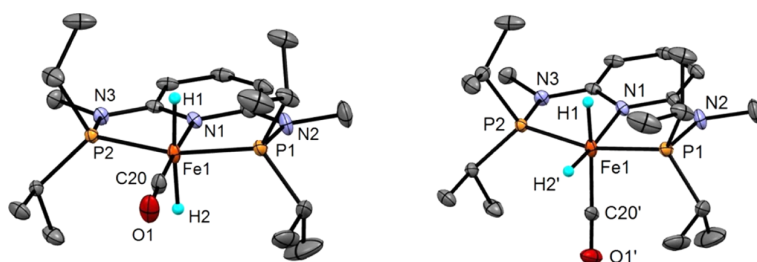


Figure 3. Structural views of (left) *trans*-[Fe(PNP^{Me}-iPr)(H)₂(CO)] (*trans*-3) and (right) *cis*-[Fe(PNP^{Me}-iPr)(H)₂(CO)] (*cis*-3) showing 50% thermal ellipsoids (most H atoms omitted for clarity). Selected bond lengths (Å) and angles (deg): Fe1–P1 2.1270(4), Fe1–P2 2.1258(4), Fe1–N1 1.9920(8), Fe1–C20 1.683(3), Fe1–C20' 1.815(3), Fe1–H1 1.46(2), Fe1–H2 1.46(4), Fe1–H2' 1.46(2); P1–Fe1–P2 164.09(2), N1–Fe1–C20 177.3(1), N1–Fe1–C20' 104.7(1).

Scheme 2. Reaction of 3 with Benzaldehyde in C₆D₆

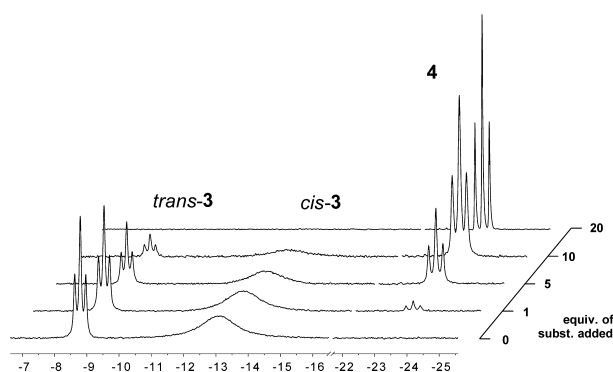
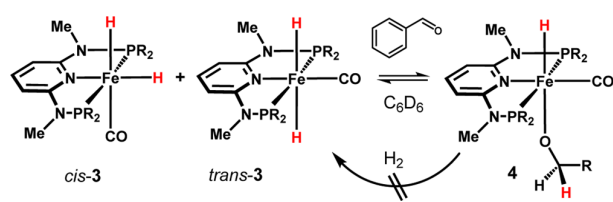
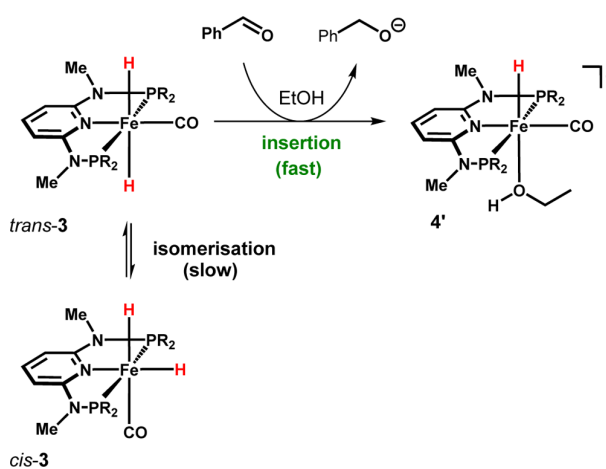


Figure 4. ¹H NMR spectra (250 MHz, C₆D₆, hydride region) of 3 in the presence of increasing amounts of benzaldehyde, showing the formation of the corresponding alkoxide complex 4.

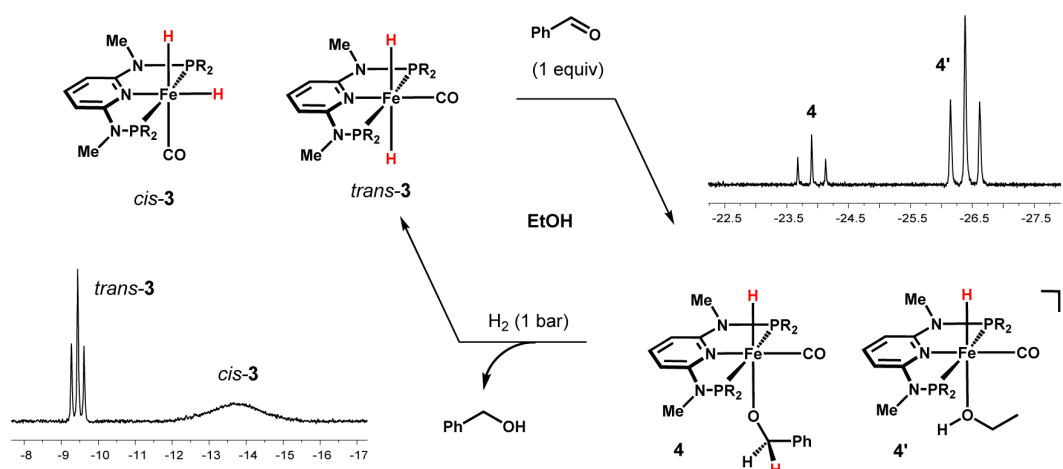
Scheme 4. Reaction of 3 with Benzaldehyde in EtOH^a



^aSee Figure 5.

The *cis*/*trans* isomerization was thought to take place within minutes, since no exchange could be observed on the NMR time scale (¹H–¹H EXSY). Thus, another experiment was performed by adding only 0.5 equiv of benzaldehyde to a solution of 3 in ethanol and the reaction was continuously

Scheme 3. Reaction of 3 with 1 equiv of Benzaldehyde in EtOH^a



^aThe inset gives the hydride region of the ¹H NMR spectra of *cis*- and *trans*-3 as well as the alkoxide and ethanol complexes 4 and 4', respectively, at room temperature.

monitored by $^{31}\text{P}\{^1\text{H}\}$ NMR spectroscopy. As depicted in Figure 5, the signal of *trans*-3 immediately disappeared and a

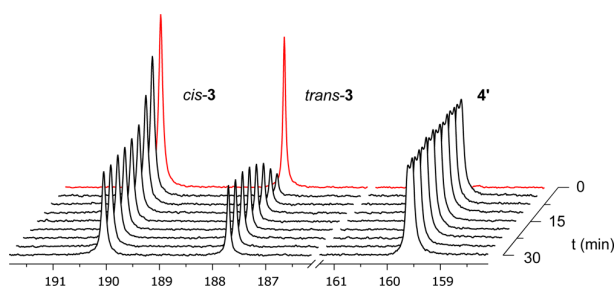


Figure 5. $^{31}\text{P}\{^1\text{H}\}$ NMR spectra (101 MHz, $\text{EtOH}/\text{C}_6\text{D}_6$) of **3** before (red) and over a period of 30 min after addition of 0.5 equiv of benzaldehyde (black) showing immediate complete conversion of *trans*-3 into the ethanol complex **4'** followed by recovery of *trans*-3 via isomerization of *cis*-3 (due to incomplete proton decoupling the signal of **4'** shows a slight residual coupling to the corresponding hydride ligand).

new signal was found again for the ethanol complex **4'**, whereas the concentration of *cis*-3 remained almost unaffected. In this case, the hydrido alkoxide complex was not observed, which might be attributed to the lower substrate concentration in comparison to the previous experiments (Scheme 4 and Figure 4). As expected, we observed recovery of the *trans*-dihydride as a result of the slow isomerization process, which required several minutes to again reach its equilibrium state.

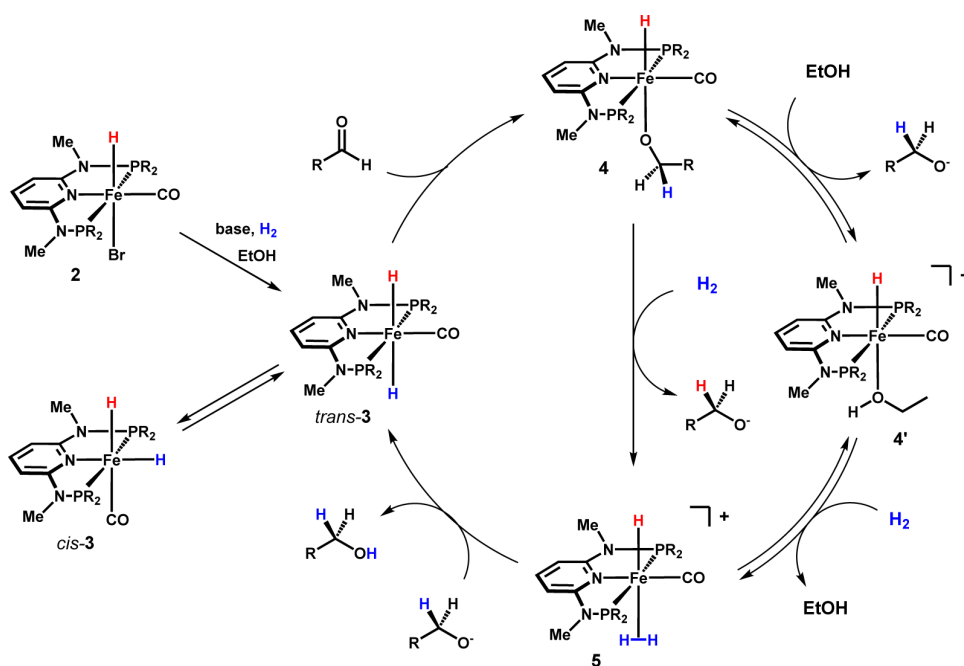
On the basis of the observations described above, a simplified catalytic cycle is depicted in Scheme 5. The precatalyst **2** readily forms complex *trans*-3 as a result of heterolytic cleavage of dihydrogen promoted by the iron metal center and the external base. Substrate insertion proceeds presumably through an

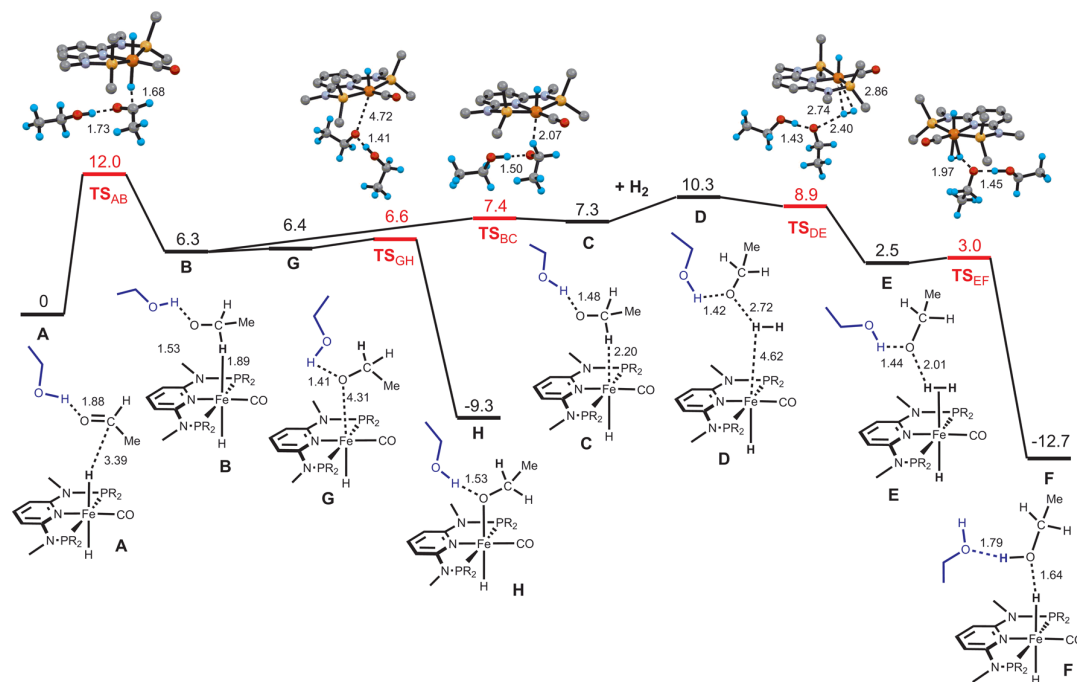
outer-sphere mechanism in which the nucleophilic dihydride directly attacks the aldehyde's carbonyl group to give the alkoxide intermediate **4**. The compound is labile, and the alkoxide ligand may be replaced either by the solvent (ethanol) to form **4'** or by dihydrogen to form complex **5**, which features an $\eta^2\text{-H}_2$ -bound dihydrogen ligand. Subsequent deprotonation of the coordinated H_2 finally leads to the regeneration of *trans*-3 and liberation of the product alcohol. Intermediate **5** may also be formed by replacement of the solvent in **4'** by H_2 . However, since intermediates **4** and **4'** could be detected by NMR spectroscopy, the question arises as to whether or not these species are indeed part of the catalytic cycle or are merely resting states.

Accordingly, the reaction mechanism was explored in detail by means of DFT calculations.¹⁶ In the model used for the calculations, acetaldehyde was taken as the substrate and *trans*-3 as the active species. In addition, an explicit ethanol molecule (solvent) was considered, providing a proton shuttle and H-bond stabilization of the intermediates. The free energy profile obtained for the reaction is represented in Scheme 6.¹⁷ The mechanism starts with nucleophilic attack of one hydride ligand of *trans*-3 to the carbonyl C atom of acetaldehyde (in A), with formation of an ethoxide ion that coordinates the metal weakly in a C–H σ complex (B). This species is further stabilized by an $\text{EtOH}\cdots\text{OH}$ bond with the neighboring ethanol molecule. The process is endergonic, with $\Delta G = 6.3$ kcal/mol, and the corresponding barrier ($\Delta G^\ddagger = 12.0$ kcal/mol) indicates a facile process.

The second step of the mechanism corresponds to dissociation of the C–H coordinated ethoxide, yielding a cationic Fe complex with one free coordination position (C). The process has a small barrier of 1.1 kcal/mol and is essentially thermoneutral ($\Delta G = 1.0$ kcal/mol). The free coordination position in C may be occupied by three different species. One possibility is, naturally, a solvent molecule

Scheme 5. Proposed Simplified Catalytic Cycle for the Chemoselective Hydrogenation of Aldehydes with Dihydrogen To Give Alcohols on the Basis of Experimental Findings



Scheme 6. Free Energy Profile Calculated (DFT) for the Hydrogenation of Acetaldehyde by H₂, Catalyzed by *trans*-3^a

^aThe free energy values (kcal/mol, solvent corrected, EtOH) are referred to the initial reactants (A), and relevant distances (Å) are indicated.

Table 1. Hydrogenation of 4-Fluorobenzaldehyde with Catalyst 2^a

entry	S/C	P (bar)	T (°C)	base (mol %)	t (h)	conversion (%) ^b	TON	TOF (h ⁻¹)
1	2000	6	room temp	<i>t</i> BuOK (1.0)	0.5	>99	2000	4000
2	10000	6	room temp	<i>t</i> BuOK (1.0)	24	>99	10000	417
3	10000	30	room temp	<i>t</i> BuOK (1.0)	1	>99	10000	10000
4	10000	30	room temp	<i>t</i> BuOK (0.5)	1	>99	10000	10000
5	10000	30	room temp	<i>t</i> BuOK (0.4)	1	50	5000	5000
6	10000	30	room temp	<i>t</i> BuOK (0.3)	1	18	1800	1800
7	10000	30	room temp	<i>t</i> BuOK (0.2)	1	<1	0	0
8	20000	30	room temp	<i>t</i> BuOK (0.5)	1	62	12300	12300
9	20000	30	room temp	<i>t</i> BuOK (1.0)	1	73	14600	14600
10	20000	30	40	<i>t</i> BuOK (1.0)	1	93	18600	18600
11	20000	30	room temp	<i>t</i> BuOK (2.5)	1	33	6600	6600
12	20000	30	room temp	DBU (1.0)	1	46	9200	9200
13	20000	30	40	DBU (1.0)	1	85	17000	17000
14	20000	30	40	DBU (5.0)	1	91	18200	18200
15	20000	30	40	DBU (1.0)	16	>99	20000	1250
16	20000	60	40	DBU (1.0)	1	>99	20000	20000
17 ^c	40000	60	40	DBU (1.0)	16	>99	40000	2500
18 ^d	80000	60	40	DBU (1.0)	48	>99	80000	1667

^aReaction conditions unless stated otherwise: 2 (0.1–1.0 μmol, 50–500 ppm), 4-fluorobenzaldehyde (2 mmol), base (0.2–5.0 mol %), EtOH (1 mL). ^bDetermined by ¹⁹F NMR spectroscopy; average of two runs. ^cReaction conditions 4-fluorobenzaldehyde (4 mmol), EtOH (2 mL). ^dReaction conditions 4-fluorobenzaldehyde (8 mmol), EtOH (4 mL).

(ethanol) producing complex 4' as depicted in Schemes 4 and 5. This is a facile process with a barrier of only 2.7 kcal/mol and a free energy balance of $\Delta G = -2.4$ kcal/mol (see Figure S1 in the Supporting Information). Alternatively, there can be O-coordination of the recently formed ethoxide ion, resulting in complex H (4) and exhibiting a negligible barrier (0.2 kcal/mol), being a considerably exergonic process ($\Delta G = -15.7$ kcal/mol). In fact, the alkoxide complex H is 9.3 kcal/mol more stable than the initial reactants, being by far the most stable intermediate along the reaction mechanism and, thus,

representing the catalyst resting state. Finally, the free coordination position in C can be occupied by one dihydrogen molecule, giving rise to formation of the dihydrogen complex E. This process is clearly exergonic ($\Delta G = -7.8$ kcal/mol) and essentially barrierless. The final step corresponds to the breaking of the H–H bond in the dihydrogen complex E, with protonation of the nearby ethoxide ion and regeneration of the dihydride species (in F). This is a facile process with a barrier of only 0.5 kcal/mol, being largely exergonic ($\Delta G = -15.2$ kcal/mol). Overall, the reaction is exergonic with $\Delta G =$

–12.7 kcal/mol, and closing the cycle exchanging one ethanol molecule (the reaction product) with a new acetaldehyde molecule (the substrate), from **F** back to **A**, is slightly endergonic, with a free energy balance of $\Delta G = 4.1$ kcal/mol. The highest barrier of the entire process corresponds to substitution of ethoxide in **H** by one H_2 molecule, in order to allow the reaction to continue. Therefore, the overall barrier for the process is the difference between the free energy values of **H** and TS_{DE} , being ca. 20 kcal/mol, in good agreement with the experimental conditions used for the reaction. It has to be noted that a similar mechanism was proposed recently by Yang, albeit for the reduction of ketones rather than aldehydes.¹⁸

Since the preliminary catalytic reactions were obtained with high catalyst loadings, more extensive test reactions were performed here in order to investigate the catalytic performance of complex **2**. Initial experiments were conducted in EtOH using 4-fluorobenzaldehyde as substrate (Table 1). In presence of 0.05 mol % of **2** together with 1.0 mol % of *t*BuOK, full conversion to the corresponding primary alcohol was achieved within 30 min at room temperature and a hydrogen pressure of 6 bar. In accordance with our observations on a stoichiometric level, no reaction took place in aprotic solvents such as THF and toluene. A possible transfer-hydrogenation mechanism in EtOH could be excluded, since the reduction of 4-fluorobenzaldehyde was not observed in the absence of dihydrogen.

Decreasing the catalyst loading led to significantly lower reaction rates. Nevertheless, although a much longer reaction time was required, full conversion could still be accomplished at a catalyst to substrate ratio of 1:10000, demonstrating the high efficiency and robustness of this system (Table 1, entry 2). As expected, the catalytic activity increased dramatically by applying higher hydrogen pressures. For example, performing the same reaction at 30 bar reduced the reaction time from 24 h to less than 1 h (entry 3), and even 73% of the primary alcohol was obtained at a catalyst to substrate ratio of 1:20000 (entry 9).

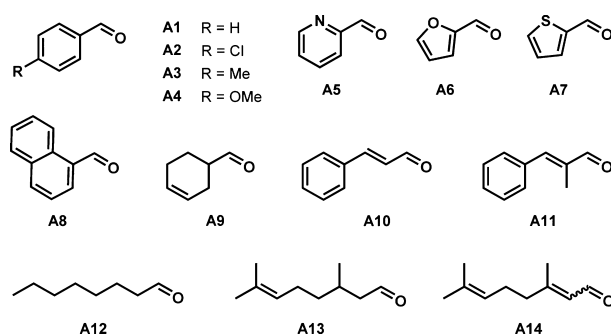
The presence of a strong base appeared mandatory for the reaction to occur. By comparing turnover frequencies after 1 h, we found that a certain amount of *t*BuOK is needed in order to maintain the catalyst in its active state. When the base loading was reduced below 1.0 mol %, the initial reaction rates dropped significantly (Table 1, entries 4–7). On the other hand, larger quantities of *t*BuOK also resulted in lower activity (entry 11). In light of the common sensitivity of aldehydes toward highly basic conditions, this result might be attributed to ongoing side reactions of the substrate, which may potentially cause catalyst deactivation. Therefore, weaker bases were also considered. At a substrate to base ratio of 1:100, amines such as NEt_3 and diisopropylethylamine were not effective, whereas DBU (1,8-diazabicyclo[5.4.0]undec-7-ene) was found to be a suitable cocatalyst. Although the catalytic activity was lower in comparison to that of *t*BuOK at room temperature, similar initial turnover frequencies were observed when the reaction temperature was raised to 40 °C and higher base loadings did not diminish the catalytic performance of complex **2** (entries 12–14). Even when a catalyst to substrate ratio of only 1:20000 was used, 73% of the primary alcohol was formed within 1 h and >99% was formed after the same time when the pressure was increased to 60 bar (entry 16), which corresponds to a turnover frequency of more than 20000 h^{-1} .

Finally, by using this protocol a turnover number of 40000 could be reached within 16 h (Table 1, entry 17) and, most

impressive, on application of a long reaction time of 48 h full conversion was still achieved at a catalyst to substrate ratio of 1:80000 (corresponds to 12.5 ppm catalyst loading, entry 18), which is one of the highest turnover numbers reached for a selective aldehyde reduction catalyst to date.¹⁹

In order to prove the general applicability of **2**, a scope of various substrates has been tested (Table 2). The catalytic

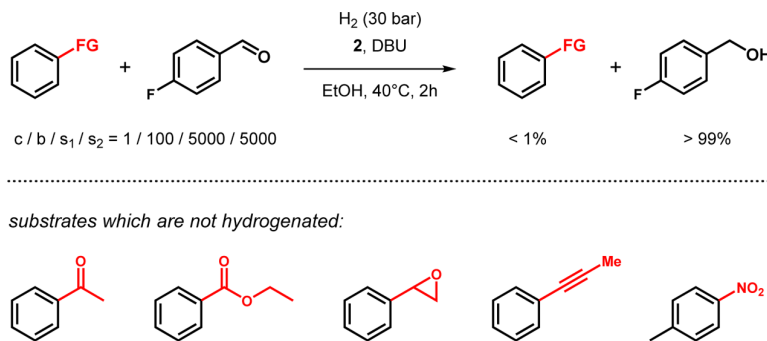
Table 2. Hydrogenation of Aldehydes A1–A14 with Catalysts 2^a



entry	S/C	substrate	conversion (%) ^b	yield (%) ^c
1	20000	A1	>99	96
2	20000	A2	>99	>99
3	15000	A3	>99	>99
4	15000	A4	98	98
5	20000	A5	>99	97
6	20000	A6	>99	>99
7	20000	A7	>99	>99
8	10000	A8	97	96
9	10000	A9	>99	98
10	10000	A10	>99	>99
11 ^d	20000	A10	>99	>99
12	10000	A11	>99	>99
13	10000	A12	>99	>99
14	10000	A13	99	97
15	10000	A14	99	99

^aReaction conditions unless stated otherwise: catalyst **2** (0.1–0.2 μ mol, 50–100 ppm), aldehyde (2 mmol), DBU (20 μ mol, 1.0 mol %), EtOH (1 mL), 30 bar of H_2 , 40 °C, 16 h. ^bDetermined by integration of 1H NMR spectra. ^cBased on integration of 1H spectra using mesitylene as internal standard. ^dReaction conditions: 60 bar of H_2 .

experiments were conducted in the presence of 50–100 ppm of catalyst together with 1 mol % of DBU at 40 °C and 30 bar of hydrogen pressure, to ensure quantitative conversion for all substrates in a reasonable reaction time (16 h). The best results could be obtained for heteroaromatic substrates and aromatic aldehydes bearing electron-withdrawing halogen substituents on the phenyl ring, while the reduction of benzaldehyde and derivatives with electron-donating groups such as 4-anisaldehyde and 4-tolylaldehyde was slightly slower. Even sterically demanding as well as aliphatic aldehydes could be reduced quantitatively at low catalyst loadings. If present, C=C double bonds remained unaffected, even in the case of challenging α,β -unsaturated substrates such as cinnamaldehydes or the industrially important citral, emphasizing the high selectivity of this system. It has to be noted that the hydrogenation of cinnamaldehyde did not proceed in the presence of *t*BuOK, revealing the benefits of employing DBU as the base in the reaction. Again, higher turnover numbers could be obtained by

Scheme 7. Hydrogenation of 4-Fluorobenzaldehyde in the Presence of Different Cosubstrates Bearing Other Reducible Functionalities


increasing the hydrogen pressure. This was exemplarily shown for cinnamaldehyde, which was quantitatively converted into the corresponding primary alcohol at a catalyst to substrate ratio of 1:20000 at 60 bar of H_2 .

Additional tests were carried out in order to investigate the catalyst's selectivity toward other reducible functionalities (Scheme 7). For this purpose, competitive experiments were performed using an equimolar mixture of 4-fluorobenzaldehyde and the respective cosubstrate at a catalyst to substrate ratio of 1:5000 with respect to the aldehyde. Gratifyingly, ketones, esters, epoxides, alkynes, and nitro groups were not hydrogenated and did also not interfere with the reaction.

Since the iron(II) dihydride is supposed to be a key intermediate in the catalytic hydrogenation, we finally conducted a series of test reactions in which the isolated complex **3** was directly used as the catalyst (Table 3). In this

Table 3. Hydrogenation of Cinnamaldehyde using **3 as Catalyst^a**

entry	amt of catalyst (mol %)	base	conversion (%) ^b	yield (%) ^c
1	0.5	none	>99	>99
2	0.1	none	0	0
3 ^d	0.1	NEt ₃	>99	>99

^aReaction conditions unless stated otherwise: catalyst **3**, cinnamaldehyde (2.0 mmol), EtOH (1 mL), 30 bar OF H_2 , room temperature.

^bDetermined by integration of 1H spectra. ^cBased on integration of 1H NMR spectra using mesitylene as internal standard. ^dReaction conditions: EtOH (0.8 mL), NEt₃ (0.4 mL).

case, the addition of an external base was not required. Using cinnamaldehyde as the substrate resulted in full conversion to the corresponding primary alcohol at a catalyst loading of 0.5 mol % within 1 h (30 bar, room temperature), but no reaction took place when the amount of **3** was lowered to 0.1 mol %. This is in accordance with our findings on the influence of the base loading on the catalytic activity, since the overall basicity of the reaction solution now exclusively depends on the amount of the product alkoxide which is initially formed by the insertion of the aldehyde into the metal–hydride bond. However, quantitative formation of cinnamyl alcohol was achieved when the same reaction was carried out in a 2:1 mixture of EtOH and NEt₃.

CONCLUSION

In sum, an inexpensive and robust homogeneous precatalyst and catalyst using earth-abundant iron, $[Fe(PNP^{Me-iPr})(CO)(H)(Br)]$ and $[Fe(PNP^{Me-iPr})(H)_2(CO)]$ (mixture of *trans* and *cis* isomers), based on the 2,6-diaminopyridine scaffold where the $PiPr_2$ moieties of the PNP ligand connect to the pyridine ring via NMe spacers, was developed and applied to the hydrogenation of several aldehydes to alcohols in the presence of DBU as base. This methodology proceeds with high chemoselectivity even in the presence of other reducible functional groups such as ketones, esters, alkynes, olefins, and α,β -unsaturated double bonds. The yields and chemoselectivities under mild conditions are exceptional in comparison with previous iron catalysts and even noble-metal catalysts. In some cases, full conversion was achieved even at a catalyst to substrate ratio of 1:80000 (12.5 ppm catalyst loading). Accordingly, $[Fe(PNP^{Me-iPr})(CO)(H)(Br)]$ and $[Fe(PNP^{Me-iPr})(H)_2(CO)]$ are some of the most efficient hydrogenation catalysts for this process to date. On the basis of stoichiometric experimental and computational studies, a mechanism which indeed proceeds via the *trans*-dihydride complex $[Fe(PNP^{Me-iPr})(H)_2(CO)]$ is proposed. Thus, the low catalyst loadings (typically 50 ppm), mild reaction conditions (40 °C, 30 bar of H_2), the broad applicability, and the mild reaction conditions make these catalysts and this procedure interesting for the synthesis of fine and bulk chemicals.³

ASSOCIATED CONTENT

Supporting Information

The Supporting Information is available free of charge on the ACS Publications website at DOI: 10.1021/acscatal.6b00436.

Complete crystallographic data, 1H , $^{13}C\{^1H\}$, and $^{31}P\{^1H\}$ NMR spectra of all complexes, and computational details and coordinates of all optimized species (PDF)

Crystallographic data for **2** and **3** (CCDC entries 1433576 (**2**) and 1433577 (**3**)) (CIF)

AUTHOR INFORMATION

Corresponding Author

*E-mail for K.K.: kkirch@mail.tuwien.ac.at.

Notes

The authors declare no competing financial interest.

ACKNOWLEDGMENTS

Financial support by the Austrian Science Fund (FWF) is gratefully acknowledged (Project No. P24583–N28). L.F.V. acknowledges the Fundação para a Ciência e Tecnologia, Projecto Estratégico- PEst-OE/UI0100/2013. The X-ray center of the Vienna University of Technology is acknowledged for financial support and for providing access to the single-crystal diffractometer.

REFERENCES

- (1) (a) *Handbook of Homogeneous Hydrogenation*; de Vries, J. G., Elsevier, C. J., Eds.; Wiley-VCH: Weinheim, Germany, 2007. (b) Dupau, P. In *Organometallics as Catalysts in the Fine Chemical Industry*; Beller, M., Blaser, H. U., Eds.; Springer-Verlag: Berlin, 2012. (c) Johnson, N. B.; Lennon, I. C.; Moran, P. H.; Ramsden, J. A. *Acc. Chem. Res.* **2007**, *40*, 1291–1299. (d) Dub, P. A.; Ikariya, T. *ACS Catal.* **2012**, *2*, 1718–1741.
- (2) (a) Noyori, R.; Ohkuma, T. *Pure Appl. Chem.* **1999**, *71*, 1493–1501. (b) Noyori, R.; Ohkuma, T. *Angew. Chem., Int. Ed.* **2001**, *40*, 40–73. (c) Noyori, R. *Angew. Chem., Int. Ed.* **2002**, *41*, 2008–2022. (d) Ohkuma, H.; Ooka, T.; Ikariya, R.; Noyori, J. *Am. Chem. Soc.* **1995**, *117*, 10417–10418.
- (3) (a) *Common Fragrance and Flavor Materials*; Surburg, H., Panten, J., Eds.; Wiley-VCH: Weinheim, Germany, 2006. (b) Saudan, L. A. *Acc. Chem. Res.* **2007**, *40*, 1309–1319.
- (4) (a) Smith, A. B.; Barbosa, J.; Wong, W.; Wood, J. L. *J. Am. Chem. Soc.* **1996**, *118*, 8316–8328. (b) Kobayakawa, Y.; Nakada, M. *J. Antibiot.* **2014**, *67*, 483–485.
- (5) Bonomo, L.; Kermorvan, L.; Dupau, P. *ChemCatChem* **2015**, *7*, 907–910.
- (6) (a) Casey, C. P.; Strotman, N. A.; Beetner, S. E.; Johnson, J. B.; Priebe, D. C.; Guzei, I. A. *Organometallics* **2006**, *25*, 1236–1244. (b) Diab, L.; Smejkal, T.; Geier, J.; Breit, B. *Angew. Chem., Int. Ed.* **2009**, *48*, 8022–8026; *Angew. Chem.* **2009**, *121*, 8166–8170.
- (7) *Catalysis Without Precious Metals*; Bullock, R. M., Ed.; Wiley-VCH: Weinheim, Germany, 2010.
- (8) Roesler, S.; Obenauf, J.; Kempe, R. *J. Am. Chem. Soc.* **2015**, *137*, 7998–8001.
- (9) (a) Morris, R. H. *Chem. Soc. Rev.* **2009**, *38*, 2282–2291. (b) Enthaler, S.; Junge, K.; Beller, M. *Angew. Chem., Int. Ed.* **2008**, *47*, 3317–3321. (c) Gaillard, S.; Renaud, J.-L. *ChemSusChem* **2008**, *1*, 505–509. (d) Bauer, G.; Kirchner, K. A. *Angew. Chem., Int. Ed.* **2011**, *50*, 5798–5800. (e) Bullock, R. M. *Science* **2013**, *342*, 1054–1055. (f) Sues, P. E.; Demmans, Z.; Morris, R. H. *Dalton Trans.* **2014**, *43*, 7650–7667. (g) Bauer, L.; Knölker, H.-J. *Chem. Rev.* **2015**, *115*, 3170–3387.
- (10) (a) Bart, S. C.; Lobkovsky, E.; Chirik, P. J. *J. Am. Chem. Soc.* **2004**, *126*, 13794–13807. (b) Bart, S. C.; Hawrelak, E. J.; Lobkovsky, E.; Chirik, P. J. *Organometallics* **2005**, *24*, 5518–5527. (c) Trovitch, R. J.; Lobkovsky, E.; Chirik, P. *Inorg. Chem.* **2006**, *45*, 7252–7260. (d) Casey, C. P.; Guan, H. *J. Am. Chem. Soc.* **2007**, *129*, 5816–5817. (e) Trovitch, R. J.; Lobkovsky, E.; Bill, E.; Chirik, P. J. *Organometallics* **2008**, *27*, 1470–1478. (f) Federsel, C.; Boddien, A.; Jackstell, R.; Jennerjahn, R.; Dyson, P. J.; Scopelliti, R.; Laurenczy, G.; Beller, M. *Angew. Chem., Int. Ed.* **2010**, *49*, 9777–9780. (g) Langer, R.; Leitius, G.; Ben-David, Y.; Milstein, D. *Angew. Chem., Int. Ed.* **2011**, *50*, 2120–2124. (h) Langer, R.; Iron, M. A.; Konstantinovski, L.; Diskin-Posner, Y.; Leitius, G.; Ben-David, Y.; Milstein, D. *Chem. - Eur. J.* **2012**, *18*, 7196–7209. (i) Yu, R. P.; Darmon, J. M.; Hoyt, J. M.; Margulieux, G. W.; Turner, Z. R.; Chirik, P. J. *ACS Catal.* **2012**, *2*, 1760–1764. (j) Ziebart, C.; Federsel, C.; Anbarasan, P.; Jackstell, R.; Baumann, W.; Spannenberg, A.; Beller, M. *J. Am. Chem. Soc.* **2012**, *134*, 20701–20704. (k) Fleischer, S.; Zhou, S.; Junge, K.; Beller, M. *Angew. Chem., Int. Ed.* **2013**, *52*, 5120–5124. (l) Srimani, D.; Diskin-Posner, Y.; Ben-David, Y.; Milstein, D. *Angew. Chem., Int. Ed.* **2013**, *52*, 14131–14134. (m) Wienhofer, G.; Baseda-Kruger, M.; Ziebart, C.; Westerhaus, F. A.; Baumann, W.; Jackstell, R.; Junge, K.; Beller, M. *Chem. Commun.* **2013**, *49*, 9089–9091. (n) Bornschein, C.; Werkmeister, S.; Wendt, B.; Jiao, H.; Alberico, E.; Baumann, W.; Junge, H.; Junge, K.; Beller, M. *Nat. Commun.* **2014**, *5*, 4111. (o) Chakraborty, S.; Dai, H.; Bhattacharya, P.; Fairweather, N. T.; Gibson, M. S.; Krause, J. A.; Guan, H. *J. Am. Chem. Soc.* **2014**, *136*, 7869–7872. (p) Chakraborty, S.; Lagaditis, P. O.; Förster, M.; Bielinski, E. A.; Hazari, N.; Holthausen, M. C.; Jones, W. D.; Schneider, S. *ACS Catal.* **2014**, *4*, 3994–4003. (q) Lagaditis, P. O.; Sues, P. E.; Sonnenberg, J. F.; Wan, K. Y.; Lough, A. J.; Morris, R. H. *J. Am. Chem. Soc.* **2014**, *136*, 1367–1380. (r) Werkmeister, S.; Junge, K.; Wendt, B.; Alberico, E.; Jiao, H.; Baumann, W.; Junge, H.; Gallou, F.; Beller, M. *Angew. Chem., Int. Ed.* **2014**, *53*, 8722–8726. (s) Bertini, F.; Mellone, I.; Ienco, A.; Peruzzini, M.; Gonsalvi, L. *ACS Catal.* **2015**, *5*, 1254–1265. (t) Rivada-Wheelaghan, O.; Dauth, A.; Leitius, G.; Diskin-Posner, Y.; Milstein, D. *Inorg. Chem.* **2015**, *54*, 4526–4538. (u) Zhang, Y.; MacIntosh, A. D.; Wong, J. L.; Bielinski, E. A.; Williard, P. G.; Mercado, B. Q.; Hazari, N.; Bernskoetter, W. H. *Chem. Sci.* **2015**, *6*, 4291–4299.
- (11) Wienhofer, G.; Westerhaus, F. A.; Junge, K.; Ludwig, R.; Beller, M. *Chem. - Eur. J.* **2013**, *19*, 7701–7707.
- (12) Zell, T.; Ben-David, Y.; Milstein, D. *Catal. Sci. Technol.* **2015**, *5*, 822–826.
- (13) Mazza, S.; Scopelliti, R.; Hu, X. *Organometallics* **2015**, *34*, 1538–1545.
- (14) Gorgas, N.; Stöger, B.; Veiros, L. F.; Pittenauer, E.; Allmaier, G.; Kirchner, K. *Organometallics* **2014**, *33*, 6905–9614.
- (15) Eisenstein, O.; Crabtree, R. H. *New J. Chem.* **2013**, *37*, 21–27.
- (16) Parr, R. G.; Yang, W. *Density Functional Theory of Atoms and Molecules*; Oxford University Press: New York, 1989.
- (17) Intermediate **D** is 1.4 kcal/mol less stable than **TS_{DE}**. This feature is the result of single-point energy calculations in species with similar stabilities. In fact, at the theory level used in the geometry optimizations, **D** is 4.2 kcal/mol below **TS_{DE}**.
- (18) Yang, X. *Inorg. Chem.* **2011**, *50*, 12836–12843.
- (19) Strohmeier, W.; Weigelt, L. *J. Organomet. Chem.* **1978**, *145*, 189–194.

Supporting Information

Highly Efficient and Selective Hydrogenation of Aldehydes: A Well-Defined Fe(II) Catalyst Exhibits Noble Metal Activity

Nikolaus Gorgas,[†] Berthold Stöger,[‡] Luis F. Veiros,[§] and Karl Kirchner^{*,†}

[†]Institute of Applied Synthetic Chemistry and [‡]Institute of Chemical Technologies and Analytics, Vienna University of Technology, Getreidemarkt 9, A-1060 Vienna, AUSTRIA, and [§]Centro de Química Estrutural, Instituto Superior Técnico, Universidade de Lisboa, Av. Rovisco Pais No. 1, 1049-001 Lisboa, PORTUGAL

General experimental information	S2
General Procedure for the Hydrogenation Reactions.....	S2
Syntheses of compound 2	S2
Syntheses of compound 3	S3
Reaction of 3 with <i>t</i> BuOK in THF under H ₂	S3
Reaction of 3 with <i>t</i> BuOK in EtOH under H ₂	S3
Reaction of 3 with benzaldehyde in C ₆ D ₆	S4
Reaction of 3 with 0.5 equiv. of benzaldehyde in EtOH.....	S4
Reaction of 2 with AgBF ₄ in EtOH.....	S4
X-ray Structure Determination.....	S4
Computational Details	S4
Details for the crystal structure determinations.....	S7
Coordinates of the optimized structures	S8
NMR spectra of isolated complexes and stoichiometric experiments.....	S16

General experimental information. All manipulations were performed under an inert atmosphere of argon by using Schlenk techniques or in a MBraun inert-gas glovebox. Hydrogen (99.999% purity) was purchased from Messer Austria and used as received. The solvents were purified according to standard procedures.¹ The deuterated solvents were purchased from Aldrich and dried over 4 Å molecular sieves. All aldehyde substrates were obtained from commercial sources and purified by distillation prior to use. The ligand N,N'-bis(diisopropylphosphino)-N,N'-dimethyl-2,6-diaminopyridine (PNP^{Me}-iPr) was prepared according to the literature.² ¹H, ¹³C{¹H}, and ³¹P{¹H} NMR spectra were recorded on Bruker AVANCE-250 and AVANCE-400 spectrometers. ¹H and ¹³C{¹H} NMR spectra were referenced internally to residual protio-solvent, and solvent resonances, respectively, and are reported relative to tetramethylsilane ($\delta = 0$ ppm). ³¹P{¹H} NMR spectra were referenced externally to H₃PO₄ (85%) ($\delta = 0$ ppm).

General procedure for the hydrogenation of aldehydes. All hydrogenation reaction were carried out in a Carl Roth 100 mL stainless steel autoclave containing a 8 mL screw cap vial equipped with a septum, a small stirring bar and a 10 inch needle (gauge 18) connecting the vial on the bottom with the head of the autoclave for injecting the reaction solution. The autoclave was evacuated, flushed several times with hydrogen gas and set to the specified temperature prior to the addition of the reaction solution. For a typical experiment, the reaction solution was prepared previously inside a glovebox by mixing the substrate (2.0 mmol), ethanol (800 μ L), the catalyst (100 μ L, 2.0mM stock solution in EtOH) and the base (100 μ L, 0.2M stock solution in EtOH). The resulting solution was taken up in a syringe via a 12 inch needle (gauge 22), removed from the glovebox and injected into the autoclave against a slight flow of hydrogen gas. The pressure was adjusted to the specified value and the reaction was run for the stated time. Afterwards, the hydrogen gas was carefully released, the vial was taken out of the autoclave and the solvent of the reaction solution was slowly removed under reduced pressure. The residue was analysed by ¹H NMR and yields were determined by integration of the spectra after addition of mesitylene (2.0 mmol) as internal standard.

Synthesis of [Fe(PNP^{Me}-iPr)(H)(Br)(CO)] (2). Anhydrous FeBr₂ (190 mg, 0.88 mmol) and PNP^{Me}-iPr (300 mg, 0.88 mmol) were dissolved in 12 mL of THF. The immediately formed yellow suspension was stirred for 1h at room temperature, after which time the amount of solvent was reduced to approximately 6 mL under reduced pressure. Diethyl ether (6 mL) was added to complete precipitation and the solvent was decanted. The residue was washed several times with diethyl ether (3 x 6 mL) and dried under high vacuum to afford [Fe(PNP^{Me}-iPr)(Br)₂] as a yellow powder, which was used as such for the next step. [Fe(PNP^{Me}-iPr)(Br)₂] was again suspended in THF and CO was bubbled through the reaction mixture for 10 min. During this time the colour changed from yellow to deep purple. The reaction solution was briefly purged with argon in order to remove excess of CO and cooled down to 0°C before a solution of Na[HBET₃] in toluene (0.97 mL, 1M, 0.97 mmol) was slowly added. The reaction mixture was stirred for 10 min at 0°C in which time the color changed from purple to dark orange. After additional 50 min at room temperature the solution was filtered and the solvent was removed under reduced pressure. The dark residue was redissolved in THF (3 mL) and the product was precipitated by addition of diethyl ether (8 mL). The precipitate was filtered off, washed with diethyl ether (3 x 8 mL) and dried under high vacuum to afford a bright yellow powder. Yield: 273 mg (58%). Anal. Calcd. for C₂₀H₃₈BrFeN₃OP₂: C 44.96; H, 7.17; N, 7.87 %. Found: C, 44.86; H, 7.22; N, 7.07%. ¹H NMR (δ , CD₂Cl₂, 20°C): 7.44 (t, *J* = 8.3 Hz, 1H, py⁴), 6.02 (d, *J* = 8.3 Hz, 2H, py^{3,5}), 3.10 (s, 6H, NCH₃), 2.93–2.75 (m, 2H, CH(CH₃)₂), 2.68–2.47 (m, 2H, CH(CH₃)₂), 1.72 (dt, *J* = 7.3 Hz, *J* = 16.6, 6H, CH(CH₃)₂), 1.60 (dt, *J* = 7.3 Hz, *J* = 14.5, 6H, CH(CH₃)₂), 1.22 (dt, *J* =

7.3 Hz, $J = 16.8$, 6H, CH(CH₃)₂), 0.83 (dt, $J = 7.0$ Hz, $J = 14.1$, 6H, CH(CH₃)₂), -21.84 (t, $J = 57.9$ Hz, 1H, FeH). ¹³C NMR (δ , CD₂Cl₂, 20°C): 222.7 (t, $J = 22.4$ Hz, CO), 162.6 (t, $J = 11.4$ Hz, py^{2,6}), 138.9 (s, py⁴), 96.6 (t, $J = 3.4$ Hz, py^{3,5}), 34.0 (t, $J = 2.5$ Hz, NCH₃), 33.6 (t, $J = 9.3$ Hz, CH(CH₃)₂), 31.2 (td, $J = 14.8$, $J = 3.2$ Hz, CH(CH₃)₂), 21.7 (s, CH(CH₃)₂), 20.3 (t, $J = 3.6$ Hz), 18.03 (s, CH(CH₃)₂), 17.8 (t, $J = 5.0$ Hz, CH(CH₃)₂). ³¹P NMR (δ , CD₂Cl₂, 20°C): 164.0 (s). IR (ATR, cm⁻¹): 1903 (ν_{CO}).

Synthesis of [Fe(PNP^{Me}-iPr)(H)₂(CO)] (3). This complex was prepared similarly to **2** by adding 2.1 equiv. of Na[HBET₃] (0.97 mL, 1.0M in toluene, 0.97 mmol) to the *in situ* prepared complex **1**. After stirring the reaction mixture for 10 min at 0°C and additional 50 min at room temperature, all volatiles were removed *in vacuo*, the residue was extracted with Et₂O (3 x 3 mL) and the resulting solution was filtered. The filtrate was concentrated to approx. 2 mL and *n*-pentane (4 mL) was added to precipitate the product. The precipitate was filtered off, washed three times with small portions of *n*-pentane (3 x 3 mL) and dried under high vacuum to afford a pale orange powder. Yield: 224 mg (56%). Anal. Calcd. for C₂₀H₃₉FeN₃OP₂: C, 52.76; H, 8.63; N, 9.23%. Found: C, 52.94; H, 8.58; N, 9.32%. *trans*-**3**: ¹H NMR (δ , benzene-*d*₆, 20°C): 6.89 (t, $J = 8.1$ Hz, 1H, py⁴), 5.42 (d, $J = 8.1$ Hz, 2H, py^{3,5}), 2.41 (s, 6H, NCH₃), 2.19–2.04 (superimposed by *cis*-**6**, m, 4H, CH(CH₃)₂), 1.47 (dt, $J = 6.8$ Hz, $J = 16.9$, 12H, CH(CH₃)₂), 1.14 (dt, $J = 6.8$ Hz, $J = 13.7$, 12H, CH(CH₃)₂), -8.76 (t, $J = 42.9$ Hz, 2H, FeH). ¹³C NMR (δ , benzene-*d*₆, 20°C): 224.1 (t, $J = 27.2$ Hz, CO), 161.7 (t, $J = 11.7$ Hz, py^{2,6}), 135.3 (s, py⁴), 94.4 (t, $J = 3.3$ Hz, py^{3,5}), 32.1–31.3 (m, NCH₃ + CH(CH₃)₂), 19.1 (t, $J = 5.3$ Hz, CH(CH₃)₂), 18.7 (s, CH(CH₃)₂). IR (ATR, cm⁻¹): 1880 (ν_{CO}). ³¹P{¹H} NMR (δ , benzene-*d*₆, 20°C): 189.6 (s). *cis*-**3**: ¹H NMR (δ , benzene-*d*₆, 20°C): 6.98 (t, $J = 8.1$ Hz, 1H, py⁴), 5.54 (d, $J = 8.1$ Hz, 2H, py^{3,5}), 2.43 (s, 6H, NCH₃), 2.17–2.05 (superimposed by *trans*-**3**, m, 2H, CH(CH₃)₂), 1.94–1.80 (m, 2H, CH(CH₃)₂), 1.47 (dt, $J = 7.0$ Hz, $J = 17.0$, 6H, CH(CH₃)₂), 1.29 (dt, $J = 7.0$ Hz, $J = 14.0$, 6H, CH(CH₃)₂), 1.24 (dt, $J = 6.8$ Hz, $J = 16.9$, 2H, CH(CH₃)₂), 0.85 (dt, $J = 6.8$ Hz, $J = 14.3$, 6H, CH(CH₃)₂), -13.02 (br, 2H, FeH). ¹³C {¹H} NMR (δ , benzene-*d*₆, 20°C): 219.5 (t, $J = 16.3$ Hz, CO), 162.9 (t, $J = 10.0$ Hz, py^{2,6}), 135.2 (s, py⁴), 94.6 (t, $J = 3.1$ Hz, py^{3,5}), 32.12–31.3 (m, NCH₃ + CH(CH₃)₂), 19.7 (t, $J = 5.3$ Hz, CH(CH₃)₂), 19.4 (t, $J = 6.4$ Hz, CH(CH₃)₂), 18.8 (s, CH(CH₃)₂), 18.3 (s, CH(CH₃)₂). ³¹P NMR (δ , benzene-*d*₆, 20°C): 191.9 (s). IR (ATR, cm⁻¹): 1880 (ν_{CO}).

Reaction of 2 with *t*BuOK in THF under H₂. A 90 mL Fisher-Porter tube was charged with a solution of **2** (80 mg, 0.15 mmol) and *t*BuOK (19 mg, 0.17 mmol) in THF (7.0 mL + 1.0 mL C₆D₆ for NMR deuterium lock). The tube was pressurized with hydrogen gas to 5 bar and the progress of the reaction was monitored periodically by running ¹H and ³¹P{¹H} NMR spectra of small samples taken from the reaction mixture. After 3 days, the spectra showed the disappearance of **2** and formation of **3** together with minor amounts of side product identified as [Fe(PNP^{Me}-iPr)(CO)₂] (δ_{P} (ppm) = 181.2 (s)).

Reaction of 2 with *t*BuOK in EtOH under H₂. A 8 mL screw cap vial equipped with a septum and a small stirring bar was charged with **3** (40 mg, 0.075 mmol) and *t*BuOK (9 mg, 0.080 mmol) dissolved in EtOH (1.5 mL + 0.5 mL C₆D₆ for NMR deuterium lock). The vial was sealed and the solution purged with hydrogen gas (1 bar) for 5 min and was stirred for additional 5 min under an atmosphere of dihydrogen. A sample (0.5 mL) was taken from the reaction mixture, filtered and analysed by ¹H and ³¹P{¹H} NMR spectroscopy revealing quantitative formation of the iron dihydride **3** (*cis/trans* = 1.75:1.00, Figures S10 and S11). ¹H NMR (δ , EtOH/C₆D₆, 20°C, hydride region): -9.57 (t, $J_{\text{PH}} = 42.2$ Hz, *trans*-**3**), -13.91 (br, *cis*-**3**). ³¹P{¹H} NMR (δ , EtOH/C₆D₆, 20°C): 189.9 (s, *trans*-**3**), 187.5 (s, *cis*-**3**). For the reference spectrum of **2** in EtOH see Figures S8 and S9.

To the above prepared solution was added benzaldehyde (7 μL , 0.075 mmol). The reaction mixture was stirred for 10 min, after which time a sample was taken (0.5 mL), filtered and analysed by ^1H and $^{31}\text{P}\{^1\text{H}\}$ NMR spectroscopy. The spectra showed the formation of **4** and **4'** in an approximate ratio of 1:6 (Figures S12 and S13). ^1H NMR (δ , EtOH/ C_6D_6 , 20°C, hydride region): -23.84 (t, $J_{\text{PH}} = 55.8$ Hz, **4**), -25.4 (t, $J_{\text{PH}} = 58.2$ Hz, **4'**). $^{31}\text{P}\{^1\text{H}\}$ NMR (δ , EtOH/ C_6D_6 , 20°C): 161.8 (s, **4**), 159.7 (s, **4'**). Purging this solution with hydrogen gas (1 bar) for 10 min leads again to the formation of the dihydride complex **3**. The described cycle can be repeated several times.

Reaction of 3 with benzaldehyde in C_6D_6 . A NMR tube was charged with **3** (22 mg, 0.049 mmol) dissolved in C_6D_6 (0.8 mL). Benzaldehyde (5 μL , 0.049 mmol) was added, the NMR tube was sealed, shaken and the sample was analysed by ^1H NMR spectroscopy (Figure 4). The experiment was repeated using the same sample as before but the amount of benzaldehyde was increased stepwise from 1 to 5 (+ 20 μL , 0.196 mmol), 10 (+ 25 μL , 0.245 mmol) and 20 (+ 50 μL , 0.490 mmol) equiv. with respect to **3**.

Reaction of 3 with 0.5 equiv. of benzaldehyde in EtOH. A NMR tube was charged with **3** (22 mg, 0.049 mmol) dissolved in EtOH (0.6 mL + 0.2 mL C_6D_6 for NMR deuterium lock). Benzaldehyde (2.6 mg, 0.025 mmol) dissolved in EtOH (0.2 mL) was added to the solution, the NMR tube was sealed, shaken and the reaction was monitored by $^{31}\text{P}\{^1\text{H}\}$ NMR by recording one spectrum every 4 min over a period of 30 min (Figure 5).

Reaction of 2 with AgBF_4 in EtOH. A vial was charged with **2** (15 mg, 0.028 mmol) dissolved in EtOH (0.6 mL + 0.2 mL C_6D_6 for NMR deuterium lock). AgBF_4 (6 mg, 0.031 mmol) was added and the reaction mixture was stirred for 5 min at room temperature. The solution was filtered into a NMR tube and analysed by ^1H and $^{31}\text{P}\{^1\text{H}\}$ NMR spectroscopy revealing the formation of **4'** (Figures S14 and S15).

Crystal Structure Determination. X-ray diffraction data of **2** and **3** were collected at $T = 100$ K in a dry stream of nitrogen on a Bruker Kappa APEX II diffractometer system using graphite-monochromatized Mo- $K\alpha$ radiation ($\lambda = 0.71073$ Å) and fine sliced φ - and ω -scans. Data were reduced to intensity values with SAINT and an absorption correction was applied with the multi-scan approach implemented in SADABS.³ The structures were solved by charge flipping using SUPERFLIP⁴ and refined against F with JANA2006.⁵ Non-hydrogen atoms were refined anisotropically. The H atoms connected to C atoms were placed in calculated positions and thereafter refined as riding on the parent atoms. The H atoms of the amine groups and the hydrides were located in difference Fourier maps. In **2**, three CO ligands were located, of which two were occupied to ca. 50%, implying a solid solution of *cis*- and *trans*-configurations. The corresponding two semi-occupied hydrides could be located in the difference Fourier maps. The sum of the occupations of both configurations was restrained to one. The Fe-H distances were restrained to 1.460(1) Å. **3** was refined as a twin by inversion. Molecular graphics were generated with the program MERCURY.⁶ Crystal data and experimental details are given in Table S1.

Computational Details. All calculations were performed using the GAUSSIAN 09 software package,⁷ without symmetry constraints. The optimized geometries were obtained with the B3LYP functional.⁸ That functional includes a mixture of Hartree-Fock⁹ exchange with DFT¹⁰ exchange-correlation, given by Becke's three parameter functional with the Lee, Yang and Parr correlation functional, which includes both local and non-local terms. The basis set used for the geometry optimizations (basis b1) consisted of the Stuttgart/Dresden ECP (SDD) basis set¹¹ to describe the electrons of iron, and a standard 6-31G(d,p) basis set¹² for all other atoms. Transition state optimizations were performed with the Synchronous Transit-Guided Quasi-Newton Method (STQN) developed by

Schlegel *et al.*,¹³ following extensive searches of the Potential Energy Surface. Frequency calculations were performed to confirm the nature of the stationary points, yielding one imaginary frequency for the transition states and none for the minima. Each transition state was further confirmed by following its vibrational mode downhill on both sides and obtaining the minima presented on the energy profiles. The electronic energies (E_{b1}) obtained at the B3LYP/b1 level of theory were converted to free energy at 298.15 K and 1 atm (G_{b1}) by using zero point energy and thermal energy corrections based on structural and vibration frequency data calculated at the same level.

Single point energy calculations were performed using the M06 functional and a standard 6-311++G(d,p) basis set,¹⁴ on the geometries optimized at the B3LYP/b1 level. The M06 functional is a hybrid meta-GGA functional developed by Truhlar and Zhao,¹⁵ and it was shown to perform very well for the kinetics of transition metal molecules, providing a good description of weak and long range interactions.¹⁶ Solvent effects (ethanol) were considered in *all* calculations (including the B3LYP/b1 geometry optimizations) using the Polarizable Continuum Model (PCM) initially devised by Tomasi and coworkers¹⁷ with radii and non-electrostatic terms of the SMD solvation model, developed by Truhler *et al.*¹⁸ The free energy values presented (G_{b2}) were derived from the electronic energy values obtained at the M06/6-311++G(d,p)//B3LYP/b1 level (E_{b2}), according to the following expression: $G_{b2}^{\text{soln}} = E_{b2}^{\text{soln}} + G_{b1} - E_{b1}$.

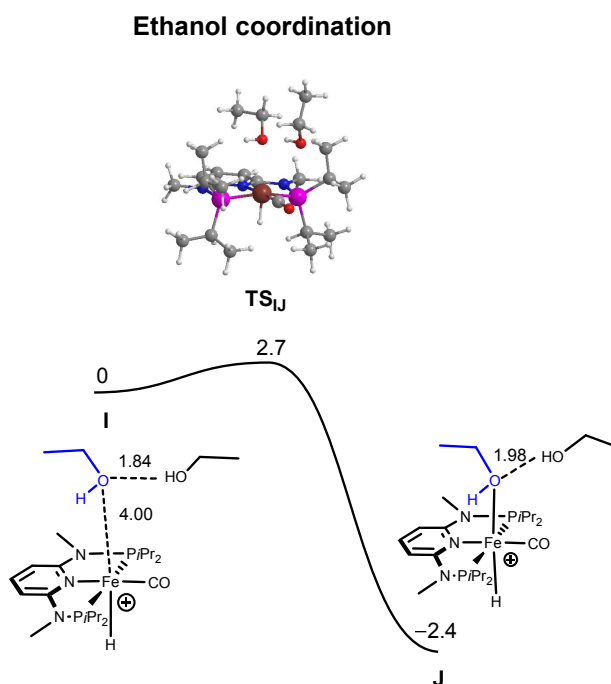


Figure S1. Free energy profile (kcal/mol) calculated for the coordination of ethanol to the 5-coordinated intermediate $[\text{Fe}(\text{PNP}^{\text{Me}}\text{-iPr})(\text{CO})(\text{H})]^+$. Distances in Å.

References

- 1 Perrin, D. D.; Armarego, W. L. F. *Purification of Laboratory Chemicals*, 3rd ed.; Pergamon: New York, **1988**.
- 2 Öztopcu, Ö.; Holzhaecker, C.; Puchberger, M.; Weil, M.; Mereiter, K.; Veiros, L. F.; Kirchner, K. *Organometallics* **2013**, *32*, 3042-3052.
- 3 Bruker computer programs: APEX2, SAINT and SADABS (Bruker AXS Inc., Madison, WI, 2012).
- 4 Palatinus, L.; Chapuis, G.J. *Appl. Cryst.* **2007**, *40*, 786-790.
- 5 Petříček, V.; Dušek, M.; Palatinus, L. JANA2006, the crystallographic computing system. (Institute of Physics, Praha, Czeck Republic, 2006).
- 6 Macrae, C. F.; Edgington, P. R.; McCabe, P.; Pidcock, E.; Shields, G. P.; Taylor, R.; Towler M.; van de Streek, J. *J. Appl. Cryst.* **2006**, *39*, 453-457.
- 7 Gaussian 09, Revision A.02, Frisch, M. J.; Trucks, G. W.; Schlegel, H. B.; Scuseria, G. E.; Robb, M. A.; Cheeseman, J. R.; Scalmani, G.; Barone, V.; Mennucci, B.; Petersson, G. A.; Nakatsuji, H.; Caricato, M.; Li, X.; Hratchian, H. P.; Izmaylov, A. F.; Bloino, J.; Zheng, G.; Sonnenberg, J. L.; Hada, M.; Ehara, M.; Toyota, K.; Fukuda, R.; Hasegawa, J.; Ishida, M.; Nakajima, T.; Honda, Y.; Kitao, O.; Nakai, H.; Vreven, T.; Montgomery, Jr., J. A.; Peralta, J. E.; Ogliaro, F.; Bearpark, M.; Heyd, J. J.; Brothers, E.; Kudin, K. N.; Staroverov, V. N.; Kobayashi, R.; Normand, J.; Raghavachari, K.; Rendell, A.; Burant, J. C.; Iyengar, S. S.; Tomasi, J.; Cossi, M.; Rega, N.; Millam, J. M.; Klene, M.; Knox, J. E.; Cross, J. B.; Bakken, V.; Adamo, C.; Jaramillo, J.; Gomperts, R.; Stratmann, R. E.; Yazyev, O.; Austin, A. J.; Cammi, R.; Pomelli, C.; Ochterski, J. W.; Martin, R. L.; Morokuma, K.; Zakrzewski, V. G.; Voth, G. A.; Salvador, P.; Dannenberg, J. J.; Dapprich, S.; Daniels, A. D.; Farkas, Ö.; Foresman, J. B.; Ortiz, J. V.; Cioslowski, J.; Fox, D. J. Gaussian, Inc., Wallingford CT, **2009**.
- 8 (a) Becke, A. D. *J. Chem. Phys.* **1993**, *98*, 5648-5652. (b) Miehlich, B.; Savin, A.; Stoll, H.; Preuss, H. *Chem. Phys. Lett* **1989**, *157*, 200-206. (c) Lee, C.; Yang, W.; Parr, G. *Phys. Rev. B* **1988**, *37*, 785-789.
- 9 Hehre, W. J.; Radom, L.; Schleyer, P. v. R.; Pople, J. A., *Ab Initio Molecular Orbital Theory*. John Wiley & Sons, New York, **1986**.
- 10 Parr, R. G.; Yang, W. *Density Functional Theory of Atoms and Molecules*, Oxford University Press, New York, 1989.
- 11 (a) Haeusermann, U.; Dolg, M.; Stoll, H.; Preuss, H. *Mol. Phys.* **1993**, *78*, 1211-1224. (b) Kuechle, W.; Dolg, M.; Stoll, H.; Preuss, H. *J. Chem. Phys.* **1994**, *100*, 7535-7542. (c) Leininger, T.; Nicklass, A.; Stoll, H.; Dolg, M.; Schwerdtfeger, P. *J. Chem. Phys.* **1996**, *105*, 1052-1059.
- 12 (a) McLean, A. D.; Chandler, G. S. *J. Chem. Phys.* **1980**, *72*, 5639-5648. (b) Krishnan, R.; Binkley, J. S.; Seeger, R.; Pople, J. A. *J. Chem. Phys.* **1980**, *72*, 650-654. (c) Wachters, A. J. H. *J. Chem. Phys.* **1970**, *52*, 1033-1036. (d) Hay, P. J. *J. Chem. Phys.* **1977**, *66*, 4377-4384. (e) Raghavachari, K.; Trucks, G. W. *J. Chem. Phys.* **1989**, *91*, 1062-1065. (f) Binning Jr., R. C.; Curtiss, L. A. *J. Comp. Chem.*, **1990**, *11*, 1206. (g) McGrath, M. P.; Radom, L. *J. Chem. Phys.* **1991**, *94*, 511-516.
- 13 (a) Peng, C.; Ayala, P.Y.; Schlegel, H.B.; Frisch, M.J. *J. Comp. Chem.* **1996**, *17*, 49-56. (b) Peng, C.; Schlegel, H.B. *Israel J. Chem.* **1993**, *33*, 449-454.
- 14 (a) McClean, A. D.; Chandler, G. S. *J. Chem. Phys.* **1980**, *72*, 5639-5648. (b) Krishnan, R.; Binkley, J. S.; Seeger, R. Pople, J. A. *J. Chem. Phys.* **1980**, *72*, 650-654. (c) Wachters, A. J. H. *J. Chem.*

-
- Phys.* **1970**, *52*, 1033-1036. (d) Hay, P. J. *J. Chem. Phys.* **1977**, *66*, 4377-4384. (e) Raghavachari, K.; Trucks, G. W. *J. Chem. Phys.* **1989**, *91*, 1062-1065. (f) Binning Jr., R. C.; Curtiss, L. A. *J. Comp. Chem.* **1990**, *11*, 1206-1216. (g) McGrath, M. P.; Radom, L. *J. Chem. Phys.* **1991**, *94*, 511-516. (h) Clark, T.; Chandrasekhar, J.; Spitznagel, G. W.; Schleyer, P. v. R. *J. Comp. Chem.* **1983**, *4*, 294-301. (i) Frisch, M. J.; Pople, J. A.; Binkley, J. S. *J. Chem. Phys.* **1984**, *80*, 3265-3269.
- 15 Zhao, Y.; Truhlar, D. G. *Theor. Chem. Acc.*, **2008**, *120*, 215-241.
- 16 (a) Zhao, Y.; Truhlar, D. G. *Acc. Chem. Res.* **2008**, *41*, 157-167. (b) Zhao, Y.; Truhlar, D.G. *Chem. Phys. Lett.* **2011**, *502*, 1-13.
- 17 (a) Cancès, M. T.; Mennucci, B.; Tomasi, J. *J. Chem. Phys.* **1997**, *107*, 3032-3041. (b) Cossi, M.; Barone, V.; Mennucci, B.; Tomasi, J. *Chem. Phys. Lett.* **1998**, *286*, 253-260. (c) Mennucci B.; Tomasi, J. *J. Chem. Phys.* **1997**, *106*, 5151-5158. (d) Tomasi, J.; Mennucci, B.; Cammi, R. *Chem. Rev.* **2005**, *105*, 2999-3094.
- 18 Marenich, A. V.; Cramer, C. J.; Truhlar, D. G. *J. Phys. Chem. B*, **2009**, *113*, 6378-6396.

Table S1. Details for the crystal structure determinations of **2** and **3**.

	2	3
formula	C ₂₀ H ₃₉ FeN ₃ OP ₂	C ₂₀ H ₃₈ BrFeN ₃ OP ₂
fw	455.3	534.2
cryst.size, mm	0.08×0.71×0.94	0.33×0.53×0.58
color, shape	translucent red plate	translucent dark yellow block
crystal system	monoclinic	monoclinic
space group	P2 ₁ /c	P2 ₁
a, Å	13.7848(7)	11.7189(10)
b, Å	11.7982(5)	12.5863(11)
c, Å	15.4447(8)	16.7721(14)
β, °	113.3317(14)	99.602(2)
V, Å ³	2306.5(2)	2439.2(4)
T, K	100	100
Z, Z'	4, 1	4, 2
ρ _{calc} , g cm ⁻³	1.3113	1.4543
μ, mm ⁻¹ (MoKα)	0.807	2.403
F(000)	976	1112
absorption correction, T _{min} -T _{max}	multi-scan, 0.71-0.94	multi-scan, 0.27-0.45
θ range, deg	1.61-35.02	1.23-32.72
no. of rflns measd	49546	65350
R _{int}	0.042	0.048
no. of rflns unique	10156	17845
no. of rflns I>3σ(I)	7395	15279
no. of params / restraints	273 / 3	514 / 2
R (I > 3σ(I)) ^a	0.0351	0.0290
R (all data)	0.0601	0.0393
wR (I > 3σ(I))	0.0390	0.0324
wR (all data)	0.0406	0.0334
Goof	1.68	1.17
Diff.Four.peaks min/max eÅ ⁻³	-0.55, 0.65	-0.28, 0.74
Flack parameter	-	0.244(3)

$$^a R = \sum |F_o| - |F_c| / \sum |F_o|, wR = \sum w(|F_o| - |F_c|) / \sum w|F_o|, Goof = \{\sum [w(F_o^2 - F_c^2)^2] / (n-p)\}^{1/2}$$

Atomic Coordinates for all the optimized molecules (B3LYP/b1)

H₂				H	5.460313	-1.569463	-2.058197
H	-0.679014	-0.385076	-1.964036	H	6.057117	-3.954301	-1.792434
H	-0.259899	-0.949217	-1.721381	H	4.326303	-3.764488	-1.528467
MeCHO				H	5.416194	-3.987183	-0.150024
O	-1.507292	-0.863535	2.774838	H	7.696214	-2.231973	-1.228375
C	-2.383138	-1.537180	2.257588	H	7.158333	-2.103432	0.447618
H	-3.130406	-1.060984	1.589505	H	7.235156	-0.656397	-0.573905
C	-2.549626	-3.010819	2.449067	H	3.524166	-3.072832	0.838376
H	-1.785816	-3.413259	3.118086	H	4.355196	-2.895387	3.154200
H	-2.500048	-3.508846	1.472243	H	4.866816	-1.224070	2.889866
H	-3.551056	-3.211670	2.850514	H	5.673832	-2.548684	2.032961
EtOH				H	1.975736	-2.315676	2.612502
O	-1.024445	-1.242582	1.816674	H	1.527208	-1.575218	1.071411
H	-0.365116	-1.595002	2.432514	H	2.381914	-0.622685	2.294042
C	-2.313351	-1.552173	2.358392	H	6.061558	3.969005	-1.702573
H	-2.436333	-1.090387	3.349537	H	7.153472	6.133559	-1.163630
H	-3.038157	-1.077416	1.687925	H	6.486248	6.111520	0.469355
C	-2.570628	-3.049940	2.440074	H	5.412358	6.274997	-0.929940
H	-1.853979	-3.533606	3.114564	H	8.381484	4.048900	-0.836678
H	-2.479843	-3.515335	1.452543	H	7.592552	2.540607	-0.359786
H	-3.578289	-3.248821	2.822616	H	7.813423	3.843801	0.821534
A				H	4.465100	5.501238	1.402154
Fe	4.684867	1.196699	0.221505	H	2.817105	4.876946	3.120449
O	0.421584	1.414784	2.390019	H	2.896938	3.173440	2.643192
P	4.276233	-0.957837	-0.100482	H	2.208926	4.373090	1.538578
O	-0.191585	3.450139	0.495341	H	5.260408	4.866441	3.658135
C	0.190431	1.740958	3.549024	H	6.479995	4.447974	2.453603
H	0.076885	2.719627	1.087051	H	5.456582	3.183102	3.155663
P	4.758604	3.410277	0.192968	H	0.383909	1.015694	4.361451
H	3.653127	1.233526	1.396281	H	5.630861	1.177545	-1.034156
C	-1.416550	3.068542	-0.138348	H	2.407582	-2.263939	-2.725626
N	3.143681	1.455780	-1.106005	H	-1.239101	2.259999	-0.864070
C	-0.344270	3.066835	3.971852	H	1.098583	-1.894953	-1.577234
H	-2.128298	2.684030	0.606992	H	2.439107	-2.916972	-1.078466
N	2.908654	-0.870862	-1.190505	H	1.830575	5.163018	-1.010642
H	-1.282114	2.912837	4.521300	H	3.174992	5.458432	-2.141759
C	-2.006864	4.277438	-0.842273	H	3.350613	5.820315	-0.416474
N	3.407504	3.767710	-0.859865	C	2.917611	5.122915	-1.130018
H	-0.505502	3.725982	3.117324	TS_{AB}			
H	-1.318647	4.662421	-1.602983	Fe	4.222716	1.330716	0.610347
C	2.526059	0.376062	-1.655988	O	0.619932	0.871990	1.716791
H	-2.211617	5.081893	-0.127067	P	4.009222	-0.862811	0.152605
H	0.357252	3.521137	4.683267	O	-0.216545	3.242547	0.680244
C	1.538566	0.520844	-2.647838	C	1.573887	1.023125	2.530504
C	1.196708	1.804663	-3.053328	H	0.040375	2.378544	1.085550
H	-2.946392	4.009116	-1.337081	P	4.553026	3.520569	0.283806
C	1.804753	2.916740	-2.485286	H	2.928735	1.480281	1.640221
C	2.781587	2.707786	-1.494215	C	-1.487352	3.071165	0.058172
C	5.554057	-1.990727	-1.048240	N	2.932047	1.534225	-0.961463
C	5.308683	-3.505951	-1.127850	C	1.542479	2.126121	3.565064
C	6.989616	-1.720274	-0.564052	H	-2.235588	2.730662	0.792137
C	3.656771	-2.077254	1.275406	N	2.749474	-0.805506	-1.056007
C	4.706869	-2.187522	2.394476	H	0.941743	1.748133	4.405103
C	2.306734	-1.613601	1.837756	C	-1.929325	4.393040	-0.547381
C	6.235335	4.245215	-0.653690	N	3.318220	3.848883	-0.909568
C	6.310976	5.777277	-0.558685	H	1.050784	3.022466	3.182178
C	7.576751	3.624383	-0.224546	H	-1.216857	4.730778	-1.308435
C	4.401743	4.453212	1.714947	C	2.350782	0.436861	-1.523941
C	2.996234	4.199546	2.276928	H	-1.999026	5.169055	0.223104
C	5.468231	4.218261	2.798570	H	2.537204	2.366382	3.947821
C	5.987857	0.980756	1.339842	C	1.396689	0.554647	-2.550642
O	6.861271	0.836106	2.107022	C	1.076324	1.824758	-3.010146
C	2.178275	-2.045954	-1.675589	H	-2.911556	4.289488	-1.021152
H	1.070123	-0.341065	-3.100491	C	1.696158	2.949468	-2.482932
H	0.448811	1.939970	-3.829733	C	2.639439	2.771158	-1.454868
H	1.545223	3.913117	-2.812670	C	5.516469	-1.586383	-0.735826
				C	5.346042	-2.929334	-1.461540
				C	6.735458	-1.642639	0.202751
				C	3.487598	-2.230885	1.349807

C	4.184414	-2.021009	2.708413
C	1.966385	-2.385259	1.533401
C	6.185313	3.924089	-0.588469
C	6.351960	5.333594	-1.176969
C	7.399803	3.574209	0.290681
C	4.337890	4.886337	1.563442
C	2.868500	5.201649	1.870842
C	5.080054	4.516416	2.861070
C	5.272443	1.157796	1.981770
O	5.970098	1.042333	2.912826
C	2.170992	-1.995920	-1.690290
H	0.929280	-0.317432	-2.983380
H	0.343528	1.938473	-3.804069
H	1.464702	3.932368	-2.866056
H	5.710011	-0.814900	-1.490459
H	6.306177	-3.210778	-1.911190
H	4.614631	-2.880973	-2.270707
H	5.060719	-3.740833	-0.783500
H	7.635651	-1.846501	-0.388777
H	6.641570	-2.448525	0.938325
H	6.899057	-0.704813	0.740645
H	3.872326	-3.163988	0.923693
H	3.999182	-2.894288	3.344471
H	3.792354	-1.142736	3.229885
H	5.267276	-1.903595	2.619226
H	1.775440	-2.986872	2.429968
H	1.501403	-2.906480	0.694208
H	1.448301	-1.431504	1.655415
H	6.156633	3.207419	-1.418314
H	7.338492	5.404095	-1.651423
H	6.309366	6.113823	-0.409507
H	5.610011	5.562195	-1.944361
H	8.302671	3.556161	-0.331014
H	7.310425	2.595846	0.770537
H	7.560374	4.325547	1.070475
H	4.807824	5.782255	1.142864
H	2.822553	5.952848	2.668491
H	2.339710	4.314699	2.223158
H	2.326299	5.601455	1.012459
H	5.048027	5.368041	3.550569
H	6.131087	4.266610	2.698243
H	4.602031	3.668127	3.361149
H	2.131340	0.135746	2.856435
H	5.380543	1.218133	-0.381172
H	2.395013	-2.024015	-2.762584
H	-1.439005	2.300421	-0.727773
H	1.084080	-2.019227	-1.559002
H	2.584404	-2.891579	-1.234519
H	1.976769	5.434134	-1.335152
H	3.300298	5.252455	-2.509697
H	3.615147	5.930397	-0.906832
C	3.036992	5.185054	-1.448052

B

Fe	4.153434	1.347480	0.631539
O	0.717662	0.897486	1.622174
P	3.959432	-0.861464	0.166796
O	-0.099309	3.120628	0.649675
C	1.806118	1.171601	2.375638
H	0.200830	2.222013	1.047773
P	4.533085	3.538531	0.286587
H	2.662804	1.685579	1.747206
C	-1.396358	2.952926	0.105445
N	2.933717	1.546824	-0.977636
C	1.547004	2.118596	3.560791
H	-2.104282	2.597262	0.874988
N	2.715419	-0.795182	-1.053171
H	0.879640	1.613622	4.270683
C	-1.891422	4.276062	-0.460082
N	3.328052	3.863576	-0.932708
H	1.045215	3.034206	3.233779
H	-1.231951	4.625975	-1.262785
C	2.347947	0.447964	-1.541298
H	-1.912898	5.045071	0.320732
H	2.470191	2.383527	4.090518
C	1.420270	0.568244	-2.590098

C	1.126248	1.837323	-3.068992
H	-2.902867	4.173584	-0.869295
C	1.744847	2.960896	-2.538782
C	2.660753	2.784695	-1.487451
C	5.483803	-1.532415	-0.728015
C	5.329472	-2.871367	-1.464396
C	6.717938	-1.571547	0.190802
C	3.431809	-2.232070	1.349427
C	4.182849	-2.078678	2.687356
C	1.912736	-2.326462	1.584819
C	6.184387	3.875647	-0.569399
C	6.377634	5.269713	-1.185818
C	7.383484	3.522945	0.328664
C	4.317511	4.912625	1.551010
C	2.846557	5.227528	1.852812
C	5.057628	4.552246	2.852537
C	5.204800	1.165759	2.016772
O	5.929366	1.039506	2.919170
C	2.126323	-1.985661	-1.679752
H	0.951512	-0.302166	-3.024344
H	0.412934	1.951240	-3.880319
H	1.529286	3.942516	-2.933960
H	5.649272	-0.749528	-1.478150
H	6.285066	-3.120932	-1.941304
H	4.576455	-2.834578	-2.253901
H	5.084228	-3.695709	-0.786574
H	7.612143	-1.737685	-0.421005
H	6.659466	-2.395115	0.909769
H	6.865418	-0.640797	0.744843
H	3.764899	-3.167636	0.886294
H	4.004722	-2.970934	3.298182
H	3.821258	-1.213051	3.250677
H	5.263807	-1.976015	2.565168
H	1.731088	-2.967523	2.455759
H	1.394146	-2.782722	0.738724
H	1.446511	-1.355993	1.773919
H	6.148181	3.142099	-1.384357
H	7.369586	5.314342	-1.651401
H	6.338929	6.065165	-0.434098
H	5.646311	5.492363	-1.965026
H	8.289681	3.474704	-0.286220
H	7.273082	2.557477	0.828922
H	7.551824	4.288483	1.092509
H	4.788808	5.803330	1.120895
H	2.800981	6.002583	2.627042
H	2.324396	4.348852	2.235755
H	2.299123	5.598408	0.984752
H	5.021528	5.409151	3.534929
H	6.109570	4.303947	2.694407
H	4.578610	3.707259	3.357153
H	2.298959	0.269975	2.779518
H	5.342092	1.217525	-0.247367
H	2.365930	-2.033202	-2.747631
H	-1.399752	2.190628	-0.693631
H	1.037649	-1.987307	-1.563520
H	2.518254	-2.881325	-1.204389
H	1.997627	5.449699	-1.385230
H	3.342274	5.263045	-2.535987
H	3.629581	5.945180	-0.929598
C	3.059286	5.199956	-1.479521

TS_{BC}

Fe	4.167467	1.322053	0.590418
O	0.616210	0.926856	1.421465
P	4.025696	-0.896522	0.155957
O	-0.073942	3.158529	0.432331
C	1.617453	1.168293	2.313423
H	0.193161	2.240057	0.835336
P	4.509136	3.519005	0.241315
H	2.543612	1.671456	1.820203
C	-1.486783	3.251143	0.440724
N	3.006836	1.482679	-1.062067
C	1.205612	2.073965	3.486630
H	-1.888725	3.104646	1.458806
N	2.889219	-0.866268	-1.166135
H	0.418237	1.568694	4.060379

C	-1.918287	4.614203	-0.080408	P	4.507493	3.516617	0.230271
N	3.253495	3.816823	-0.937752	H	2.512415	1.653122	1.962655
H	0.796202	3.022038	3.124552	C	-1.455183	3.288048	0.471588
H	-1.555661	4.768527	-1.103476	N	3.027197	1.471036	-1.085089
C	2.511344	0.365282	-1.674577	C	1.069648	2.078267	3.528693
H	-1.512650	5.415463	0.548200	H	-1.832388	3.146299	1.499934
H	2.040597	2.283646	4.167084	N	2.923805	-0.878110	-1.191591
C	1.651982	0.457228	-2.782538	H	0.222210	1.592107	4.028910
C	1.325108	1.718012	-3.261488	C	-1.874416	4.661517	-0.032881
H	-3.010473	4.704572	-0.087787	N	3.241538	3.807329	-0.939655
C	1.842441	2.862377	-2.671384	H	0.721289	3.043344	3.146765
C	2.696006	2.715547	-1.565283	H	-1.535594	4.813449	-1.064478
C	5.623337	-1.575474	-0.591463	C	2.542632	0.351410	-1.701803
C	5.522542	-2.898254	-1.364864	H	-1.436791	5.452277	0.587591
C	6.752357	-1.652456	0.451577	H	1.848894	2.258713	4.280642
C	3.410971	-2.237622	1.331646	C	1.687076	0.440400	-2.812936
C	4.035028	-2.025683	2.725187	C	1.347443	1.700607	-3.284796
C	1.877881	-2.341206	1.430208	H	-2.964445	4.773738	-0.011750
C	6.112550	3.895789	-0.686601	C	1.847839	2.847655	-2.685017
C	6.326613	5.367774	-1.069731	C	2.701121	2.703775	-1.578434
C	7.366322	3.334472	0.006295	C	5.647366	-1.590977	-0.581875
C	4.289733	4.906478	1.480352	C	5.546903	-2.914401	-1.354338
C	2.863923	4.968107	2.041284	C	6.762603	-1.674034	0.475340
C	5.309072	4.787618	2.626373	C	3.409149	-2.231734	1.322985
C	5.169665	1.191556	2.018094	C	4.016267	-2.005457	2.721460
O	5.864035	1.111832	2.949022	C	1.873910	-2.318285	1.400298
C	2.364006	-2.073425	-1.818210	C	6.099732	3.904166	-0.710749
H	1.257899	-0.428210	-3.258452	C	6.296503	5.378226	-1.095071
H	0.663820	1.809811	-4.118458	C	7.364852	3.351445	-0.031577
H	1.600421	3.838762	-3.063827	C	4.284287	4.892714	1.479798
H	5.878187	-0.783674	-1.305645	C	2.871194	4.908608	2.074992
H	6.522540	-3.174500	-1.720261	C	5.333495	4.796277	2.600666
H	4.878235	-2.820272	-2.242535	C	5.187683	1.191975	2.004654
H	5.163059	-3.722841	-0.740220	O	5.890182	1.119473	2.930091
H	7.704622	-1.819523	-0.064760	C	2.399098	-2.087407	-1.840297
H	6.605362	-2.490243	1.140550	H	1.303542	-0.446367	-3.294966
H	6.852664	-0.737088	1.040419	H	0.687675	1.790120	-4.143196
H	3.795333	-3.184016	0.933736	H	1.593126	3.823514	-3.070647
H	3.796585	-2.888728	3.357331	H	5.916073	-0.801723	-1.293865
H	3.628515	-1.134559	3.212863	H	6.549706	-3.199991	-1.694041
H	5.123156	-1.930594	2.697941	H	4.916734	-2.832568	-2.241884
H	1.623589	-2.974914	2.288256	H	5.170476	-3.734247	-0.733410
H	1.440207	-2.809697	0.546089	H	7.719546	-1.850695	-0.029000
H	1.390214	-1.372500	1.570158	H	6.600144	-2.508751	1.164573
H	5.956103	3.317010	-1.606560	H	6.863629	-0.757722	1.062516
H	7.226016	5.446752	-1.692084	H	3.791774	-3.185170	0.940565
H	6.485916	5.998772	-0.189180	H	3.755659	-2.853383	3.365241
H	5.496255	5.783317	-1.644957	H	3.616776	-1.099123	3.186226
H	8.214347	3.404299	-0.684967	H	5.106085	-1.927721	2.707884
H	7.252941	2.285370	0.289683	H	1.598810	-2.927695	2.269513
H	7.630747	3.904796	0.901644	H	1.445800	-2.803901	0.520740
H	4.501628	5.835179	0.939367	H	1.395304	-1.340757	1.508581
H	2.743001	5.893931	2.615785	H	5.938594	3.324751	-1.629525
H	2.682170	4.133253	2.720805	H	7.190122	5.466137	-1.724529
H	2.090651	4.949198	1.269288	H	6.456176	6.010689	-0.215627
H	5.156671	5.617995	3.325288	H	5.457393	5.785336	-1.663725
H	6.343951	4.837440	2.280207	H	8.202855	3.420723	-0.735028
H	5.177104	3.856773	3.186909	H	7.259541	2.303320	0.258926
H	2.040972	0.243686	2.745936	H	7.639296	3.927586	0.856920
H	5.384344	1.195563	-0.233382	H	4.456826	5.830045	0.939657
H	2.676083	-2.126176	-2.866728	H	2.739571	5.822885	2.665340
H	-1.941986	2.463567	-0.186515	H	2.727617	4.059267	2.746560
H	1.270250	-2.092926	-1.775433	H	2.081051	4.879476	1.320786
H	2.737937	-2.957980	-1.308822	H	5.174124	5.618919	3.307113
H	1.785821	5.270389	-1.377069	H	6.358066	4.877045	2.230739
H	3.207286	5.320656	-2.449421	H	5.240135	3.859685	3.159341
H	3.317761	5.914165	-0.786580	H	1.928932	0.239061	2.844382
C	2.872888	5.150451	-1.419803	H	5.409734	1.190392	-0.228237
				H	2.716399	-2.146173	-2.886881
				H	-1.946034	2.512586	-0.144411
				H	1.305081	-2.103846	-1.802915
				H	2.768076	-2.970467	-1.324707
				H	1.747605	5.238783	-1.357436
				H	3.163707	5.326597	-2.435062
				H	3.270611	5.903675	-0.766120
				C	2.836474	5.139396	-1.406127
C							
Fe	4.184030	1.314509	0.578040				
O	0.609755	0.944892	1.420179				
P	4.044510	-0.904354	0.144684				
O	-0.046595	3.165694	0.422303				
C	1.558555	1.174900	2.383041				
H	0.216520	2.240982	0.834683				

D

Fe	-0.135989	0.377728	-0.675548
O	-2.026691	1.055413	2.266270
H	0.673472	0.977503	4.407646
P	-0.849254	-1.730645	-0.992636
H	0.162274	1.086693	3.877920
O	-3.460711	1.611490	0.312889
C	-2.795160	0.607817	3.343051
H	-2.868374	1.395775	1.172192
P	0.616769	2.482422	-0.989487
C	-4.430397	2.591180	0.628209
H	-2.279186	-0.195152	3.910148
N	-1.257989	0.778476	-2.308206
H	-3.971996	3.461238	1.129929
C	-3.145053	1.723547	4.338775
N	-1.914421	-1.479389	-2.349842
C	-5.139244	3.063257	-0.635130
H	-3.725929	2.515413	3.849454
N	-0.521935	3.008797	-2.207435
H	-5.632121	2.224152	-1.140328
H	-2.234468	2.182519	4.743545
C	-1.974434	-0.217399	-2.912462
H	-4.428206	3.511298	-1.339292
H	-3.736448	1.342264	5.182287
C	-2.747187	0.029681	-4.060059
H	-5.902698	3.813087	-0.396981
C	-2.779231	1.320270	-4.568479
C	-2.054597	2.342808	-3.971204
C	-1.284134	2.039817	-2.836265
C	0.441409	-2.968454	-1.610042
C	-0.008898	-4.436458	-1.679283
C	1.768265	-2.867511	-0.837380
C	-1.909883	-2.639715	0.256467
C	-1.163670	-2.733866	1.599426
C	-3.283488	-1.977552	0.431570
C	2.302791	2.603675	-1.832782
C	2.816213	4.030086	-2.079513
C	3.378425	1.753276	-1.135047
C	0.547735	3.845443	0.290139
C	-0.874301	4.034657	0.837919
C	1.549740	3.591039	1.429467
C	0.882024	0.019238	0.705813
O	1.610481	-0.235705	1.575552
C	-2.720279	-2.552084	-2.945326
H	-3.295484	-0.763974	-4.545392
H	-3.370202	1.531249	-5.455336
H	-2.068205	3.339044	-4.387710
H	0.618264	-2.606997	-2.631560
H	0.786063	-5.025827	-2.151029
H	-0.915467	-4.585757	-2.269288
H	-0.174612	-4.855352	-0.681359
H	2.498725	-3.542309	-1.298550
H	1.657369	-3.172201	0.208138
H	2.185161	-1.859128	-0.861762
H	-2.056849	-3.654761	-0.127450
H	-1.739850	-3.360893	2.289283
H	-1.055400	-1.745669	2.057332
H	-0.169993	-3.180867	1.501580
H	-3.836188	-2.500667	1.220976
H	-3.886336	-2.027388	-0.479271
H	-3.195622	-0.927946	0.722906
H	2.089985	2.137286	-2.803857
H	3.742953	3.978506	-2.663201
H	3.050949	4.545483	-1.142713
H	2.111019	4.644690	-2.643111
H	4.298724	1.785435	-1.730099
H	3.078753	0.707142	-1.043635
H	3.621859	2.129835	-0.137114
H	0.852790	4.765455	-0.220360
H	-0.888519	4.915449	1.491217
H	-1.198228	3.173334	1.430363
H	-1.605214	4.203248	0.042190
H	1.452961	4.391195	2.172274
H	2.586110	3.592129	1.082670
H	1.359587	2.642294	1.940488
H	-3.750220	0.146617	3.008930

H	0.995936	-0.026410	-1.529453
H	-5.185324	2.193709	1.330431
H	-2.338642	-2.843448	-3.930572
H	-3.764067	-2.240774	-3.047344
H	-2.703994	-3.424164	-2.295793
H	-1.648283	4.723012	-2.718013
H	-0.195854	4.477986	-3.719865
H	-0.052670	5.052539	-2.050944
C	-0.607016	4.386664	-2.708036

TS_{DE}

Fe	0.318851	0.390032	-0.448157
O	-2.972469	1.714440	1.183521
H	-0.257445	0.632660	2.338770
P	-0.677965	-1.605723	-0.792105
H	-0.867175	0.872493	1.978684
O	-4.745224	0.488334	-0.060174
C	-3.425496	1.839513	2.494336
H	-3.992524	1.026864	0.460442
P	1.163077	2.467257	-0.664214
C	-5.912297	1.278948	-0.139920
H	-2.646268	1.551570	3.234298
N	-1.098533	1.069983	-1.718749
H	-5.670353	2.321308	-0.414327
C	-3.884938	3.262050	2.851572
N	-2.042982	-1.083231	-1.741100
C	-6.872939	0.702142	-1.172374
H	-4.703572	3.584369	2.195477
N	-0.096275	3.194346	-1.626560
H	-7.140345	-0.329775	-0.915492
H	-3.061389	3.977506	2.730721
C	-2.043340	0.216701	-2.216457
H	-6.415527	0.696002	-2.168356
H	-4.237931	3.324356	3.890112
C	-2.987204	0.641345	-3.166738
H	-7.796743	1.290447	-1.222916
C	-2.948023	1.961604	-3.591709
C	-1.997789	2.843519	-3.095326
C	-1.071665	2.365769	-2.153919
C	0.243497	-2.809505	-1.922800
C	-0.390111	-4.202838	-2.060711
C	1.736619	-2.936381	-1.574261
C	-1.431323	-2.639842	0.575983
C	-0.331512	-3.137734	1.530266
C	-2.525187	-1.893062	1.351234
C	2.716310	2.606864	-1.731385
C	3.332261	4.010268	-1.843187
C	3.797180	1.582389	-1.345808
C	1.380494	3.661602	0.762859
C	0.046791	3.998275	1.444728
C	2.393091	3.104791	1.778565
C	1.607260	-0.224515	0.568791
O	2.494037	-0.643490	1.193482
C	-3.126780	-1.979250	-2.164023
H	-3.715986	-0.044458	-3.572382
H	-3.664334	2.307390	-4.331575
H	-1.961347	3.864898	-3.444287
H	0.168196	-2.294733	-2.889752
H	0.147651	-4.762302	-2.835151
H	-1.441378	-4.169196	-2.355268
H	-0.311461	-4.775212	-1.130969
H	2.218320	-3.588740	-2.312089
H	1.894733	-3.385518	-0.588910
H	2.249293	-1.972563	-1.599735
H	-1.880384	-3.514325	0.092563
H	-0.786884	-3.772063	2.299384
H	0.165072	-2.305887	2.040725
H	0.432033	-3.733964	1.023904
H	-2.956783	-2.574325	2.094316
H	-3.338720	-1.535280	0.716106
H	-2.115134	-1.033712	1.886875
H	2.321438	2.320052	-2.714970
H	4.141092	3.982410	-2.582798
H	3.768900	4.337709	-0.894048
H	2.618787	4.768853	-2.172190
H	4.612258	1.635618	-2.076990

H	3.416083	0.559373	-1.346664
H	4.227908	1.789652	-0.361383
H	1.797296	4.581113	0.337175
H	0.222826	4.743342	2.229421
H	-0.394787	3.117252	1.916183
H	-0.685527	4.415648	0.748915
H	2.553575	3.845431	2.570388
H	3.366635	2.888484	1.330609
H	2.022526	2.189861	2.252128
H	-4.276212	1.152566	2.702289
H	1.168699	0.044939	-1.603222
H	-6.432166	1.333845	0.835019
H	-3.057412	-2.229040	-3.229007
H	-4.095070	-1.511382	-1.966995
H	-3.084023	-2.902749	-1.590516
H	-1.101516	5.044956	-1.822288
H	0.155293	4.761817	-3.052297
H	0.599139	5.161052	-1.384185
C	-0.111583	4.614184	-1.999493

E

Fe	0.264134	0.415828	-0.379528
O	-2.942362	1.781007	0.952621
H	-0.475234	0.751864	1.118402
P	-0.695126	-1.574583	-0.750601
H	-1.117744	0.968058	0.694330
O	-4.807179	0.495298	-0.093485
C	-3.147205	1.781528	2.328530
H	-4.024908	1.051668	0.343696
P	1.136653	2.466528	-0.623179
C	-5.973779	1.291788	-0.115791
H	-2.206710	1.569007	2.886239
N	-1.096495	1.077178	-1.733190
H	-5.743819	2.323818	-0.434295
C	-3.705868	3.110769	2.859798
N	-2.051239	-1.065621	-1.719987
C	-7.001461	0.691332	-1.066420
H	-4.667912	3.342435	2.385484
N	-0.101615	3.197403	-1.610491
H	-7.262626	-0.328361	-0.759210
H	-3.020212	3.938614	2.639822
C	-2.036931	0.223752	-2.226604
H	-6.603472	0.645846	-2.086966
H	-3.862306	3.079809	3.946717
C	-2.963239	0.639466	-3.198548
H	-7.921219	1.287627	-1.083036
C	-2.905330	1.952750	-3.643841
C	-1.959848	2.836675	-3.140992
C	-1.058579	2.366797	-2.171072
C	0.236159	-2.788236	-1.861766
C	-0.398396	-4.182138	-1.992980
C	1.727987	-2.914021	-1.508126
C	-1.451448	-2.596607	0.623423
C	-0.351637	-3.119687	1.564709
C	-2.511421	-1.823698	1.419195
C	2.709592	2.610490	-1.659714
C	3.333136	4.013359	-1.736688
C	3.779889	1.574883	-1.274927
C	1.336416	3.652549	0.811683
C	0.002642	3.929100	1.517494
C	2.383116	3.121866	1.807034
C	1.561179	-0.212589	0.618498
O	2.448579	-0.641031	1.233701
C	-3.133942	-1.963816	-2.140426
H	-3.692981	-0.046707	-3.602350
H	-3.605225	2.292210	-4.402162
H	-1.911780	3.854277	-3.499997
H	0.166323	-2.280786	-2.833242
H	0.141437	-4.748340	-2.761043
H	-1.448477	-4.149048	-2.291663
H	-0.324767	-4.747735	-1.058760
H	2.212363	-3.566403	-2.244168
H	1.883894	-3.362189	-0.522044
H	2.240878	-1.950233	-1.533653
H	-1.928956	-3.459909	0.147022
H	-0.813313	-3.738633	2.342567

H	0.170902	-2.297784	2.066186
H	0.390306	-3.737256	1.052317
H	-2.963833	-2.500691	2.153563
H	-3.314618	-1.423457	0.796142
H	-2.060258	-0.993510	1.969825
H	2.330352	2.341779	-2.654672
H	4.155734	3.996119	-2.461278
H	3.752247	4.321752	-0.773464
H	2.628566	4.780674	-2.064941
H	4.603502	1.632018	-1.996167
H	3.393544	0.553971	-1.293726
H	4.200609	1.767170	-0.283079
H	1.712906	4.592500	0.393526
H	0.152497	4.697857	2.284420
H	-0.374995	3.032522	2.016409
H	-0.766621	4.290564	0.830261
H	2.511686	3.850098	2.616020
H	3.362943	2.966355	1.348004
H	2.063200	2.177915	2.261535
H	-3.849822	0.978028	2.643055
H	1.122308	0.066908	-1.556146
H	-6.426023	1.376184	0.890080
H	-3.050985	-2.236686	-3.198812
H	-4.101346	-1.484677	-1.967401
H	-3.106759	-2.875217	-1.546742
H	-1.112281	5.039157	-1.841115
H	0.196350	4.772769	-3.019791
H	0.567419	5.168992	-1.332781
C	-0.111956	4.618135	-1.979344

TS_{EF}

Fe	0.259215	0.416704	-0.376148
O	-2.920742	1.773405	0.941590
H	-0.487048	0.750279	1.117058
P	-0.696296	-1.574560	-0.749634
H	-1.132734	0.977441	0.699436
O	-4.799344	0.496319	-0.100788
C	-3.130043	1.775933	2.317220
H	-4.014577	1.048057	0.331926
P	1.132870	2.466421	-0.621309
C	-5.963232	1.297416	-0.121128
H	-2.191302	1.561715	2.877172
N	-1.100949	1.077541	-1.729922
H	-5.729902	2.328225	-0.440683
C	-3.687509	3.106606	2.845826
N	-2.051526	-1.067167	-1.721118
C	-6.994075	0.699624	-1.069859
H	-4.647805	3.339903	2.368847
N	-0.107134	3.198219	-1.606054
H	-7.257908	-0.319097	-0.761751
H	-2.999870	3.933168	2.627595
C	-2.039021	0.223110	-2.225761
H	-6.597823	0.652509	-2.090984
H	-3.847106	3.076193	3.932302
C	-2.964881	0.638465	-3.198351
H	-7.912004	1.298706	-1.085271
C	-2.909038	1.952547	-3.641530
C	-1.965451	2.837342	-3.136606
C	-1.063977	2.367375	-2.166910
C	0.238811	-2.786367	-1.859977
C	-0.393355	-4.181114	-1.993289
C	1.730248	-2.910102	-1.503810
C	-1.453797	-2.599581	0.621636
C	-0.355010	-3.121389	1.564861
C	-2.516870	-1.829587	1.416034
C	2.703386	2.607365	-1.662074
C	3.326569	4.010012	-1.745572
C	3.774930	1.573192	-1.276839
C	1.338550	3.654254	0.811346
C	0.007061	3.934437	1.519917
C	2.386336	3.123090	1.805332
C	1.554529	-0.210492	0.624122
O	2.440935	-0.638180	1.241558
C	-3.131457	-1.967098	-2.144836
H	-3.692895	-0.048493	-3.604040
H	-3.608839	2.291894	-4.399951

H	-1.918708	3.855453	-3.494324
H	0.170024	-2.278339	-2.831220
H	0.148362	-4.745909	-2.761078
H	-1.443078	-4.149454	-2.293404
H	-0.320180	-4.747418	-1.059430
H	2.217066	-3.560913	-2.239640
H	1.885104	-3.359024	-0.517891
H	2.241598	-1.945475	-1.527398
H	-1.928618	-3.463322	0.143381
H	-0.817061	-3.742258	2.340954
H	0.164496	-2.298827	2.068405
H	0.389550	-3.736663	1.053489
H	-2.969303	-2.508057	2.149025
H	-3.319653	-1.430414	0.791777
H	-2.068313	-0.998951	1.968104
H	2.321584	2.335294	-2.655144
H	4.146936	3.990486	-2.472631
H	3.748594	4.321781	-0.784676
H	2.620791	4.776042	-2.074215
H	4.595849	1.626929	-2.001405
H	3.388283	0.552278	-1.289614
H	4.199453	1.769729	-0.287461
H	1.716087	4.592729	0.390795
H	0.161025	4.701448	2.287849
H	-0.372688	3.038228	2.017889
H	-0.761986	4.299670	0.834467
H	2.518698	3.852760	2.612435
H	3.364705	2.963949	1.344491
H	2.064993	2.181044	2.262728
H	-3.835093	0.974135	2.630059
H	1.117909	0.068031	-1.552842
H	-6.413063	1.383544	0.885529
H	-3.045988	-2.238419	-3.203427
H	-4.100350	-1.490506	-1.973045
H	-3.103188	-2.879234	-1.552317
H	-1.116865	5.040643	-1.835644
H	0.188930	4.772557	-3.016995
H	0.564062	5.169447	-1.331023
C	-0.117191	4.618661	-1.975730

F

Fe	0.419237	0.352030	-0.484868
O	-2.804601	1.826247	1.049064
H	-0.458858	0.686407	0.790136
P	-0.602049	-1.597757	-0.769655
H	-1.969396	1.325010	0.906898
O	-4.983244	0.514583	-0.040278
C	-3.113132	1.831410	2.454329
H	-4.188773	1.002293	0.270971
P	1.196379	2.426234	-0.638494
C	-5.918558	1.463865	-0.551102
H	-2.183732	1.825331	3.036225
N	-1.077263	1.059795	-1.686252
H	-5.475367	2.041436	-1.376927
C	-3.932371	3.067627	2.780134
N	-2.010414	-1.087972	-1.675195
C	-7.153260	0.726993	-1.041572
H	-4.857615	3.089679	2.193711
N	-0.085036	3.176957	-1.565411
H	-7.616188	0.158402	-0.227355
H	-3.365928	3.980466	2.566297
C	-2.038077	0.214283	-2.147719
H	-6.897767	0.028285	-1.846123
H	-4.203456	3.070718	3.841532
C	-3.022033	0.647380	-3.055553
H	-7.893153	1.436327	-1.427948
C	-2.994634	1.971929	-3.473025
C	-2.026245	2.848643	-3.000797
C	-1.070406	2.358137	-2.093128
C	0.228964	-2.874221	-1.898220
C	-0.447213	-4.251260	-1.993040
C	1.726758	-3.047121	-1.589513
C	-1.329733	-2.592838	0.646021
C	-0.214935	-3.109529	1.572261
C	-2.372429	-1.805727	1.451449
C	2.753590	2.705314	-1.683002

C	3.340539	4.125512	-1.687020
C	3.862652	1.685447	-1.367174
C	1.389883	3.569724	0.839830
C	0.060474	3.823765	1.561955
C	2.438570	3.011797	1.818120
C	1.710840	-0.251979	0.501993
O	2.584501	-0.657730	1.166926
C	-3.115384	-1.979543	-2.044556
H	-3.767686	-0.034516	-3.437414
H	-3.735284	2.324585	-4.185426
H	-2.000317	3.874169	-3.339661
H	0.146379	-2.377809	-2.874732
H	0.063244	-4.848382	-2.758357
H	-1.500660	-4.195925	-2.276141
H	-0.373657	-4.803067	-1.050223
H	2.174168	-3.706554	-2.342804
H	1.894022	-3.509767	-0.611754
H	2.266942	-2.098372	-1.616756
H	-1.824317	-3.462084	0.198791
H	-0.662073	-3.699308	2.381088
H	0.338986	-2.285175	2.033958
H	0.499766	-3.754353	1.054289
H	-2.820087	-2.468961	-2.201338
H	-3.181999	-1.413275	0.830437
H	-1.911863	-0.967413	1.982563
H	2.376028	2.481320	-2.689836
H	4.157360	4.171954	-2.417359
H	3.762906	4.390689	-0.712384
H	2.614525	4.892590	-1.964637
H	4.675702	1.803668	-2.093451
H	3.507969	0.654697	-1.430121
H	4.290991	1.839976	-0.371746
H	1.761129	4.526963	0.457765
H	0.217088	4.557502	2.361666
H	-0.321587	2.908254	2.021542
H	-0.709192	4.219018	0.893594
H	2.562822	3.710512	2.653760
H	3.420737	2.878591	1.356569
H	2.124212	2.049771	2.236741
H	-3.675758	0.924445	2.715488
H	1.194096	0.058351	-1.803989
H	-6.204203	2.186124	0.229745
H	-3.096303	-2.235501	-3.110703
H	-4.073404	-1.506114	-1.810652
H	-3.056595	-2.901623	-1.469968
H	-1.118307	5.016999	-1.707425
H	0.147643	4.794254	-2.939157
H	0.576770	5.145894	-1.256832
C	-0.121141	4.605921	-1.892825

G

Fe	1.589530	-1.485640	0.268177
O	-1.533889	-0.239842	3.784483
P	0.757401	-3.562326	0.060207
O	-2.366350	-0.253750	1.451032
C	-2.476830	-0.876311	4.621364
H	-1.918616	-0.225041	2.787473
P	2.222997	0.652185	0.025002
C	-3.597365	0.382384	1.330981
H	-1.944988	-1.486729	5.369790
N	0.181020	-1.010393	-1.087853
H	-3.716525	1.211614	2.065700
C	-3.381739	0.117494	5.351576
N	-0.598419	-3.225473	-0.984726
C	-3.833302	0.977786	-0.063086
H	-3.971430	0.707024	4.639461
N	0.976952	1.201285	-1.065354
H	-3.802956	0.192564	-0.828729
H	-2.784792	0.813553	5.953057
C	-0.673289	-1.968310	-1.559218
H	-3.053792	1.711185	-0.304504
H	-4.078509	-0.399545	6.023561
C	-1.597646	-1.686975	-2.578507
H	-4.807262	1.480864	-0.132136
C	-1.628536	-0.402279	-3.104569
C	-0.778806	0.586876	-2.627679

N	-0.024608	-0.889424	-1.248026	O	-1.380917	0.553325	2.687657
H	-1.592286	0.584683	0.262931	P	-0.159105	-2.107704	-0.766885
C	-1.941797	0.415573	5.341377	O	-3.176952	1.144856	0.621045
N	-0.731580	-3.130288	-1.308699	C	-1.917276	0.414866	4.008083
C	-3.207690	-0.666589	0.909582	H	-2.103388	0.803402	2.072742
H	-2.411340	0.918177	4.487602	P	1.185376	2.148586	-0.647035
N	0.754097	1.322381	-1.097171	C	-4.225724	2.129655	0.715481
H	-3.562490	-1.193182	1.803517	H	-1.126968	-0.045686	4.611121
H	-1.230275	1.113351	5.798148	N	-0.625671	0.417694	-2.029503
C	-0.744541	-1.862694	-1.872703	H	-3.738790	3.042960	1.069112
H	-3.138289	-1.394483	0.093377	C	-2.331902	1.748647	4.615294
H	-2.725044	0.197970	6.078001	N	-1.291730	-1.838078	-2.066706
C	-1.477075	-1.595286	-3.043483	C	-4.907604	2.364985	-0.622090
H	-3.968531	0.076615	0.635427	H	-3.129911	2.217079	4.027552
C	-1.440685	-0.308055	-3.562229	N	0.119099	2.646541	-1.936122
C	-0.699918	0.690488	-2.944944	H	-5.398675	1.452038	-0.978637
C	0.006759	0.368050	-1.771712	H	-1.482784	2.440005	4.654692
C	1.723750	-4.483628	-0.689186	C	-1.354043	-0.574863	-2.627155
C	1.309133	-5.789072	-1.384988	H	-4.183690	2.687254	-1.378446
C	2.846244	-4.763891	0.325709	H	-2.704991	1.605846	5.636289
C	-0.602165	-4.557520	1.203039	C	-2.138088	-0.323191	-3.765306
C	0.090328	-4.580342	2.580541	H	-5.673711	3.142729	-0.525973
C	-2.085536	-4.205039	1.385413	C	-2.159681	0.965494	-4.279988
C	3.518960	0.829089	-0.550778	C	-1.419500	1.983059	3.693714
C	4.065408	2.220679	-0.905361	C	-0.647094	1.678947	-2.560112
C	4.573039	0.042508	0.248145	C	1.133855	-3.287145	-1.479590
C	1.749382	2.197298	1.442321	C	0.694294	-4.752367	-1.628464
C	0.332582	2.593583	1.876407	C	2.474738	-3.207010	-0.728646
C	2.600102	1.855158	2.679566	C	-1.153556	-3.078864	0.488764
C	1.919743	-1.670144	1.902584	C	-0.319518	-3.350444	1.752434
O	2.644679	-1.932651	2.779157	C	-2.465465	-2.364948	0.841250
C	-1.534655	-4.179117	-1.949694	C	2.927467	2.400587	-1.335752
H	-2.045486	-2.369532	-3.537329	C	3.412345	3.856894	-1.411758
H	-1.993050	-0.081135	-4.469969	C	3.976381	1.529108	-0.623161
H	-0.665110	1.685031	-3.365056	C	0.933278	3.458429	0.669615
H	2.126129	-3.803545	-1.450230	C	-0.551055	3.656064	1.005204
H	2.209715	-6.292016	-1.757952	C	1.738678	3.113705	1.933813
H	0.656068	-5.621346	-2.243396	C	1.525158	-0.352950	0.968228
H	0.812162	-6.486342	-0.701989	O	2.236808	-0.609975	1.850923
H	3.727246	-5.137441	-0.209014	C	-2.127926	-2.898414	-2.643007
H	2.553462	-5.535908	1.044031	H	-2.697850	-1.113233	-4.243279
H	3.152085	-3.874744	0.882432	H	-2.754832	1.178509	-5.163511
H	-0.534638	-5.560894	0.766938	H	-1.424691	2.976807	-4.116348
H	-0.391199	-5.338498	3.209228	H	1.285320	-2.864370	-2.481409
H	-0.011783	-3.615578	3.087996	H	1.491025	-5.309147	-2.135506
H	1.153191	-4.826757	2.528704	H	-0.212970	-4.871011	-2.224533
H	-2.547150	-4.956340	2.037708	H	0.532768	-5.228999	-0.656258
H	-2.646167	-4.197814	0.448682	H	3.208151	-3.836382	-1.245851
H	-2.205751	-3.231712	1.864528	H	2.394737	-3.575579	0.298718
H	3.338538	0.280468	-1.484345	H	2.870948	-2.190052	-0.699788
H	5.015265	2.104093	-1.441290	H	-1.392147	-4.042968	0.026882
H	4.270932	2.817502	-0.010508	H	-0.908047	-3.964763	2.443400
H	3.397810	2.793182	-1.552488	H	-0.062730	-2.421806	2.272107
H	5.461055	-0.099551	-0.379131	H	0.605450	-3.892559	1.538980
H	4.222726	-0.945733	0.553111	H	-3.045569	-2.993332	1.527184
H	4.895399	0.584513	1.142206	H	-3.088163	-2.176222	-0.038093
H	2.214865	3.052855	0.941411	H	-2.271632	-1.414466	1.346274
H	0.386327	3.506995	2.480592	H	2.814149	2.015977	-2.357892
H	-0.119051	1.813977	2.494043	H	4.380799	3.879825	-1.924754
H	-0.331542	2.794279	1.032045	H	3.560696	4.287695	-0.416196
H	2.604378	2.716404	3.357911	H	2.735001	4.506745	-1.969837
H	3.640323	1.628369	2.436146	H	4.937452	1.641192	-1.138565
H	2.182200	1.006151	3.229266	H	3.712532	0.469807	-0.638784
H	-1.970051	-1.560956	4.469260	H	4.127624	1.831898	0.417365
H	2.161713	-1.669744	-0.324063	H	1.328935	4.393316	0.258158
H	-2.028314	0.782517	1.952151	H	-0.651376	4.488830	1.711301
H	-1.191625	-4.384234	-2.970026	H	-0.967875	2.766045	1.483581
H	-2.589431	-3.887335	-1.988363	H	-1.153053	3.896819	0.124881
H	-1.462659	-5.100241	-1.375451	H	1.640979	3.931596	2.656832
H	-0.302317	3.065795	-1.662036	H	2.804633	2.979659	1.732754
H	1.182993	2.776258	-2.598601	H	1.360840	2.203798	2.410545
H	1.273554	3.351830	-0.927451	H	-2.768695	-0.280876	4.003189
C	0.727795	2.699013	-1.604486	H	1.670247	-0.333140	-1.265014
				H	-4.956333	1.821905	1.474709
				H	-1.783840	-3.185777	-3.643043
				H	-3.170433	-2.572843	-2.707465
				H	-2.100502	-3.776960	-2.002873
I							
Fe	0.514855	0.010711	-0.417063				

H	-0.984376	4.365364	-2.492574	H	2.922862	3.206863	1.582236
H	0.501442	4.106645	-3.441056	H	1.525250	2.461804	2.382903
H	0.586854	4.688894	-1.769899	H	-2.075520	-0.262455	4.378179
C	0.053675	4.022869	-2.444362	H	1.427345	-0.261268	-1.051760
H	-3.582861	0.294365	0.394747	H	-3.915922	1.700781	1.560645
TS_{ij}				H	-1.856379	-3.004911	-3.760241
Fe	0.214934	0.145374	-0.326144	H	-3.291751	-2.456114	-2.861513
O	-0.888633	1.116574	3.353652	H	-2.222573	-3.667146	-2.159719
P	-0.397415	-1.985921	-0.756121	H	-0.987237	4.503210	-2.538509
O	-2.155258	0.881155	0.820339	H	0.501678	4.163742	-3.454917
C	-1.681531	0.759146	4.488945	H	0.585593	4.775297	-1.795838
H	-1.433857	1.040984	2.545068	C	0.034786	4.118720	-2.464721
P	1.058088	2.217922	-0.616667	H	-2.457152	-0.036415	0.882903
C	-3.328485	1.711516	0.634146	J			
H	-0.996804	0.749090	5.344586	Fe	0.145567	0.148417	-0.300148
N	-0.748788	0.535322	-2.058990	O	-0.739643	1.138010	3.506829
H	-2.948860	2.724128	0.489052	P	-0.436958	-1.977685	-0.783287
C	-2.822663	1.734585	4.744132	O	-1.730491	0.674415	0.777823
N	-1.456262	-1.708180	-2.116806	C	-1.730365	0.911244	4.515216
C	-4.186738	1.278236	-0.540935	H	-1.163381	1.083891	2.631732
H	-3.536884	1.731950	3.912559	P	0.984916	2.228775	-0.570775
N	0.030772	2.751731	-1.927890	C	-2.824142	1.555382	0.386413
H	-4.553610	0.254187	-0.407282	H	-1.182890	0.850248	5.462360
H	-2.440697	2.754244	4.866801	N	-0.800755	0.557242	-2.054531
C	-1.460065	-0.446641	-2.689675	H	-2.395363	2.258904	-0.325553
H	-3.636523	1.332802	-1.484893	C	-2.773960	2.018269	4.582227
H	-3.367533	1.460441	5.655105	N	-1.480732	-1.692521	-2.152602
C	-2.177565	-0.186844	-3.869454	C	-4.008166	0.819798	-0.210708
H	-5.059191	1.937416	-0.615862	H	-3.351549	2.073911	3.652176
C	-2.149286	1.100438	-4.388181	N	-0.037917	2.774704	-1.882268
C	-1.423920	2.107301	-3.766103	H	-4.438777	0.110615	0.504426
C	-0.717802	1.793999	-2.592026	H	-2.299377	2.991188	4.750919
C	1.007528	-3.040365	-1.463571	C	-1.486441	-0.423243	-2.711133
C	0.627739	-4.459126	-1.914948	H	-3.739422	0.282774	-1.123999
C	2.246423	-3.090388	-0.552893	H	-3.476456	1.833008	5.403146
C	-1.382210	-3.125796	0.367198	C	-2.181744	-0.157592	-3.903514
C	-0.645235	-3.333248	1.701940	H	-4.786216	1.549767	-0.461470
C	-2.822100	-2.658037	0.623475	C	-2.145053	1.133021	-4.413636
C	2.799916	2.237346	-1.351974	C	-1.435602	2.136690	-3.769088
C	3.386632	3.628034	-1.638015	C	-0.760818	1.817475	-2.577709
C	3.803811	1.386850	-0.554054	C	0.982457	-3.012815	-1.483381
C	0.992790	3.636791	0.608059	C	0.598006	-4.326370	-2.180868
C	-0.439272	3.987217	1.033638	C	2.099139	-3.271786	-0.456777
C	1.869986	3.345973	1.838335	C	-1.406731	-3.134264	0.341255
C	1.106924	-0.209071	1.143143	C	-0.732796	-3.209700	1.724707
O	1.767983	-0.466511	2.064413	C	-2.888318	-2.767081	0.511941
C	-2.246048	-2.763883	-2.764905	C	2.728257	2.259486	-1.307627
H	-2.729858	-0.967215	-4.371417	C	3.312876	3.653480	-1.582166
H	-2.695094	1.320884	-5.301288	C	3.739578	1.403380	-0.525431
H	-1.393968	3.100494	-4.189219	C	0.934815	3.646482	0.658458
H	1.273116	-2.453766	-2.352863	C	-0.487210	4.022183	1.094978
H	1.500296	-4.921978	-2.391229	C	1.810474	3.336309	1.885873
H	-0.183521	-4.473742	-2.645456	C	1.078457	-0.221246	1.134861
H	0.345646	-5.096588	-1.070768	O	1.769141	-0.478043	2.035654
H	3.073852	-3.547148	-1.108069	C	-2.259493	-2.745485	-2.819342
H	2.075377	-3.703891	0.336570	H	-2.720751	-0.936585	-4.422013
H	2.571801	-2.099154	-0.231060	H	-2.670331	1.357921	-5.337638
H	-1.425055	-4.090353	-0.150136	H	-1.396259	3.132399	-4.185599
H	-1.215393	-4.036476	2.319635	H	1.379136	-2.325089	-2.240630
H	-0.559633	-2.395194	2.260381	H	1.511433	-4.807391	-2.550858
H	0.357191	-3.748606	1.575801	H	-0.056002	-4.173729	-3.041206
H	-3.383437	-3.472843	1.094586	H	0.116346	-5.034592	-1.498476
H	-3.354340	-2.372130	-0.286611	H	2.993357	-3.619125	-0.986740
H	-2.851591	-1.818523	1.326879	H	1.819351	-4.057352	0.251517
H	2.625543	1.729981	-2.309994	H	2.379249	-2.380751	0.109747
H	4.338603	3.507959	-2.168640	H	-1.349499	-4.124507	-0.124700
H	3.596305	4.178530	-0.715142	H	-1.250244	-3.959378	2.334240
H	2.741097	4.244887	-2.267051	H	-0.803048	-2.250337	2.248306
H	4.742289	1.326224	-1.117481	H	0.319766	-3.496542	1.677957
H	3.446450	0.367694	-0.392719	H	-3.393551	-3.577944	1.049199
H	4.037155	1.827109	0.419597	H	-3.415051	-2.617106	-0.432119
H	1.422401	4.501400	0.091119	H	-3.011216	-1.863957	1.117815
H	-0.421839	4.918714	1.611348	H	2.551571	1.761758	-2.270295
H	-0.864827	3.211519	1.675521	H	4.258420	3.540095	-2.125722
H	-1.104955	4.141589	0.180130	H	3.535059	4.191055	-0.654592
H	1.812017	4.198673	2.524633				

H	2.660579	4.279970	-2.194476
H	4.673679	1.348748	-1.096868
H	3.385611	0.382328	-0.370038
H	3.980924	1.835678	0.449867
H	1.377888	4.506380	0.145117
H	-0.442422	4.934508	1.701258
H	-0.933328	3.239181	1.713265
H	-1.151180	4.220801	0.249842
H	1.774991	4.191162	2.571115
H	2.859137	3.171860	1.627791
H	1.445677	2.462004	2.432731
H	-2.219282	-0.062137	4.361460
H	1.359240	-0.228905	-1.072345
H	-3.132675	2.113835	1.276558
H	-1.877808	-2.954817	-3.824651
H	-3.311297	-2.452509	-2.897973
H	-2.210636	-3.664057	-2.238757
H	-1.060486	4.520148	-2.499147
H	0.456234	4.211292	-3.379988
H	0.489178	4.802746	-1.712055
C	-0.035774	4.147675	-2.402978
H	-2.112003	-0.129069	1.161000

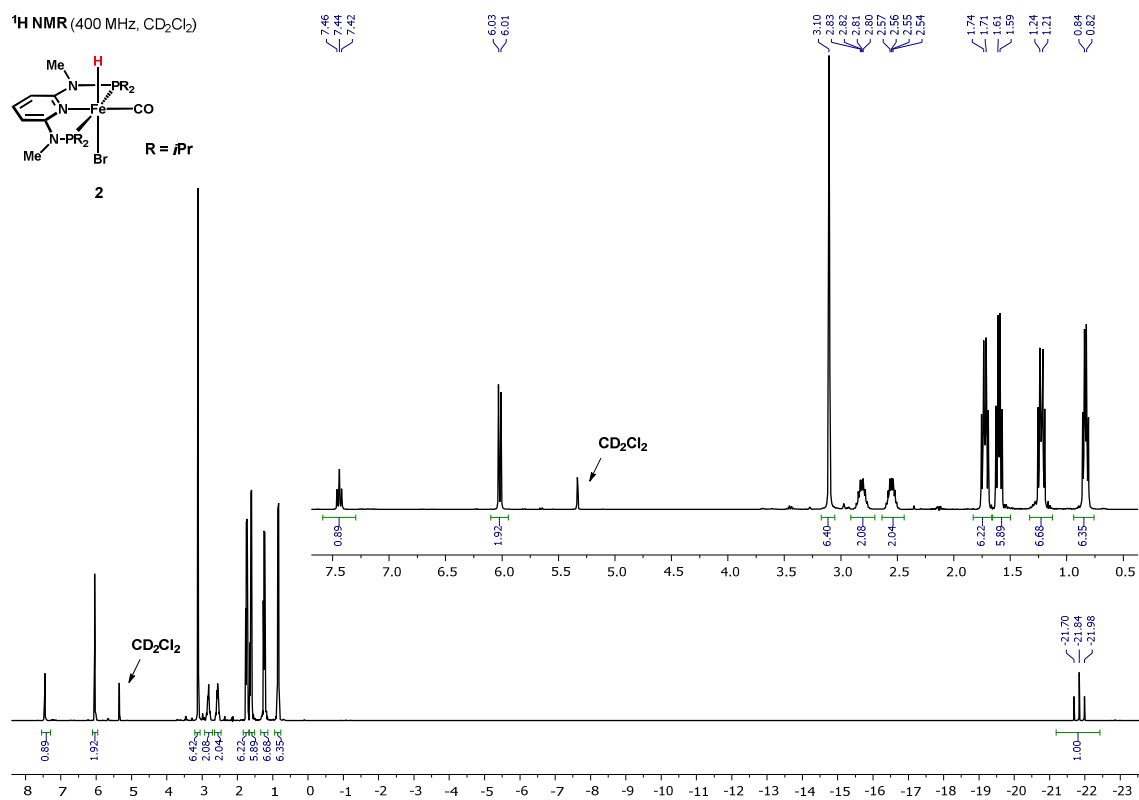


Figure S2. ¹H NMR spectrum of **2**

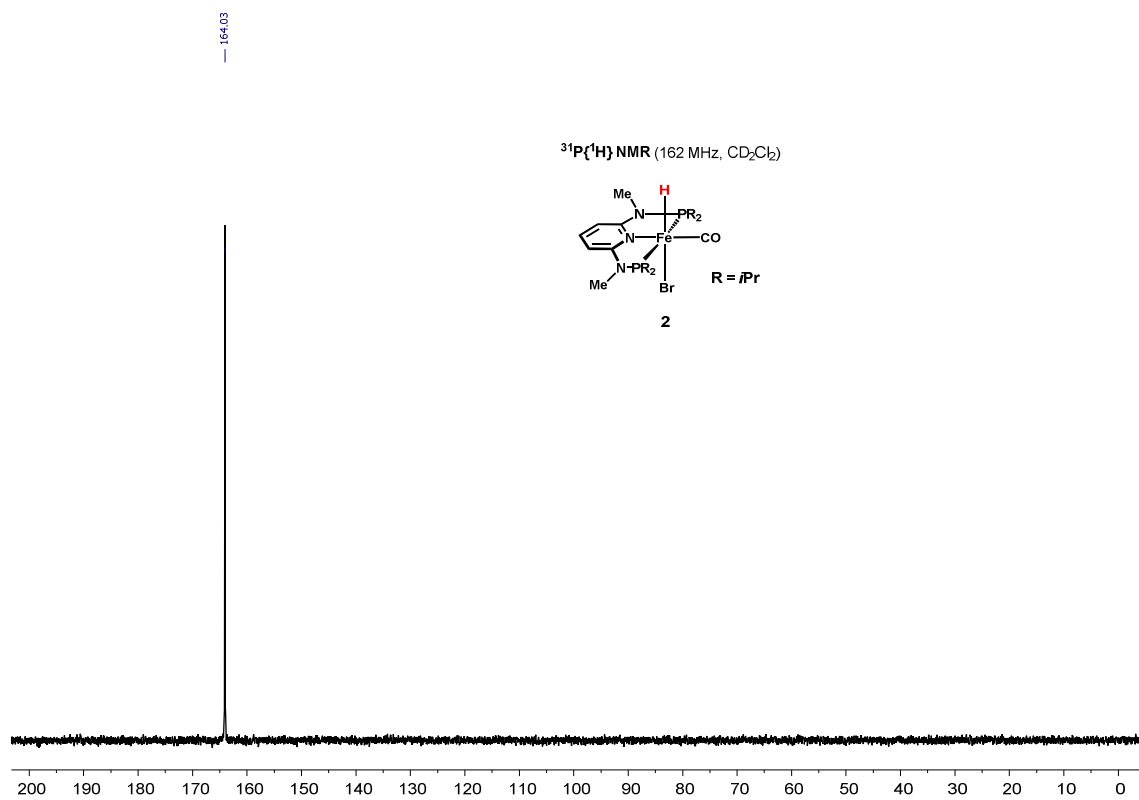


Figure S3. ³¹P{¹H} NMR spectrum of **2**

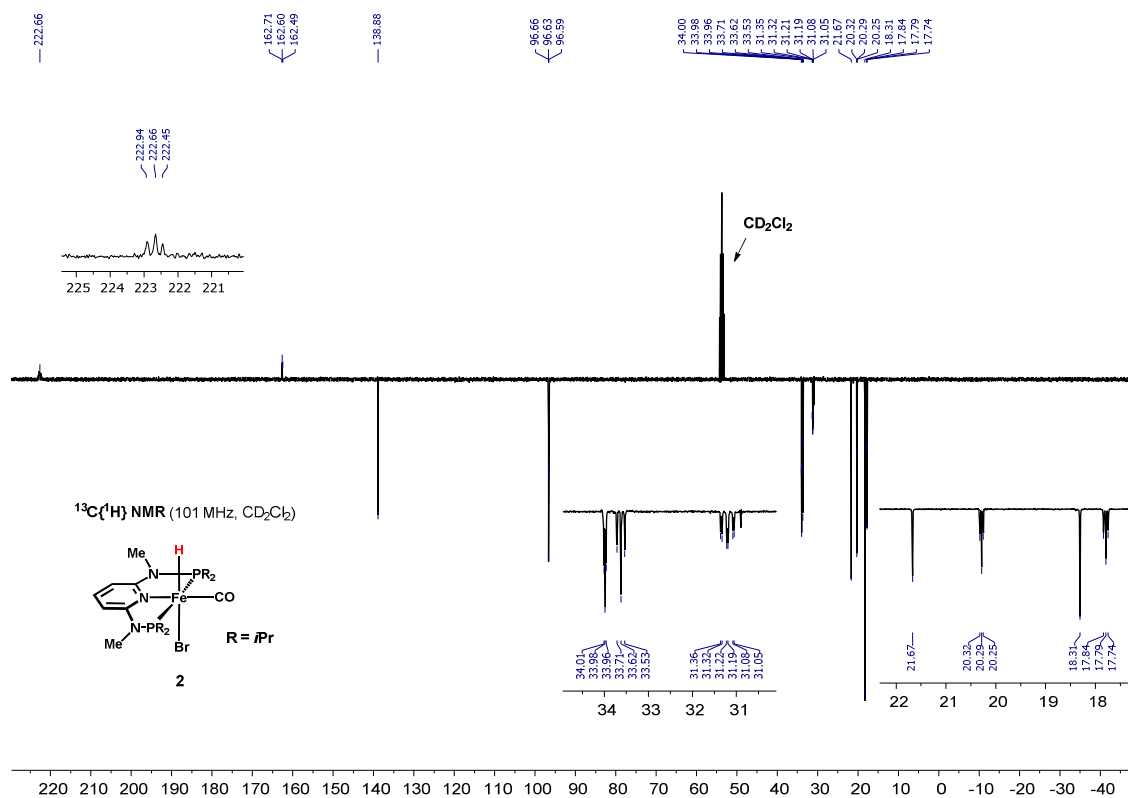


Figure S4. $^{13}\text{C}\{^1\text{H}\}$ APT NMR spectrum of **2**

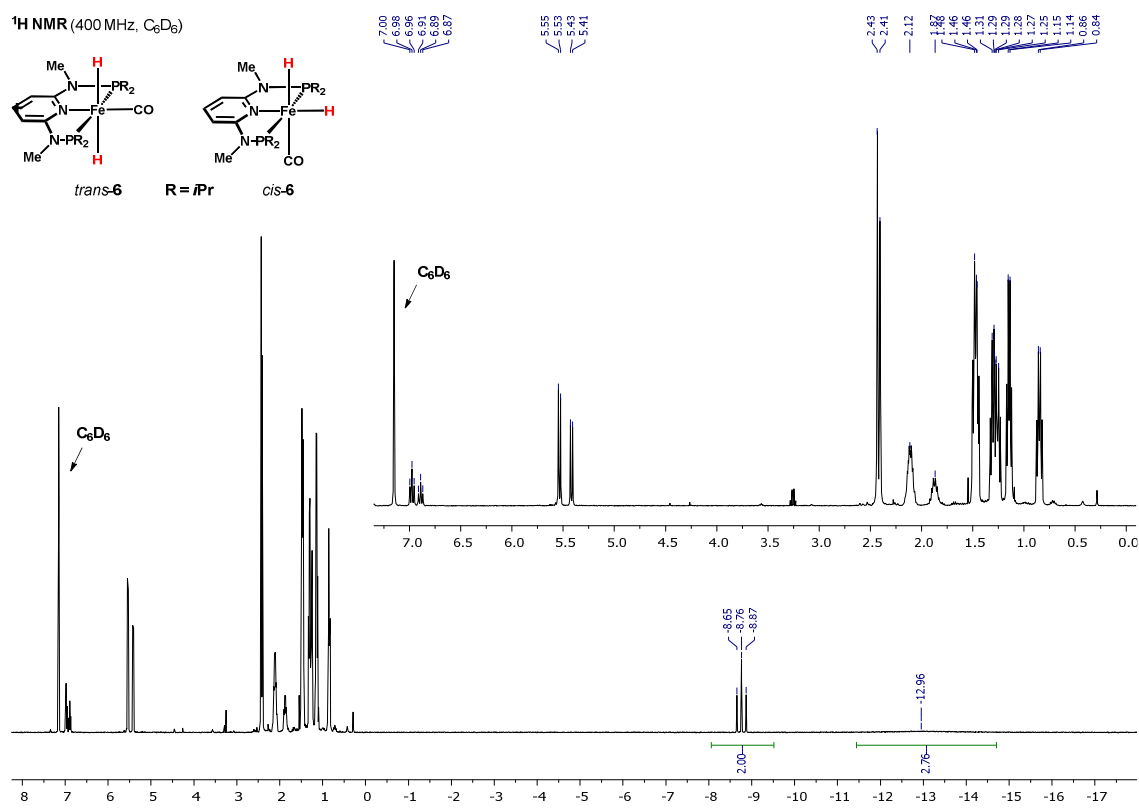


Figure S5. ^1H NMR spectrum of **3**

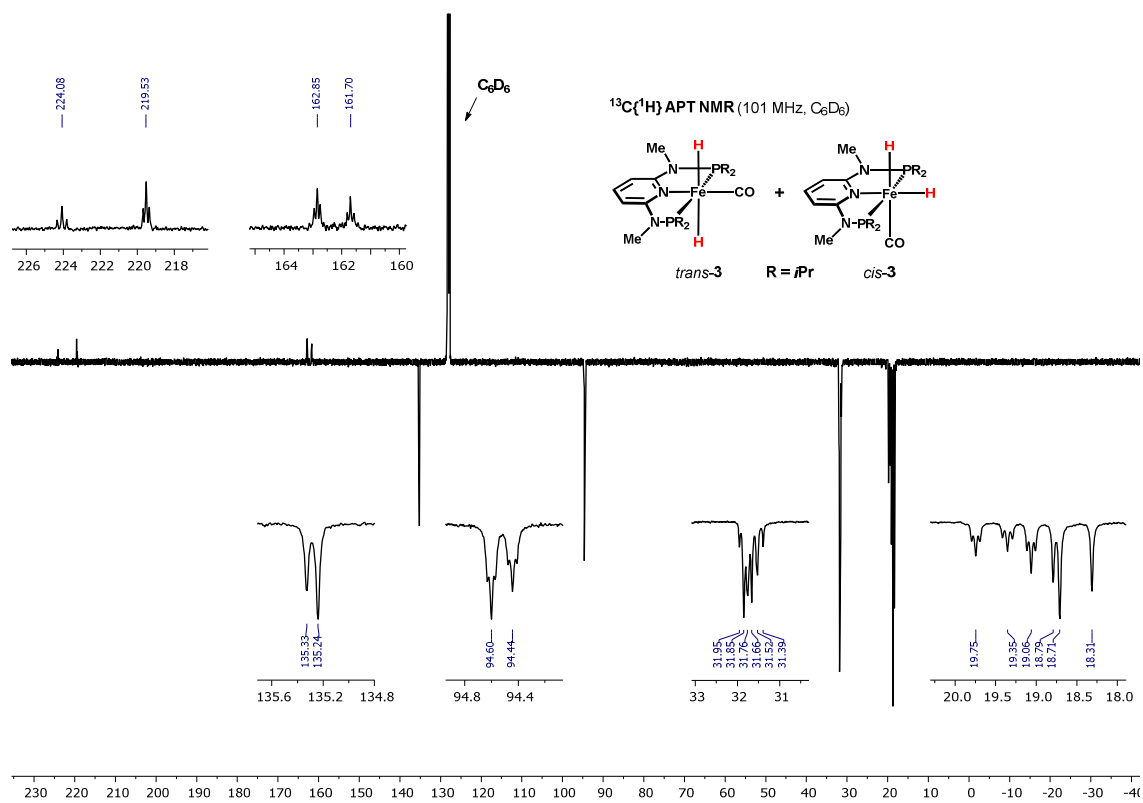


Figure S8. $^{13}\text{C}\{^1\text{H}\}$ APT NMR spectrum of **3**

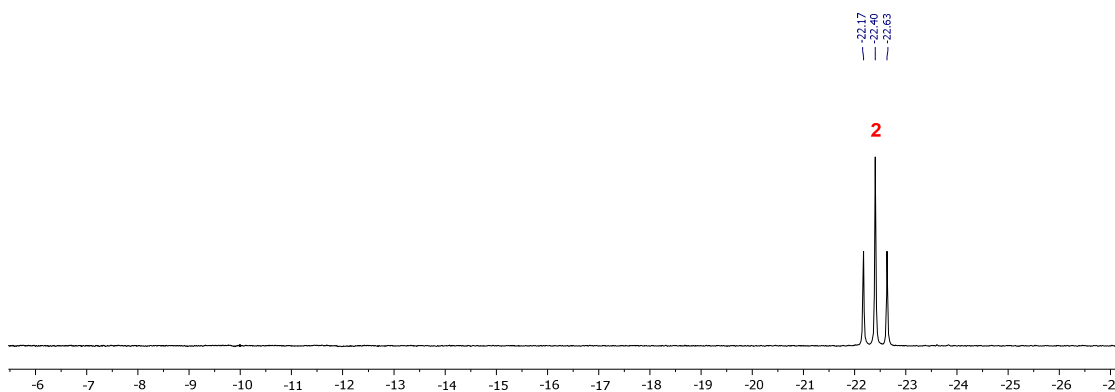


Figure S9. ^1H NMR (250 MHz, 20°C , hydride region) of **2** in EtOH

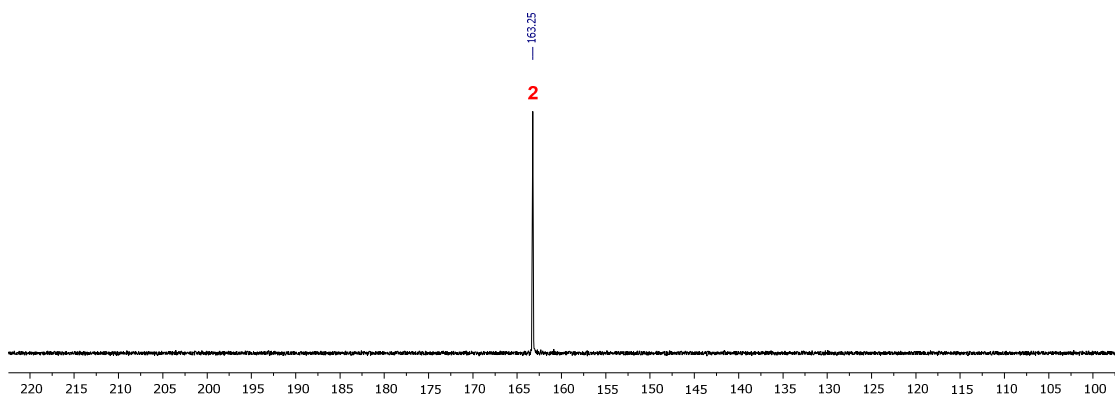


Figure S10. $^{31}\text{P}\{^1\text{H}\}$ NMR (101 MHz, 20°C) of **2** in EtOH

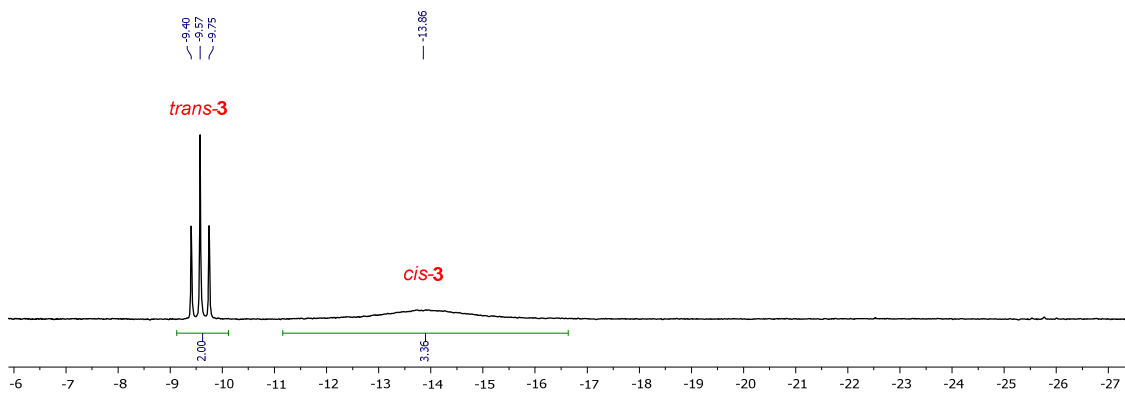


Figure S11. ^1H NMR (250 MHz, 20°C , hydride region) after reaction of **2** with *t*BuOK under H_2 in EtOH

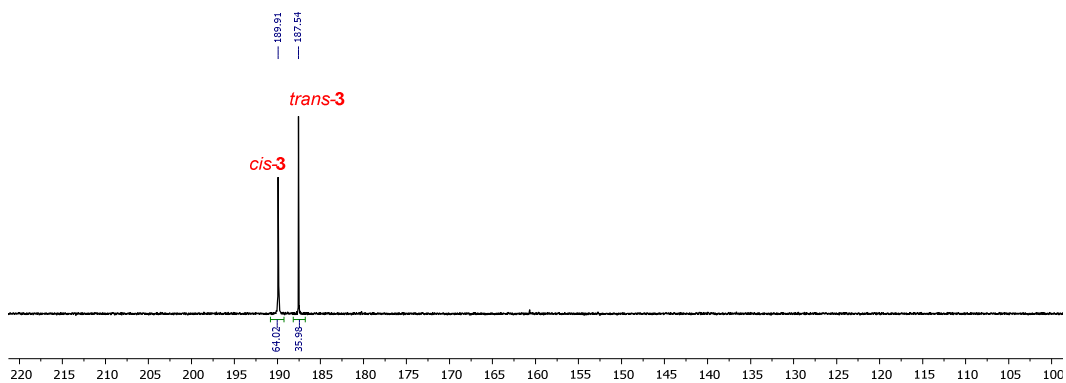


Figure S12. $^{31}\text{P}\{^1\text{H}\}$ NMR (101 MHz, 20°C) after reaction of **2** with *t*BuOK under H_2 in EtOH

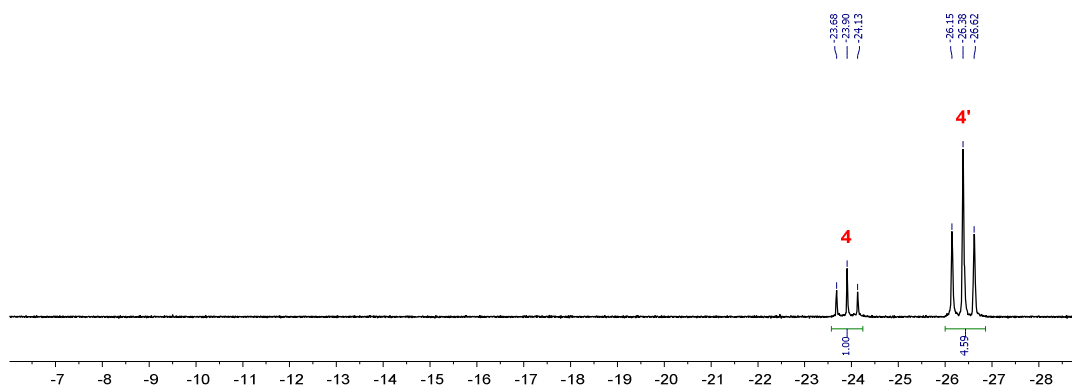


Figure S13. ^1H NMR (250 MHz, 20°C , hydride region) after addition of 1 equiv. of benzaldehyde to a solution of **3** in EtOH

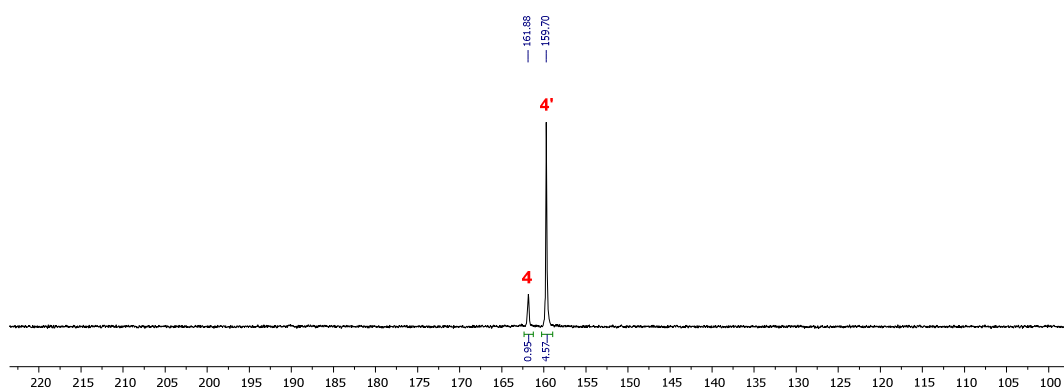


Figure S14. $^{31}\text{P}\{^1\text{H}\}$ NMR (101 MHz, 20°C) after addition of 1 equiv. of benzaldehyde to a solution of **3** in EtOH

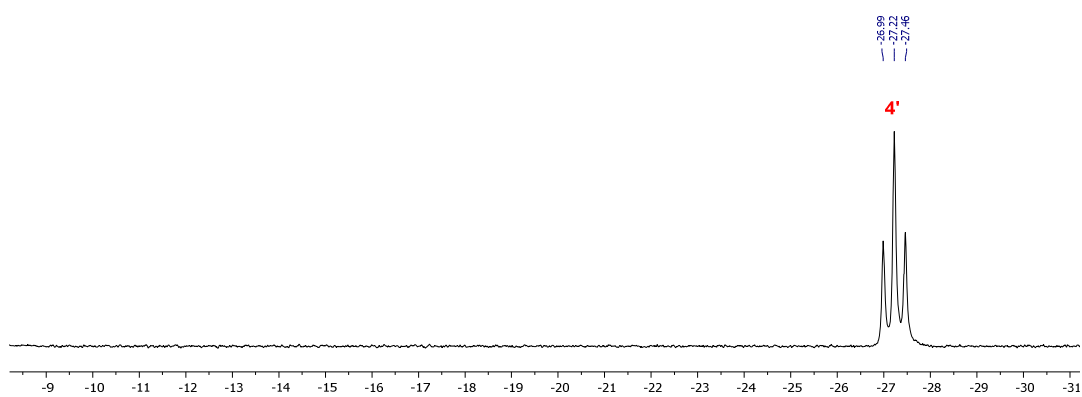


Figure S15. ^1H NMR (250 MHz, 20°C , hydride region) showing the formation of **4'** after the reaction of **2** with AgBF_4

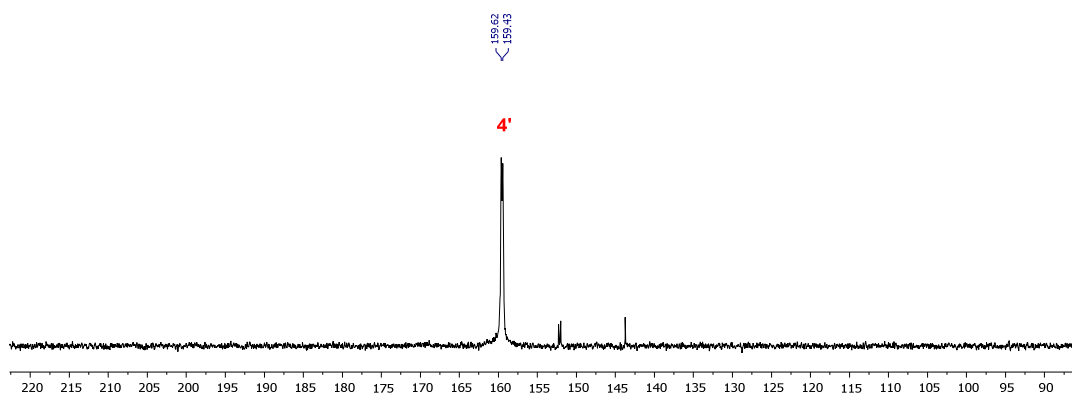


Figure S16. $^{31}\text{P}\{^1\text{H}\}$ NMR (101 MHz, 20°C) showing the formation of **4'** after the reaction of **2** with AgBF_4

Results and Discussion – Part III

Efficient and Mild Carbon Dioxide Hydrogenation to Formate Catalyzed by Fe(II) Hydrido Carbonyl Complexes Bearing 2,6-(Diaminopyridyl)diphosphine Pincer Ligands.

Reprinted with permission from *ACS Catal.* **2016**, 6, 2889–2893. Copyright 2016 American Chemical Society.

Efficient and Mild Carbon Dioxide Hydrogenation to Formate Catalyzed by Fe(II) Hydrido Carbonyl Complexes Bearing 2,6-(Diaminopyridyl)diphosphine Pincer Ligands

Federica Bertini,[†] Nikolaus Gorgas,[‡] Berthold Stöger,[§] Maurizio Peruzzini,[†] Luis F. Veiros,^{||} Karl Kirchner,^{*,‡} and Luca Gonsalvi^{*,†}

[†]Consiglio Nazionale delle Ricerche (CNR), Istituto di Chimica dei Composti Organometallici (ICCOM), Via Madonna del Piano 10, 50019 Sesto Fiorentino (Firenze), Italy

[‡]Institute of Applied Synthetic Chemistry and [§]Institute of Chemical Technologies and Analytics, Vienna University of Technology, Getreidemarkt 9/163-AC, A-1060 Wien, Austria

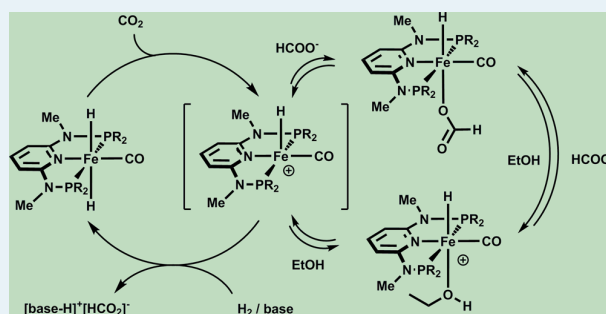
[§]Institute of Chemical Technologies and Analytics, Vienna University of Technology, Getreidemarkt 9/163-AC, A-1060 Wien, Austria

^{||}Centro de Química Estrutural, Instituto Superior Técnico, Universidade de Lisboa, Av. Rovisco Pais No. 1, 1049-001 Lisboa, Portugal

Supporting Information

ABSTRACT: Fe(II) hydrido carbonyl complexes supported by PNP pincer ligands based on the 2,6-diaminopyridine scaffold were found to promote the catalytic hydrogenation of CO₂ and NaHCO₃ to formate in protic solvents in the presence of bases, reaching quantitative yields and high TONs under mild reaction conditions, with pressures as low as 8.5 bar and temperatures as low as 25 °C. NMR and DFT studies highlighted the role of dihydrido and hydrido formate complexes in catalysis.

KEYWORDS: CO₂ hydrogenation, iron pincer complexes, homogeneous catalysis, mechanistic studies, DFT calculations

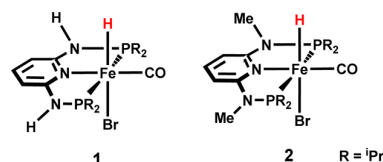


INTRODUCTION

The use of CO₂ as a C1 source is a matter of great interest due to its high abundance, availability, and low cost. In particular, its reduction to HCOOH or derivatives has attracted significant attention in recent years, since it holds the potential for reversible hydrogen storage.¹ The reduction of NaHCO₃ is also of interest, as CO₂ can be easily trapped in basic solutions and reversible hydrogen storage cycles based on bicarbonate and formate have been proposed.² The most efficient catalysts for CO₂ hydrogenation are typically based on expensive noble metals such as ruthenium and iridium.³ In the quest for cheaper alternatives, the preparation of well-defined earth-abundant metal catalysts of comparable activity is highly desirable and important progress has been made recently.⁴ Efficient iron-based catalysts supported by tetraphosphine ligands have been reported by Beller^{4a,b} and some of us,^{4c} whereas Milstein reported that the iron pincer complex [Fe(PNP)(H)₂(CO)] (PNP = 2,6-bis(di-*tert*-butylphosphinomethyl)pyridine) catalyzes CO₂ hydrogenation at low pressure.^{4d} More recently, Hazari and co-workers achieved impressive catalytic activities in Fe-catalyzed CO₂ hydrogenation, reaching turnover numbers (TONs) up to 79600 using iron PNP pincer complexes in the presence of Lewis acid (LA) cocatalysts.^{4e} In recent years, some

of us developed a new class of PNP pincer complexes based on the 2,6-diaminopyridine scaffold where the PR₂ moieties of the PNP ligand are connected to the pyridine ring via NH, N-alkyl, or N-aryl spacers.⁵ Among these, the iron hydrido carbonyl complexes [Fe(PNP^H-iPr)(H)(CO)(Br)] (**1**) and [Fe(PNP^{Me}-iPr)(H)(CO)(Br)] (**2**), shown in Scheme 1, were shown to be active catalysts for hydrogenation reactions.^{5c} Mechanistic studies showed that the N–H spacer of the PNP ligand in **1** can work as a bifunctional catalyst promoting metal–ligand cooperation,^{5c,d} while the N–Me spacer in complex **2** prevents

Scheme 1. Fe-PNP Pincer Complexes **1** and **2**



Received: February 10, 2016

Revised: March 26, 2016

Published: March 30, 2016

such a possibility. In addition, the presence of a labile bromide and strongly σ donating H and CO ligands could give an ideal donor set suitable for catalytic CO₂ hydrogenation.^{4d} Thus, we investigated the activities of these complexes for CO₂ and NaHCO₃ hydrogenation reactions.

RESULTS AND DISCUSSION

Catalytic Studies. Initially, the catalytic activities of **1** and **2** in NaHCO₃ hydrogenation were tested in different solvents using 0.05 mol % of catalyst at 80 °C, 90 bar of H₂, and 24 h (Table S1 in the Supporting Information). The best results were obtained in H₂O/THF (4/1) mixtures which ensure good solubility of both catalysts and substrate, reaching 98% formate yield and TON = 1964 for **1** and 52% formate yield and TON = 1036 for **2**, respectively. In MeOH, TONs and yields decrease by ca. 50% with both catalysts, whereas the reaction does not proceed in neat THF, indicating the need for a protic solvent. In all cases, **1** performed better than **2** under analogous conditions (see the Supporting Information for details). On the basis of the solvent screening results, the hydrogenation of NaHCO₃ in H₂O/THF was then studied with **1** under different conditions of temperature, pressure, and catalyst loading (Table 1). In the presence of only 0.005 mol % of **1**, TONs up to 4560

Table 1. Hydrogenation of NaHCO₃ to NaHCO₂ with **1 at Different Catalyst Loadings, Temperatures, and Pressures^a**

entry ^a	amt of cat. 1 (mol %)	T (°C)	P (bar)	TON ^b	t (h)	yield ^c (%)
1	0.05	80	90	1964	24	98
2	0.005	80	90	4560	24	23
3	0.005	100	90	400	24	2
4	0.005	60	90	2360	24	12
5	0.05	25	90	188	72	9
6	0.005	80	60	640	24	3
7	0.005	80	30	80	24	<1
8	0.1	80	8.5	140	16	14

^aGeneral reaction conditions: 20 mmol of NaHCO₃, 0.01–0.001 mmol of catalyst, 25 mL of H₂O/THF 4/1, 80 °C, 90 bar, 24 h. ^bTON = (mmol of formate)/(mmol of catalyst). ^cYields calculated from the integration of ¹H NMR signals due to NaHCO₂, using DMF as internal standard.

could be achieved at 80 °C and 90 bar of H₂ after 24 h (entry 2). Either higher or lower temperatures resulted in lower turnover numbers (entries 3 and 4). It is worth noting that the reaction proceeds *even at room temperature*, giving TON = 188 after 72 h (entry 5). Reducing the H₂ pressure resulted in a drop of TONs (entries 6 and 7), yet at higher catalyst loadings (0.1 mol %) sodium formate was obtained (14% yield) with a TON of 140 at only 8.5 bar of H₂ (Milstein's conditions)^{4d} after 16 h (entry 8).

Next, the hydrogenation of CO₂ to formate in H₂O/THF (4/1) in the presence of **1** and NaOH as base was studied (Table 2), reaching TONs up to 1220 with nearly quantitative yield under the optimized conditions (catalyst/NaOH = 1/1250, CO₂/H₂ = 40/40 bar, 80 °C, 21 h).

Higher NaOH/catalyst ratios gave worse results regardless of concentration (Table 2, entries 2–4). We then tested the hydrogenation of CO₂ with **1** in EtOH in the presence of different amine bases. Quite surprisingly, formate was not formed using either DBU (1,8-diazabicyclo[5.4.0]undec-7-ene) or DMOA (*N,N*-dimethyloctylamine), whereas in the presence

Table 2. Hydrogenation of CO₂ to Formate with **1 using Different Solvents and Bases^a**

entry	amt of cat. 1 (mol %)	base	solvent	TON ^c	yield ^f (%)
1	0.08	NaOH	H ₂ O/THF	1220	98
2 ^b	0.04	NaOH	H ₂ O/THF	608	24
3 ^c	0.008	NaOH	H ₂ O/THF	120	1
4 ^d	0.04	NaOH	H ₂ O/THF	656	26
5	0.08	DBU	EtOH	0	0
6	0.08	DMOA	EtOH	0	0
7	0.08	NEt ₃	EtOH	288	23
8	0.08		EtOH	0	0
9	0.08	DBU	THF	0	0

^aGeneral reaction conditions: 12.5 mmol of base, 0.01 mmol of catalyst, 25.0 mL of solvent, 80 °C, 80 bar total pressure, 21 h. ^b25.0 mmol of base. ^c0.001 mmol of catalyst. ^d0.005 mmol of catalyst. ^eTON = (mmol of formate)/(mmol of catalyst). ^fYields calculated from the integration of ¹H NMR signals due to NaHCO₂, using DMF as internal standard.

of NEt₃ formate was obtained only in low yields (entries 5–7). The observation that complex **1** fails to catalyze the hydrogenation of CO₂ in EtOH in the presence of amine bases such as DBU and DMOA may be attributed to the fact that EtOH appears to prevent the formation of dihydrides,^{5c} which are expected to be the catalytically active species in this reaction. No reaction occurred in EtOH in the absence of base (entry 8) or in THF with DBU as base due to catalyst decomposition (entry 9).

A complete screening of the effects of catalyst concentration, nature of base, solvent, and temperature for CO₂ hydrogenation in the presence of **2** was then carried out (Table 3).

As for NaHCO₃ hydrogenation, catalyst **2** showed poorer performance in comparison to **1** in the hydrogenation of CO₂ in H₂O/THF (4/1) in the presence of NaOH (Table 3, entries 1 and 2, vs Table 2, entries 1 and 2). Among the alcohols, reactions in EtOH gave activity comparable to that observed in H₂O/THF (entry 4), whereas worse performance was achieved in MeOH (Table 3, entry 3). On the basis of the solvent screening results, amine screening was then studied for CO₂ hydrogenation with **2** in EtOH. To our delight, using DBU as base gave nearly quantitative formate yield (>90%) with a TON of 1153 at 80 °C under 80 bar total pressure (entry 5). Using either DMOA or NEt₃ instead of DBU resulted in lower TONs (entries 6 and 7), and no reaction occurred in the absence of base (entry 8) or with DBU in THF (entry 9) under otherwise analogous conditions.

The potential of catalyst **2** was then further explored under milder reaction conditions. At first, the effect of lower total pressure was determined. In the presence of 0.1 mol % of **2** a TON of 480 was reached after 21 h at 80 °C under only 8.5 bar of H₂/CO₂ (1/1) (Table 3, entry 10), an activity comparable to that of other known iron pincer catalysts.^{4d,f} Then, temperature effects were studied. At 25 °C, catalyst **2** manifested a remarkable catalytic activity, affording sodium formate in high yields⁶ with a TON of 856 after 21 h and of 1032 after 72 h under 80 bar initial pressure (entries 11 and 12) in the presence of 0.1 mol % catalyst. To the best of our knowledge, these are the highest TONs obtained for Fe-catalyzed CO₂ hydrogenation at room temperature to date.

Finally, the effect of catalyst loading was studied. At lower catalyst loading (0.01 mol %) sodium formate was still obtained in excellent yield (98%) with a TON of 9840 after 21 h at 80

Table 3. Hydrogenation of CO₂ to Formate with **2 using Different Solvents and Bases^a**

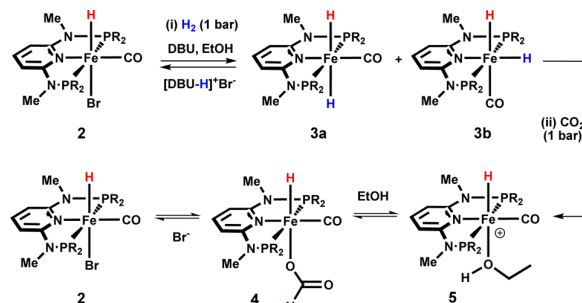
entry	amt of cat. 2 (mol %)	base	solvent	T (°C)	TON ^f	yield ^g (%)
1	0.08	NaOH	H ₂ O/THF	80	680	54
2 ^b	0.04	NaOH	H ₂ O/THF	80	372	15
3	0.08	NaOH	MeOH	80	220	18
4	0.08	NaOH	EtOH	80	654	53
5	0.08	DBU	EtOH	80	1153	92
6	0.08	DMOA	EtOH	80	452	36
7	0.08	NEt ₃	EtOH	80	686	55
8	0.08		EtOH	80	0	0
9	0.08	DBU	THF	80	0	0
10 ^{c,d}	0.1	DBU	EtOH	80	480	48
11 ^c	0.1	DBU	EtOH	25	856	86
12 ^{c,e}	0.1	DBU	EtOH	25	1032	103
13 ^{c,f}	0.01	DBU	EtOH	80	9840	98
14	0.01	DBU	EtOH	25	465	5
15	0.005	DBU	EtOH	80	10275	21
16 ^{c,g}	0.001	DBU	EtOH	80	5000	5
17 ^{c,h}	0.01	DBU	EtOH	80	620	6
18 ^a		DBU	EtOH	80	0	0
19 ^k	0.08	DBU	EtOH	80	1163	93

^aGeneral reaction conditions: 12.5 mmol of base, 0.01 mmol of catalyst, 25.0 mL of solvent, 21 h. ^b25.0 mmol of base. ^c10.0 mmol of base. ^d8.5 bar (CO₂/H₂ = 1/1) total pressure. ^e72 h. ^f0.001 mmol of catalyst. ^g0.0001 mmol of catalyst. ^hIn the presence of LiOTf as Lewis acid additive, DBU/LiOTf = 7.5. ⁱTON = (mmol of formate)/(mmol of catalyst). ^jYields calculated from the integration of ¹H NMR signals due to NaHCO₃, using DMF as internal standard. ^kAs for footnote a, Hg(0) added.

°C (Table 3, entry 13), whereas a TON of 465 was achieved at 25 °C after 21 h at 80 bar (entry 14). On further reduction of the catalyst loading to 0.005 mol %, CO₂ hydrogenation to formate was still achieved with a high TON of 10275, albeit in low yield with respect to the base (21%, entry 15). Lowering the catalyst amount further (0.001 mol %) under the same conditions resulted in a lower TON of 5000 (entry 16). We also tested the effect of additives at high substrate to catalyst ratios. Surprisingly, in contrast to what was observed by Hazari et al.,^{4c} the use of a LA cocatalyst such as LiOTf negatively affected the performance (entry 17). Colloidal metal catalysis was ruled out by carrying out a Hg poisoning test, which gave results comparable to those observed in the original run (entry 19 vs 5).

Mechanistic Studies. In order to gain insights into the reaction mechanism, the reactivity of complex **2** was investigated in stoichiometric reactions by NMR techniques. Exposure of an EtOH solution of **2** to H₂ (1 bar) in the presence of KOtBu resulted in the quantitative formation of dihydrides **3a,b** (cis and trans isomers).^{5c,7} The ³¹P{¹H} NMR spectrum exhibits two singlets at 187.5 ppm (**3a**) and 189.9 ppm (**3b**), while the ¹H NMR exhibits a triplet at -9.57 ppm for **3a** and a broad resonance at -13.86 ppm for **3b**. When the temperature is lowered to -50 °C, the broad signal starts to split into two separate triplets centered at -8.82 and -17.64 ppm.⁷ Using DBU as base, NMR analysis revealed that only 40% of **2** was converted into the Fe(II) dihydrides **3**, even after prolonged standing under an hydrogen atmosphere, suggesting that **2** and **3** are in equilibrium with each other (Scheme 2, step

i). This may be explained by the lower pK_a value of [DBU-H]⁺ in comparison to that of tBuOH.⁸

Scheme 2. Stepwise Reaction of **2 with H₂ (i) and CO₂ (ii) in the Presence of DBU as Base in EtOH**

Next, the EtOH/base solution containing in situ formed **3** was stirred under an atmosphere of CO₂ for 30 min. Regardless of the base used, we observed the formation of the hydrido formate complex [Fe(PNP^{Me}-iPr)(H)(CO)(η¹-O₂CH)] (**4**; Scheme 2, step ii) characterized by a triplet at -24.71 ppm for the hydride and a singlet at 7.96 ppm for the proton of the formate ligand, which both integrate to 1 in the ¹H NMR spectrum (see the Supporting Information).

Under these reaction conditions, **4** is in equilibrium with **2** due to the presence of bromide anions in solution. As a result, a broad signal at 8.65 ppm due to free formate salt appeared in the corresponding ¹H NMR spectrum. In addition, the cationic hydride complex [Fe(PNP^{Me}-iPr)(H)(CO)(EtOH)]⁺ (**5**) was present (Scheme 2), exhibiting a ¹H NMR triplet resonance at -25.57 ppm. The ³¹P{¹H} NMR chemical shift of **5** is very close to that of formate complex **4**. However, no signal for the free formate counteranion could be found in the ¹H spectrum of **5**. It is worth noting that complex **5** was independently synthesized by treatment of **2** with silver salts in EtOH.⁷ In a separate experiment, stirring a mixture of **2** and sodium formate (4 equiv) in EtOH for 1 h also affords a mixture of **2**, **4**, and **5**. In another experiment, this time starting from isolated **3**, the reaction with CO₂ in EtOH afforded **5** with minor traces of **4**. Evidently, the formate ligand is easily displaced by an excess of solvent under these conditions.

Single crystals of **4** suitable for X-ray diffraction analysis were obtained by slow diffusion of pentane into a concentrated solution of the complex in THF under an atmosphere of CO₂. The solid-state structure of **4** confirms the geometry proposed on the basis of NMR data. A structural view is depicted in Figure 1 with selected bond distances given in the caption. Complex **4** adopts a distorted-octahedral geometry around the metal center with the formate and hydride ligands trans to each other and in positions cis to the CO ligand. The hydride could be unambiguously located in the difference Fourier maps. The Fe-H distance was refined to 1.46(2) Å.

On the basis of the experimental evidence, a catalytic cycle for CO₂ hydrogenation starting from **2** can be proposed, encompassing formation of dihydrides **3** and CO₂ insertion to give the hydrido formate complex **4** followed by hydrogenolysis and formate elimination giving back **3** in the presence of base. Solvent-assisted formate decoordination in **4** may occur to leave a highly reactive, unobserved pentacoordinate cationic Fe(II) hydrido carbonyl species, which can be stabilized by EtOH coordination to give **5**, observed by NMR (Scheme 3).

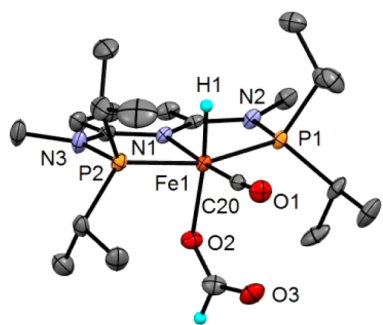
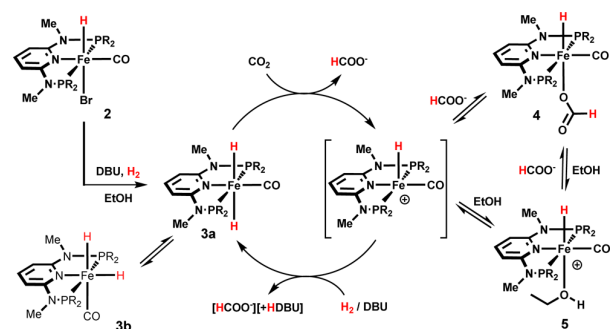


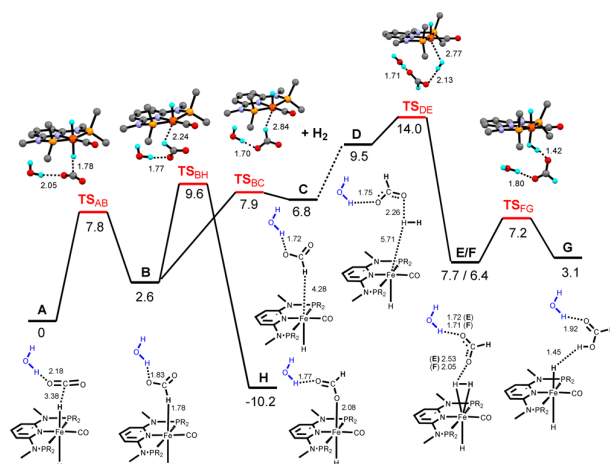
Figure 1. Structural view of **4** showing 50% thermal ellipsoids (most H atoms and a second independent complex omitted for clarity). Selected bond lengths (Å) and angles (deg): Fe1–P1 2.1765(7), Fe1–P2 2.1789(7), Fe1–N1 2.004(2), Fe1–C20 1.737(2), Fe1–O2 2.032(2), Fe1–H1 1.46(2); P1–Fe1–P2 162.57(2), N1–Fe1–C20 175.58(8).

Scheme 3. Proposed Catalytic Cycle for CO₂ Hydrogenation with **3a**



Further mechanistic details on the CO₂ hydrogenation mechanism were obtained by DFT calculations using **3a** as the initial active species. The free energy profile is shown in Scheme 4. Computational details are presented as Supporting Information. The model used in the calculations included one

Scheme 4. Free Energy Profile Calculated (DFT) for the Hydrogenation of CO₂ Catalyzed by **3a** (Denoted as A)⁴



⁴The free energy values (kcal/mol) are referenced to the initial reactants, and relevant distances (Å) are indicated.

explicit water molecule that provides H-bond stabilization of the intermediates. The highlights of the calculated mechanism are presented in Scheme 4 with relevant intermediates and the corresponding free energy values.⁹

In the first step of the calculated mechanism, from **A** to **B**, the hydride attack from complex **3a** to a CO₂ molecule results in a H-bonded formate complex. This is a facile process with a barrier of 7.8 kcal/mol. In the resulting intermediate (**B**) the formate ion is stabilized by a H-bond with the water molecule. From **B**, formate can coordinate the metal, giving complex **4** (**H** in Scheme 4), where the formate ligand is bonded through the O atom. This intermediate represents the potential well of the mechanism; thus, it may be viewed as the catalyst resting state. Alternatively, the formate ion dissociates from the metal in **B** to give **C**, opening one coordination position that is occupied by a molecule of H₂ in the following step. Both processes are competitive with barriers within 2 kcal/mol. The reaction pathway proceeds with H₂ addition to **C**, yielding the dihydrogen complex **F**. This process has an energy barrier of 14 kcal/mol, corresponding to the highest barrier of the entire mechanism. In the final step, the formate ion is protonated by **F**, regenerating the initial complex **3a** and producing formic acid. Given the excess of base present in the reaction medium under experimental conditions, the acid formed will then be deprotonated in an acid–base reaction that provides the final driving force for the entire process. Importantly, the free formate ion (the reaction product under the experimental conditions) is stabilized by a H bond with the nearby water molecule in intermediates **E**/**F**.⁹ This facilitates the opening of the coordination position that will be used by H₂ in the following step of the mechanism, justifying the need for a protic solvent in the catalytic reaction. A similar reaction mechanism was recently proposed for the selective hydrogenation of aldehydes in EtOH with **3** as catalyst⁷ and by other authors on related systems.¹⁰

CONCLUSIONS

In conclusion, selected Fe(II) pincer-type complexes of 2,6-diaminopyridylbis(diisopropylphosphine) gave high activities as catalysts for CO₂ and NaHCO₃ reduction to formate under very mild to moderate conditions, even at room temperature. Mechanistic details were obtained by NMR techniques, highlighting the role of dihydride and hydrido formate complexes. DFT calculations indicate an outer-sphere mechanism with a hydrido formate complex as the catalyst resting state and suggest that the overall reaction is pushed forward by the acid–base reaction between the product (formic acid) and the excess base present in solution. Protic solvents promote catalysis by stabilizing the reaction intermediates and assisting formate elimination from the coordination sphere of the metal.

ASSOCIATED CONTENT

Supporting Information

The Supporting Information is available free of charge on the ACS Publications website at DOI: 10.1021/acscatal.6b00416.

General materials and methods, synthetic procedures, NMR experiments and spectra, Cartesian coordinates of the computed structures, crystallographic data for the X-ray structure of **4**, and additional catalytic data (PDF) Crystallographic data for the X-ray structure of **4** (CIF)

AUTHOR INFORMATION

Corresponding Authors

*E-mail for K.K.: karl.kirchner@tuwien.ac.at.

*E-mail for L.G.: l.gonsalvi@iccom.cnr.it.

Notes

The authors declare no competing financial interest.

ACKNOWLEDGMENTS

Financial contributions by the CNR and ECRF through projects EFOR and HYDROLAB-2.0, respectively, are gratefully acknowledged. This work was also supported by COST Action CM1205 CARISMA (Catalytic Routines for Small Molecule Activation). L.F.V. acknowledges the Fundação para a Ciência e Tecnologia, grant UID/QUI/00100/2013. N.G. and K.K. gratefully acknowledge financial support by the Austrian Science Fund (FWF) (Project No. P24583-N28).

REFERENCES

- (1) (a) Joó, F. *ChemSusChem* **2008**, *1*, 805–808. (b) Enthaler, S.; von Langermann, J.; Schmidt, T. *Energy Environ. Sci.* **2010**, *3*, 1207–1217. (c) Loges, B.; Boddien, A.; Gärtner, F.; Junge, H.; Beller, M. *Top. Catal.* **2010**, *53*, 902–914.
- (2) (a) Papp, G.; Csorba, J.; Laurenczy, G.; Joó, F. *Angew. Chem., Int. Ed.* **2011**, *50*, 10433–10435. (b) Boddien, A.; Gärtner, F.; Federsel, C.; Sponholz, P.; Mellmann, D.; Jackstell, R.; Junge, H.; Beller, M. *Angew. Chem., Int. Ed.* **2011**, *50*, 6411–6414.
- (3) Wang, W.-H.; Himeda, Y.; Muckerman, J. T.; Manbeck, G. F.; Fujita, E. *Chem. Rev.* **2015**, *115*, 12936–12973.
- (4) (a) Federsel, C.; Boddien, A.; Jackstell, R.; Jennerjahn, R.; Dyson, P. J.; Scopelliti, R.; Laurenczy, G.; Beller, M. *Angew. Chem., Int. Ed.* **2010**, *49*, 9777–9780. (b) Ziebart, C.; Federsel, C.; Anbarasan, P.; Jackstell, R.; Baumann, R.; Spannenberg, W. A.; Beller, M. *J. Am. Chem. Soc.* **2012**, *134*, 20701–20704. (c) Bertini, F.; Mellone, I.; Ienco, A.; Peruzzini, M.; Gonsalvi, L. *ACS Catal.* **2015**, *5*, 1254–1265. (d) Langer, R.; Diskin-Posner, Y.; Leitus, G.; Shimon, L. J. W.; Ben-David, Y.; Milstein, D. *Angew. Chem., Int. Ed.* **2011**, *50*, 9948–9952. (e) Zhang, Y.; MacIntosh, A. D.; Wong, J. L.; Bielinski, E. A.; Williard, P. G.; Mercado, B. Q.; Hazari, N.; Bernskoetter, W. *Chem. Sci.* **2015**, *6*, 4291–4299. (f) Rivada-Wheelaghan, O.; Dauth, A.; Leitus, G.; Diskin-Posner, Y.; Milstein, D. *Inorg. Chem.* **2015**, *54*, 4526–4538.
- (5) (a) Bichler, B.; Glatz, M.; Stöger, B.; Mereiter, K.; Veiros, L. F.; Kirchner, K. *Dalton Trans* **2014**, *43*, 14517–15419. (b) de Aguiar, S. R. M. M.; Öztöpcü, Ö.; Stöger, B.; Mereiter, K.; Veiros, L. F.; Pittenauer, E.; Allmaier, G.; Kirchner, K. *Dalton Trans* **2014**, *43*, 14669–14679. (c) Gorgas, N.; Stöger, B.; Veiros, L. F.; Pittenauer, E.; Allmaier, G.; Kirchner, K. *Organometallics* **2014**, *33*, 6905–6914. (d) Bichler, B.; Holzhaecker, C.; Stöger, B.; Puchberger, M.; Veiros, L. F.; Kirchner, K. *Organometallics* **2013**, *32*, 4114–4121. (e) Benito-Garagorri, D.; Becker, E.; Wiedermann, J.; Lackner, W.; Pollak, M.; Mereiter, K.; Kisala, J.; Kirchner, K. *Organometallics* **2006**, *25*, 1900–1913. (f) Benito-Garagorri, D.; Wiedermann, J.; Pollak, M.; Mereiter, K.; Kirchner, K. *Organometallics* **2007**, *26*, 217–222. (g) Benito-Garagorri, D.; Puchberger, M.; Mereiter, K.; Kirchner, K. *Angew. Chem., Int. Ed.* **2008**, *47*, 9142–9145.
- (6) Over-quantitative yields of formate have been reported with DBU as base; see: Hsu, S.-F.; Rommel, S.; Eversfield, P.; Müller, K.; Klemm, E.; Thiel, W. R.; Plietker, B. *Angew. Chem., Int. Ed.* **2014**, *53*, 7074–7078. See also ref 4e and references cited therein.
- (7) Gorgas, N.; Stöger, B.; Veiros, L. F.; Kirchner, K. *ACS Catal.* **2016**, *6*, 2664–2672.
- (8) The pK_a for DBU is ca. 11.5–11.9; see: Kaupmees, K.; Trummal, A.; Leito, I. *Croat. Chem. Acta* **2014**, *87*, 385–395. The pK_a for *t*BuOH in water is 17.
- (9) Free energy values were obtained at the B3LYP/VDZP level using the Gaussian 09 package. All calculations included solvent effects (THF) using the PCM/SMD model. A full account of the

computational details and a complete list of references are provided as Supporting Information.

(10) Yang, X. *Inorg. Chem.* **2011**, *50*, 12836–12843.

SUPPORTING INFORMATION

Efficient and Mild Carbon Dioxide Hydrogenation to Formate Catalyzed by Fe(II) Hydridocarbonyl Complexes bearing 2,6-(diaminopyridyl)diphosphine Pincer Ligands

Federica Bertini,^a Nikolaus Gorgas,^b Berthold Stöger,^c Maurizio Peruzzini,^a Luis F. Veiros,^d Karl Kirchner^{*,b} and Luca Gonsalvi.^{*,a}

^a Consiglio Nazionale delle Ricerche (CNR), Istituto di Chimica dei Composti Organometallici (ICCOM), Via Madonna del Piano 10, 50019 Sesto Fiorentino, Italy. E-mail: l.gonsalvi@iccom.cnr.it.

^b Institute of Applied Synthetic Chemistry, Vienna University of Technology, Getreidemarkt 9/163-AC, A-1060 Wien, Austria. E-mail: karl.kirchner@tuwien.ac.at.

^c Institute of Chemical Technologies and Analytics, Vienna University of Technology, Getreidemarkt 9/163-AC, A-1060 Wien, Austria.

^d Centro de Química Estrutural, Instituto Superior Técnico, Universidade de Lisboa, Av. Rovisco Pais No. 1, 1049-001 Lisboa, Portugal.

1. GENERAL METHODS AND MATERIALS
2. SYNTHETIC PROCEDURES, NMR EXPERIMENTS AND RELATED SPECTRA
3. COMPUTATIONAL DETAILS AND ATOMIC COORDINATES
4. X-RAY CRYSTAL STRUCTURE DATA COLLECTION
5. ADDITIONAL TABLE FOR CATALYTIC TESTS
6. REFERENCES

1. General Methods and Materials

All syntheses were performed using standard Schlenk techniques under an atmosphere of dry nitrogen or argon. Complexes **1-3** were synthesized following literature procedures.^{1,2} Solvents were freshly distilled over appropriate drying agents, collected over Linde type 3Å or 4Å molecular sieves under nitrogen, and degassed with nitrogen or argon gas. Deuterated solvents for NMR measurements were purchased from commercial suppliers and stored onto activated 4Å molecular sieves under Ar before use. The ¹H, ¹³C{¹H}, and ³¹P{¹H} NMR spectra were recorded on a Bruker AVANCE-250 spectrometer (operating at 250.13, 101.26, and 62.90 MHz, respectively), on a Bruker Avance II 300 spectrometer (operating at 300.13, 75.47, and 121.50 MHz, respectively) and a Bruker Avance II 400 spectrometer (operating at 400.13, 100.61, and 161.98 MHz, respectively) at room temperature. Peak positions are relative to tetramethylsilane and were calibrated against the residual solvent resonance (¹H) or the deuterated solvent multiplet (¹³C). ³¹P{¹H} NMR were referenced to 85% H₃PO₄, with the downfield shift taken as positive. Infrared spectra were measured on an ATR crystal using a Bruker Tensor 27 mid-range FTIR spectrophotometer. X-ray single crystal diffraction data at T = 298 K were obtained on a Bruker KAPPA APEX CCD diffractometer using graphite monochromatized Mo K_α radiation.

2. Synthetic procedures, NMR experiments and related spectra

2a. Synthesis of [Fe(PNP^{Me}-iPr)(H)(CO)(η¹-O₂CH)] (4**).** A Schlenk tube equipped with a septum and a stirring bar was charged with **3** (80 mg, 0.15 mmol) dissolved in THF (2.0 mL). The solution was purged with carbon dioxide (1 bar) for 5 min and stirred for additional 20 min under an atmosphere of CO₂. The solution was filtered and the product was precipitated by addition of *n*-pentane (8.0 mL). The solvent was decanted, the residue washed three times with small portions of *n*-pentane and briefly dried under high vacuum to afford **4** as a yellow powder. Yield: 68 mg (91%). Crystals were grown by slow diffusion of *n*-pentane into a concentrated solution of **4** in THF under an atmosphere of CO₂. In absence of carbon dioxide, **4** is slowly converted into the corresponding dihydride complex **3**. Therefore, **4** was stored and handled under an atmosphere of carbon dioxide including its characterization by NMR spectroscopy. ¹H NMR (δ, benzene-*d*₆, 20°C, Figure S4): 8.92 (s, 1H, HCO₂), 7.03 (t, *J*_{HH} = 8.2 Hz, 1H, py⁴), 5.58 (d, *J*_{HH} = 8.2 Hz, 2H, py^{3,5}), 2.38 (t, *J*_{HP} = 1.6 Hz, 6H, NCH₃), 2.35–2.25 (m, 2H, CH(CH₃)₂), 2.01–1.85 (m, 2H, CH(CH₃)₂), 1.68 (td, *J*_{HP} = 17.3, *J*_{HH} = 7.1 Hz, 6H, CH(CH₃)₂), 1.24–1.15 (m, 12H), 0.70 (td, *J*_{HP} = 13.8, *J*_{HH} = 6.8 Hz, 6H, CH(CH₃)₂), -23.59 (t, *J*_{HP} = 55.2 Hz, 1H, FeH). ¹H{³¹P} NMR (δ, benzene-*d*₆, 20°C, Figure S5): 8.92 (s, 1H), 7.03 (t, *J* = 8.2 Hz, 1H), 5.58 (d, *J* = 8.2 Hz, 2H), 2.38 (s, 6H), 2.31 (hept, *J* = 7.1 Hz, 2H), 1.93 (hept, *J* = 6.8 Hz, 2H), 1.68 (d, *J* = 7.1 Hz, 6H), 1.20 (d, *J* = 6.8 Hz, 6H), 1.19 (d, *J* = 7.1 Hz, 6H), 0.70 (d, *J* = 6.8 Hz, 6H), -23.59 (s, 1H). ¹³C{¹H} NMR (δ, benzene-*d*₆, 20°C, Figure S7): 222.4 (t, *J*_{CP} = 24.3 Hz), 169.8 (s, HCO₂), 163.1 (t, *J*_{CP} = 10.8 Hz, py^{2,6}), 138.5 (s, py⁴), 96.1 (t, *J*_{CP} = 3.3 Hz, py^{3,5}), 32.6 (t, *J*_{CP} = 2.8 Hz, NCH₃), 31.3 (t, *J*_{CP} = 7.5 Hz, CH(CH₃)₂), 30.8 (td, *J*_{CP} = 13.7, *J*_{HP} = 3.8 Hz (hydride residual coupling), CH(CH₃)₂), 19.3 (t, *J*_{CP} = 5.3 Hz, CH(CH₃)₂), 19.2 (s, CH(CH₃)₂), 18.4 (s, CH(CH₃)₂), 18.3 (t, *J*_{CP} = 4.5 Hz, CH(CH₃)₂). ³¹P{¹H} NMR (δ, benzene-*d*₆, 20°C, Figure S6): 165.1 (s). IR (ATR, cm⁻¹): 1915 (ν_{CO}), 1610 (ν_{HCOO}).

2b. In situ formation of 3a and 3b by the reaction of 2 with H₂ in presence of base in EtOH. A 8 mL screw cap vial equipped with a septum and a small stirring bar was charged with **2** (40 mg, 0.075 mmol) and DBU (112 μL, 0.75 mmol) dissolved in EtOH (2.7 mL + 0.3 mL C₆D₆ for NMR deuterium lock). The vial was sealed, the solution purged with hydrogen gas (1 bar) for 5 min and stirred for additional 25 min under an

atmosphere of dihydrogen. A sample (0.5 ml) was taken from the reaction mixture, filtered and analyzed by ^1H and $^{31}\text{P}\{^1\text{H}\}$ NMR spectroscopy (see Figures S8 and S9). The spectra revealed partial conversion (ca. 40%) of **2** into the iron dihydrides **3a** (*cis* isomer) and **3b** (*trans* isomer). The relative intensities of the observed signals did not change after prolonged exposure of the reaction solution to an atmosphere of dihydrogen (1 bar, 1h), indicating reversibility of this reaction. Selected proton resonances (δ , EtOH/ C_6D_6 , 20°C): -9.57 (t, $J_{\text{PH}} = 42.2$ Hz, FeH_2 of **3a**), -13.91 (br, FeH_2 of **3b**), -22.45 (t, $J_{\text{PH}} = 58.1$ Hz, FeH of **2**). $^{31}\text{P}\{^1\text{H}\}$ NMR (δ , EtOH/ C_6D_6 , 20°C): 189.9 (s, **3b**), 187.5 (s, **3a**), 163.24 (s, **2**). Approx. rel. ratio: **3a** (14%), **3b** (29%), **2** (57%). An analogous experiment using KOtBu instead of DBU gave quantitative formation of **3**.

2c. Reaction of the *in situ* formed mixture containing **3a and **3b** with CO_2 in EtOH.** The above prepared solution was purged with carbon dioxide for 5 min and stirred under for additional 25 min under an atmosphere of CO_2 . Again, a sample was taken (0.5 mL), filtered and analyzed by ^1H and $^{31}\text{P}\{^1\text{H}\}$ NMR spectroscopy. The spectra showed disappearance of **3a/3b**, the presence of the hydride complexes **2**, **4** and **5** as well as the formation of free formate salt (see Figures S10 and S11). Approx. rel. ratio: **2** (78%), **4** (18%), **2** (4%). Stirring this mixture under an atmosphere of H_2 and CO_2 (1:1, 1bar) for 1h resulted in a significant increase of **4** and free formate relative to **2** and **5** (see Figures S12 and S13). Approx. rel. ratio: **2** (29%), **4** (27%), **2** (44%). Selected proton resonances (δ , EtOH/ C_6D_6 , 20°C): -25.57 (t, $J_{\text{PH}} = 56.6$ Hz, FeH of **5**), -24.71 (t, $J_{\text{PH}} = 56.1$ Hz, FeH of **4**), -22.40 (t, $J_{\text{PH}} = 58.1$ Hz, FeH of **2**), 7.96 (s, HCO_2 of **4**), 8.65 (br, free formate salt). $^{31}\text{P}\{^1\text{H}\}$ NMR (δ , EtOH/ C_6D_6 , 20°C): 189.9 (s, **3b**), 187.5 (s, **3a**), 163.24 (s, **2**).

2d. Reaction of **2 with sodium formate in EtOH.** To a solution of **2** (15 mg, 0.028 mmol) in EtOH (0.8 mL + 0.2 mL C_6D_6 for NMR deuterium lock) was added HCO_2Na (19 mg, 0.28 mmol) and the resulting orange suspension was stirred for 1h at room temperature. The reaction mixture was filtered and analysed by ^1H and $^{31}\text{P}\{^1\text{H}\}$ NMR spectroscopy. Again, the NMR spectra revealed a mixture of complexes **2**, **4** and **5** together with free formate salt (see Figures S14 and S15). Approx. rel. ratio: **2** (36%), **4** (6%), **5** (58%).

2e. Reaction of isolated **3 with CO_2 in EtOH.** A 8 mL screw cap vial equipped with a septum and a small stirring bar was charged with **3** (15 mg, 0.033 mmol) dissolved in EtOH (2.7 mL + 0.3 mL C_6D_6 for NMR deuterium lock). The vial was sealed, the solution purged with CO_2 (1 bar) for 5 min and stirred for additional 25 min under an atmosphere of CO_2 . The solution was filtered into a NMR tube and analyzed by ^1H and $^{31}\text{P}\{^1\text{H}\}$ NMR spectroscopy (see Figures S16 and S17). The spectra revealed formation of **5** together with trace amounts of **4**.

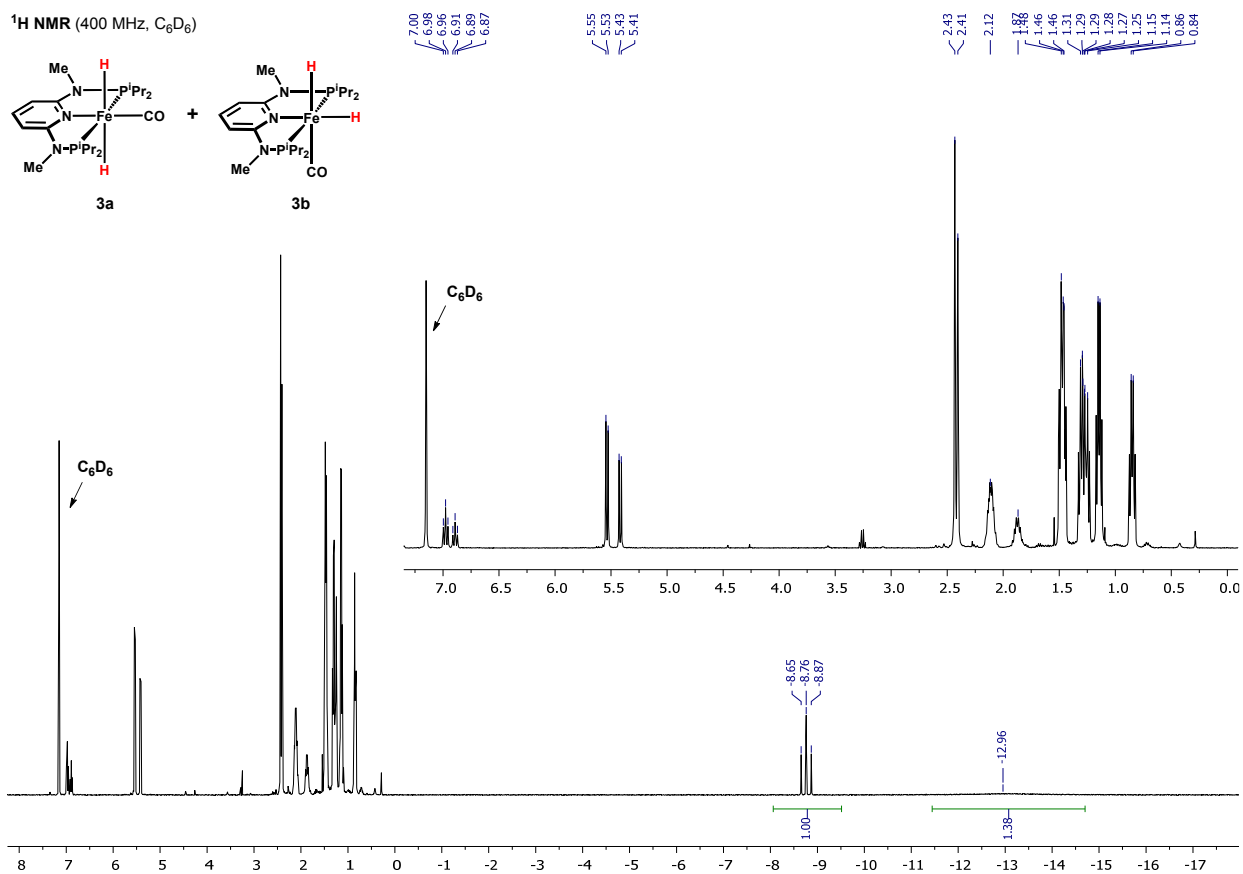


Figure S1. ¹H NMR spectrum of **3**

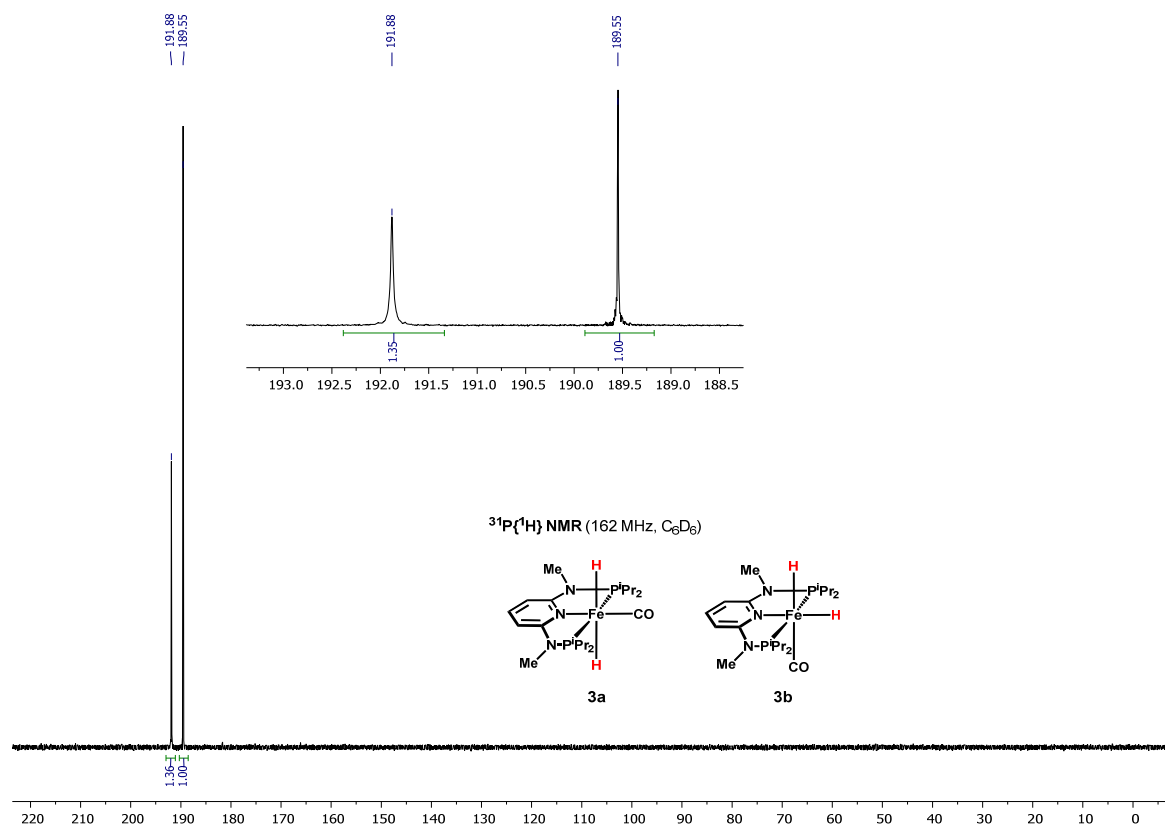


Figure S2. ³¹P{¹H} NMR spectrum of **3**

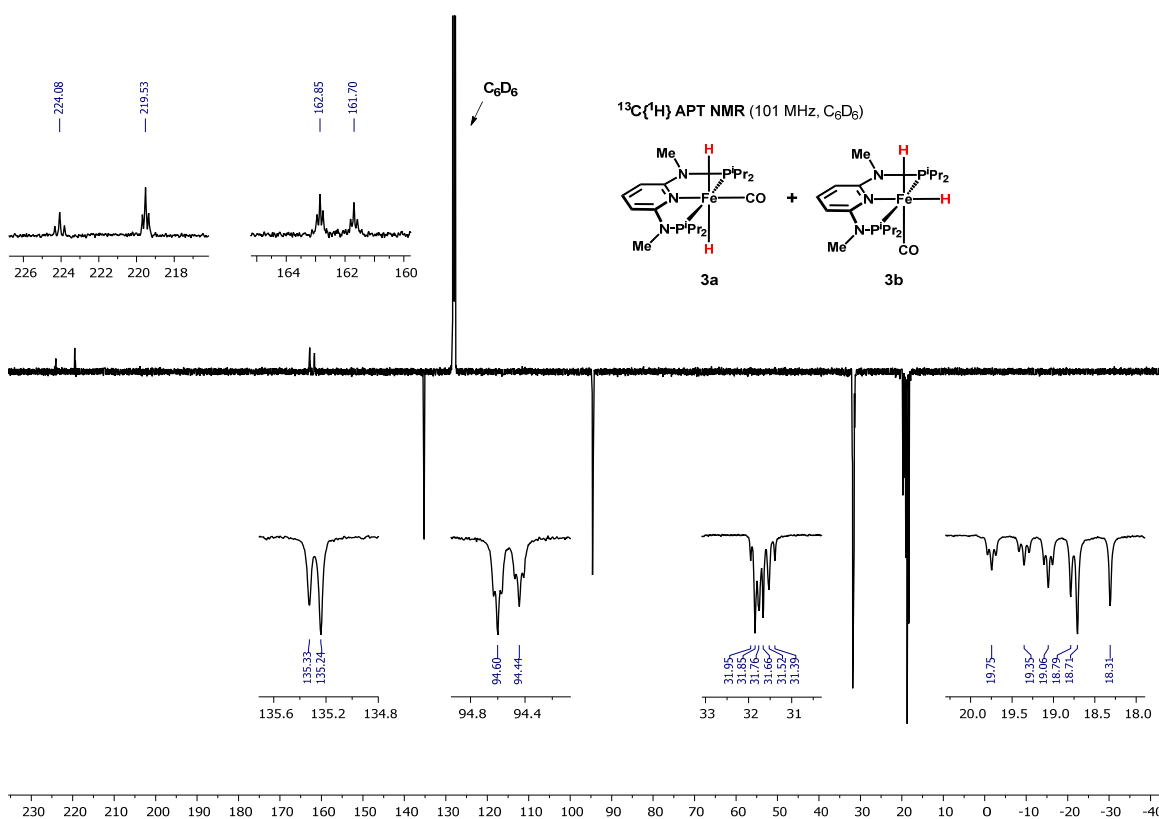


Figure S3. $^{13}\text{C}\{^1\text{H}\}$ APT NMR spectrum of **3**

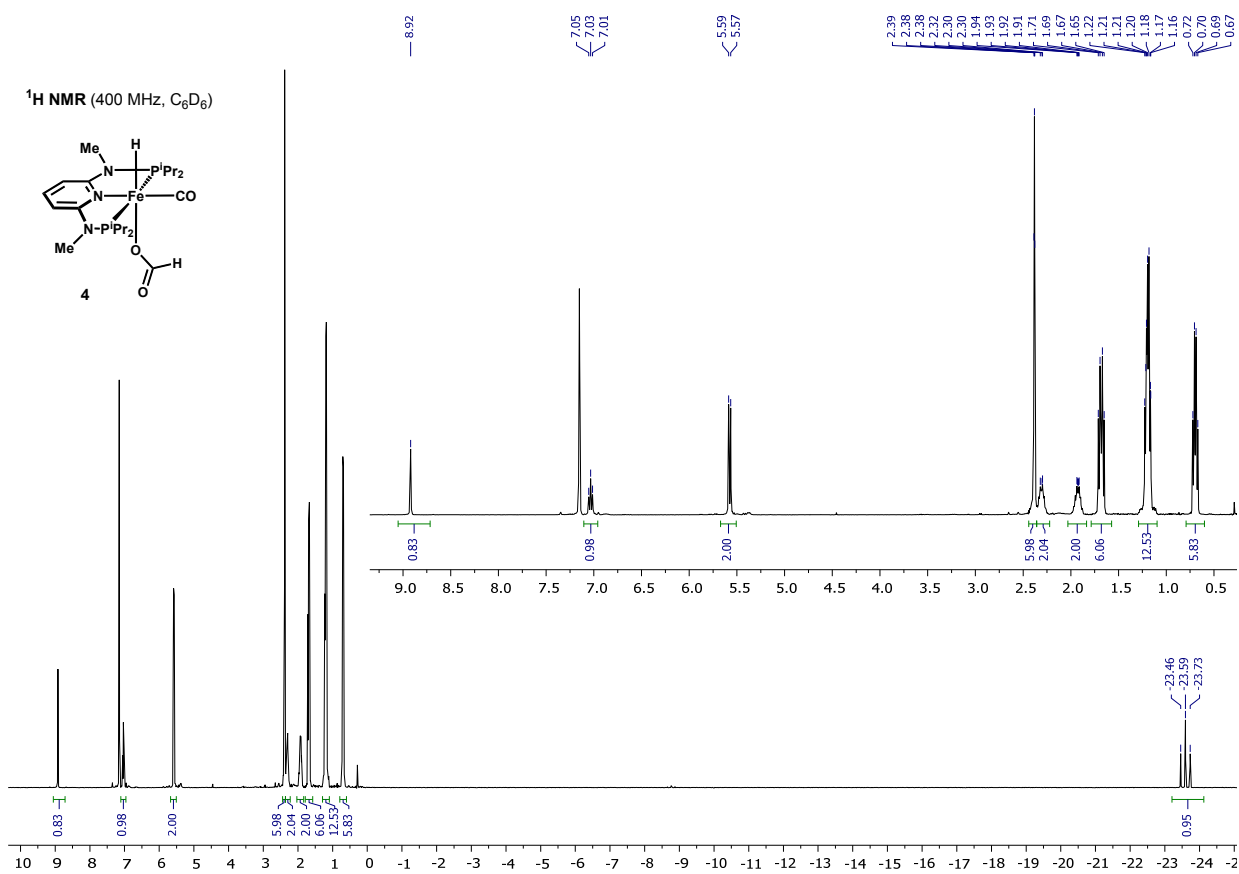


Figure S4. ^1H NMR spectrum of **4**

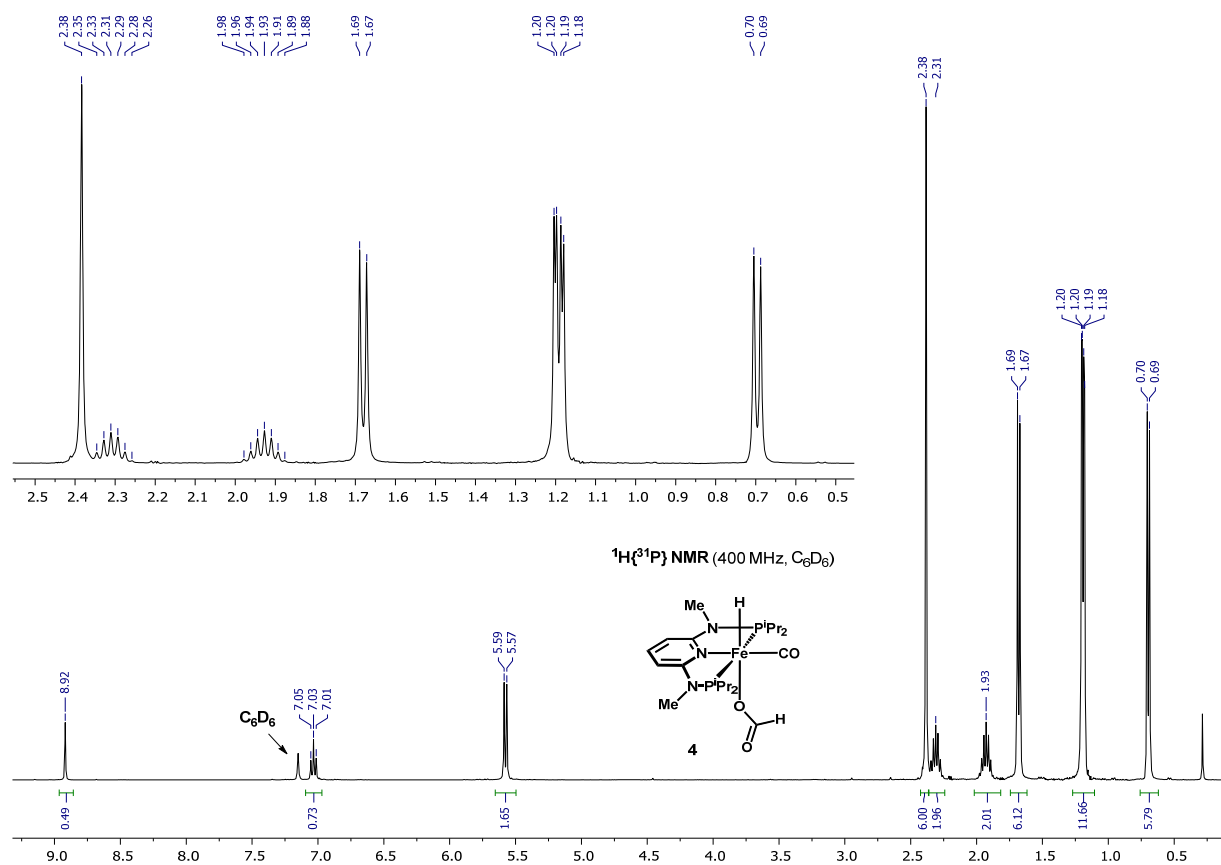


Figure S5. $^1\text{H}\{^{31}\text{P}\}$ NMR spectrum of **4** (positive region)

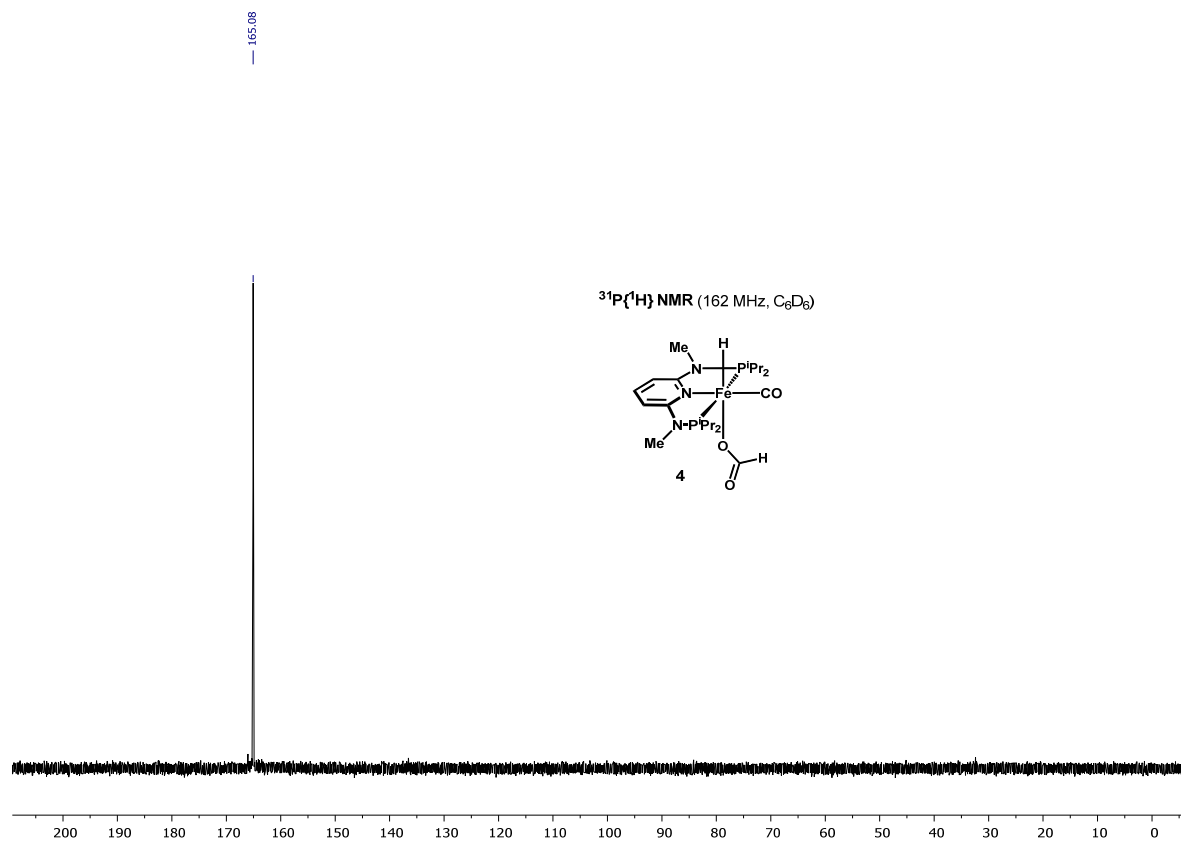


Figure S6. $^{31}\text{P}\{^1\text{H}\}$ NMR spectrum of **4**

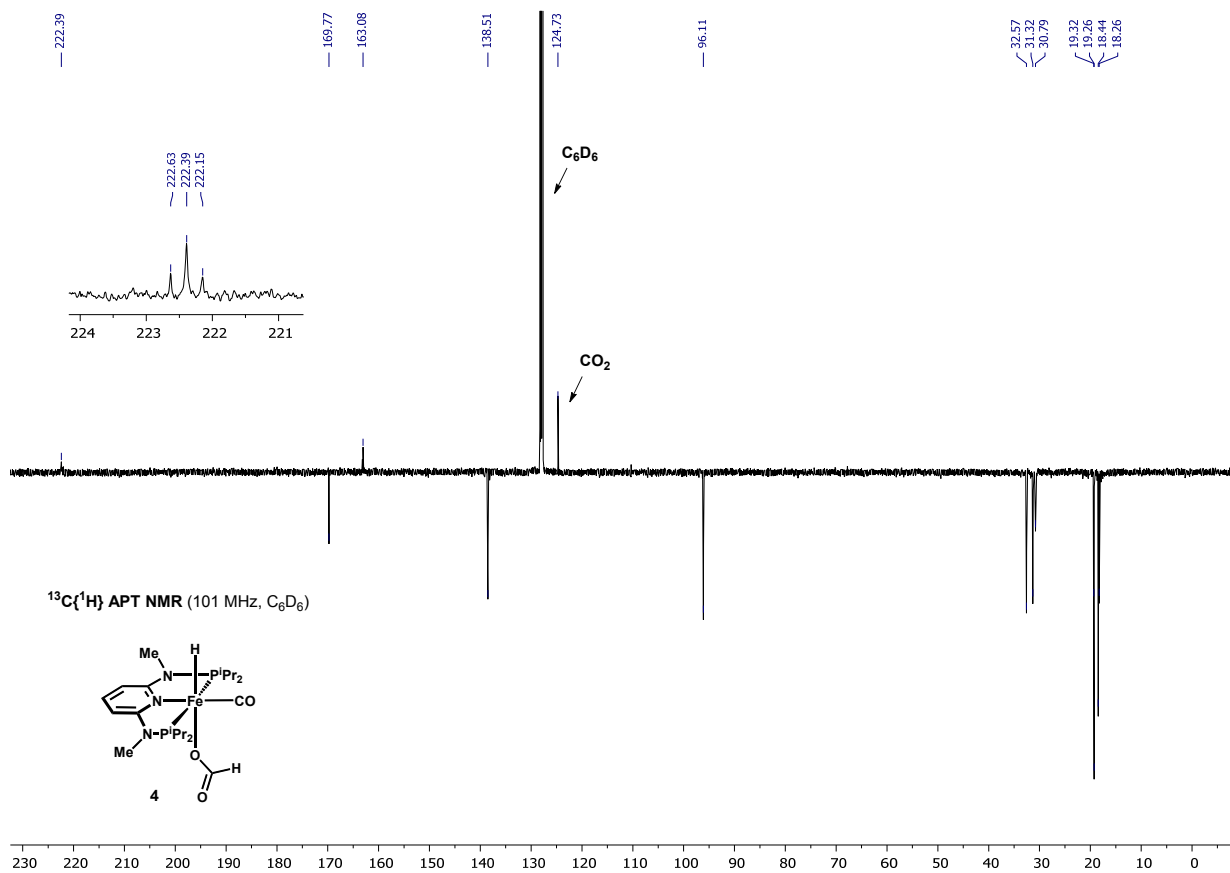


Figure S7. $^{13}\text{C}\{^1\text{H}\}$ APT NMR spectrum of **4**

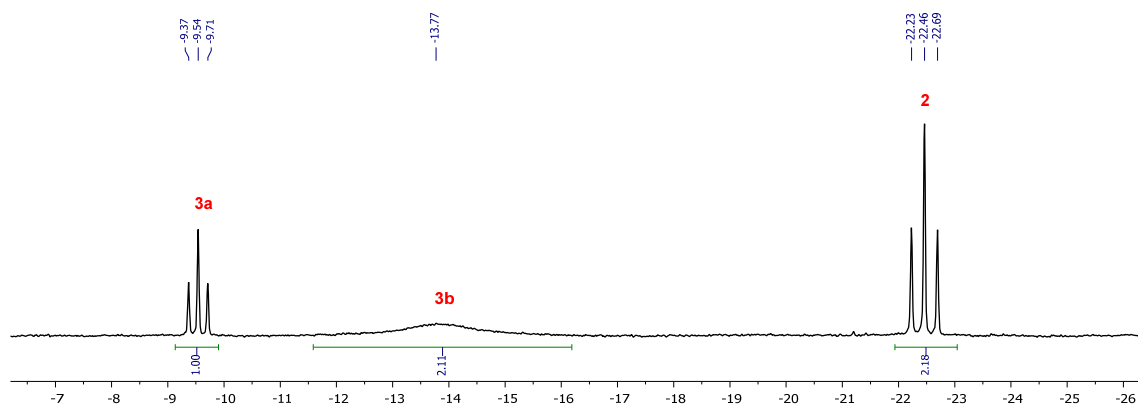


Figure S8. ^1H NMR (250 MHz, 20°C) after reaction of **2** with DBU under H_2

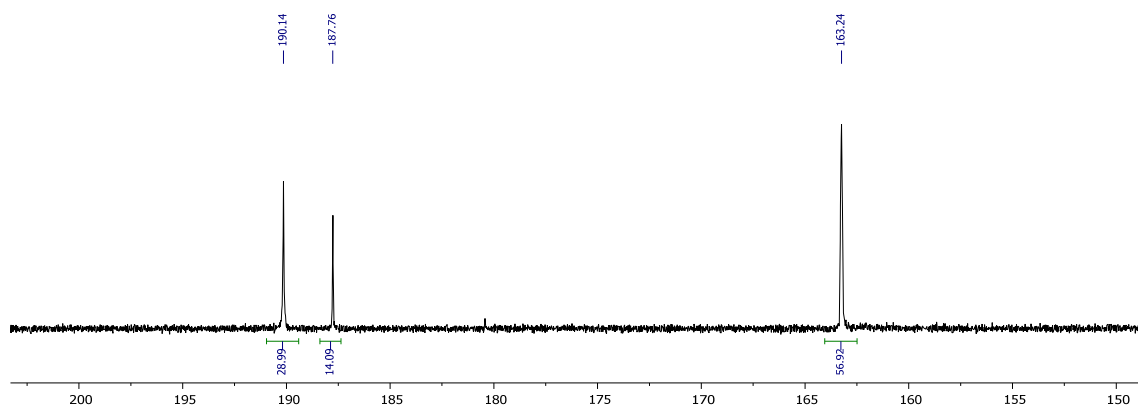


Figure S9. $^{31}\text{P}\{^1\text{H}\}$ NMR (101 MHz, 20°C) after reaction of **2** with DBU under H_2

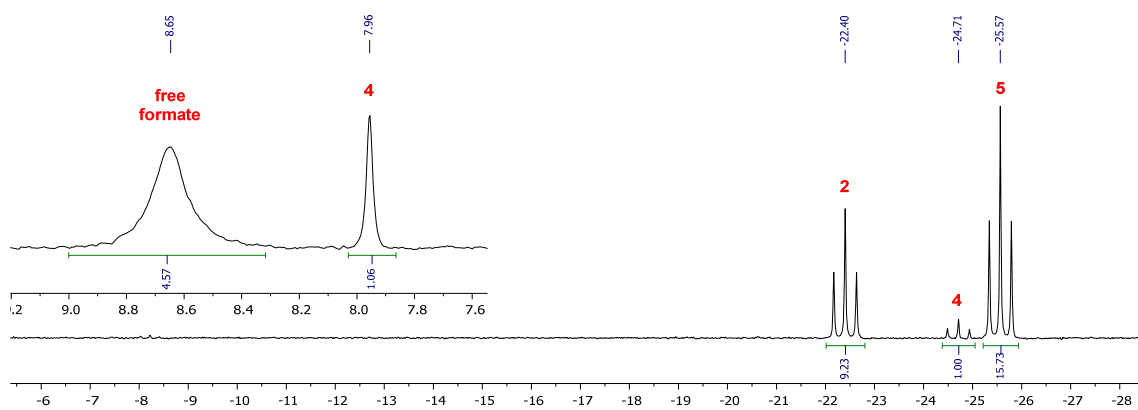


Figure S10. ^1H NMR (250 MHz, 20°C) after reaction of **3a/3b** with CO_2

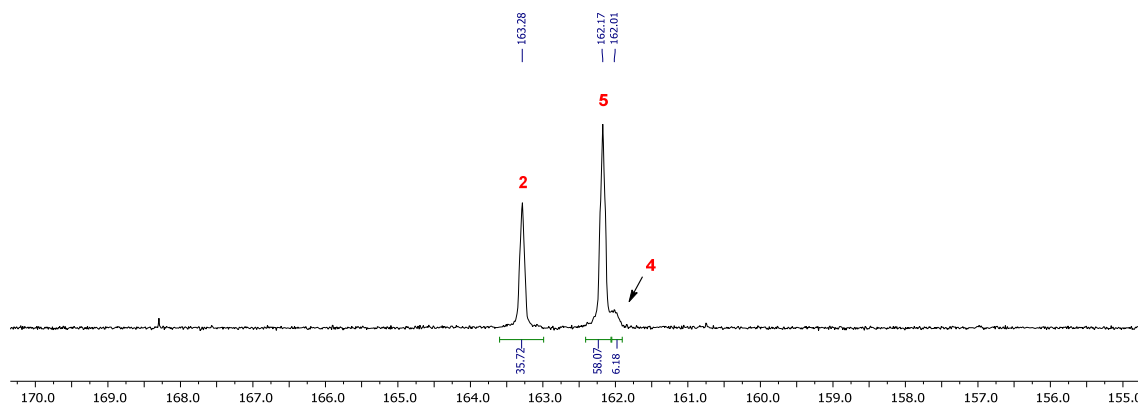


Figure S11. $^{31}\text{P}\{^1\text{H}\}$ NMR (101 MHz, 20°C) after reaction of **3a/3b** with CO_2

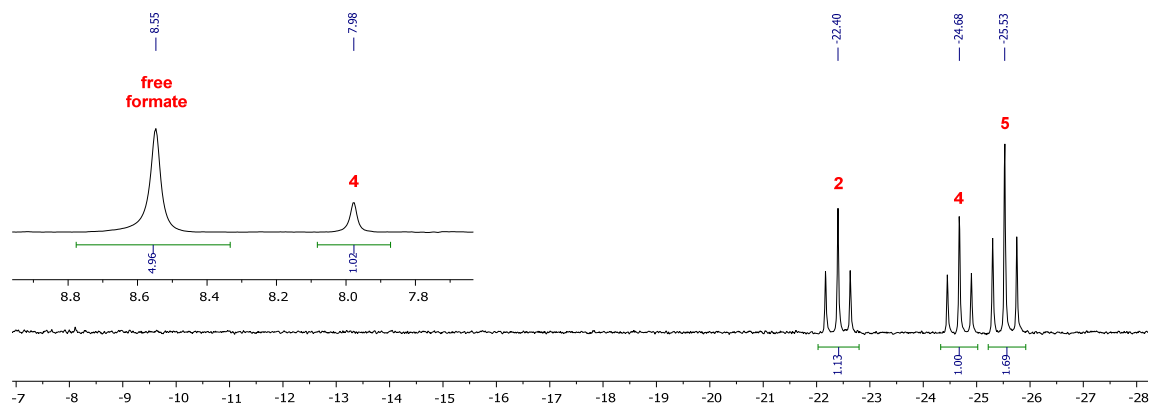


Figure S12. ^1H NMR (250 MHz, 20°C) after reaction of **3a/3b** with H_2/CO_2

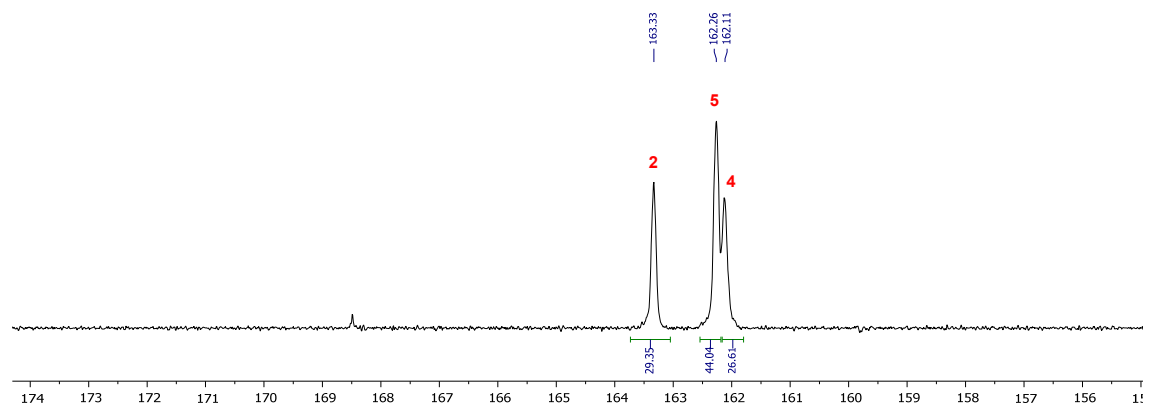


Figure S13. $^{31}\text{P}\{^1\text{H}\}$ NMR (101 MHz, 20°C) after reaction of **3a/3b** with H_2/CO_2

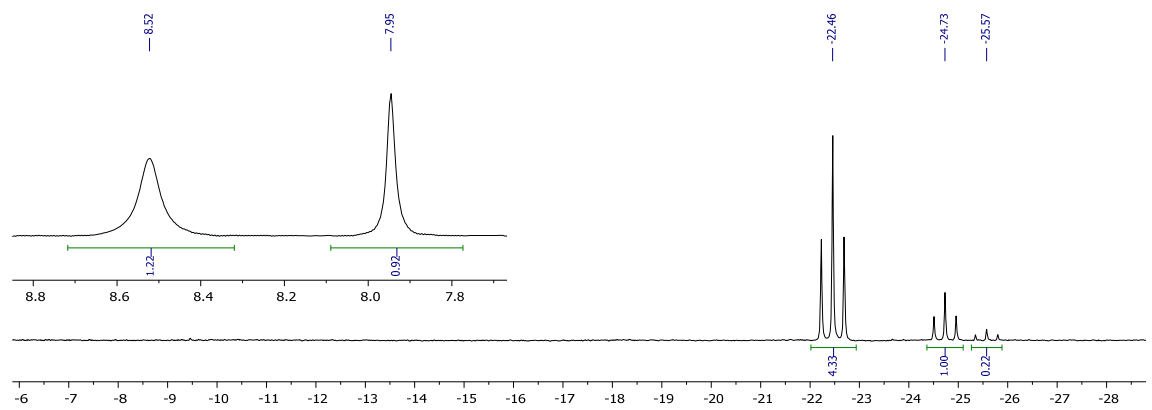


Figure S14. ^1H NMR (250 MHz, 20°C) after reaction of **2** with sodium formate

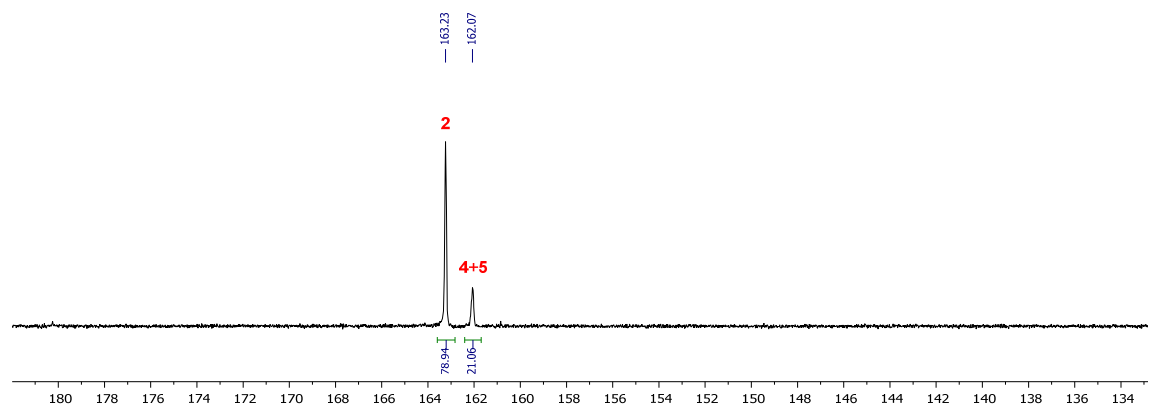


Figure S15. $^{31}\text{P}\{^1\text{H}\}$ NMR (101 MHz, 20°C) after reaction of **2** with sodium formate

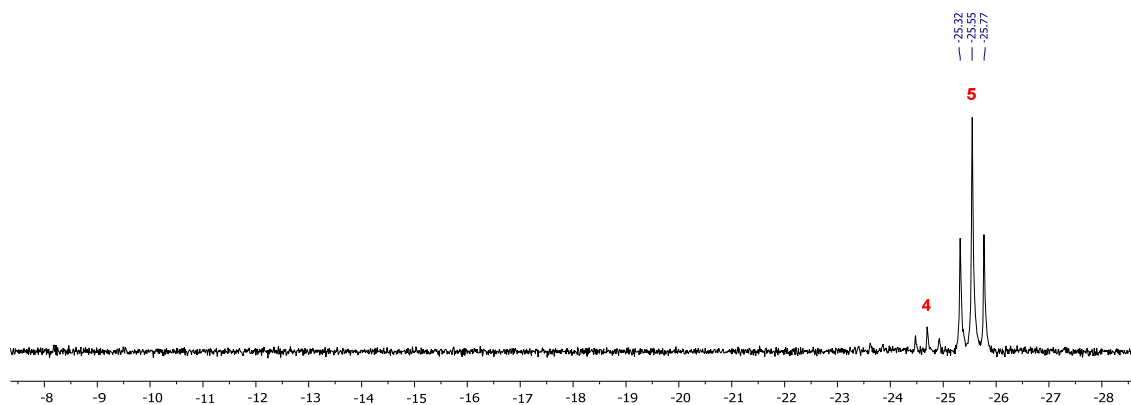


Figure S16. ^1H NMR (250 MHz, 20°C) after reaction of isolated **3** with CO_2 in EtOH

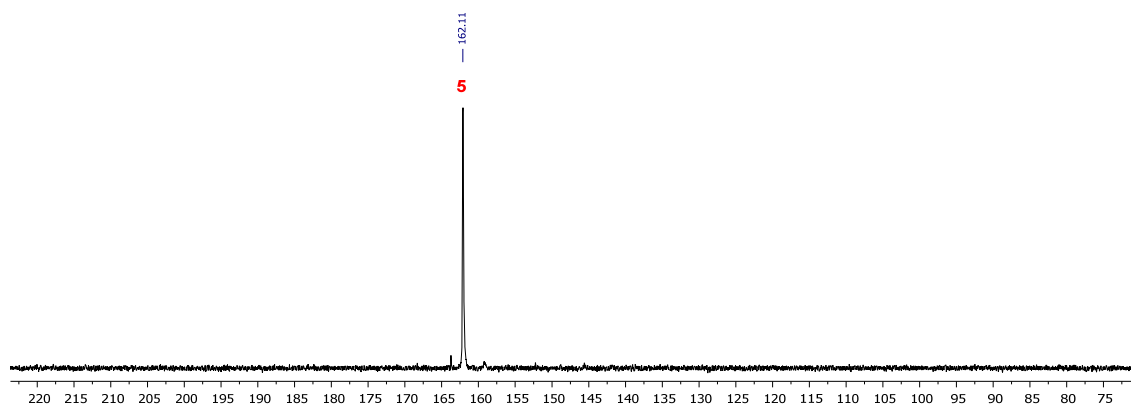


Figure S17. $^{31}\text{P}\{^1\text{H}\}$ NMR (101 MHz, 20°C) after reaction of isolated **3** with CO_2 in EtOH

3. Computational details and atomic coordinates

All calculations were performed using the GAUSSIAN 09 software package³ without symmetry constraints. The optimized geometries were obtained with the B3LYP functional.⁴ That functional includes a mixture of Hartree-Fock⁵ exchange with DFT⁶ exchange-correlation, given by Becke's three parameter functional with the Lee, Yang and Parr correlation functional, which includes both local and non-local terms. The basis set used for the geometry optimizations (basis b1) consisted of the Stuttgart/Dresden ECP (SDD) basis set⁷ to describe the electrons of iron, and a standard 6-31G(d,p) basis set⁸ for all other atoms. Transition state optimizations were performed with the Synchronous Transit-Guided Quasi-Newton Method (STQN) developed by Schlegel *et al.*,⁹ following extensive searches of the Potential Energy Surface. Frequency calculations were performed to confirm the nature of the stationary points, yielding one imaginary frequency for the transition states and none for the minima. Each transition state was further confirmed by following its vibrational mode downhill on both sides and obtaining the minima presented on the energy profiles. The electronic energies (E_{b1}) obtained at the B3LYP/b1 level of theory were converted to free energy at 298.15 K and 1 atm (G_{b1}) by using zero point energy and thermal energy corrections based on structural and vibration frequency data calculated at the same level.

Ethanol coordination

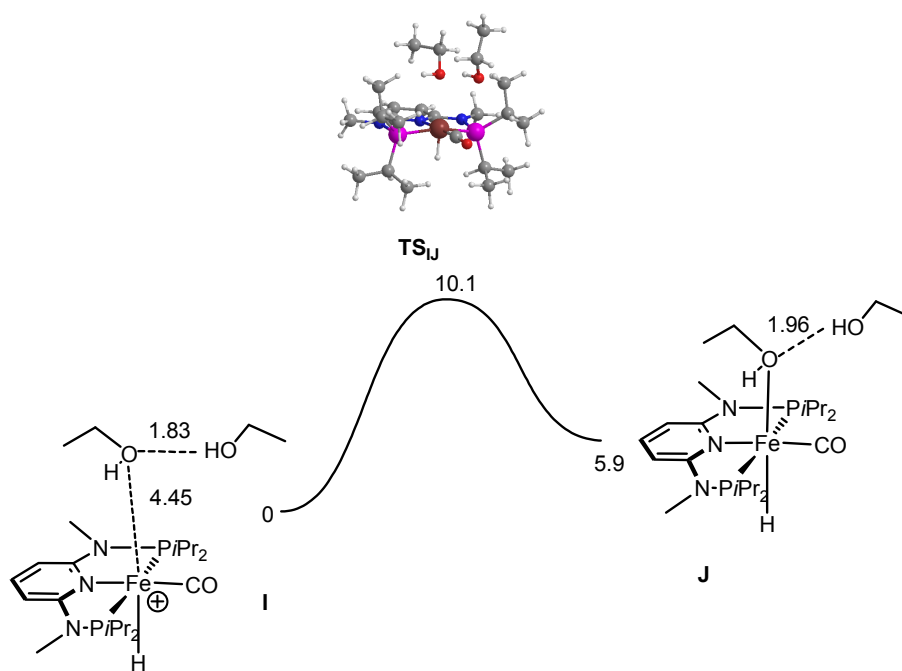


Figure S18. Free energy profile calculated for the coordination of ethanol to the 5-coordinated cation $[\text{Fe}(\text{PNP}^{\text{Me-/iPr}})(\text{H})(\text{CO})]^+$. The free energy values (kcal/mol) are referred to I and relevant distances are presented (\AA).

3.1. Atomic coordinates for all the optimized structures (B3LYP/b1)

H₂				H	-0.243420	4.205365	-2.214260
H	-0.678981	-0.385119	-1.964018	H	-0.106075	4.667290	-0.510603
H	-0.259932	-0.949174	-1.721399	C	-0.535556	3.936775	-1.192083
A				TS_{AB}			
Fe	1.130125	0.065872	0.431157	Fe	0.859358	0.091944	0.617326
O	-3.462692	0.518571	1.620907	O	-2.718582	0.482827	1.890795
P	0.741765	-2.097084	0.163925	P	0.616826	-2.087134	0.223130
O	-3.856369	2.958298	-0.290789	O	-3.690961	2.705651	0.109574
C	-3.122020	0.350601	2.729302	C	-1.840463	0.320723	2.679087
H	-3.785125	2.325474	0.436460	H	-3.435206	2.048842	0.774654
P	1.204999	2.275531	0.322758	P	1.083658	2.293663	0.380995
H	0.049989	0.133172	1.566336	H	-0.403096	0.185413	1.634393
H	-3.512519	2.463241	-1.049087	H	-3.399871	2.302353	-0.720983
N	-0.355995	0.273614	-0.966061	N	-0.461324	0.286223	-0.927194
O	-2.802494	0.182481	3.839179	O	-1.372666	0.189181	3.761549
N	-0.619951	-2.049750	-0.941215	N	-0.672116	-2.046478	-0.964239
N	-0.075496	2.591570	-0.829875	N	-0.152427	2.607166	-0.819372
C	-0.976568	-0.824060	-1.475153	C	-1.035199	-0.815330	-1.482996
C	-1.942060	-0.718880	-2.495377	C	-1.960216	-0.711354	-2.539725
C	-2.256075	0.544296	-2.976068	C	-2.280776	0.552949	-3.011131
C	-1.645501	1.677832	-2.450868	C	-1.696780	1.687872	-2.460058
C	-0.692713	1.507912	-1.424658	C	-0.770532	1.520214	-1.410784
C	2.030630	-3.145174	-0.751639	C	2.055029	-2.930437	-0.683028
C	1.786162	-4.661470	-0.810988	C	1.899849	-4.427876	-0.992384
C	3.460671	-2.862945	-0.258000	C	3.411495	-2.673738	-0.002380
C	0.111279	-3.195731	1.552839	C	0.006562	-3.371335	-1.453312
C	1.177350	-3.354173	2.650412	C	1.006576	-3.542585	2.609265
C	-1.202567	-2.677291	2.152437	C	-1.394137	-3.060415	1.997873
C	2.722365	3.102727	-0.460981	C	2.682180	2.885213	-0.450039
C	2.808056	4.634960	-0.367213	C	2.849003	4.401993	-0.631639
C	4.039523	2.475974	0.028546	C	3.941656	2.291313	0.204560
C	0.739292	3.374786	1.773926	C	0.720290	3.580840	1.702985
C	-0.690867	3.112397	2.265320	C	-0.718963	3.505825	2.231180
C	1.747820	3.205018	2.922300	C	1.723591	3.475154	2.864177
C	2.392713	-0.110493	1.616970	C	1.964835	-0.068742	1.958308
O	3.229137	-0.229641	2.422734	O	2.696017	-0.175350	2.860112
C	-1.354609	-3.237572	-1.385930	C	-1.319726	-3.243031	-1.512270
H	-2.411988	-1.597876	-2.911765	H	-2.402875	-1.590752	-2.983288
H	-2.982102	0.648831	-3.777418	H	-2.988154	0.657854	-3.828860
H	-1.863444	2.657054	-2.853392	H	-1.922500	2.667693	-2.855187
H	1.946882	-2.737830	-1.768163	H	2.054362	-2.376738	-1.631050
H	2.550448	-5.123239	-1.447598	H	2.758316	-4.760419	-1.588332
H	0.813713	-4.925691	-1.231666	H	1.000421	-4.657119	-1.567798
H	1.867822	-5.124360	0.177966	H	1.887687	-5.033436	-0.080156
H	4.176329	-3.367376	-0.918100	H	4.215239	-3.022464	-0.661610
H	3.626975	-3.244745	0.754487	H	3.506886	-3.219472	0.941433
H	3.693516	-1.796436	-0.265305	H	3.579750	-1.613246	0.195244
H	-0.072872	-4.184503	1.118435	H	-0.040550	-4.320511	0.908356
H	0.797740	-4.022884	3.431760	H	0.624194	-4.292345	3.311681
H	1.409902	-2.394245	3.122514	H	1.140509	-2.609094	3.164820
H	2.109524	-3.784690	2.274801	H	1.988264	-3.882956	2.271002
H	-1.579976	-3.400083	2.885432	H	-1.769751	-3.933199	2.544824
H	-1.980814	-2.530416	1.397649	H	-2.115611	-2.825472	1.210687
H	-1.042440	-1.727641	2.670013	H	-1.365774	-2.225000	2.701262
H	2.593005	2.823188	-1.515242	H	2.578381	2.426251	-1.442271
H	3.680981	4.979947	-0.934141	H	3.759425	4.594255	-1.211987
H	2.941147	4.970629	0.666618	H	2.963312	4.917391	0.327588
H	1.933796	5.143168	-0.779931	H	2.019101	4.863430	-1.171360
H	4.872889	2.888369	-0.552691	H	4.814183	2.525995	-0.416576
H	4.048443	1.391487	-0.096464	H	3.883053	1.205236	0.300270
H	4.233132	2.703603	1.081796	H	4.126336	2.713952	1.196988
H	0.799103	4.409672	1.419589	H	0.862017	4.557766	1.228311
H	-0.946102	3.839098	3.045712	H	-0.929322	4.401827	2.827239
H	-0.770790	2.112218	2.701674	H	-0.843573	2.644326	2.891421
H	-1.436000	3.201839	1.469147	H	-1.471176	3.447187	1.439932
H	1.481162	3.876878	3.746590	H	1.490539	4.241183	3.612878
H	2.771785	3.444140	2.622197	H	2.757284	3.632279	2.546084
H	1.737881	2.182182	3.312829	H	1.661304	2.501445	3.360288
H	2.127501	0.013712	-0.780727	H	1.979268	0.016282	-0.435563
H	-1.120192	-3.498245	-2.425066	H	-1.035915	-3.415943	-2.557031
H	-2.433886	-3.075699	-1.300799	H	-2.409189	-3.151078	-1.455730
H	-1.101874	-4.085594	-0.754066	H	-1.034978	-4.116058	-0.930282
H	-1.623695	4.001348	-1.097532	H	-1.644990	4.063319	-1.148006

H	-0.276901	4.143025	-2.291418
H	-0.089203	4.699813	-0.622677
C	-0.561553	3.948543	-1.250877

B

Fe	0.801235	0.106640	0.640378
O	-2.642315	0.484258	1.850920
P	0.582241	-2.090110	0.240774
O	-3.549502	2.614247	0.262296
C	-1.561791	0.291064	2.431982
H	-3.233677	1.893975	0.846593
P	1.061728	2.314034	0.384073
H	-0.622138	0.324483	1.685258
H	-3.403759	2.257593	-0.624101
N	-0.471744	0.293575	-0.921297
O	-1.243380	0.076129	3.602391
N	-0.679972	-2.044119	-0.968187
N	-0.176088	2.620308	-0.809912
C	-1.032106	-0.811794	-1.491325
C	-1.935249	-0.708173	-2.564479
C	-2.251699	0.556457	-3.038726
C	-1.684266	1.692539	-2.475591
C	-0.778370	1.529699	-1.410219
C	2.054119	-2.882798	-0.651053
C	1.922535	-4.377312	-0.983882
C	3.394944	-2.614444	0.054746
C	-0.027842	-3.384741	1.456153
C	0.956594	-3.543029	2.627642
C	-1.443040	-3.095961	1.976861
C	2.663299	2.849604	-0.468087
C	2.841540	4.361321	-0.677615
C	3.918671	2.247973	0.186545
C	0.726824	3.600308	1.709611
C	-0.702972	3.522242	2.263905
C	1.753901	3.499205	2.850380
C	1.919709	-0.056521	1.985238
O	2.682791	-0.166140	2.853737
C	-1.316191	-3.241496	-1.530184
H	-2.366266	-1.587999	-3.018092
H	-2.944452	0.659666	-3.868996
H	-1.913064	2.672349	-2.868198
H	2.058526	-2.316306	-1.591306
H	2.790437	-4.686656	-1.578235
H	1.030659	-4.608624	-1.569786
H	1.911868	-4.996790	-0.081255
H	4.212174	-2.956116	-0.591133
H	3.478811	-3.159062	1.000011
H	3.551057	-1.552627	0.254129
H	-0.046568	-4.331229	0.904634
H	0.582734	-4.316698	3.308053
H	1.048832	-2.616857	3.203107
H	1.954727	-3.847831	2.304021
H	-1.799741	-3.968578	2.536750
H	-2.159733	-2.902956	1.174106
H	-1.447670	-2.241350	2.657339
H	2.544421	2.375089	-1.451121
H	3.746893	4.534654	-1.271186
H	2.969283	4.891618	0.271560
H	2.008149	4.818111	-1.216070
H	4.788977	2.466875	-0.443049
H	3.848493	1.163308	0.291873
H	4.114976	2.677128	1.173569
H	0.861517	4.574190	1.226355
H	-0.897730	4.418100	2.865663
H	-0.819190	2.656653	2.920727
H	-1.469191	3.464676	1.486272
H	1.535136	4.272665	3.595431
H	2.781727	3.651599	2.512230
H	1.697370	2.531181	3.357709
H	1.944795	0.010591	-0.317486
H	-1.011402	-3.411537	-2.569186
H	-2.406169	-3.149598	-1.492819
H	-1.040872	-4.114428	-0.943311
H	-1.689551	4.053662	-1.116628
H	-0.326957	4.166707	-2.268438
H	-0.139090	4.712340	-0.596513
C	-0.605244	3.960368	-1.228753

Fe	0.900741	0.069201	0.583446
O	-3.329872	1.237287	2.428923
P	0.664358	-2.131454	0.187056
O	-3.640293	2.789130	0.241514
C	-2.292693	0.521559	2.463444
H	-3.541111	2.207943	1.043896
P	1.119841	2.299345	0.369469
H	-1.794578	0.326958	1.465659
H	-3.521425	2.182087	-0.500232
N	-0.406813	0.270065	-0.936653
O	-1.738129	-0.002213	3.456017
N	-0.556134	-2.072543	-1.059759
N	-0.184033	2.603490	-0.750475
C	-0.927145	-0.834447	-1.552678
C	-1.822457	-0.719969	-2.629541
C	-2.187076	0.550988	-3.051577
C	-1.668181	1.684232	-2.439828
C	-0.754408	1.515553	-1.383707
C	2.135855	-2.988634	-0.638273
C	2.015204	-4.511579	-0.809051
C	3.476513	-2.638862	0.030787
C	-0.025543	-3.346346	1.435003
C	0.916624	-3.459139	2.645903
C	-1.446088	-2.970774	1.878510
C	2.664375	2.882404	-0.546891
C	2.795858	4.404518	-0.708245
C	3.960531	2.283154	0.025093
C	0.818869	3.521413	1.756470
C	-0.561934	3.318042	2.393559
C	1.927242	3.442158	2.819915
C	2.074785	-0.102971	1.887504
O	2.887489	-0.216546	2.708228
C	-1.172966	-3.268960	-1.645493
H	-2.217418	-1.595890	-3.121808
H	-2.880898	0.661087	-3.880044
H	-1.940378	2.669467	-2.788011
H	2.127633	-2.524075	-1.633079
H	2.867342	-4.869494	-1.398545
H	1.107640	-4.817564	-1.333646
H	2.046820	-5.030529	0.154365
H	4.291129	-3.085379	-0.551078
H	3.546166	-3.037941	1.047381
H	3.647746	-1.561557	0.069974
H	-0.053872	-4.320965	0.935233
H	0.519541	-4.206754	3.341880
H	0.986259	-2.510115	3.187110
H	1.927150	-3.771669	2.369404
H	-1.830509	-3.757750	2.538873
H	-2.136868	-2.887314	1.034010
H	-1.462677	-2.028154	2.436303
H	2.505595	2.440196	-1.538921
H	3.668608	4.622925	-1.334762
H	2.952375	4.902658	0.253759
H	1.927351	4.857601	-1.192015
H	4.798110	2.557360	-0.626680
H	3.920725	1.192889	0.074106
H	4.186694	2.665161	1.024813
H	0.860650	4.518921	1.305780
H	-0.756481	4.139387	3.093667
H	-0.599134	2.384134	2.960360
H	-1.374779	3.299402	1.663754
H	1.702292	4.157478	3.619130
H	2.914390	3.692763	2.424153
H	1.980408	2.449264	3.277149
H	2.031510	-0.012149	-0.359767
H	-0.835832	-3.433878	-2.675247
H	-2.263634	-3.180552	-1.640055
H	-0.912162	-4.143051	-1.053184
H	-1.768062	3.973714	-0.927251
H	-0.455560	4.205610	-2.130825
H	-0.225634	4.683255	-0.444728
C	-0.686945	3.941720	-1.092749

C

Fe	1.043698	0.031328	0.554557
O	-3.394884	1.820298	2.156875
P	0.760847	-2.163916	0.180917
O	-4.055233	2.979852	-0.207778
C	-2.828544	0.695261	2.110329

TS_{Bc}

H	-3.865124	2.549718	0.666132	H	-3.004604	1.023497	3.894148
P	1.177940	2.277515	0.411240	N	-0.599916	0.867702	-1.088836
H	-3.170603	0.009606	1.281401	O	-1.051516	1.186257	3.412520
H	-3.820071	2.296932	-0.849074	N	-1.556561	-1.280782	-1.054712
N	-0.364529	0.242433	-0.868873	N	0.411638	2.989606	-1.057101
O	-1.945578	0.236808	2.876072	C	-1.595521	0.026367	-1.501736
N	-0.479666	-0.2098674	-1.043179	C	-2.634266	0.474603	-2.337938
N	-0.206534	2.573802	-0.608143	C	-2.623103	1.799731	-2.752566
C	-0.878791	-0.856627	-1.501056	C	-1.616320	2.665041	-2.349703
C	-1.794766	-0.732648	-2.558996	C	-0.608190	2.170201	-1.504201
C	-2.186510	0.541188	-2.946832	C	0.739512	-2.974142	-1.318345
C	-1.682493	1.668354	-2.311954	C	0.025372	-4.307033	-1.589580
C	-0.753925	1.490900	-1.270489	C	2.206033	-3.213959	-0.920081
C	2.190996	-3.084412	-0.645032	C	-0.878818	-2.812746	1.244090
C	2.041733	-4.611039	-0.744525	C	0.227243	-3.391816	2.143193
C	3.552620	-2.729444	-0.023093	C	-1.874343	-1.989161	2.074597
C	0.053153	-3.306679	1.484844	C	3.221243	2.404822	-1.192622
C	0.978023	-3.336370	2.714109	C	3.831278	3.808019	-1.336415
C	-1.378818	-2.909589	1.873584	C	4.311357	1.391570	-0.803102
C	2.639075	2.951628	-0.577098	C	1.909348	3.477597	1.317228
C	2.734210	4.483299	-0.644547	C	0.574815	3.822191	1.995324
C	3.985315	2.343964	-0.146987	C	2.910166	2.914780	2.341835
C	0.935276	3.423015	1.870297	C	2.111590	-0.378266	1.226402
C	-0.445073	3.244927	2.514340	O	2.976243	-0.777465	1.890036
C	2.052312	3.216389	2.908814	C	-2.707031	-2.146342	-1.351069
C	2.306286	-0.143874	1.768343	H	-3.408360	-0.199702	-2.672765
O	3.177329	-0.258866	2.526768	H	-3.409854	2.161963	-3.408081
C	-1.111337	-3.293562	-1.615598	H	-1.606700	3.690403	-2.687623
H	-2.180725	-1.603963	-3.066547	H	0.742467	-2.386482	-2.245596
H	-2.889813	0.658499	-3.766258	H	0.592993	-4.870214	-2.339610
H	-1.971401	2.657069	-2.635790	H	-0.985228	-4.173638	-1.981459
H	2.165481	-2.662104	-1.658221	H	-0.033205	-4.928921	-0.690394
H	2.880385	-5.010313	-1.326559	H	2.701232	-3.782316	-1.715814
H	1.122956	-4.924940	-1.244296	H	2.294617	-3.797796	0.000676
H	2.076143	-5.086150	0.241173	H	2.755652	-2.279349	-0.789762
H	4.345343	-3.218846	-0.600578	H	-1.406956	-3.652954	0.779204
H	3.636720	-3.082128	1.009602	H	-0.239220	-3.967908	2.950379
H	3.744054	-1.654999	-0.038209	H	0.825192	-2.602327	2.609431
H	0.036978	4.311084	1.047482	H	0.901095	-4.065600	1.608448
H	0.601952	-4.074800	3.431110	H	-2.341071	-2.645842	2.818805
H	0.999329	-2.365820	3.220553	H	-2.672834	-1.542417	1.475795
H	2.006187	-3.614131	2.463955	H	-1.368090	-1.182392	2.612414
H	-1.733528	-3.589351	2.658266	H	2.814619	2.099117	-2.165625
H	-2.070367	-2.998847	1.030361	H	4.642884	3.766668	-2.072145
H	-1.443689	-1.884316	2.259785	H	4.263381	4.160814	-0.394297
H	2.410665	2.572647	-1.581765	H	3.115936	4.554880	-1.687319
H	3.527073	4.760715	-1.348996	H	5.116901	1.434338	-1.545239
H	2.997128	4.914132	0.326897	H	3.932801	0.368000	-0.780845
H	1.810783	4.953653	-0.990082	H	4.753986	1.617995	0.171643
H	4.765768	2.681174	-0.839099	H	2.338602	4.389627	0.886947
H	3.967877	1.252082	-0.169340	H	0.763418	4.545157	2.798443
H	4.280685	2.662788	0.857271	H	0.099085	2.940009	2.439810
H	1.021615	4.444359	1.482438	H	-0.136470	4.280854	1.302518
H	-0.534782	3.941955	3.356888	H	3.092311	3.667965	3.116698
H	-0.602807	2.231093	2.894128	H	3.877077	2.658307	1.900287
H	-1.266513	3.451088	1.826670	H	2.510200	2.024321	2.836704
H	1.934298	3.956358	3.708358	H	1.711695	-0.180622	-0.974139
H	3.055615	3.341112	2.492851	H	-2.799368	-2.337510	-2.425923
H	1.989236	2.224534	3.367080	H	-3.624680	-1.681705	-0.977795
H	2.116527	-0.033586	-0.457328	H	-2.587862	-3.102065	-0.846328
H	-0.785560	-3.468697	-2.647317	H	-0.585391	4.854324	-1.160525
H	-2.200993	-3.195895	-1.600286	H	0.552566	4.552107	-2.497793
H	-0.852911	-4.165670	-1.018632	H	1.148933	4.946668	-0.876027
H	-1.840714	3.893111	-0.758662	C	0.378943	4.410050	-1.425146
H	-0.508519	4.239724	-1.908584				
H	-0.334645	4.628618	-0.191175				
C	-0.753467	3.909715	-0.892209				
D							
Fe	0.842693	0.203608	0.154431				
O	-2.755167	1.590438	1.971180				
H	-0.615477	0.660135	6.345958				
P	-0.156861	-1.794253	-0.149188				
H	-0.727371	0.791252	5.615924				
O	-4.621843	0.141939	0.610480				
C	-2.262311	1.266592	3.084973				
H	-4.012811	0.647987	1.202521				
P	1.684101	2.274434	-0.100792				
H	-4.413403	0.504597	-0.260711				
TS_{DE}							
Fe	0.892292	0.176542	0.185287				
O	-2.981279	1.537718	1.962351				
H	0.526050	0.367361	2.928585				
P	-0.150127	-1.802170	-0.089877				
H	-0.079497	0.9720720	3.202205				
O	-4.716087	0.059783	0.514953				
C	-2.823755	1.403972	3.210713				
H	-4.128608	0.584645	1.122192				
P	1.706754	2.268601	-0.021121				
H	-4.552859	0.472865	-0.343123				
H	-3.705002	0.966924	3.761284				
N	-0.581009	0.868876	-1.016004				
O	-1.830219	1.699850	3.910109				

N	-1.542111	-1.276944	-0.995447
N	0.438521	2.985794	-0.978818
C	-1.570728	0.029190	-1.444873
C	-2.593012	0.476958	-2.301238
C	-2.570979	1.799671	-2.721182
C	-1.568700	2.663624	-2.303396
C	-0.577903	2.168665	-1.438329
C	0.699010	-3.049555	-1.226396
C	0.017785	-4.423357	-1.330534
C	2.195507	-3.218822	-0.912270
C	-0.885900	-2.766743	1.335243
C	0.220571	-3.309003	2.256137
C	-1.900463	-1.928960	2.128881
C	3.261021	2.458111	-1.081596
C	3.886100	3.861829	-1.126165
C	4.338578	1.415331	-0.737094
C	1.891041	3.449631	1.423634
C	0.543498	3.805724	2.070321
C	2.877042	2.880236	2.458688
C	2.218845	-0.445526	1.163316
O	3.120273	-0.866623	1.760402
C	-2.690490	-2.141221	-1.305246
H	-3.361743	-0.197417	-2.647994
H	-3.343827	2.161114	-3.393434
H	-1.547861	3.686750	-2.647479
H	0.615876	-2.543710	-2.197357
H	0.536116	-5.019993	-2.090168
H	-1.031235	-4.360419	-1.628127
H	0.076020	-4.975533	-0.387199
H	2.640998	-3.888338	-1.657127
H	2.362908	-3.668142	0.071304
H	2.734328	-2.270102	-0.954467
H	-1.405659	-3.624407	0.893623
H	-0.239760	-3.890516	3.062962
H	0.790533	-2.498213	2.721014
H	0.920239	-3.967711	1.734796
H	-2.371618	-2.569453	2.884077
H	-2.693326	-1.504774	1.507486
H	-1.411002	-1.105468	2.654469
H	2.869036	2.217636	-2.078572
H	4.697911	3.862041	-1.862740
H	4.321775	4.140300	-0.161346
H	3.181419	4.641942	-1.421763
H	5.171987	1.520283	-1.441296
H	3.963077	0.393556	-0.815762
H	4.742580	1.559595	0.269771
H	2.327552	4.366758	1.012086
H	0.720571	4.527861	2.876528
H	0.033209	2.944173	2.511774
H	-0.143873	4.273060	1.359812
H	3.049003	3.627144	3.241931
H	3.849473	2.630863	2.024287
H	2.476273	1.983601	2.940956
H	1.703115	-0.171325	-0.998658
H	-2.759108	-2.347141	-2.379375
H	-3.611899	-1.666217	-0.955160
H	-2.586618	-3.090491	-0.784537
H	-0.555971	4.848716	-1.124579
H	0.631885	4.544978	-2.417732
H	1.165207	4.944147	-0.774967
C	0.417747	4.404964	-1.352037

E

Fe	0.755527	0.216894	0.378757
O	-3.028003	1.644268	1.979149
H	-0.095668	0.990574	1.621216
P	-0.187158	-1.773529	-0.004556
H	-0.441262	0.272353	1.547490
O	-4.708304	0.074516	0.544831
C	-2.631728	1.296109	3.128715
H	-4.150442	0.631475	1.148985
P	1.629416	2.257821	0.105948
H	-4.522495	0.455853	-0.323323
H	-3.395638	0.755327	3.757275
N	-0.627411	0.876263	-0.957636
O	-1.513535	1.477543	3.660502
N	-1.562932	-1.272572	-0.947014
N	0.399427	2.981019	-0.895788
C	-1.590081	0.029125	-1.414836

C	-2.581335	0.463849	-2.313352
C	-2.543621	1.782500	-2.747387
C	-1.555710	2.651091	-2.304967
C	-0.601487	2.165285	-1.393898
C	0.745618	-2.971009	-1.128387
C	0.095584	-4.352266	-1.305687
C	2.228652	-3.123246	-0.750025
C	-0.935872	-2.795358	1.373765
C	0.154729	-3.322793	2.322042
C	-1.999668	-2.016585	2.161965
C	3.205949	2.368617	-0.930964
C	3.828433	3.766976	-1.070786
C	4.279852	1.357169	-0.497220
C	1.825077	3.467159	1.524257
C	0.477479	3.884161	2.131757
C	2.753174	2.881474	2.603333
C	2.031236	-0.395961	1.432007
O	2.889936	-0.811780	2.089101
C	-2.682421	-2.157631	-1.297747
H	-3.335896	-0.215988	-2.680685
H	-3.291472	2.135945	-3.451364
H	-1.520135	3.670492	-2.659477
H	0.699724	-2.436488	-2.086516
H	0.649661	-4.912322	-2.067900
H	-0.944069	-4.296022	-1.636021
H	0.131462	-4.937298	-0.381211
H	2.729856	-2.726840	-1.515494
H	2.358709	-3.637186	0.207074
H	2.742429	-2.161114	-0.698487
H	-1.412381	-3.657242	0.893545
H	-0.314134	-3.945537	3.092233
H	0.668156	-2.502301	2.833857
H	0.903315	-3.936572	1.814759
H	-2.491891	-2.703287	2.860777
H	-2.772294	-1.570510	1.529577
H	-1.546480	-1.218010	2.757252
H	2.828985	2.052833	-1.912899
H	4.656861	3.714845	-1.786741
H	4.241118	4.122836	-0.121172
H	3.127276	4.516564	-1.443262
H	5.099942	1.377333	-1.224178
H	3.895470	0.336354	-0.460403
H	4.705223	1.604408	0.480200
H	2.311572	4.354717	1.104125
H	0.663125	4.621943	2.921966
H	-0.062771	3.044406	2.584856
H	-0.182679	3.528891	1.396701
H	2.929469	3.638331	3.375914
H	3.728440	2.580931	2.210309
H	2.297481	2.014120	3.092028
H	1.622438	-0.134468	-0.795451
H	-2.710190	-2.363902	-2.373634
H	-3.624256	-1.699236	-0.981839
H	-2.579953	-3.104754	-0.772951
H	-0.572835	4.848724	-1.097216
H	0.655468	4.522540	-2.345260
H	1.136904	4.936573	-0.690001
C	0.405134	4.395902	-1.285728

F

Fe	0.608149	0.170841	0.120711
O	-2.573004	1.382989	1.871952
H	-0.308075	0.539213	1.367312
P	-0.380567	-1.792099	-0.183736
H	-1.639476	1.051176	1.659563
O	-4.770505	0.244812	0.213050
C	-2.724922	1.566028	3.187909
H	-4.098822	0.610722	0.811147
P	1.401297	2.235536	-0.075150
H	-4.478742	0.549639	-0.658041
H	-3.755041	1.886222	3.412345
N	-0.849537	0.851263	-1.142816
O	-1.867032	1.410624	4.029009
N	-1.762934	-1.305223	-1.143437
N	0.137993	2.970347	-1.044102
C	-1.797808	-0.004046	-1.611682
C	-2.788102	0.423299	-2.519253
C	-2.766522	1.747347	-2.943066
C	-1.799659	2.627244	-2.478235

C	-0.842898	2.144656	-1.564655
C	0.509078	-3.050473	-1.287787
C	-0.172119	-4.416742	-1.463991
C	1.983278	-3.246590	-0.893381
C	-1.153935	-2.803433	1.197084
C	-0.075603	-3.314887	2.167770
C	-2.231118	-2.026073	1.965990
C	2.969174	2.471200	-1.114219
C	3.556948	3.889776	-1.179747
C	4.073755	1.465929	-0.741955
C	1.582088	3.433810	1.361227
C	0.250651	3.695366	2.077777
C	2.640221	2.929431	2.357615
C	1.860392	-0.417377	1.184005
O	2.690437	-0.813240	1.901144
C	-2.868621	-2.198704	-1.507885
H	-3.520261	-0.267949	-2.911174
H	-3.510066	2.093948	-3.655214
H	-1.775615	3.650550	-2.822975
H	0.492297	-2.524657	-2.251759
H	0.385902	-5.003855	-2.203291
H	-1.200996	-4.340954	-1.822321
H	-0.176005	-4.991470	-0.531972
H	2.484964	-3.842776	-1.664788
H	2.084446	-3.788303	0.052169
H	2.517422	-2.298481	-0.805168
H	-1.623343	-3.673314	0.724247
H	-0.552022	-3.910637	2.955111
H	0.447018	-2.485029	2.654774
H	0.668301	-3.950971	1.681480
H	-2.745811	-2.710283	2.651042
H	-2.984197	-1.575322	1.314315
H	-1.781898	-1.233365	2.570025
H	2.599442	2.199694	-2.112050
H	4.384275	3.900375	-1.899502
H	3.965017	4.202992	-0.213323
H	2.836199	4.642455	-1.506529
H	4.888408	1.540904	-1.471970
H	3.712294	0.435872	-0.748755
H	4.500481	1.673062	0.244523
H	1.940504	4.379669	0.940209
H	0.385303	4.501048	2.809328
H	-0.089277	2.810505	2.621939
H	-0.542990	4.001907	1.390388
H	2.753822	3.659049	3.167937
H	3.623830	2.793899	1.900036
H	2.339341	1.979364	2.810711
H	1.433075	-0.154323	-1.152740
H	-2.868833	-2.429213	-2.579788
H	-3.823687	-1.739549	-1.235227
H	-2.781872	-3.133515	-0.958850
H	-0.886251	4.813930	-1.214921
H	0.370486	4.558925	-2.449484
H	0.812667	4.940003	-0.777248
C	0.107212	4.392928	-1.398044

TSFG

Fe	0.443063	0.158845	0.018711
O	-2.431275	1.080629	3.699309
H	-0.483567	0.470181	1.897980
P	-0.489464	-1.845115	-0.320288
H	-0.757286	0.597674	1.060528
O	-3.498536	2.009939	1.306113
C	-1.310907	0.665427	4.043734
H	-3.096590	1.625276	2.116249
P	1.197589	2.258853	-0.153280
H	-3.002436	2.828875	1.182747
H	-1.124176	0.524973	5.133014
N	-0.880397	0.764592	-1.420962
O	-0.309585	0.365131	3.305571
N	-1.732668	-1.417286	-1.469986
N	0.028974	2.919113	-1.271375
C	-1.748865	-0.127596	-1.971377
C	-2.629657	0.243283	-3.003722
C	-2.600670	1.555680	-3.453359
C	-1.723401	2.477980	-2.900093
C	-0.865061	2.048691	-1.871772
C	0.536428	-3.157089	-1.225474
C	-0.071837	-4.566453	-1.304198

C	1.980582	-3.239654	-0.702571
C	-1.435617	-2.760848	1.016072
C	-0.507467	-3.084993	2.200310
C	-2.673156	-1.986795	1.490789
C	2.862640	2.529607	-1.015983
C	3.414464	3.964087	-1.002542
C	3.943864	1.550349	-0.527754
C	1.159550	3.470159	1.278266
C	-0.266595	3.750383	1.771983
C	2.045319	2.964101	2.430112
C	1.695837	-0.401205	1.120477
O	2.557232	-0.784417	1.796784
C	-2.729785	-2.370650	-1.967603
H	-3.301349	-0.475459	-3.449367
H	-3.266335	1.862758	-4.254987
H	-1.693101	3.494242	-3.264019
H	0.573358	-2.735419	-2.238770
H	0.563032	-5.193327	-1.941396
H	-1.075587	-4.580770	-1.733906
H	-0.114377	-5.043918	-0.319925
H	2.549711	-3.934285	-1.331515
H	2.025086	-3.617390	0.323594
H	2.485268	-2.272713	-0.736322
H	-1.767398	-3.705578	0.571213
H	-1.044489	-3.716412	2.917730
H	-0.205668	-2.170983	2.720878
H	0.392663	-3.672784	1.897208
H	-3.215925	-2.596097	2.223449
H	-3.364688	-1.758753	0.675142
H	-2.403275	-1.048077	1.980850
H	2.613046	2.260660	-2.051123
H	4.322336	4.002218	-1.616063
H	3.693848	4.280432	0.007815
H	2.718546	4.699647	-1.411165
H	4.843801	1.677335	-1.140711
H	3.626337	0.509814	-0.614053
H	4.228667	1.740628	0.511726
H	1.585366	4.408399	0.906156
H	-0.226406	4.492294	2.578416
H	-0.737797	2.851031	2.175265
H	-0.907770	4.157259	0.984430
H	2.097552	3.733785	3.208976
H	3.069861	2.749325	2.113179
H	1.621302	2.062248	2.881819
H	1.380501	-0.180856	-1.131522
H	-2.531148	-2.663454	-3.005275
H	-3.734367	-1.940827	-1.908677
H	-2.721470	-3.265004	-1.348544
H	-1.012158	4.725023	-1.626691
H	0.387695	4.466107	-2.695356
H	0.618844	4.915461	-0.995743
C	0.006446	4.328407	-1.676519

G

Fe	0.393613	0.021226	-0.001437
O	-2.162476	1.890668	3.729640
H	-0.458264	0.566668	2.585120
P	-1.041024	-1.650292	-0.319356
H	-0.512936	0.672624	1.136666
O	-3.023258	3.013091	1.210439
C	-1.321401	1.163103	4.229512
H	-2.722014	2.570674	2.023370
P	1.659587	1.841688	-0.182908
H	-2.315098	3.643447	1.025275
H	-1.243157	1.013428	5.317302
N	-0.760247	0.965683	-1.414318
O	-0.401153	0.459630	3.592256
N	-2.175246	-0.899235	-1.419795
N	0.709418	2.785011	-1.309009
C	-1.853077	0.345341	-1.933888
C	-2.624287	0.938873	-2.950804
C	-2.244272	2.188175	-3.420687
C	-1.132167	2.834816	-2.899188
C	-0.403169	2.192077	-1.881417
C	-0.426312	-3.171892	-1.270376
C	-1.396027	-4.358464	-1.390304
C	0.937873	-3.668099	-0.760964
C	-2.154503	-2.329630	1.032262
C	-1.311358	-2.914449	2.179040

C	-3.138576	-1.277335	1.559777
C	3.343373	1.663282	-1.039412
C	4.256857	2.899307	-1.048658
C	4.128768	0.443530	-0.528064
C	1.950165	3.047391	1.229156
C	0.653684	3.720547	1.699806
C	2.658367	2.340478	2.398057
C	1.422139	-0.817773	1.134224
O	2.119432	-1.387293	1.874275
C	-3.399051	-1.548563	-1.899589
H	-3.479233	0.430225	-3.371252
H	-2.817688	2.661157	-4.212975
H	-0.828683	3.798527	-3.280908
H	-0.271158	-2.744212	-2.269926
H	-0.958113	-5.111806	-2.056101
H	-2.367574	-4.085851	-1.807183
H	-1.563260	-4.842623	-0.422256
H	1.309584	-4.452006	-1.431501
H	0.864739	-4.104543	0.240262
H	1.682169	-2.870194	-0.735699
H	-2.730678	-3.148071	0.587944
H	-1.973925	-3.392886	2.909729
H	-0.755791	-2.130625	2.702056
H	-0.598364	-3.670697	1.838492
H	-3.748263	-1.717676	2.357585
H	-3.818642	-0.913246	0.785044
H	-2.616159	-0.413201	1.978001
H	3.032618	1.449379	-2.070936
H	5.137233	2.687969	-1.667346
H	4.618798	3.141825	-0.043953
H	3.778327	3.789479	-1.462210
H	5.024484	0.308091	-1.145729
H	3.542364	-0.475145	-0.583197
H	4.463600	0.577728	0.505536
H	2.622358	3.825576	0.851139
H	0.876665	4.394159	2.535658
H	-0.076012	2.986671	2.051637
H	0.184370	4.316246	0.911588
H	2.902576	3.075381	3.173890
H	3.592861	1.859402	2.095643
H	2.014738	1.581366	2.852358
H	1.201869	-0.553160	-1.196629
H	-3.306536	-1.871152	-2.943656
H	-4.250940	-0.866286	-1.817848
H	-3.620139	-2.420863	-1.288505
H	0.198036	4.804763	-1.675384
H	1.452425	4.159880	-2.759779
H	1.829211	4.546179	-1.071185
C	1.066931	4.141699	-1.733302

TS_{BH}

Fe	0.810544	0.113484	0.659924
O	-2.802185	0.169650	2.048753
P	0.576673	-2.088667	0.255945
O	-3.557119	2.288707	0.449465
C	-1.564906	0.309303	2.202031
H	-3.345502	1.523501	1.037835
P	1.079292	2.329203	0.400158
H	-1.070401	1.013937	1.471824
H	-3.370314	1.949275	-0.435496
N	-0.466075	0.310615	-0.903942
O	-0.799894	-0.219202	3.047540
N	-0.639541	-2.030371	-0.999550
N	-0.197756	2.640128	-0.753851
C	-1.003657	-0.793419	-1.500659
C	-1.901629	-0.681280	-2.577533
C	-2.243199	0.587739	-3.021259
C	-1.700097	1.722038	-2.430636
C	-0.789974	1.552683	-1.370855
C	2.077125	-2.878325	-0.590432
C	1.951636	-4.361863	-0.971056
C	3.387182	-2.645014	0.182509
C	-0.075268	-3.380581	1.454761
C	0.779767	-3.390660	2.734741
C	-1.558124	-3.196675	1.811122
C	2.656183	2.828391	-0.515513
C	2.831025	4.331701	-0.779771
C	3.930471	2.240958	0.115450
C	0.808612	3.635245	1.722796

C	-0.596373	3.586600	2.343640
C	1.882570	3.538921	2.820325
C	1.916945	-0.058752	2.023119
O	2.672147	-0.166845	2.895640
C	-1.248072	-3.226331	-1.594900
H	-2.314591	-1.557942	-3.053365
H	-2.937313	0.696688	-3.849641
H	-1.952231	2.705608	-2.798198
H	2.129701	-2.287497	-1.513987
H	2.845609	-4.659797	-1.531614
H	1.088257	-4.570599	-1.605515
H	1.895211	-5.007537	-0.088692
H	4.228995	-2.976083	-0.436831
H	3.423612	-3.220868	1.112360
H	3.547029	-1.522177	0.422416
H	0.048707	-4.344913	0.949681
H	0.452425	-4.214922	3.379144
H	0.649099	-2.457240	3.288745
H	1.844981	-3.563182	2.536430
H	-1.878355	-4.048930	2.423215
H	-2.207781	-3.164793	0.932591
H	-1.709741	-2.283525	2.390248
H	2.503581	2.322187	-1.477705
H	3.718609	4.482915	-1.405355
H	2.988307	4.892651	0.147151
H	1.982411	4.772601	-1.307676
H	4.775404	2.416105	-0.506665
H	3.852317	1.163762	0.278208
H	4.175153	2.715924	1.070018
H	0.934497	4.600272	1.219911
H	-0.760121	4.506305	2.917730
H	-0.684025	2.745784	3.037151
H	-1.399473	3.497961	1.606615
H	1.695900	4.316958	3.569301
H	2.894909	3.689291	2.438428
H	1.847754	2.573825	3.335276
H	1.947803	0.009284	-0.277854
H	-0.918336	-3.373417	-2.629772
H	-2.339832	-3.150975	-1.580180
H	-0.971350	-4.105154	-1.017157
H	-1.726537	4.065258	-1.027673
H	-0.381710	4.199629	-2.194612
H	-0.173484	4.730109	-0.520411
C	-0.642773	3.980642	-1.153035

H

Fe	0.909134	0.131774	0.620997
O	-2.756115	0.509593	2.683248
P	0.612835	-2.064305	0.235411
O	-4.831139	1.560817	1.229271
C	-1.848595	0.559196	1.828170
H	-4.148947	1.211420	1.849506
P	1.184592	2.345378	0.363427
H	-2.107945	0.936177	0.818635
H	-5.170929	0.761083	0.807436
N	-0.373561	0.344097	-0.963617
O	-0.637025	0.209397	2.012620
N	-0.634159	-1.987997	-0.988980
N	-0.042591	2.664529	-0.842224
C	-0.926149	-0.754104	-1.549269
C	-1.768151	-0.642987	-2.671034
C	-2.019090	0.622661	-3.182477
C	-1.452789	1.750597	-2.604506
C	-0.623686	1.579319	-1.481262
C	2.036996	-2.979019	-0.617366
C	1.863516	-4.494549	-0.808001
C	3.400957	-2.689003	0.033235
C	-0.078812	-3.281620	1.487127
C	0.871391	-3.399647	2.691529
C	-1.500119	-2.930472	1.948288
C	2.796760	-2.895036	-0.469123
C	3.011754	4.410467	-0.606739
C	4.042468	2.242762	0.154947
C	0.853652	3.636944	1.687879
C	-0.598070	3.642130	2.186322
C	1.828243	3.452513	2.864183
O	2.110029	-0.056692	1.888667
C	2.922911	-0.183409	2.709224
C	-1.286403	-3.174593	-1.553529

H	-2.195005	-1.517985	-3.138295
H	-2.657484	0.731192	-4.054696
H	-1.635909	2.730728	-3.019295
H	2.034790	-2.501622	-1.606292
H	2.693630	-4.874037	-1.415672
H	0.937954	-4.764568	-1.321044
H	1.893737	-5.027971	0.147800
H	4.192505	-3.129945	-0.584142
H	3.483698	-3.131778	1.030800
H	3.599897	-1.618748	0.113792
H	-0.106381	-4.255412	0.985587
H	0.478973	-4.147050	3.390837
H	0.951070	-2.451173	3.231949
H	1.878497	-3.715553	2.406747
H	-1.876185	-3.735769	2.590975
H	-2.197595	-2.824509	1.112157
H	-1.512271	-2.000169	2.517959
H	2.669921	2.469907	-1.473490
H	3.909333	4.589941	-1.210413
H	3.175902	4.886293	0.365595
H	2.181856	4.920168	-1.100804
H	4.918325	2.483496	-0.459032
H	3.957691	1.155505	0.202157
H	4.239770	2.617705	1.163905
H	1.064363	4.609260	1.229203
H	-0.753290	4.518439	2.826860
H	-0.815904	2.751950	2.778998
H	-1.325606	3.694296	1.371577
H	1.655725	4.242931	3.603741
H	2.876284	3.513619	2.559661
H	1.672972	2.492002	3.366062
H	2.014218	0.028359	-0.413812
H	-0.924322	-3.396564	-2.564457
H	-2.370904	-3.033066	-1.592081
H	-1.091358	-4.036700	-0.919577
H	-1.474720	4.136524	-1.342549
H	0.014340	4.206885	-2.316346
H	0.013201	4.754453	-0.631540
C	-0.387977	4.009770	-1.315511

4. X-Ray Crystal Structure Data Collection

Single crystals of **4** were obtained by slow diffusion of pentane into a concentrated solution of the complex in THF under an atmosphere of CO₂. X-ray diffraction data of **4** were collected at $T = 100$ K in a dry stream of nitrogen on a Bruker Kappa APEX II diffractometer system using graphite-monochromatized Mo-K α radiation ($\lambda = 0.71073$ Å) and fine sliced φ - and ω -scans. Data were reduced to intensity values with SAINT and an absorption correction was applied with the multi-scan approach implemented in SADABS.¹⁰ The structures were solved by charge flipping using SUPERFLIP¹¹ and refined against F with JANA2006.¹² Non-hydrogen atoms were refined anisotropically. The H atoms connected to C atoms were placed in calculated positions and thereafter refined as riding on the parent atoms. The H atoms of the amine groups and the hydrides were located in difference Fourier maps. Molecular graphics were generated with the program MERCURY. CCDC 1442681 contains the supplementary crystallographic data for this paper. These data are provided free of charge by The Cambridge Crystallographic Data Centre.

5. Additional catalytic data

Table S1. Solvent screening for the hydrogenation of NaHCO₃ with **1** and **2**.^a

Entry	Cat	Cat.[mol%]	Solvent	TON ^b	Yield [%]
1	1	0.05	H ₂ O/THF	1964	98
2	2	0.05	H ₂ O/THF	1036	52
3	1	0.05	MeOH	1120	56
4	2	0.05	MeOH	516	26
5	1	0.05	THF	0	0
6	2	0.05	THF	0	0

^a General reaction conditions: 20 mmol NaHCO₃, 0.01 mmol catalyst, 25 ml solvent, 80 °C, 90 bar H₂, 24h. ^b Defined as (mmol product)/(mmol catalyst).

6. References

- 1 Gorgas, N.; Stöger, B.; Veiros, L. F.; Pittenauer, E.; Allmaier, G.; Kirchner, K. *Organometallics*, **2014**, *33*, 6905–6914.
- 2 Gorgas, N.; Stöger, B.; Veiros, L. F.; Kirchner, K. *ACS Catal.* **2016**, *6*, 2664–2672.
- 3 Gaussian 09, Revision A.02, Frisch, M. J.; Trucks, G. W.; Schlegel, H. B.; Scuseria, G. E.; Robb, M. A.; Cheeseman, J. R.; Scalmani, G.; Barone, V.; Mennucci, B.; Petersson, G. A.; Nakatsuji, H.; Caricato, M.; Li, X.; Hratchian, H. P.; Izmaylov, A. F.; Bloino, J.; Zheng, G.; Sonnenberg, J. L.; Hada, M.; Ehara, M.; Toyota, K.; Fukuda, R.; Hasegawa, J.; Ishida, M.; Nakajima, T.; Honda, Y.; Kitao, O.; Nakai, H.; Vreven, T.; Montgomery, Jr., J. A.; Peralta, J. E.; Ogliaro, F.; Bearpark, M.; Heyd, J. J.; Brothers, E.; Kudin, K. N.; Staroverov, V. N.; Kobayashi, R.; Normand, J.; Raghavachari, K.; Rendell, A.; Burant, J. C.; Iyengar, S. S.; Tomasi, J.; Cossi, M.; Rega, N.; Millam, J. M.; Klene, M.; Knox, J. E.; Cross, J. B.; Bakken, V.; Adamo, C.; Jaramillo, J.; Gomperts, R.; Stratmann, R. E.; Yazyev, O.; Austin, A. J.; Cammi, R.; Pomelli, C.; Ochterski, J. W.; Martin, R. L.; Morokuma, K.; Zakrzewski, V. G.; Voth, G. A.; Salvador, P.; Dannenberg, J. J.; Dapprich, S.; Daniels, A. D.; Farkas, Ö.; Foresman, J. B.; Ortiz, J. V.; Cioslowski, J.; Fox, D. J. Gaussian, Inc., Wallingford CT, **2009**.
- 4 (a) Becke, A. D. *J. Chem. Phys.* **1993**, *98*, 5648–5652. (b) Miehlich, B.; Savin, A.; Stoll, H.; Preuss, H. *Chem. Phys. Lett* **1989**, *157*, 200–206. (c) Lee, C.; Yang, W.; Parr, G. *Phys. Rev. B* **1988**, *37*, 785–789.

-
- 5 Hehre, W. J.; Radom, L.; Schleyer, P. v. R.; Pople, J. A., *Ab Initio Molecular Orbital Theory*. John Wiley & Sons, New York, **1986**.
- 6 Parr, R. G.; Yang, W. *Density Functional Theory of Atoms and Molecules*, Oxford University Press, New York, **1989**.
- 7 (a) Haeusermann, U.; Dolg, M.; Stoll, H.; Preuss, H. *Mol. Phys.* **1993**, *78*, 1211-1224. (b) Kuechle, W.; Dolg, M.; Stoll, H.; Preuss, H. *J. Chem. Phys.* **1994**, *100*, 7535-7542. (c) Leininger, T.; Nicklass, A.; Stoll, H.; Dolg, M.; Schwerdtfeger, P. *J. Chem. Phys.* **1996**, *105*, 1052-1059.
- 8 (a) McLean, A. D.; Chandler, G. S. *J. Chem. Phys.* **1980**, *72*, 5639-5648. (b) Krishnan, R.; Binkley, J. S.; Seeger, R.; Pople, J. A. *J. Chem. Phys.* **1980**, *72*, 650-654. (c) Wachters, A. J. H. *J. Chem. Phys.* **1970**, *52*, 1033-1036. (d) Hay, P. J. *J. Chem. Phys.* **1977**, *66*, 4377-4384. (e) Raghavachari, K.; Trucks, G. W. *J. Chem. Phys.* **1989**, *91*, 1062-1065. (f) Binning Jr., R. C.; Curtiss, L. A. *J. Comp. Chem.*, **1990**, *11*, 1206. (g) McGrath, M. P.; Radom, L. *J. Chem. Phys.* **1991**, *94*, 511-516.
- 9 (a) Peng, C.; Ayala, P.Y.; Schlegel, H.B.; Frisch, M.J. *J. Comp. Chem.* **1996**, *17*, 49-56. (b) Peng, C.; Schlegel, H.B. *Israel J. Chem.* **1993**, *33*, 449-454.
- 10 Bruker computer programs: APEX2, SAINT and SADABS (Bruker AXS Inc., Madison, WI, **2012**).
- 11 Palatinus, L.; Chapuis, G. *J. Appl. Cryst.* **2007**, *40*, 786-790.
- 12 Petříček, V.; Dušek, M.; Palatinus, L. JANA2006, the crystallographic computing system (Institute of Physics, Praha, Czeck Republic, **2006**).

Results and Discussion – Part IV

Selective Formic Acid Dehydrogenation Catalyzed by Fe-PNP Pincer Complexes Based on the 2,6-Diaminopyridine Scaffold.

Reprinted with permission from *Organometallics* **2016**, 35, 3344–3349. Copyright 2016 American Chemical Society.

Selective Formic Acid Dehydrogenation Catalyzed by Fe-PNP Pincer Complexes Based on the 2,6-Diaminopyridine Scaffold

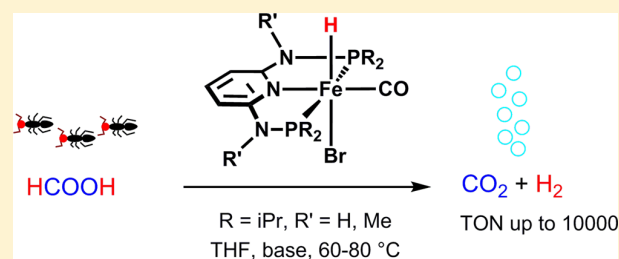
Irene Mellone,[†] Nikolaus Gorgas,[‡] Federica Bertini,[†] Maurizio Peruzzini,[†] Karl Kirchner,^{*,‡} and Luca Gonsalvi^{*,†}

[†]Consiglio Nazionale delle Ricerche (CNR), Istituto di Chimica dei Composti Organometallici (ICCOM), Via Madonna del Piano 10, 50019 Sesto Fiorentino (Firenze), Italy

[‡]Institute of Applied Synthetic Chemistry, Vienna University of Technology, Getreidemarkt 9/163-AC, A-1060 Wien, Austria

Supporting Information

ABSTRACT: Fe(II) hydrido carbonyl complexes supported by PNP pincer ligands based on the 2,6-diaminopyridine scaffold were studied as homogeneous, non-precious-metal-based catalysts for selective formic acid dehydrogenation to hydrogen and carbon dioxide, reaching quantitative yields and high TONs under mild reaction conditions.



INTRODUCTION

A global issue that scientists worldwide are called to answer is to provide solutions for sustainable energy production, by cleaner and renewable alternatives to fossil fuels. Hydrogen has been identified as an important energy vector, as its chemical bond energy can be converted into electricity using mature fuel cell technology.¹ Some of the major limitations to the widespread use of hydrogen for energy applications remain its efficient handling and storage, overcoming its safety issues, and improving its cost effectiveness.^{2,3} As a possible answer, a great deal of research has been carried out to identify suitable hydrogen-rich molecules from which hydrogen can be extracted reversibly under mild conditions of temperature and pressure.

Among several candidates,^{4–6} liquid organic hydrogen carriers (LOHCs),⁷ from which hydrogen can be released on demand by catalytic dehydrogenation, are receiving increasing attention. Among these, formic acid (FA), a liquid under ambient conditions having 4.4% in weight of hydrogen, can be safely handled, stored, and transported easily. Formic acid can be dehydrogenated under mild conditions in the presence of a suitable catalyst to afford fuel cell grade H₂ and CO₂ as the sole byproduct. In principle, CO₂ can be rehydrogenated to HCOOH, so a zero-carbon-emission energy storage cycle can be contemplated.⁸

In recent years, many different heterogeneous and homogeneous catalyst systems for the dehydrogenation of formic acid have been studied. In the case of homogeneous catalysts, the best results were obtained with noble-metal-based complexes, such as Ru⁹ and Ir.¹⁰ At present, an important target in organometallic catalysis is the replacement of noble-metal-based catalysts with non-precious-metal catalysts of comparable activity. Beller's group reported efficient hydrogen generation from formic acid catalyzed by either the in situ catalytic system

obtained from Fe(BF₄)₂·6H₂O and PP₃ ligand (PP₃ = tris[2-(diphenylphosphino)ethyl]phosphine) or the well-defined complexes [FeH(PP₃)BF₄], [FeH(η²-H₂)(PP₃)BF₄], [FeH(η²-H₂)(PP₃)BPh₄], and [FeCl(PP₃)BF₄] in propylene carbonate (PC) as solvent, without the need for an additional base. Except for [FeCl(PP₃)BF₄], excellent activities were observed for all these systems, with a maximum TOF of 1942 h⁻¹ after 3 h at 40 °C using Fe(BF₄)₂·6H₂O/PP₃. Remarkably, this system showed a good performance¹¹ in continuous hydrogen production at 80 °C with TON = 92000 and TOF = 9425 h⁻¹. Lately, some of us reported hydrogen generation from formic acid catalyzed by iron complexes bearing the linear tetraphosphine 1,1,4,7,10,10-hexaphenyl-1,4,7,10-tetraphosphadecane (tetraphos-1), under mild reaction conditions with good activities.¹² Laurency and co-workers described the first Fe-based catalyst for the formic acid dehydrogenation in aqueous solution, using Fe(II) salts together with the water-soluble meta-trisulfonated analogue of PP₃, namely PP₃TS.¹³ Recently, Milstein and co-workers described the iron dihydride pincer complex *trans*-[Fe-(tBuPNP)(H)₂(CO)] (tBuPNP = 2,6-bis(di-*tert*-butylphosphinomethyl)pyridine), which showed an outstanding activity and selectivity in formic acid dehydrogenation at 40 °C in the presence of trialkylamines, with TONs up to 100000.¹⁴ Finally, Schneider, Hazari, Bernskoetter and co-workers reported a new pincer-type iron catalyst that, without the need for added base or free ligand, in the presence of a Lewis acid (LA) as cocatalyst (10 mol %) at 60 °C, achieved the highest TON (ca. 1000000) reported for formic acid dehydrogenation using a first-row transition-metal catalyst.¹⁵

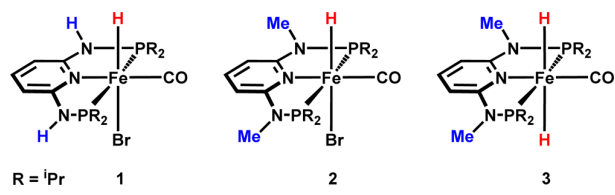
Received: July 8, 2016

Published: September 22, 2016



In recent times, some of us synthesized new transition-metal complexes containing PNP pincer ligands based on the 2,6-diaminopyridine scaffold containing NH and NR linkers between the aromatic pyridine ring and the phosphine moieties.¹⁶ In particular, the iron complexes $[\text{Fe}(\text{PNP}^{\text{H}}\text{-iPr})(\text{H})(\text{CO})(\text{Br})]$ (**1**) and $[\text{Fe}(\text{PNP}^{\text{Me}}\text{-iPr})(\text{H})(\text{CO})(\text{Br})]$ (**2**) proved to be active catalysts for ketone and aldehyde hydrogenation.^{16c,h} Very recently we used complexes **1** and **2** (Chart 1) as catalysts for CO_2 and NaHCO_3 hydrogenation,

Chart 1. Fe-PNP Pincer Complexes 1–3



obtaining good results even under very mild conditions of temperature and pressure.¹⁷ A key role in catalysis was played by the in situ formed complex *trans*- $[\text{Fe}(\text{PNP}^{\text{Me}}\text{-iPr})(\text{H})_2(\text{CO})]$ (**3**). Encouraged by these results, we decided to explore the possible application of these complexes as catalysts for formic acid dehydrogenation. Hereby we present a series of experimental results including detailed screening of reaction conditions and mechanistic considerations based on stoichiometric NMR reactions, which allowed for the description of a proposed catalytic cycle for these systems.

RESULTS AND DISCUSSION

Formic Acid Dehydrogenation Tests. We have tested complexes **1** and **2** for catalytic formic acid dehydrogenation under isobaric conditions at atmospheric pressure in the presence of added bases and additives and different solvents, temperatures, and catalyst loadings. The development of gases during the catalytic tests was measured with a manual gas buret. Aliquots of the gas mixtures produced were analyzed off-line by FT-IR, showing the absence of CO for all tests (see the Experimental Section).

Initially, we checked the activity of complexes **1** and **2** using formic acid without added base, but no activity was observed under these conditions, in contrast to the iron phosphine based systems reported in the literature.^{11,12,15}

We therefore applied the reaction conditions previously described by Milstein et al.¹⁴ for a similar pincer complex: i.e., adding 50 mol % of NEt_3 (0.5 equiv to FA) as base. To our delight, complexes **1** and **2** were found to be catalytically active under these reaction conditions. Using 0.1 mol % of the catalysts at 60 °C, formic acid dehydrogenation took place with $\text{TOF}_{1\text{h}}$ s (turnover frequencies at 1 h) of 95 and 276 h^{-1} and TONs (turnover numbers) of 200 and 653 within 3 h in the case of **1** and **2**, respectively (Table 1, entries 1 and 2).

The presence of a base appeared to be mandatory for the reaction to occur. Initially, we tested the effect of different amounts of NEt_3 as base on the catalytic activity (Table 1). For complex **2**, lowering the amount of NEt_3 to 25 mol % led to a significant decrease in the catalytic activity (TON = 204, entry 3). On the other hand, better performances were obtained in

Table 1. Formic Acid Dehydrogenation using Fe-PNP complexes 1–3 Screening FA/Base Ratios, FA Concentrations, Nature of Base, Solvent, Temperature, and Catalyst Concentration Effects^{a,c}

entry	catalyst	[FA] (mol/L)	solvent	base (mol %)	T (°C)	$\text{TOF}_{1\text{h}}$ (h^{-1}) ^c	TON ^d	conversion (%)
1	1	2.5	THF	NEt_3 (50)	60	95	200 (3)	20
2	2	2.5	THF	NEt_3 (50)	60	276	653 (3)	65
3	2	2.5	THF	NEt_3 (25)	60	102	204 (3)	20
4	2	2.5	THF	NEt_3 (100)	60	398	816 (3)	82
5	2	2.5	THF	NEt_3 (200)	60	418	827 (3)	83
6	1	2.5	THF	NEt_3 (100)	60	174	369 (3)	37
7	2	5.0	THF	NEt_3 (100)	60	612	1000 (2.5)	100
8	2	10.0	THF	NEt_3 (100)	60	770	1000 (2)	100
9	1	5.0	THF	NEt_3 (100)	60	716	1000 (2)	100
10	2	5.0	THF	NEt_3 (50)	60	593	980 (3)	98
11	2	5.0	THF	DMOA (50)	60	673	980 (3)	98
12	2	5.0	THF	DBU (50)	60	459	571 (3)	57
13	1	5.0	THF	DMOA (50)	60	51	76 (3)	2
14	2	5.0	PC	NEt_3 (100)	60	500	1000 (3)	100
15	2	5.0	1,4-dioxane	NEt_3 (100)	60	378	878 (3)	88
16	2	5.0	EtOH	NEt_3 (100)	60	165	650 (3)	65
17	2	5.0	THF	NEt_3 (100)	40	79	180 (3)	18
18	2	5.0	PC	NEt_3 (100)	60	500	1000 (3)	100
19 ^c	2	5.0	PC	NEt_3 (100)	80	1800	1000 (0.6)	100
20 ^b	2	10.0	THF	NEt_3 (100)	60	918	2245 (6)	22
21 ^b	2	10.0	PC	NEt_3 (100)	80	2635	10000 (6)	100
22 ^b	2	5.0	PC	NEt_3 (100)	80	1714	6286 (6)	63
23	3	5.0	THF	-	60	0	0 (3)	0
24	3	5.0	THF	NEt_3 (100)	60	633	1000 (2)	100

^aReaction conditions unless specified otherwise: 10.0 μmol of catalyst; 10.0 mmol of FA, specified amount of base, specified solvent. ^bReaction conditions: 5.0 μmol of catalyst; 50.0 mmol of FA, specified amount of base, specified solvent. Gas evolution was measured with a manual gas buret.

^cDefined as $\text{mmol}_{\text{H}_2\text{ produced}}/(\text{mmol}_{\text{catalyst}} \text{ h})$, calculated after 1 h. ^dDefined as $\text{mmol}_{\text{H}_2\text{ produced}}/\text{mmol}_{\text{catalyst}}$. Run times (h) are given in parentheses.

^eTOF calculated after 20 min due to fast reaction. All tests were repeated at least twice to check for reproducibility (error $\pm 10\%$).

the presence of 100 mol % (1 equiv to FA) of NEt_3 (TON = 816, entry 4). It is worth noting that under these conditions the activity shown by **2** was comparable to that of Milstein's catalyst.¹⁴ A further increase of amine content to 200 mol % did not lead to a significant improvement (TON = 827, entry 5). The catalytic activity of complex **1** also increased using 100 mol % of NEt_3 (entry 6 vs 1), although also under these conditions catalyst **1** performed less efficiently than **2** (TON = 369, entry 6).

Substrate concentration effects were then studied (Table 1, entries 4–9). For catalyst **2**, increasing the FA concentration from 2.5 to 10.0 mol/L resulted in an increase of $\text{TOF}_{1\text{h}}$ from 398 to 770 h^{-1} (entry 4 vs 8), and full conversions were achieved with FA concentrations of 5.0 and 10.0 mol/L (entries 7 and 8). Interestingly, catalyst **2** achieved complete conversion using a FA concentration of 5.0 mol/L, showing in this case a faster initial rate in comparison to **1** with a $\text{TOF}_{1\text{h}}$ of 716 h^{-1} (entry 9). A comparison of reaction profiles at various NEt_3 and FA concentrations is shown in Figure 1.

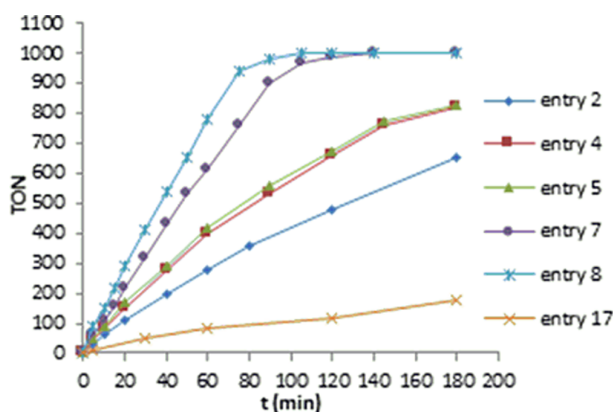


Figure 1. Reaction profiles of selected FA dehydrogenation tests run at 60 °C with **2** (0.1 mol %) with increasing amounts of NEt_3 (50 mol %, Table 1, entry 2; 100 mol %, entry 4; 200 mol %, entry 5), with increasing FA amounts (5.0 mol/L, entry 7; 10.0 mol/L, entry 8), and at a different temperature (40 °C, 5.0 mol/L FA, 100 mol % NEt_3 , entry 17). Other details are given in the footnotes of Table 1.

On the basis of these results, the effect of different amines and solvents on the catalytic activity was examined (Table 1, entries 10 to 12), showing that replacement of NEt_3 with other bases did not lead to any remarkable improvement.^{14,18} Using complex **2**, with 50 mol % of dimethyloctylamine (DMOA), the TON was unchanged in comparison to that with NEt_3 , although $\text{TOF}_{1\text{h}}$ slightly increased from 593 to 673 h^{-1} (entry 10 vs 11). With DBU as base, the catalytic performance dropped with a TON of 571 and $\text{TOF}_{1\text{h}}$ of 459 h^{-1} (entry 12). Complex **1** showed no activity with DBU and was almost inactive with DMOA (entry 13).

The results of solvent screening showed that the highest catalytic activity was achieved in aprotic solvents such as THF ($\text{TOF}_{1\text{h}}$ = 612 h^{-1} , Table 1, entry 7), propylene carbonate (PC, $\text{TOF}_{1\text{h}}$ = 500 h^{-1} , entry 14), and 1,4-dioxane ($\text{TOF}_{1\text{h}}$ = 378 h^{-1} , entry 15), whereas the use of a protic solvent such as EtOH resulted in significantly lower reaction rates ($\text{TOF}_{1\text{h}}$ = 165 h^{-1} , entry 16). The same order THF > PC > 1,4-dioxane > EtOH was observed for TONs and FA conversions at 3 h reaction time.

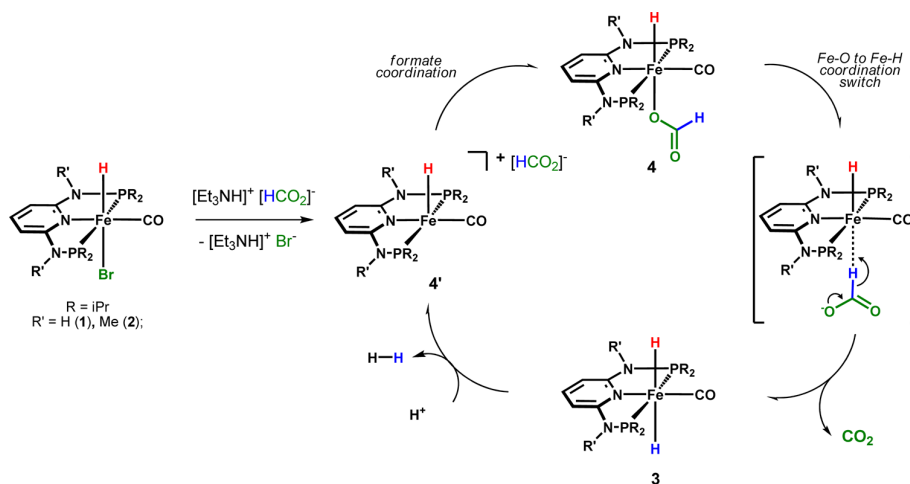
The effect of Lewis acids as cocatalysts was then tested. As recently reported by Hazari et al. for other Fe pincer based systems,¹⁵ such additives can accelerate FA dehydrogenation dramatically. However, this was not the case for our systems, as no FA conversion was observed under standard reaction conditions in the presence of LiBF_4 (10 mol %) instead of bases using complexes **1**–**3**.

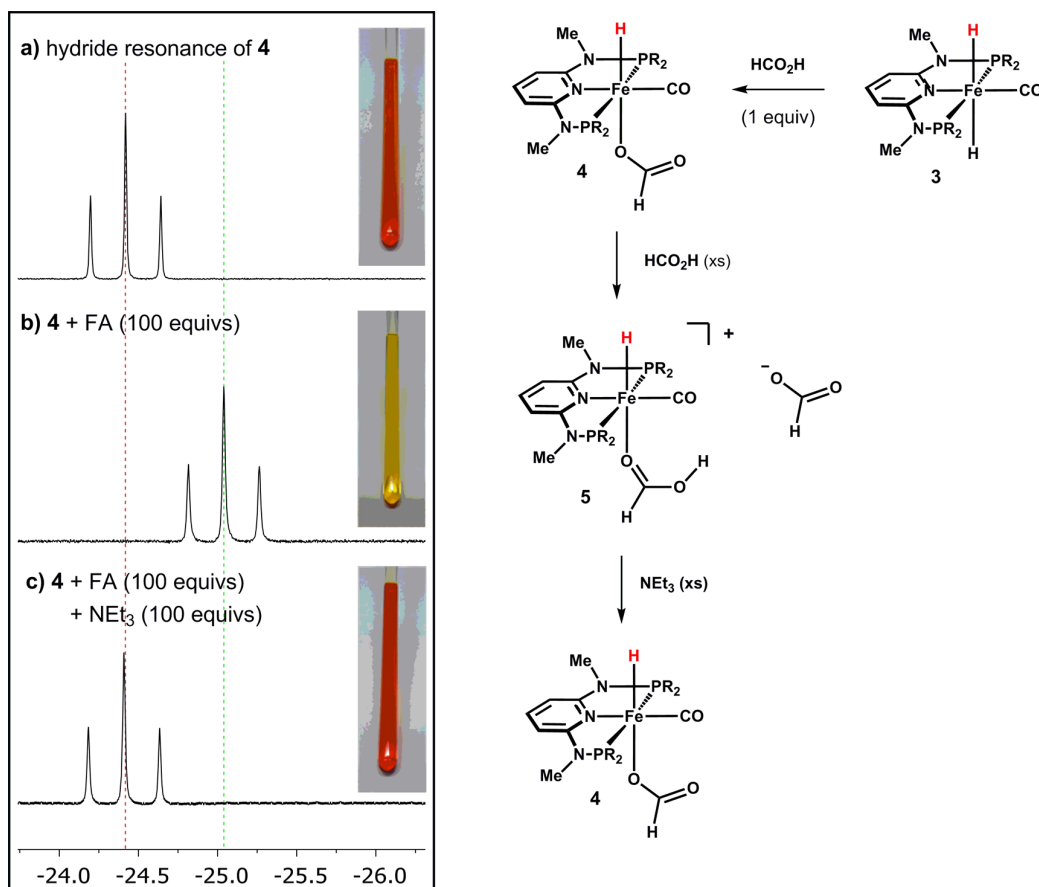
The effect of temperature was then evaluated for **2** (Table 1, entries 17–19). TON = 180 and $\text{TOF}_{1\text{h}}$ = 79 h^{-1} were obtained at 40 °C using a 2:FA ratio of 1:1000 (entry 17) after 3 h. To test higher temperature conditions, PC was used as a solvent. In this case, complete conversion (TON = 1000) was achieved at 80 °C after only 30 min, with a high $\text{TOF}_{1\text{h}}$ = 1000 h^{-1} (entry 19).

The effect of catalyst loading was studied in the case of reactions catalyzed by **2**.

When a catalyst to substrate ratio of 1:10000 was used at 60 °C with a FA concentration of 10.0 mol/L in THF, TON = 2245 was achieved after 6 h with a 22% conversion (Table 1, entry 20). When the test was run in PC at 80 °C, full conversion was reached within the same period, giving a rewarding TON of ca. 10000 (entry 21). Decreasing the FA

Scheme 1. Proposed Simplified Catalytic Cycle for FA Dehydrogenation Catalyzed by **1** and **2** (R = *i*Pr; R' = H, Me)



Scheme 2. Effect of Excess FA and Added Base on the Shift of the ^1H NMR Hydride Resonance of 4

concentration to 5.0 mol/L led to a significant decrease in the catalyst activity with a TON of 6286 and a conversion of 63% at 80 °C (entry 22).

Complex 3 was inactive in FA dehydrogenation in the absence of amine (entry 23), similarly to Milstein's catalyst,¹⁴ whereas it gave activity comparable to that of 1 and 2 in the presence of NEt_3 under the same test conditions (Table 1, entry 24 vs 7 and 9).

Then, a series of experiments with 2 were carried out to test catalyst deactivation vs product inhibition, by adding neat HCOOH aliquots (0.47 mL each) after the first run had reached 50% substrate conversion (see the Experimental Section). Using this procedure, an overall TON = 12170 was reached after ca. 8.5 h with an initial catalyst to substrate ratio of 1:5000 on running the test in PC at 80 °C. A decrease in activity was observed after the fourth addition. At an initial catalyst to substrate ratio of 1:1000, a higher number of consecutive cycles (11) was possible, reaching however a lower overall TON = 5574 after 4.5 h (see Table S7 and Figure S7 in the Supporting Information). Complex 3 (1:5000 catalyst to substrate ratio) gave results comparable to those for 2 under otherwise identical conditions (overall TON = 12300 after ca. 9 h).

Mechanistic Studies. A plausible mechanism for the catalytic dehydrogenation of formic acid with our complexes is outlined in Scheme 1. On the basis of our recent studies¹⁷ related to carbon dioxide hydrogenation, i.e. the reverse reaction of FA dehydrogenation, using catalysts 1 and 2, we

envisage that the latter proceeds via a very similar but reverse reaction pathway. The precatalysts (1 and 2) are activated by bromide abstraction, giving the coordinatively unsaturated cationic intermediate $[\text{Fe}(\text{PNP-}i\text{Pr})(\text{H})(\text{CO})]^+$ (4'). Subsequently, the formate ion may coordinate the iron metal center on the vacant site via the O atom, resulting in neutral $[\text{Fe}(\text{PNP}^{\text{Me}}-i\text{Pr})(\text{H})(\text{CO})(\eta^1\text{-OCOH})]$ (4). Then, the formate ligand switches from $\eta^1\text{-O}$ to $\eta^1\text{-H}$ coordination to Fe. Facile carbon dioxide elimination occurs, yielding 3, which upon hydride protonation releases H_2 to give back 4'.

To understand the role of the base in the mechanism, we performed a series of stoichiometric NMR experiments on the reactivity of precatalyst 2 with FA. No reaction could be observed after the addition of 10 equiv of neat FA to a solution of 2 in THF (with 20% C_6D_6 for deuterium lock), even upon heating the NMR tube to 60 °C for 1 h. On the other hand, when the experiment was repeated adding also 10 equiv of NEt_3 under otherwise identical conditions, the spectra revealed partial formation of complex 4 (ca. 25% on the basis of integration) and conversion of the substrate, as demonstrated by a decrease in the signals due to free formate. These observations confirm that a base is needed to activate the precatalyst, facilitating bromide dissociation and freeing a coordination site on the metal center.

It was observed experimentally (see above) that another role of amine is to promote catalytic turnover. This was confirmed by NMR experiments showing that addition of FA (1 equiv) to a solution of 3 in THF/ C_6D_6 (20%) caused immediate

formation of **4**, as demonstrated by the disappearance of the ^1H NMR triplet at -8.76 ppm ($J_{\text{PH}} = 42.9$ Hz) due to **3** and the appearance of a new triplet due to **4** at -24.4 ppm. Under these conditions, **4** proved to be stable in solution without evolving further. In a separate NMR experiment, addition of a known excess of FA (100 equiv) led to a slight shift of the hydride resonance of **4** in the ^1H NMR spectrum (-25.1 ppm), along with a significant color change of the respective solution from orange to bright yellow (Scheme 2). When NEt_3 (1 equiv to FA) was placed in the NMR tube, the hydride resonance shifted back to its initial value and also the color of the reaction solution turned back to orange.

We attribute this upfield shift of the hydride resonance to the change from an anionic (formate) to a neutral (FA) oxygen ligand coordinated trans to it. An excess of FA might thus lead to substitution/reprotonation of the formate ligand, resulting in the cationic complex $[\text{Fe}(\text{PNP}^{\text{Me}}\text{-iPr})(\text{H})(\text{CO})(\eta^1\text{-HCOOH})](\text{HCO}_2)$ (**5**), which in turn gives back **4** in the presence of added base.

The trend of the hydride resonances to shift toward more negative values is known for similar systems.^{16c,h,19} In our case, DFT calculations confirmed the chemical shift trend (see Scheme S1 in the Supporting Information). Thus, the role of the base in this step is to deprotonate the formic acid ligand in **5** to give back **4**, which in turn eliminates CO_2 and regenerates **3** by β -hydride elimination, closing the catalytic cycle.

CONCLUSIONS

In summary, we have shown that $\text{Fe}(\text{PNP})$ pincer-type complexes bearing the easily accessible and tunable 2,6-diaminopyridine scaffold are efficient catalysts for selective formic acid dehydrogenation, in the presence of added base, under mild reaction conditions. Studies are in progress to fine-tune the structure of the complexes in order to obtain more robust catalysts, allowing for improved long-term stability and more efficient recycling.

EXPERIMENTAL SECTION

General Methods and Materials. Complexes **1–3** were prepared according to recently reported procedures.^{16c} Formic acid, triethylamine, dimethyloctylamine, and DBU were purchased from commercial suppliers and degassed under nitrogen prior to use. All manipulations were carried out using standard Schlenk and glovebox techniques. Solvents were freshly distilled over appropriate drying agents, collected over Linde type 3 or 4 Å molecular sieves under nitrogen, and degassed with nitrogen or argon gas. Deuterated solvents for NMR measurements were purchased from commercial suppliers and stored onto activated 4 Å molecular sieves under Ar before use. The ^1H , $^{13}\text{C}\{^1\text{H}\}$, and $^{31}\text{P}\{^1\text{H}\}$ NMR spectra were recorded on a Bruker AVANCE-250 spectrometer (operating at 250.13, 101.26, and 62.90 MHz, respectively), on a Bruker Avance II 300 spectrometer (operating at 300.13, 75.47, and 121.50 MHz, respectively), and on a Bruker Avance II 400 spectrometer (operating at 400.13, 100.61, and 161.98 MHz, respectively) at room temperature. Peak positions are relative to tetramethylsilane and were calibrated against the residual solvent resonance (^1H) or the deuterated solvent multiplet (^{13}C). $^{31}\text{P}\{^1\text{H}\}$ NMR spectra were referenced to 85% H_3PO_4 , with downfield shifts taken as positive.

Typical Procedure for FA Dehydrogenation Tests. In a typical experiment, a solution of catalyst (typically 0.010 mmol) in THF (2.0 mL) was placed under a nitrogen atmosphere in a magnetically stirred glass reaction vessel thermostated by external liquid circulation and connected to a reflux condenser and gas buret (2 mL scale). After the solution was heated to the desired temperature, NEt_3 (1.38 mL, 0.01 mol) and FA (0.38 mL, 0.01 mol) were added and the experiment was

started. The gas evolution was monitored throughout the experiment by reading the values of liquid displacement reached on the burets. The gas mixtures were analyzed off-line by FTIR spectroscopy using a 10 cm gas cell (KBr windows) to check for CO formation (detection limit 0.02%).²⁰ Each test was repeated at least twice for reproducibility.

Typical Procedure for Slow Substrate Feed Experiments. In a typical experiment carried out with the experimental setup described above, using either **2** or **3** (0.005 mmol), FA (initial amount 50 mmol), and NEt_3 (50 mmol) at a set temperature of 80 °C in PC as solvent, once 50% of the initial amount of FA had converted, neat FA (0.47 mL, 12.5 mmol) was added by syringe to the reaction vessel. The procedure was repeated until no further gas evolution was observed.

ASSOCIATED CONTENT

Supporting Information

The Supporting Information is available free of charge on the ACS Publications website at DOI: 10.1021/acs.organomet.6b00551.

Additional tables for catalytic tests for screening of various effects and corresponding reaction profiles and computational details for **4'** and **5** (PDF)

Cartesian coordinates for the calculated structure of **4'** (XYZ)

Cartesian coordinates for the calculated structure of **5** (XYZ)

AUTHOR INFORMATION

Corresponding Authors

*E-mail for K.K.: karl.kirchner@tuwien.ac.at.

*E-mail for L.G.: lgonsalvi@iccom.cnr.it.

Author Contributions

All authors have given approval to the final version of the manuscript.

Notes

The authors declare no competing financial interest.

ACKNOWLEDGMENTS

Financial contributions by the ECRF through projects HYDROLAB-2.0 and ENERGYLAB are gratefully acknowledged. This work was also supported by COST Action CM1205 CARISMA (Catalytic Routines for Small Molecule Activation) through an STSM for N.G. to the CNR. N.G. and K.K. gratefully acknowledge financial support by the Austrian Science Fund (FWF) (Project No. P28866–N34).

REFERENCES

- (1) (a) *Hydrogen as a future energy carrier*; Züttel, A., Boggschulte, A., Schlapbach, L., Eds.; Wiley: Hoboken, NJ, 2011. (b) Mazloomi, K.; Gomes, C. *Renewable Sustainable Energy Rev.* **2012**, *16*, 3024–3033. (c) Turner, J. A. *Science* **2004**, *305*, 972–974.
- (2) Crabtree, G. W.; Dresselhaus, M. S.; Buchanan, M. V. *Phys. Today* **2004**, *57*, 39–44.
- (3) (a) Schlapbach, L.; Züttel, A. *Nature* **2001**, *414*, 353–358. (b) Eberle, U.; Felderhoff, M.; Schüth, F. *Angew. Chem.* **2009**, *121*, 6732–6757.
- (4) (a) Darkrim, F. L.; Malbrunot, P.; Tartaglia, G. P. *Int. J. Hydrogen Energy* **2002**, *27*, 193–202. (b) Ströbel, R.; Garcke, J.; Moseley, P. T.; Jörissen; Wolf, L. G. *J. Power Sources* **2006**, *159*, 781–801.
- (5) (a) Sakintuna, B.; Lamari-Darkrim, F.; Hirscher, M. *Int. J. Hydrogen Energy* **2007**, *32*, 1121–1140. (b) Ley, M. B.; Jepsen, B.; Lars, H.; Young-Su, L.; Young-Whan, C.; von Colbe, B.; Dornheim, J. M.; Rokni, M.; Jensen, M.; Sloth, J. O.; Filinchuk, M.; Jørgensen, Y.

- Besenbacher, J. E.; Jensen, F.; Torben, R. *Mater. Today* **2014**, *17*, 122–128.
- (6) Langmi, H. W.; Ren, J.; North, B.; Mathe, M. K.; Bessarabov, D. *Electrochim. Acta* **2014**, *128*, 368–392.
- (7) (a) Okada, Y.; Sasaki, E.; Watanabe, E.; Hyodo, S.; Nishijima, H. *Int. J. Hydrogen Energy* **2006**, *31*, 1348–1356. (b) Wang, Z.; Tonks, I.; Belli, J.; Jensen, C. M. *J. Organomet. Chem.* **2009**, *694*, 2854–2857. (c) Wang, J.; Zhang, X. B.; Wang, Z.-L.; Wang, L.-M.; Zhang, Y. *Energy Environ. Sci.* **2012**, *5*, 6885–6888. (d) Johnson, T. C.; Morris, D. J.; Wills, M. *Chem. Soc. Rev.* **2010**, *39*, 81–88. (e) Alsabeh, P. G.; Mellmann, D.; Junge, H.; Beller, M. *Top. Organomet. Chem.* **2014**, *48*, 45–80. (f) Nielsen, M.; Alberico, E.; Baumann, W.; Drexler, H.-J.; Junge, H.; Gladiali, S.; Beller, M. *Nature* **2013**, *495*, 85–89. (g) Zeng, G.; Sakaki, S.; Fujita, K. I.; Sano, H.; Yamaguchi, R. *ACS Catal.* **2014**, *4*, 1010–1020. (h) Polukeev, A. V.; Petrovskii, P. V.; Peregudov, A. S.; Ezernitskaya, M. G.; Koridze, A. A. *Organometallics* **2013**, *32*, 1000–1015. (i) Kawahara, R.; Fujita, K. I.; Yamaguchi, R. *J. Am. Chem. Soc.* **2012**, *134*, 3643–3646. (j) Spasyuk, D.; Smith, S.; Gusev, D. G. *Angew. Chem., Int. Ed.* **2012**, *51*, 2772–2775. (l) Putignano, E.; Bossi, G.; Rigo, P.; Baratta, W. *Organometallics* **2012**, *31*, 1133–1142. (m) Bertoli, M.; Choualeb, A.; Lough, A. J.; Moore, B.; Spasyuk, D.; Gusev, D. G. *Organometallics* **2011**, *30*, 3479–3482. (n) Baratta, W.; Boss, G.; Putignano, E.; Rigo, P. *Chem. - Eur. J.* **2011**, *17*, 3474–3481. (o) Alberico, E.; Sponholz, P.; Cordes, C.; Nielsen, M.; Drexler, H. J.; Baumann, W.; Junge, H.; Beller, M. *Angew. Chem., Int. Ed.* **2013**, *52*, 14162–14166.
- (8) (a) Joó, F. *ChemSusChem* **2008**, *1*, 805–808. (b) Enthaler, S.; von Langermann, J.; Schmidt, T. *Energy Environ. Sci.* **2010**, *3*, 1207–1217. (c) Loges, B.; Boddien, A.; Gärtner, F.; Junge, H.; Beller, M. *Top. Catal.* **2010**, *53*, 902–914.
- (9) (a) Gao, Y.; Kuncheria, J.; Puddephatt, R. J.; Yap, G. P. A. *Chem. Commun.* **1998**, 2365–2366. (b) Fellay, C.; Dyson, P. J.; Laurenczy, G. *Angew. Chem., Int. Ed.* **2008**, *47*, 3966–3968. (c) Loges, B.; Boddien, A.; Junge, H.; Beller, M. *Angew. Chem., Int. Ed.* **2008**, *47*, 3962–3965. (d) Boddien, A.; Loges, B.; Junge, H.; Beller, M. *ChemSusChem* **2008**, *1*, 751–758. (e) Majewski, A.; Morris, D. J.; Kendall, K.; Wills, M. *ChemSusChem* **2010**, *3*, 431–434. (f) Boddien, A.; Loges, B.; Junge, H.; Gärtner, F.; Noyes, J. R.; Beller, M. *Adv. Synth. Catal.* **2009**, *351*, 2517–2520. (g) Li, X.; Ma, X.; Shi, F.; Deng, Y. *ChemSusChem* **2010**, *3*, 71–74. (h) Boddien, A.; Gärtner, F.; Federsel, C.; Sponholz, P.; Mellmann, D.; Jackstell, R.; Junge, H.; Beller, M. *Angew. Chem., Int. Ed.* **2011**, *50*, 6411–6414. (i) Boddien, A.; Federsel, C.; Sponholz, P.; Mellmann, D.; Jackstell, R.; Junge, H.; Laurenczy, G.; Beller, M. *Energy Environ. Sci.* **2012**, *5*, 8907–8911. (j) Rodriguez-Lugo, R. E.; Trincado, M.; Vogt, M.; Tewes, F.; Santiso-Quinones, G.; Grützmacher, H. *Nat. Chem.* **2013**, *5*, 342–347. (k) Mellone, I.; Peruzzini, M.; Rosi, L.; Mellmann, D.; Junge, H.; Beller, M.; Gonsalvi, L. *Dalton Trans.* **2013**, *42*, 2495–2501. (l) Sponholz, P.; Mellmann, D.; Junge, H.; Beller, M. *ChemSusChem* **2013**, *6*, 1172–1176. (m) Czaun, M.; Goepfert, A.; Kothandaraman, J.; May, R. B.; Haiges, R. G.; Prakash, K. S.; Olah, G. A. *ACS Catal.* **2014**, *4*, 311–320. (n) Filonenko, G. A.; Putten, R. V.; Schulpen, E. N.; Hensen, M. E. J.; Pidko, E. A. *ChemCatChem* **2014**, *6*, 1526–1530. (o) Pan, Y.; Pan, C.-L.; Zhang, Y.; Li, H.; Min, S.; Guo, X.; Zheng, B.; Chen, H.; Anders, A.; Lai, Z.; Zheng, J.; Huang, K.-W. *Chem. - Asian J.* **2016**, *11*, 1357–1360.
- (10) (a) Himeda, Y. *Green Chem.* **2009**, *11*, 2018–2022. (b) Tanaka, R.; Yamashita, M.; Chung, L. W.; Morokuma, K.; Nozaki, K. *Organometallics* **2011**, *30*, 6742–6750. (c) Hull, J. F.; Himeda, Y.; Wang, W. H.; Hashiguchi, B.; Periana, R.; Szalda, D. J.; Muckerman, J. T.; Fujita, E. *Nat. Chem.* **2012**, *4*, 383–388. (d) Maenaka, Y.; Suenobu, T.; Fukuzumi, S. *Energy Environ. Sci.* **2012**, *5*, 7360–7367. (e) Barnard, J. H.; Wang, C.; Berry, N. G.; Xiao, C. *Chem. Sci.* **2013**, *4*, 1234–1244. (f) Fukuzumi, S.; Kobayashi, T.; Suenobu, T. *J. Am. Chem. Soc.* **2010**, *132*, 1496–1497. (g) Oldenhof, S.; de Bruin, B.; Lutz, M.; Siegler, M. A.; Patureau, F. W.; van der Vlugt, J. I.; Reek, J. N. H. *Chem. - Eur. J.* **2013**, *19*, 11507–11511. (h) Suna, Y.; Ertem, M. Z.; Wang, W. H.; Kambayashi, H.; Manaka, Y.; Muckerman, J. T.; Fujita, E.; Himeda, Y. *Organometallics* **2014**, *33*, 6519–6530. (i) Wang, W. H.; Xu, S.; Manaka, Y.; Suna, Y.; Kambayashi, H.; Muckerman, J. T.; Fujita, E.; Himeda, Y. *ChemSusChem* **2014**, *7*, 1976–1983. (j) Wang, Z.; Lu, S.-M.; Li, J.; Wang, J.; Li, C. *Chem. - Eur. J.* **2015**, *21*, 12592–12595. (k) Papp, G.; Olveti, G.; Horváth, H.; Kathó, Á.; Joó, F. *Dalton Trans.* **2016**, DOI: 10.1039/C6DT01695B. (l) Celaje, J. J. A.; Lu, Z.; Kedzie, E. A.; Terrile, N. J.; Lo, J. N.; Williams, T. J. *Nat. Commun.* **2016**, *7*, 11308.
- (11) Boddien, A.; Mellmann, D.; Gaertner, F.; Jackstell, R.; Junge, H.; Dyson, P. J.; Laurenczy, G.; Ludwig, R.; Beller, M. *Science* **2011**, *333*, 1733–1736.
- (12) Bertini, F.; Mellone, I.; Ienco, A.; Peruzzini, M.; Gonsalvi, L. *ACS Catal.* **2015**, *5*, 1254–1265.
- (13) Montandon-Clerc, M.; Dalebrook, A. F.; Laurenczy, G. *J. Catal.* **2015**, DOI: 10.1016/j.jcat.2015.11.012.
- (14) Zell, T.; Butschke, B.; Ben-David, Y.; Milstein, D. *Chem. - Eur. J.* **2013**, *19*, 8068–8072.
- (15) Bielinski, E. A.; Lagaditis, P. O.; Zhang, Y.; Mercado, B. Q.; Würtele, C.; Bernskoetter, W. H.; Hazari, N.; Schneider, S. *J. Am. Chem. Soc.* **2014**, *136*, 10234–10237.
- (16) (a) Bichler, B.; Glatz, M.; Stöger, B.; Mereiter, K.; Veiros, L. F.; Kirchner, K. *Dalton Trans.* **2014**, *43*, 14517–15419. (b) de Aguiar, S. R. M. M.; Öztöpcü, Ö.; Stöger, B.; Mereiter, K.; Veiros, L. F.; Pittenauer, E.; Allmaier, G.; Kirchner, K. *Dalton Trans.* **2014**, *43*, 14669–14679. (c) Gorgas, N.; Stöger, B.; Veiros, L. F.; Pittenauer, E.; Allmaier, G.; Kirchner, K. *Organometallics* **2014**, *33*, 6905–6914. (d) Bichler, B.; Holzhaacker, C.; Stöger, B.; Puchberger, M.; Veiros, L. F.; Kirchner, K. *Organometallics* **2013**, *32*, 4114–4121. (e) Benito-Garagorri, D.; Becker, E.; Wiedermann, J.; Lackner, W.; Pollak, M.; Mereiter, K.; Kivala, J.; Kirchner, K. *Organometallics* **2006**, *25*, 1900–1913. (f) Benito-Garagorri, D.; Wiedermann, J.; Pollak, M.; Mereiter, K.; Kirchner, K. *Organometallics* **2007**, *26*, 217–222. (g) Benito-Garagorri, D.; Puchberger, M.; Mereiter, K.; Kirchner, K. *Angew. Chem., Int. Ed.* **2008**, *47*, 9142–9145. (h) Gorgas, N.; Stöger, B.; Veiros, L. F.; Kirchner, K. *ACS Catal.* **2016**, *6*, 2664–2672.
- (17) Bertini, F.; Gorgas, N.; Stöger, B.; Peruzzini, M.; Veiros, L. F.; Kirchner, K.; Gonsalvi, L. *ACS Catal.* **2016**, *6*, 2889–2893.
- (18) Junge, H.; Boddien, A.; Capitta, F.; Loges, B.; Noyes, J. R.; Gladiali, S.; Beller, M. *Tetrahedron Lett.* **2009**, *50*, 1603–1606.
- (19) Langer, R.; Iron, M. A.; Konstantinovski, L.; Diskin-Posner, Y.; Leitun, G.; Ben-David, Y.; Milstein, D. *Chem. - Eur. J.* **2012**, *18*, 7196–7209.
- (20) Gas mixture analyses were carried out by FTIR spectroscopic methods described in previous publications. For details see: (a) Morris, D. J.; Clarkson, G. J.; Wills, M. *Organometallics* **2009**, *28*, 4133–4140. (b) Guerriero, A.; Bricout, H.; Sordakis, K.; Peruzzini, M.; Monflier, E.; Hapiot, F.; Laurenczy, G.; Gonsalvi, L. *ACS Catal.* **2014**, *4*, 3002–3012.

SUPPORTING INFORMATION

Selective formic acid dehydrogenation catalyzed by Fe-PNP pincer complexes based on the 2,6-diaminopyridine scaffold

Irene Mellone,^a Nikolaus Gorgas,^b Maurizio Peruzzini,^a Karl Kirchner,^{*,b} and Luca Gonsalvi^{*,a}

^a Consiglio Nazionale delle Ricerche (CNR), Istituto di Chimica dei Composti Organometallici (ICCOM), Via Madonna del Piano 10, 50019 Sesto Fiorentino (Firenze), Italy.

^b Institute of Applied Synthetic Chemistry, Vienna University of Technology, Getreidemarkt 9/163-AC, A-1060 Wien, Austria.

1. General Methods and Materials
2. Additional Tables and Reaction Profiles
3. DFT Calculations
4. References

1. GENERAL METHODS AND MATERIALS

All manipulations were carried out using standard schlenk and glovebox techniques. Solvents were freshly distilled over appropriate drying agents, collected over Linde type 3Å or 4Å molecular sieves under nitrogen, and degassed with nitrogen or argon gas. Deuterated solvents for NMR measurements were purchased from commercial suppliers and stored onto activated 4Å molecular sieves under Ar before use. The ^1H , $^{13}\text{C}\{^1\text{H}\}$, and $^{31}\text{P}\{^1\text{H}\}$ NMR spectra were recorded on a Bruker AVANCE-250 spectrometer (operating at 250.13, 101.26, and 62.90 MHz, respectively), on a Bruker Avance II 300 spectrometer (operating at 300.13, 75.47, and 121.50 MHz, respectively) and a Bruker Avance II 400 spectrometer (operating at 400.13, 100.61, and 161.98 MHz, respectively) at room temperature. Peak positions are relative to tetramethylsilane and were calibrated against the residual solvent resonance (^1H) or the deuterated solvent multiplet (^{13}C). $^{31}\text{P}\{^1\text{H}\}$ NMR were referenced to 85% H_3PO_4 , with the downfield shift taken as positive.

2. ADDITIONAL TABLES AND REACTION PROFILES

Table S1. Effect of the FA/NEt₃ ratio on the catalytic activity of **2**.^[a]

Entry	NEt ₃ (mol%)	TOF _{1h} ^[b]	TON ^[c]	conversion (%)
1	25	102	204 (3)	20
2	50	276	653 (3)	65
3	100	398	816 (3)	82
4	200	418	827 (3)	83

^[a] Reaction conditions: **2** (0.01 mmol); FA (10 mmol); specified amount of NEt₃, THF (4.0 mL), 60 °C. Gas evolution measured by manual gas buret. ^[b] Defined as mmol_{H₂ produced} / mmol_{catalyst} × h⁻¹ (calculated after 1h). ^[c] Defined as mmol_{H₂ produced} / mmol_{catalyst}. Run time (h) in parenthesis.

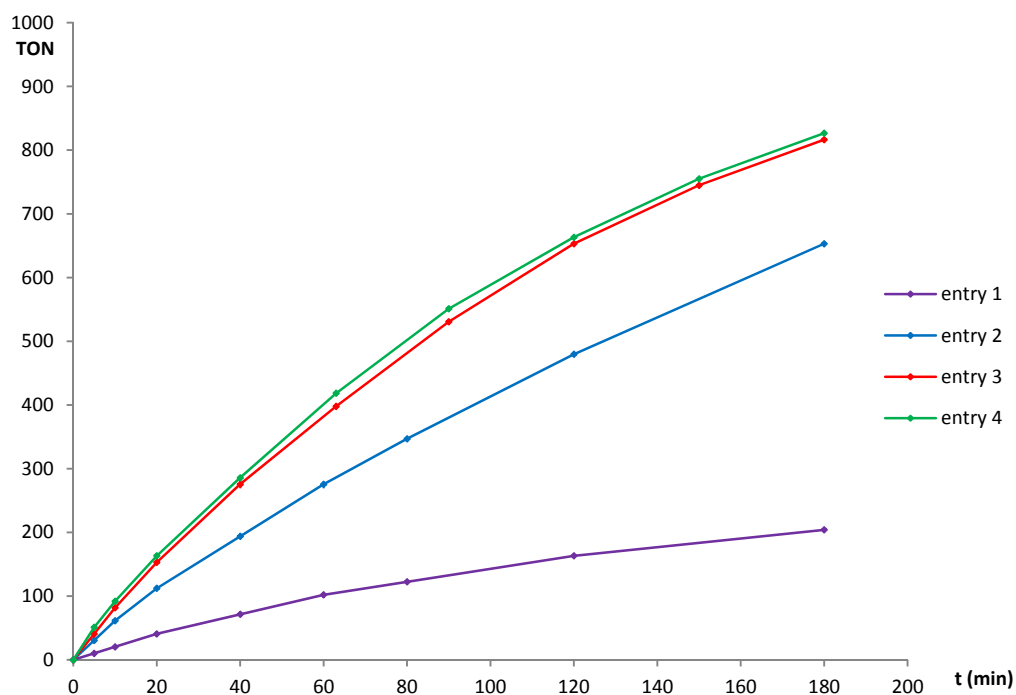


Table S2. Effect of different solvents on the catalytic activity of **2**.^[a]

Entry	solvent	TOF _{1h} ^[b]	TON ^[c]	conversion (%)
1	THF	612	1000 (3)	100
2	PC	500	1000 (3)	100
3	dioxane	378	878 (3)	88
4	EtOH	165	650 (3)	65

^[a] Reaction conditions: **2** (0.01 mmol); FA (10 mmol); NEt₃ (100 mol%), solvent (2.0 mL), 60 °C. Gas evolution measured by manual gas buret. ^[b] Defined as mmol_{H₂} produced / mmol_{catalyst} × h⁻¹ (calculated after 1h). ^[c] Defined as mmol_{H₂} produced / mmol_{catalyst}. Run time (h) in parenthesis.

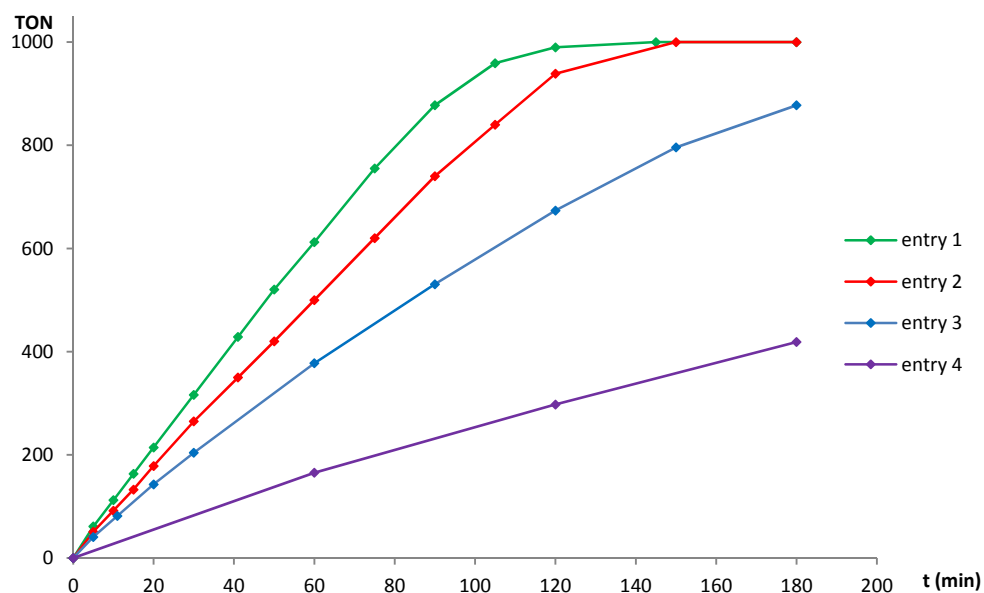


Table S3. Effect of different amines on the catalytic activity of **2**.^[a]

Entry	amine (mol%)	TOF _{1h} ^[b]	TON ^[c]	conv. (%)
1	NEt ₃ (50)	593	980 (3)	98
2	DMOA (50)	673	980 (3)	98
3	DBU (50)	459	571 (3)	57

^[a] Reaction conditions: **2** (0.01 mmol); FA (10 mmol); specified amine (50 mol%), THF (2.0 mL), 60 °C. Gas evolution measured by manual gas buret. ^[b] Defined as $\text{mmol}_{\text{H}_2 \text{ produced}} / \text{mmol}_{\text{catalyst}} \times \text{h}^{-1}$ (calculated after 1h). ^[c] Defined as $\text{mmol}_{\text{H}_2 \text{ produced}} / \text{mmol}_{\text{catalyst}}$. Run time (h) in parenthesis.

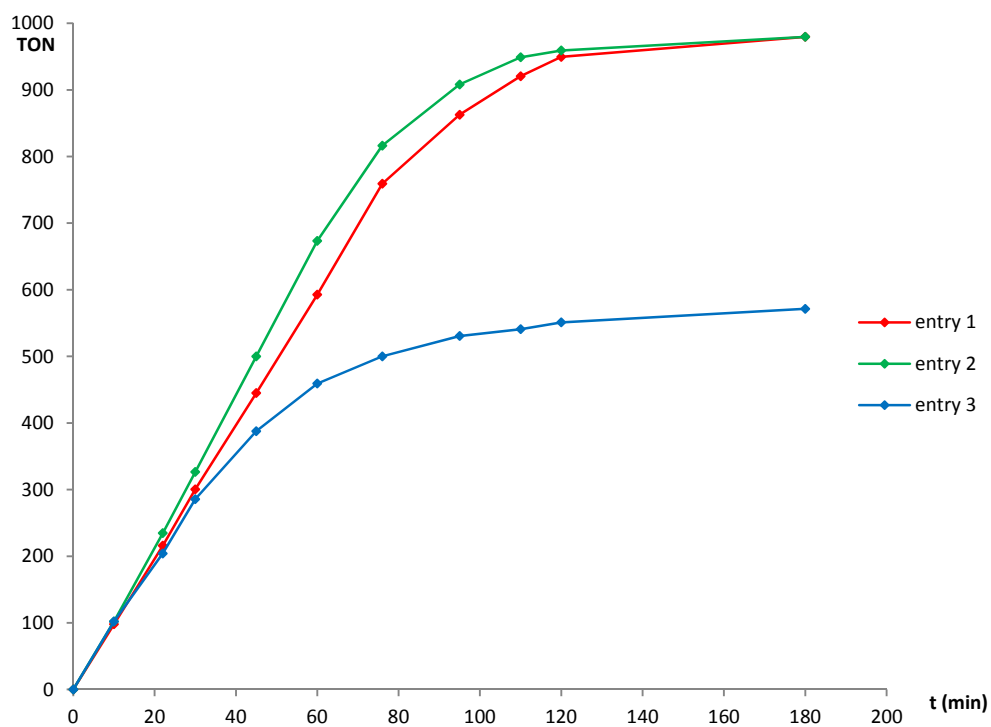


Table S4. Effect of the reaction temperature on the catalytic activity of **2**.

Entry	Solvent	T (°C)	TOF _{1h} ^[b]	TON ^[c]	conv. (%)
1	THF	40	79	180 (3)	18
2	THF	60	612	1000 (3)	100
3	PC	60	500	1000 (3)	100
4	PC	80	1800 ^[c]	1000 (0.6)	100

^[a] Reaction conditions: **2** (0.01 mmol); FA (10 mmol); NEt₃ (100 mol%), solvent (2.0 mL). Gas evolution measured by manual gas buret.

^[b] Defined as mmol_{H₂ produced} / mmol_{catalyst} × h⁻¹ (calculated after 1h). ^[c] Defined as mmol_{H₂ produced} / mmol_{catalyst}. Run time (h) in parenthesis.

^[c] TOF calculated after 20 min due to fast reaction.

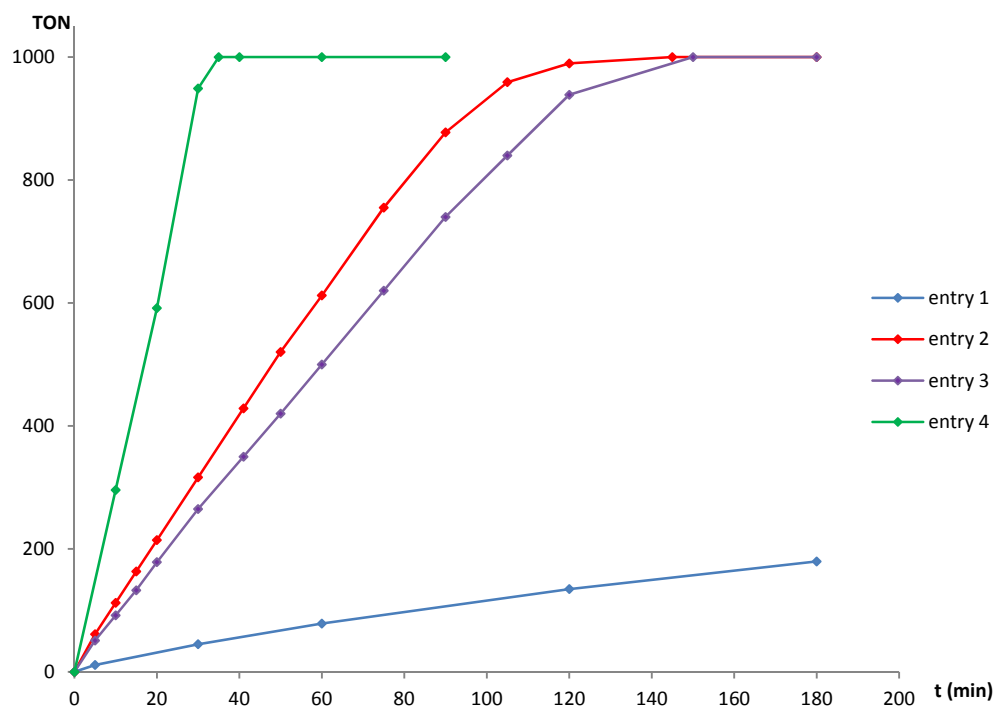


Table S5. Effect of the substrate concentration on the catalytic activity of **2**.

Entry	[FA] (mol/L)	TOF _{1h} ^[d]	TON ^[e]	conversion (%)
1 ^[a]	2.5	398	816 (3)	82
2 ^[b]	5.0	612	1000 (2.5)	100
3 ^[c]	10.0	770	1000 (2)	100

Reaction conditions: ^[a] **2** (0.01 mmol); FA (10 mmol); NEt₃ (100 mol%), THF (4.0 mL), 60°C. ^[b] THF (2.0 mL). ^[c] THF (1.0 mL). Gas evolution measured by manual gas buret. ^[d] Defined as mmol_{H₂} produced / mmol_{catalyst} × h⁻¹ (calculated after 1 h). ^[e] Defined as mmol_{H₂} produced / mmol_{catalyst}. Run time (h) in parenthesis.

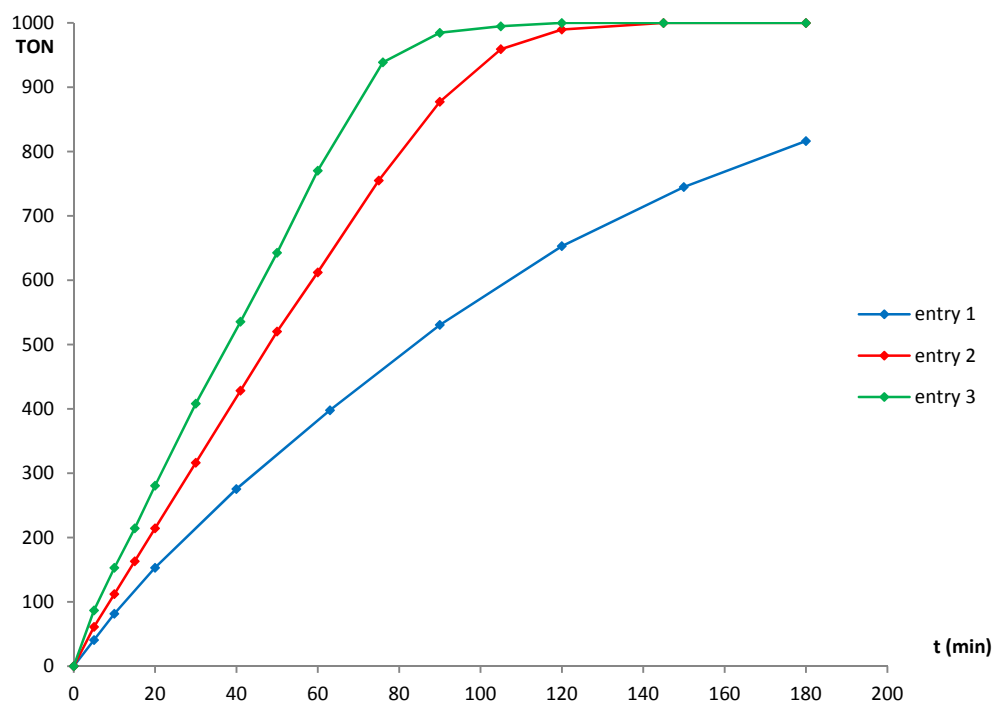


Table S6. Effect of low catalyst loading and temperature on the catalytic activity of **2**.

Entry	[FA](mol/L)	solvent	T (°C)	TOF _{1h} ^[d]	TON ^[e]	conversion (%)
1 ^[a]	10.0	THF	60	918	2245 (6)	22
2 ^[b]	5.0	PC	80	1714	6286 (6)	63
3 ^[c]	10.0	PC	80	2635	10000 (6)	100

Reaction conditions: ^[a] **2** (0.005 mmol); FA (50 mmol); NEt₃ (100 mol%), THF (5.0 mL), 60 °C. ^[b] **2** (0.005 mmol); FA (50 mmol); NEt₃ (100 mol%), PC (10.0 mL), 80 °C. ^[c] **2** (0.005 mmol); FA (50 mmol); NEt₃ (100 mol%), PC (5.0 mL), 80 °C. Gas evolution measured by manual gas buret. ^[d] Defined as mmol_{H2 produced} / mmol_{catalyst} × h⁻¹ (calculated after 1h). ^[e] Defined as mmol_{H2 produced} / mmol_{catalyst}. Run time (h) in parenthesis.

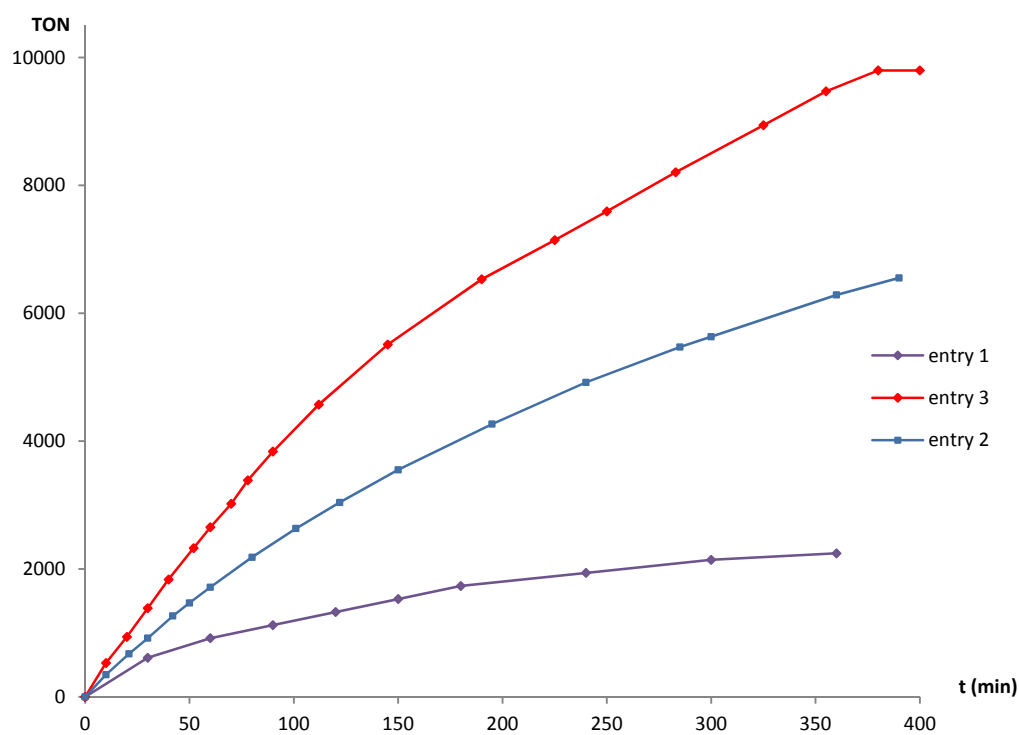
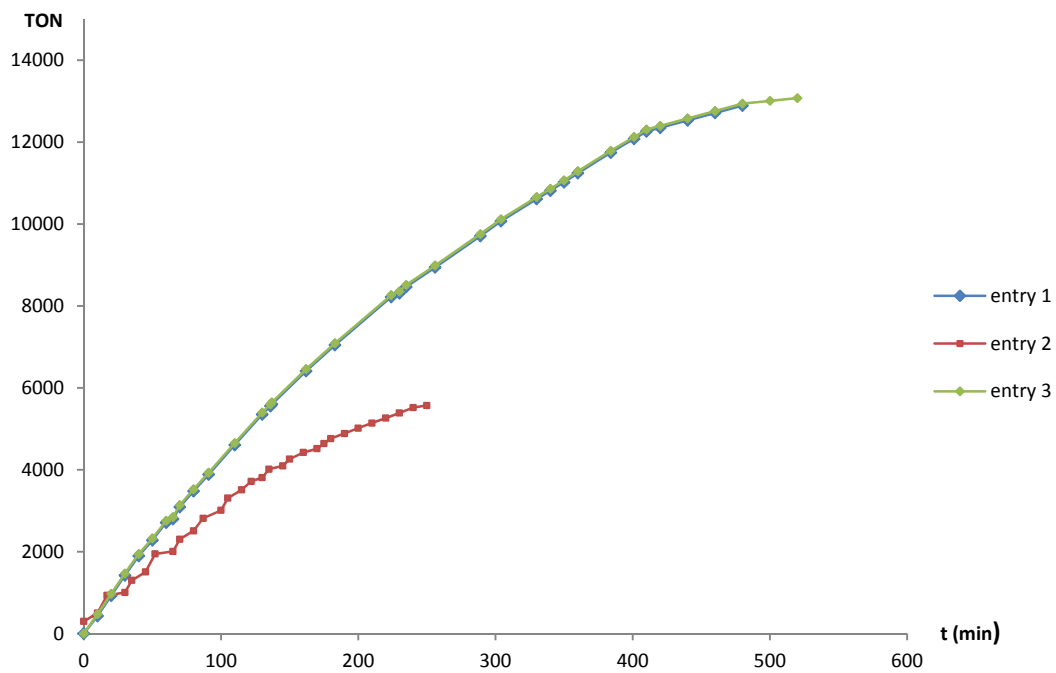


Table S7. Catalyst recycling by neat FA addition in the presence of **2** and **3** and NEt₃.

Entry	No. run	Initial FA/cat	TOF _{10 min} ^[d]	TON ^[e]	conversion (%)
1 ^[a]	1	5000	2574	2755	50 (65)
	2		2628	2755	50 (135)
	3		2439	2755	50 (230)
	4		2140	2755	50 (350)
	5		1874	2009	36 (520)
2 ^[b]	1	1000	1782	502	50 (17)
	2		1715	502	50 (35)
	3		1668	502	50 (52)
	4		1795	502	50 (70)
	5		1727	502	50 (87)
	6		1701	502	50 (105)
	7		1724	502	50 (122)
	8		1710	502	50 (145)
	9		1616	502	50 (175)
	10		1517	502	50 (210)
	11		1401	502	50 (250)
	12		1279	52	5 (270)
3 ^[c]	1	5000	2844	2755	50 (60)
	2		2664	2755	50 (130)
	3		2494	2755	50 (225)
	4		2141	2755	50 (345)
	5		1882	2122	38 (550)

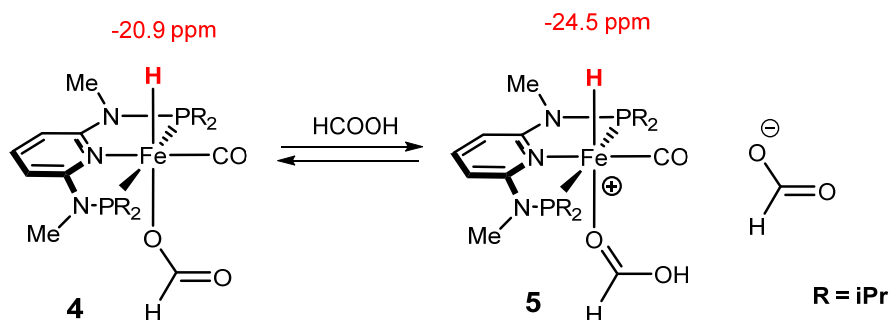
Reaction conditions: ^[a] **2** (0.005 mmol); FA (25 mmol, initial); NEt₃ (100 mol%), PC (5.0 mL), 80 °C. ^[b] **2** (0.01 mmol); FA (10 mmol, initial); NEt₃ (100 mol%), PC (5.0 mL), 80 °C. ^[c] **3** (0.005 mmol); FA (25 mmol, initial); NEt₃ (100 mol%), PC (5.0 mL), 80 °C. ^[d] Defined as mmol_{H₂} produced / mmol_{catalyst} × h⁻¹ (calculated after 10 min). ^[e] Defined as mmol_{H₂} produced / mmol_{catalyst}. Run time (min) in parenthesis.



Neat FA (12.5 mmol aliquots) added after 65, 135, 230, 350 min (entry 1); 17, 35, 52, 70, 87, 105, 122, 145, 175, 210, 250 min (entry 2); 60, 130, 225, 345 min (entry 3).

3. COMPUTATIONAL DETAILS

Calculations were performed using the GAUSSIAN 09 software package,¹ without symmetry constraints. The optimized geometries were obtained with the B3LYP functional.² That functional includes a mixture of Hartree-Fock³ exchange with DFT⁴ exchange-correlation, given by Becke's three parameter functional with the Lee, Yang and Parr correlation functional, which includes both local and non-local terms. The basis set used consists of the Stuttgart/Dresden ECP (SDD) basis set⁵ to describe the electrons of the iron atom, and a standard 6-31g(d,p) basis set⁶ for all other atoms. Frequency calculations were performed to confirm the nature of the stationary points yielding no imaginary frequency for the the minima. ¹H chemical shifts were calculated at the B3LYP level of theory for the optimized structures of *trans*-[Fe(PNP^{Me}-iPr)(H)(CO)(κ¹-OCOH)] (4) and *trans*-[Fe(PNP^{Me}-iPr)(H)(CO)(κ¹-HCOOH)]⁺ (5) using the gauge-independent atomic orbital (GIAO) method in Gaussian 09 with the above basis sets. Chemical shifts are given with respect to Si(Me₃)₄ (TMS) at the same computational level.⁷



Scheme S1. Calculated ¹H NMR hydride shifts for *trans*-[Fe(PNP^{Me}-iPr)(H)(CO)(κ¹-OCOH)] (4) and *trans*-[Fe(PNP^{Me}-iPr)(H)(CO)(κ¹-HCOOH)]⁺ (5).

Atomic coordinates

trans-[Fe(PNP^{Me}-iPr)(H)(CO)(κ¹-OCOH)] (4)

26	-0.006874000	-0.467660000	0.118446000	1	-2.145493000	-2.693205000	2.049140000
15	-2.210393000	-0.270927000	0.197924000	1	-3.556678000	-2.867483000	0.998851000
15	2.215235000	-0.187877000	0.143634000	1	-3.336280000	-0.418036000	3.826616000
7	-0.041874000	1.573026000	0.082817000	1	-2.782701000	0.985463000	2.899298000
7	-2.377999000	1.471292000	0.235813000	1	-1.677655000	-0.360115000	3.192637000
7	2.302602000	1.553367000	-0.045780000	1	2.315366000	-0.846229000	-2.082686000
6	-1.226375000	2.237750000	0.123117000	1	4.702571000	-0.863198000	-2.760337000
6	-1.288876000	3.639850000	0.054730000	1	5.211354000	-0.302972000	-1.168280000
6	-0.097776000	4.345099000	-0.040043000	1	4.202606000	0.728162000	-2.212532000
6	1.119221000	3.681482000	-0.067230000	1	3.601673000	-2.927572000	-2.036373000
6	1.116635000	2.274929000	-0.012370000	1	2.402786000	-2.959514000	-0.748164000
6	-3.216772000	-0.816056000	-1.308050000	1	4.109859000	-2.662820000	-0.367971000
6	-4.747554000	-0.845435000	-1.165956000	1	2.800958000	0.321545000	2.374446000
6	-2.692433000	-2.160806000	-1.849865000	1	3.167813000	-1.905737000	3.402692000
6	-3.201688000	-0.807331000	1.701011000	1	2.996090000	-2.695758000	1.833673000
6	-3.163294000	-2.336957000	1.870080000	1	1.619728000	-1.835305000	2.543653000
6	-2.718374000	-0.103400000	2.977711000	1	5.091081000	-0.596968000	2.730644000
6	3.103711000	-0.949703000	-1.327500000	1	5.097544000	0.503018000	1.358008000
6	4.378752000	-0.296750000	-1.879636000	1	5.124347000	-1.245631000	1.093587000
6	3.311835000	-2.458720000	-1.089787000	1	-0.000904000	-0.379224000	1.635835000
6	3.166040000	-0.505628000	1.750688000	6	0.020091000	-2.208455000	0.323813000
6	2.702448000	-1.816275000	2.414191000	8	0.037472000	-3.352070000	0.530918000
6	4.704014000	-0.450335000	1.715412000	6	3.549738000	2.318311000	-0.095755000
1	-2.235289000	4.159777000	0.057826000	1	3.668952000	2.949781000	0.794069000
1	-0.118700000	5.429621000	-0.096121000	1	4.393026000	1.638842000	-0.150263000
1	2.040947000	4.238051000	-0.139709000	1	3.582296000	2.956964000	-0.985531000
1	-2.947694000	-0.045318000	-2.041002000	6	-3.659951000	2.161584000	0.358463000
1	-5.191262000	-1.120028000	-2.129614000	1	-3.938700000	2.676911000	-0.569411000
1	-5.177085000	0.117840000	-0.879666000	1	-4.439349000	1.440518000	0.595047000
1	-5.076135000	-1.594496000	-0.438097000	1	-3.632482000	2.896404000	1.170974000
1	-3.220916000	-2.405297000	-2.778449000	8	0.118353000	-0.521569000	-1.937601000
1	-2.867653000	-2.984715000	-1.150167000	6	-0.052722000	0.418675000	-2.812792000
1	-1.625037000	-2.100647000	-2.067809000	8	0.512539000	0.508727000	-3.896862000
1	-4.244181000	-0.516538000	1.518401000	1	-0.800926000	1.200885000	-2.525457000
1	-3.774275000	-2.624062000	2.733172000				

trans-[Fe(PNP^{Me}-*i*Pr)(H)(CO)(κ¹-HCOOH)]⁺ (5)

26	0.054929000	-0.511116000	-0.003161000	1	3.589160000	-3.023477000	-0.597440000
15	2.272352000	-0.321273000	-0.187763000	1	3.261757000	-1.055561000	-3.778562000
15	-2.171597000	-0.299731000	-0.220593000	1	2.687154000	0.462765000	-3.078008000
7	0.063746000	1.489437000	-0.334507000	1	1.618189000	-0.944487000	-3.127305000
7	2.404271000	1.394956000	-0.507797000	1	-2.475790000	-0.649045000	2.086481000
7	-2.289573000	1.450788000	-0.275617000	1	-4.910314000	-0.601069000	2.525336000
6	1.243904000	2.152704000	-0.507473000	1	-5.259826000	-0.283965000	0.829973000
6	1.282284000	3.547395000	-0.675396000	1	-4.372176000	0.909134000	1.801809000
6	0.080271000	4.239705000	-0.709618000	1	-3.732144000	-2.729469000	2.212366000
6	-1.130493000	3.571897000	-0.584623000	1	-2.445156000	-2.935786000	1.028203000
6	-1.111150000	2.178634000	-0.401182000	1	-4.116369000	-2.693072000	0.493803000
6	3.344302000	-0.593449000	1.349106000	1	-2.527709000	-0.180319000	-2.544402000
6	4.868979000	-0.614493000	1.142196000	1	-2.834147000	-2.542309000	-3.215917000
6	2.889746000	-1.846720000	2.124122000	1	-2.828316000	-3.068462000	-1.533493000
6	3.189272000	-1.107196000	-1.620163000	1	-1.372628000	-2.345745000	-2.241125000
6	3.156570000	-2.643940000	-1.526767000	1	-4.786174000	-1.144495000	-2.954202000
6	2.652799000	-0.625273000	-2.976745000	1	-4.906062000	0.173077000	-1.799231000
6	-3.178870000	-0.863414000	1.273030000	1	-4.988602000	-1.507068000	-1.244943000
6	-4.503369000	-0.158096000	1.609654000	1	0.083220000	-0.736003000	-1.473164000
6	-3.370484000	-2.393936000	1.235168000	6	0.052261000	-2.269434000	0.156737000
6	-2.963313000	-0.891499000	-1.829299000	8	0.053354000	-3.426185000	0.192756000
6	-2.461758000	-2.297015000	-2.216013000	6	-3.548751000	2.182841000	-0.470002000
6	-4.497270000	-0.827810000	-1.946511000	1	-3.593501000	2.642293000	-1.464222000
1	2.220089000	4.072832000	-0.777069000	1	-4.385172000	1.501091000	-0.368538000
1	0.085791000	5.317186000	-0.843450000	1	-3.665922000	2.966517000	0.285865000
1	-2.059533000	4.118648000	-0.634725000	6	3.668435000	2.063354000	-0.836560000
1	3.094092000	0.285515000	1.959473000	1	3.999153000	2.730848000	-0.032150000
1	5.360865000	-0.716899000	2.115233000	1	4.443687000	1.318423000	-1.000378000
1	5.256873000	0.297036000	0.682408000	1	3.569792000	2.644481000	-1.758845000
1	5.184407000	-1.467141000	0.533423000	8	-0.031931000	-0.094836000	2.119843000
1	3.453709000	-1.917120000	3.060092000	6	0.054615000	0.919707000	2.785575000
1	3.080266000	-2.766020000	1.562878000	8	-0.073624000	0.872732000	4.105724000
1	1.827458000	-1.814834000	2.372172000	1	0.236104000	1.910979000	2.343589000
1	4.234132000	-0.788468000	-1.525707000	1	0.019773000	1.755013000	4.497466000
1	3.737866000	-3.066045000	-2.352706000				
1	2.137120000	-3.028627000	-1.610028000				

4. REFERENCES

-
- ¹ Gaussian 09, Revision A.02, Frisch, M. J.; Trucks, G. W.; Schlegel, H. B.; Scuseria, G. E.; Robb, M. A.; Cheeseman, J. R.; Scalmani, G.; Barone, V.; Mennucci, B.; Petersson, G. A.; Nakatsuji, H.; Caricato, M.; Li, X.; Hratchian, H. P.; Izmaylov, A. F.; Bloino, J.; Zheng, G.; Sonnenberg, J. L.; Hada, M.; Ehara, M.; Toyota, K.; Fukuda, R.; Hasegawa, J.; Ishida, M.; Nakajima, T.; Honda, Y.; Kitao, O.; Nakai, H.; Vreven, T.; Montgomery, Jr., J. A.; Peralta, J. E.; Ogliaro, F.; Bearpark, M.; Heyd, J. J.; Brothers, E.; Kudin, K. N.; Staroverov, V. N.; Kobayashi, R.; Normand, J.; Raghavachari, K.; Rendell, A.; Burant, J. C.; Iyengar, S. S.; Tomasi, J.; Cossi, M.; Rega, N.; Millam, J. M.; Klene, M.; Knox, J. E.; Cross, J. B.; Bakken, V.; Adamo, C.; Jaramillo, J.; Gomperts, R.; Stratmann, R. E.; Yazyev, O.; Austin, A. J.; Cammi, R.; Pomelli, C.; Ochterski, J. W.; Martin, R. L.; Morokuma, K.; Zakrzewski, V. G.; Voth, G. A.; Salvador, P.; Dannenberg, J. J.; Dapprich, S.; Daniels, A. D.; Farkas, Ö.; Foresman, J. B.; Ortiz, J. V.; Cioslowski, J.; Fox, D. J. Gaussian, Inc., Wallingford CT, **2009**.
- ² (a) Becke, A. D. *J. Chem. Phys.* **1993**, *98*, 5648-5652. (b) Miehlich, B.; Savin, A.; Stoll, H.; Preuss, H. *Chem. Phys. Lett.* **1989**, *157*, 200-206. (c) Lee, C.; Yang, W.; Parr, G. *Phys. Rev. B* **1988**, *37*, 785-789.
- ³ Hehre, W. J.; Radom, L.; Schleyer, P. v. R.; Pople, J. A., *Ab Initio Molecular Orbital Theory*. John Wiley & Sons, New York, **1986**.
- ⁴ Parr, R. G.; Yang, W. *Density Functional Theory of Atoms and Molecules*, Oxford University Press, New York, **1989**.
- ⁵ (a) Haeusermann, U.; Dolg, M.; Stoll, H.; Preuss, H. *Mol. Phys.* **1993**, *78*, 1211-1224. (b) Kuechle, W.; Dolg, M.; Stoll, H.; Preuss, H. *J. Chem. Phys.* **1994**, *100*, 7535-7542. (c) Leininger, T.; Nicklass, A.; Stoll, H.; Dolg, M.; Schwerdtfeger, P. *J. Chem. Phys.* **1996**, *105*, 1052-1059.
- ⁶ (a) Ditchfield, R.; Hehre, W. J.; Pople, J. A. *J. Chem. Phys.* **1971**, *54*, 724-728; (b) Hehre, W. J.; Ditchfield, R.; Pople, J. A. *J. Chem. Phys.* **1972**, *56*, 2257-2261; (c) Hariharan, P. C.; Pople, J. A. *Mol. Phys.* **1974**, *27*, 209-214; (d) Gordon, M. S. *Chem. Phys. Lett.* **1980**, *76*, 163-168; (e) Hariharan, P. C.; Pople, J. A. *Theor. Chim. Acta* **1973**, *28*, 213-222.

Abstract

This work describes the synthesis, characterization and catalytic application of a new class of well-defined iron based PNP-pincer complexes. In particular, iron hydride complexes of the type $[\text{Fe}(\text{PNP})(\text{H})(\text{CO})(\text{L})]$ have been prepared and tested as catalysts for the hydrogenative reduction of C-O double bonds. The metal center in these complexes is stabilized by PNP-pincer ligands that are based on 2,6-diaminopyridine scaffolds. In contrast to related pyridine derived pincer systems, these ligands allow for a modification of the linker's substituents, which might have a decisive impact on the reactivity of the corresponding complexes.

In the first part of this thesis is focused on the hydrogenative reduction of carbonyl compounds has been investigated. Complexes $[\text{Fe}(\text{PNP}^{\text{H-Pr}})(\text{H})(\text{CO})(\text{L})]$ containing labile co-ligands ($\text{L} = \text{Br}^-$, CH_3CN , BH_4^-) and N-H spacers are efficient catalysts for the hydrogenation of both ketones and aldehydes, while those containing inert ligands ($\text{L} = \text{pyridine}$, PMe_3 , SCN^- , CO) are catalytically inactive. Interestingly, complex $[\text{Fe}(\text{PNP}^{\text{Me-Pr}})(\text{H})(\text{CO})(\text{Br})]$, featuring N-Me spacers, is an efficiently catalyzes the hydrogenation of aldehydes, but was found to be unreactive towards ketones. Based on detailed experimental and computational studies, it could be shown that the hydrogenation of ketones takes place via an inner-sphere reaction mechanism in which the catalytically active species is formed upon deprotonation of one N-H group. The second type of catalysts instead proceed via a different intermediate, since they are not capable undergoing this type of metal ligand cooperation. Further studies on this catalyst revealed an outer-sphere mechanism, in which an iron(II) dihydride was identified to be the catalytically active species. This intermediate could even be isolated, structurally characterized and independently employed in catalytic hydrogenation reaction. This catalyst appeared to be highly active and productive achieving turnover numbers of up to 80.000 and TOFs of more than 20.000 h^{-1} . Moreover, a remarkable degree of chemoselectivity could be reached, as other reducible functionalities including ketones, conjugated C-C double bonds, esters, epoxides and nitrosyl groups remain unaffected in course of the reaction.

The second part of this work is concerned with the application of these complexes as catalysts in the reversible hydrogenation/dehydrogenation of carbon dioxide or formic acid, which is considered to serve as a potential hydrogen storage technology for future energy supply. Both complexes, those bearing N-H as well as those bearing N-Me linker substituents, were found to promote the catalytic hydrogenation of CO_2 and NaHCO_3 to formates, reaching quantitative yields and high TONs even under mild reaction conditions. NMR and DFT studies highlighted the role of dihydrido and hydrido formate complexes in catalysis, strongly resembling the mechanism previously proposed for the selective hydrogenation of aldehydes. Moreover, the described catalysts are also capable for the reverse dehydrogenation of formic acid to yield carbon dioxide and molecular hydrogen. Formic acid decomposition takes place in presence of a stoichiometric amount of triethyl amine reaching turnover numbers of more than 10.000.

Zusammenfassung

Die vorliegende Arbeit beschreibt die Synthese, Charakterisierung und katalytische Anwendung wohl-definierter Eisen Pincer-Komplexe. Im Speziellen wurden Eisen-Hydrid-Komplexe des Typs $[\text{Fe}(\text{PNP})(\text{H})(\text{CO})(\text{L})]$ hergestellt und als Katalysatoren für die Hydrierung von C-O Doppelbindungen getestet. Das Metallzentrum in diesen Komplexen wird durch sogenannte PNP-Pincer Liganden stabilisiert, welche auf einem 2,6-Diaminopyridine-Grundgerüst aufbauen. Im Gegensatz zu anderen Pyridin-basierten Pincer-Systemen können bei diesen Liganden unterschiedlich substituierte Linker eingeführt werden, welche in vielen Fällen weitreichende Auswirkungen auf die Reaktivität der resultierenden Komplexe haben können.

Im ersten Teil der Arbeit wurde die katalytische Hydrierung von Carbonylverbindungen untersucht. Komplexe des Typs $[\text{Fe}(\text{PNP-}i\text{Pr})(\text{H})(\text{CO})(\text{L})]$, welche sowohl über *N*-H Gruppen als auch über labile Co-Liganden ($\text{L} = \text{Br}^-$, CH_3CN , BH_4^-) verfügen, erwiesen sich als effiziente Katalysatoren für die Hydrierung von Aldehyden und Ketonen, während jene mit inerten Liganden ($\text{L} = \text{Pyridin}$, PMe_3 , SCN^- , CO) katalytisch inaktiv sind. Mechanistische Studien weisen auf einen *Inner-Sphere* Mechanismus hin, der über die Insertion des Substrats in die Metall-Hydrid Bindung verläuft. Der Komplex $[\text{Fe}(\text{PNP}^{\text{Me}}\text{-}i\text{Pr})(\text{H})(\text{CO})(\text{Br})]$ hingegen, welcher über *N*-Me Linker verfügt, ist ein effizienter Katalysator für die Hydrierung von Aldehyden, zeigt jedoch keine Reaktivität gegenüber Ketonen. Dieser Umstand legt einen alternativen Reaktionsmechanismus nahe, da hier eine Aktivierung unter Beteiligung des PNP-Liganden nicht möglich ist. In diesem Fall wurde ein *Outer-Sphere* Mechanismus vorgeschlagen, der über ein Eisen(II)-Dihydrid verläuft. Dieses Intermediat konnte sogar isoliert, charakterisiert und direkt in Testreaktionen eingesetzt werden. Mit TONs bis zu 80.000 und TOFs über 20.000 h^{-1} weist dieser Katalysator eine erstaunliche Aktivität und Produktivität auf. Darüber hinaus ist die Reaktion äußerst chemoselektiv, da andere reduzierbare funktionelle Gruppen wie Ketone, konjugierte Doppelbindungen, Ester, Epoxide und Nitrosylverbindungen nicht umgesetzt werden.

Der zweite Teil dieser Arbeit beschäftigt sich mit der Anwendung der oben genannten Komplexe als Katalysatoren für die reversible Hydrierung / Dehydrogenierung von Kohlendioxid bzw. Ameisensäure als potentielle Wasserstoff-Speichertechnologie. Beide Komplexe, sowohl jene mit *N*-H als auch jene mit *N*-Me Linkern, konnten erfolgreich in der katalytischen Hydrierung von CO_2 bzw. NaCO_3 zu Formiaten eingesetzt werden. Basierend auf NMR-Experimenten und DFT-Rechnungen konnten die entsprechenden Eisen(II)-Dihydrid und Hydrido-Formiat Spezies als Schlüssel-Intermediate im Katalyse-Zyklus identifiziert werden, welcher, wie im Fall der selektiven Hydrierung von Aldehyden, über einem *Outer-Sphere* Mechanismus verläuft. Darüber hinaus sind diese Katalysatoren in der Lage, auch die formal entgegengesetzte Reaktion (d.h. die Dehydrogenierung von Ameisensäure) zu katalysieren. In Anwesenheit einer stöchiometrischen Menge von Triethylamin konnten TONs über 10.000 erreicht werden.

